

EVOLUTIONARY STRUCTURAL OPTIMIZATION OF MULTIPLE LOAD
CASE GENERIC AIRCRAFT COMPONENTS

A THESIS SUBMITTED TO THE GRADUATE SCHOOL OF NATURAL AND
APPLIED SCIENCES
OF
MIDDLE EAST TECHNICAL UNIVERSITY

BY

MURAT ATACAN AVGIN

IN PARTIAL FULFILLMENT OF THE REQUIREMENTS
FOR
THE DEGREE OF MASTER OF SCIENCE
IN
MECHANICAL ENGINEERING

JULY 2012

Approval of the thesis:

**EVOLUTIONARY STRUCTURAL OPTIMIZATION OF MULTIPLE LOAD
CASE GENERIC AIRCRAFT COMPONENTS**

submitted by **MURAT ATACAN AVGIN** in partial fulfillment of the requirements for the degree of **Master of Science in Mechanical Engineering, Middle East Technical University** by,

Prof. Dr. Canan Özgen
Dean, **Graduate School of Natural and Applied Sciences** _____

Prof. Dr. Suha Oral
Head of Department, **Mechanical Engineering** _____

Assist. Prof. Dr. Ergin Tönük
Supervisor, Mechanical Engineering Dept., **METU** _____

Examining Committee Members:

Prof. Dr. Suha Oral (*)
Mechanical Engineering Dept., **METU** _____

Assist. Prof. Dr. Ergin Tönük (**)
Mechanical Engineering Dept., **METU** _____

Prof. Dr. Haluk Darendeliler
Mechanical Engineering Dept., **METU** _____

Prof. Dr. Fevzi Suat Kadioğlu
Mechanical Engineering Dept., **METU** _____

Erhan Çiftçi, M.Sc.
Specialist Design Engineer, **TAI** _____

Date: **13.07.2012**

* Head of the examining committee

** Thesis supervisor

I hereby declare that all information in this document has been obtained and presented in accordance with academic rules and ethical conduct. I also declare that, as required by these rules and conduct, I have fully cited and referenced all material and results that are not original to this work.

Murat Atacan Avgin

ABSTRACT

EVOLUTIONARY STRUCTURAL OPTIMIZATION OF MULTIPLE LOAD CASE GENERIC AIRCRAFT COMPONENTS

Avgın, Murat Atacan

M.Sc., Department of Mechanical Engineering

Supervisor: Assist. Prof. Dr. Ergin Tönük

July 2012, 159 pages

Structural optimization is achieving the best objective function from a predefined medium, well bounded by constraints. Optimization methods have been utilized on different engineering applications to minimize the conceptual design effort that creates the necessity of new optimization techniques. Evolutionary Structural Optimization (*ESO*) is a topological optimization algorithm, which is defined as removing of inefficient elements from a design domain. ESO stress based method is applied to linear elastic, isotropic aircraft components for multiple load case. The bulk structure is modeled and discretized into three dimensional solid hexahedron or tetrahedron mesh, afterwards constraints, load and boundary conditions are defined in MSC.PATRAN. MSC.NASTRAN is utilized as finite element solver. The stress results are collected and evaluated by program developed in MICROSOFT VISUAL BASIC. The elements which are below the stress limit are eliminated. The remaining elements are operated after increasing the stress limit. The iteration process continued until prescribed rejection ratio is reached. Well known examples in literature are solved using program code and similar results are obtained which is a check for the code developed. Four generic aircraft components, *the clevis, the lug, the main landing fitting and power control unit fitting* were structurally optimized. The stress distribution in optimized results and existing aircraft designs are compared.

Keywords: evolutionary structural optimization, stress based method, aircraft, multiple load cases, topological optimization.

ÖZ

ÇOKLU YÜK ALTINDAKİ GENEL UÇAK PARÇALARININ EVRİMSEL YAPISAL OPTİMİZASYONU

Avgın, Murat Atacan

Yüksek Lisans, Makina Mühendisliği Bölümü

Tez Yöneticisi: Yard. Doç. Dr. Ergin Tönük

Temmuz 2012, 159 sayfa

Yapısal optimizasyon, iyi belirlenmiş sınırlara sahip önceden belirlenmiş bir ortamdan en iyi hedef fonksiyonu elde etmektir. Optimizasyon metotları yeni teknikler geliştirilmesi ihtiyacını doğuran kavram tasarım çabalarını en aza indirmek için çeşitli mühendislik uygulamalarında kullanılmaktadır. Evrimsel Yapısal Optimizasyon (EYO) tasarım alanından yük taşıma kapasitesi düşük elemanların çıkarılması olarak tanımlanan bir topolojik optimizasyon çözüm yoludur. EYO çoklu yük durumundaki doğrusal elastik, eşyönsüz (izotropik) uçak parçalarına uygulanan, gerilme tabanlı bir metottur. Yığın yapı modellenir ve üç boyutlu katı altı yüzlü ya da dört yüzlü parçalara ayrılır. Ardından kısıtlar, yük ve sınır koşulları MSC.PATRAN yardımıyla belirlenir. MSC.NASTRAN yazılımı ile sonlu elemanlar çözümü yapılır. Gerilme analizi sonuçları, MICROSOFT VISUAL BASIC'teki kod ile toplanır ve değerlendirilir. Gerilme sınırının altında kalan elemanlar elenir. Kalan elemanlar gerilme sınırı arttırıldıktan sonra tekrar işleme konur. Tekrar süreci, önceden belirlenmiş ret oranı yakalanıncaya kadar devam eder. Kodun doğruluğunun sınanması için literatürde bilinen örnekler denenmiş ve literatürdekilerle uyumlu sonuç elde edilmiştir. Ardından uçakta kullanılan dört parça, *çatal*, *kulp*, *uçuş ana bağlantı parçası* ve *güç kontrol ünitesi bağlantı parçası* EYO ile optimize edilmiştir. Optimize edilmiş sonuçlar ile uçak üzerinde var olan tasarımlardaki gerilme dağılımı karşılaştırılmıştır.

Anahtar Kelimeler: evrimsel yapısal optimizasyon, gerilme tabanlı metot, hava taşıtı, çoklu yük durumu, topolojik optimizasyon.

To who believe in me.

ACKNOWLEDGMENTS

Firstly, I would like to present my gratitude and respect to my supervisor, Assist. Prof. Dr. Ergin Tönük, who guide me through the study with his precious and wise instructions. It is an honor for me to face with his generosity, courtesy and patience.

I would like to thank my colleagues Sinan Karabulut, Mehmet Yaşartekin, Deniz Can Erdayı, and Barış Gider who have great contributions on my study.

I would also appreciate my family who provide me to able to walk on my way and my love Seda who give intangible support during my work. Especially I would like to memorialize my grandfather due to his humanity and unyielding personality.

TABLE OF CONTENTS

ABSTRACT	iv
ÖZ	v
ACKNOWLEDGMENTS	vii
TABLE OF CONTENTS	viii
LIST OF FIGURES	x
CHAPTER	
1.INTRODUCTION	1
1.1. OBJECTIVE	1
1.2. METHODOLOGY	1
1.3. OUTLINE	2
2.OPTIMIZATION	3
2.1. STRUCTURAL OPTIMIZATION	3
2.2. COMPUTATIONAL ALGORITHMS	6
2.2.1. GRADIENT-BASED ALGORITHMS	7
2.2.2. DISCRETE VARIABLE ALGORITHMS	8
2.2.3. GLOBAL SOLUTION ALGORITHMS	9
2.2.4. MULTIOBJECTIVE OPTIMIZATION	9
2.3. FINITE ELEMENT ANALYSIS	10
2.4. TYPES OF STRUCTURAL OPTIMIZATION	11
2.4.1. SIZE OPTIMIZATION	11
2.4.2. SHAPE OPTIMIZATION	11
2.4.3. TOPOLOGY OPTIMIZATION	12
2.5. SOLID ISOTROPIC MATERIAL WITH PENALIZATION (SIMP) METHOD	14
2.6. HOMOGENIZATION METHOD	14
2.7. LEVEL SET METHOD	17
2.8. EVOLUTIONARY STRUCTURAL OPTIMIZATION	18
2.9. BI-DIRECTIONAL EVOLUTIONARY STRUCTURAL OPTIMIZATION	26
2.10. GENETIC ALGORITHMS	29
2.10.1. SELECTION	30
2.10.2. CROSSOVER	30
2.10.3. MUTATION	31
3.PROGRAM FOR EVOLUTIONARY STRUCTURAL OPTIMIZATION AND VALIDATION	33
3.1. EVOLUTIONARY STRUCTURAL OPTIMIZATION	33
3.2. PROGRAM ALGORITHM	34
3.2.1. BUILDING THE “BDF” FILE	37

3.2.2. “F06” CREATION AND INTERFACE CODE	37
3.2.3. REJECTION AND STOPPING CRITERION	38
3.2.4. POST PROCESSING.....	39
3.2.5. PROGRAM MANUAL.....	40
3.3. PROGRAM VALIDATION.....	42
3.3.1. TWO BAR FRAME.....	42
3.3.2. MICHELL TYPE STRUCTURES WITH TWO FIXED SUPPORTS	50
3.3.3. MICHELL TYPE STRUCTURES WITH A ROLLER AND FIXED SUPPORT	54
3.3.4. BRIDGE WITH A MOVING LOAD	57
3.3.5. TORSION BEAM.....	59
3.4. RESULTS AND DISCUSSION	63
4.OPTIMIZATION OF GENERIC AIRCRAFT COMPONENTS	64
4.1. ENVIRONMENT OF LUG AND CLEVIS	64
4.2. LUG.....	67
4.3. CLEVIS	79
4.4. MAIN LANDING FITTING	88
4.5. POWER CONTROL EQUIPMENT SUPPORT	103
5.DISCUSSION AND CONCLUSION	114
5.1. DISCUSSION.....	114
5.2. LIMITATIONS OF CURRENT STUDY	116
5.3. RECOMMENDATIONS FOR FUTURE WORK.....	116
APPENDICES	122
A. MICROSOFT VISUAL BASIC INTERFACE CODE	122
B. THE EVALUATION OF THE AIRCRAFT COMPONENTS	133
B.1. THE EVALUATION OF LUG.....	133
B.2. THE EVALUATION OF CLEVIS	144
B.3. THE EVALUATION OF MAIN LANDING FITTING	151
B.4. THE EVALUATION OF SUPPORT FITTING.....	154

LIST OF FIGURES

Figure 2.1 Finding the best structure to transmit the load F to the support.....	4
Figure 2.2 Initial design domains and optimized results of size, shape and topology optimization respectively.....	11
Figure 2.3 Shape optimization problem and solution defined by Galileo in 1638.	12
Figure 2.4 Topological optimization of a satellite frame. a) Design domain showing instruments around which frame is to be designed. b) Optimized topology c) Optimized topology with instruments	13
Figure 2.5 A unit cell describing the microstructure with a rectangle void.....	15
Figure 2.6 Assumption of continuous change in microstructures	16
Figure 2.7 Initial design domain and ESO results for different iterations of an object hanging in the air with own weight.....	23
Figure 2.8 Photograph of Gaudi's original drawing for Passion Façade.....	24
Figure 2.9 Evolution of Passion Façade.....	24
Figure 3.1 Flow chart of the program interactions.....	35
Figure 3.2 General flow chart of the program.....	36
Figure 3.3 Rejection and stopping criterion of the program.....	39
Figure 3.4 Program interface for single load case input.....	41
Figure 3.5 Program interface for multiple load case input.....	41
Figure 3.6 Design domain of the two bar frame.....	43
Figure 3.7 Result of two bar for $RR=3\%$ and optimized structure.....	43
Figure 3.8 Result of two bar for $RR=6\%$ and optimized structure	44
Figure 3.9 Result of two bar for $RR=9\%$ and optimized structure	44

Figure 3.10 Result of two bar for RR=12% and optimized structure	45
Figure 3.11 Result of two bar for RR=15% and optimized structure	45
Figure 3.12 Result of two bar for RR=18% and optimized structure	46
Figure 3.13 Result of two bar for RR=21% and optimized structure	46
Figure 3.14 Result of two bar for RR=24% and optimized structure	47
Figure 3.15 Result of two bar for RR=30% and optimized structure	47
Figure 3.16 Total progress time vs. iteration number for two bar frame optimized structure...	48
Figure 3.17 Volume reduction vs. iteration numbers for two bar frame optimized structure...	49
Figure 3.18 Maximum von Mises Stress vs. iteration numbers for two bar frame optimized structure.....	49
Figure 3.19 Design domain of Michell type structure with two fixed support.....	50
Figure 3.20 Result of Michell truss with two fixed supports for RR=5% and optimized structure.....	51
Figure 3.21 Result of Michell truss with two fixed supports for RR=10% and optimized structure.....	51
Figure 3.22 Result of Michell truss with two fixed supports for RR=15% and optimized structure	51
Figure 3.23 Result of Michell truss with two fixed supports for RR=20% and optimized structure	52
Figure 3.24 Result of Michell truss with two fixed supports for RR=25% and optimized structure	52
Figure 3.25 Total progress time vs. iteration numbers for Michell truss with two fixed supports optimized structure.....	53
Figure 3.26 Volume reduction vs. iteration numbers for Michell truss with two fixed supports optimized structure.....	53

Figure 3.27 Maximum von Mises Stress vs. iteration numbers for Michell truss with two fixed supports optimized structure.....	54
Figure 3.28 Result of Michell truss with a roller and fixed support with volumetric approach and optimized structure.....	54
Figure 3.29 Result of Michell truss with a roller and fixed support with volumetric approach and optimized structure	55
Figure 3.30 Result of Michell truss with a roller and fixed support with volumetric approach and optimized structure	55
Figure 3.31 Total progress time vs. iteration numbers for Michell truss with a roller and fixed support optimized structure	56
Figure 3.32 Volume reduction vs. iteration numbers for Michell truss with a roller and fixed support optimized structure	56
Figure 3.33 Maximum von Mises Stress vs. iteration numbers for Michell truss with a roller and fixed support optimized structure	57
Figure 3.34 Initial model of the bridge with loading and boundary conditions.	58
Figure 3.35 Optimal design for the bridge with nine load cases.....	58
Figure 3.36 The optimum geometry at Rejection Ratio 12%.....	59
Figure 3.37 The design domain, colored as green, the support is colored as pink.....	60
Figure 3.38 The design domain is solid rectangular beam with square profile. Left figure is the section cut of design domain.....	60
Figure 3.39 The code output at Rejection Ratio % 62.....	61
Figure 3.40 The hollow shape is constant in all sections except loading and support transient regions. Left figure corresponds to section cut.....	61
Figure 3.41 Total progress time vs. iteration numbers for torsion beam.....	62
Figure 3.42 Volume reduction vs. iteration numbers for torsion beam optimized structure..	62

Figure 3.43 Maximum von Mises Stress vs. iteration numbers for torsion beam optimized structure.....	63
Figure 4.1 The front view of the lug, clevis assembly.....	64
Figure 4.2 The left view of the lug, clevis assembly and load case directions.....	65
Figure 4.3 The free body diagram of the instrument panel.....	66
Figure 4.4 The half and full model of lug.....	67
Figure 4.5 The half model is constraint from the symmetry plane.....	68
Figure 4.6 The load distribution in bearing hole for load case 1 on the left and for load case 2 on the right.....	68
Figure 4.7 Support nodes around the rivet.....	69
Figure 4.8 The contact elements and compression rivets at the bottom of lug in load case 1..	70
Figure 4.9 The contact elements and compression rivets at the bottom of lug in load case 2..	70
Figure 4.10 The support points of rivet head in tension regions.....	71
Figure 4.11 Rivet head spacing.....	71
Figure 4.12 The design and non-design domain of bearing.....	72
Figure 4.13 The design and non-design domain of rivets.....	72
Figure 4.14 The front, top, right side and isometric view of the optimized lug.....	73
Figure 4.15 Total progress time vs. iteration numbers for optimized lug.....	74
Figure 4.16 Volume reduction vs. iteration numbers for optimized lug.....	74
Figure 4.17 Maximum von Mises Stress vs. iteration numbers for optimized lug.....	75
Figure 4.18 The von Mises stress distribution of existing design lug for load case 1.....	76
Figure 4.19 The von Mises stress distribution of optimized lug for load case 1.....	76
Figure 4.20 The von Mises stress distribution of existing design lug for load case 2.....	77

Figure 4.21 The von Mises stress distribution of optimized lug for load case 2.....	77
Figure 4.22 Top, front, right side and isometric view of existing design and optimized lug. Existing design is red, optimized topology is blue.....	78
Figure 4.23 The half and full bulk model of clevis.....	79
Figure 4.24 The load distribution in bushing holes for load case 1 on the left and for load case 2 on the right.....	80
Figure 4.25 The support elements of the clevis end.....	80
Figure 4.26 The design and non-design domain of clevis.....	81
Figure 4.27 The front, top, right view of the optimized clevis.....	82
Figure 4.28 The isometric view of the optimized clevis.....	82
Figure 4.29 Total progress time vs. iteration numbers for optimized clevis.....	83
Figure 4.30 Volume reduction vs. iteration numbers for optimized clevis.....	83
Figure 4.31 Maximum von Mises Stress vs. iteration numbers for optimized clevis.....	84
Figure 4.32 The von Mises stress distribution of existing design clevis for load case 1.....	85
Figure 4.33 The von Mises stress distribution of optimized clevis for load case 1.....	85
Figure 4.34 The von Mises stress distribution of existing design clevis for load case 2.....	86
Figure 4.35 The von Mises stress distribution of optimized clevis for load case 2.....	86
Figure 4.36 Top, front, right side and isometric view of existing design and optimized clevis. Existing design is red, optimized topology is blue.....	87
Figure 4.37 Components of main landing assembly.....	88
Figure 4.38 The load and boundary conditions of the main landing fitting.....	89
Figure 4.39 The connection of main landing fitting and actuator rod end.....	90
Figure 4.40 The connection of main landing fitting and torque link.....	90

Figure 4.41 The bulk model of main lading fitting.....	92
Figure 4.42 The sinusoidal load distribution in bushing holes via actuator on the left and via torque link on the right.....	92
Figure 4.43 The MPC force distribution from CG of landing light to rivet holes.....	93
Figure 4.44 The support elements of main landing fitting.....	93
Figure 4.45 Design and non-design domain of main landing fitting.....	94
Figure 4.46 The front, top, right view of the optimized main landing fitting.....	95
Figure 4.47 Section A-A of the Figure 4.46.....	95
Figure 4.48 Section B-B of the Figure 4.46.....	96
Figure 4.49 Total progress time vs. iteration numbers for optimized main landing fitting.....	96
Figure 4.50 Volume reduction vs. iteration numbers for optimized main landing fitting.....	97
Figure 4.51 Maximum von Mises Stress vs. iteration numbers for optimized main landing fitting.....	98
Figure 4.52 The von Mises stress distribution of existing design main landing fitting.....	99
Figure 4.53 The von Mises stress distribution of optimized main landing fitting.....	99
Figure 4.54 The total displacement distribution of existing design main landing fitting.....	100
Figure 4.55 The total displacement distribution of optimized main landing fitting.....	100
Figure 4.56 Isometric view of existing design and optimized main landing fitting. Existing design is red, optimized topology is blue.....	101
Figure 4.57 Top, front and right side views of existing design and optimized main landing fitting	102
Figure 4.58 Power control and distribution unit and system installation brackets.....	103
Figure 4.59 Power control unit and support fittings connected to firewall.....	104
Figure 4.60 The bulk model of equipment support fitting and MPC of equipment.....	105

Figure 4.61 The boundary elements of the support fittings.....	105
Figure 4.62 The design and non-design domain of support fittings	106
Figure 4.63 The front, top, right view of the optimized support fitting.....	107
Figure 4.64 Total progress time vs. iteration numbers for optimized support fittings.....	107
Figure 4.65 Volume reduction vs. iteration numbers for optimized support fitting.....	108
Figure 4.66 Maximum von Mises Stress vs. iteration numbers for optimized support fitting	109
Figure 4.67 The von Mises stress distribution of existing design support fitting for load case 1	110
Figure 4.68 The von Mises stress distribution of optimized support fitting for load case 1...110	
Figure 4.69 The von Mises stress distribution of existing design support fitting for load case 2	111
Figure 4.70 The von Mises stress distribution of optimized support fitting for load case 2...111	
Figure 4.71 Isometric view of existing design and optimized support fitting. Existing design is red, optimized topology is blue.....	112
Figure 4.72 Top, front and right side views of existing design and optimized support fitting	113
Figure B.1 The von Mises stress distribution of lug at RR=2.5% for load case 1.....	134
Figure B.2 The von Mises stress distribution of lug at RR=5% for load case 1	134
Figure B.3 The von Mises stress distribution of lug at RR=7.5% for load case 1.....	135
Figure B.4 The von Mises stress distribution of lug at RR=10% for load case 1.....	135
Figure B.5 The von Mises stress distribution of lug at RR=12.5% for load case 1.....	136
Figure B.6 The von Mises stress distribution of lug at RR=15% for load case 1.....	136
Figure B.7 The von Mises stress distribution of lug at RR=17.5% for load case 1.....	137
Figure B.8 The von Mises stress distribution of lug at RR=20% for load case 1.....	137

Figure B.9 The von Mises stress distribution of lug at RR=22.5% for load case 1.....	138
Figure B.10 The von Mises stress distribution of lug at RR=25% for load case 1.....	138
Figure B.11 The von Mises stress distribution of lug at RR=2.5% for load case 2.....	139
Figure B.12 The von Mises stress distribution of lug at RR=5% for load case 2.....	139
Figure B.13 The von Mises stress distribution of lug at RR=7.5% for load case 2.....	140
Figure B.14 The von Mises stress distribution of lug at RR=10% for load case 2.....	140
Figure B.15 The von Mises stress distribution of lug at RR=12.5% for load case 2.....	141
Figure B.16 The von Mises stress distribution of lug at RR=15% for load case 2.....	141
Figure B.17 The von Mises stress distribution of lug at RR=17.5% for load case 2.....	142
Figure B.18 The von Mises stress distribution of lug at RR=20% for load case 2.....	142
Figure B.19 The von Mises stress distribution of lug at RR=22.5% for load case 2.....	143
Figure B.20 The von Mises stress distribution of lug at RR=25% for load case 2.....	143
Figure B.21 The von Mises stress distribution of clevis at RR=3% for load case 1.....	144
Figure B.22 The von Mises stress distribution of clevis at RR=6% for load case 1.....	144
Figure B.23 The von Mises stress distribution of clevis at RR=9% for load case 1.....	145
Figure B.24 The von Mises stress distribution of clevis at RR=12% for load case 1.....	145
Figure B.25 The von Mises stress distribution of clevis at RR=15% for load case 1.....	145
Figure B.26 The von Mises stress distribution of clevis at RR=18% for load case 1.....	146
Figure B.27 The von Mises stress distribution of clevis at RR=21% for load case 1.....	146
Figure B.28 The von Mises stress distribution of clevis at RR=24% for load case 1.....	146
Figure B.29 The von Mises stress distribution of clevis at RR=27% for load case 1.....	147
Figure B.30 The von Mises stress distribution of clevis at RR=30% for load case 1.....	147

Figure B.31 The von Mises stress distribution of clevis at RR=3% for load case 2.....147

Figure B.32 The von Mises stress distribution of clevis at RR=6% for load case 2.....148

Figure B.33 The von Mises stress distribution of clevis at RR=9% for load case 2.....148

Figure B.34 The von Mises stress distribution of clevis at RR=12% for load case 2.....148

Figure B.35 The von Mises stress distribution of clevis at RR=15% for load case 2.....149

Figure B.36 The von Mises stress distribution of clevis at RR=18% for load case 2.....149

Figure B.37 The von Mises stress distribution of clevis at RR=21% for load case 2.....149

Figure B.38 The von Mises stress distribution of clevis at RR=24% for load case 2.....150

Figure B.39 The von Mises stress distribution of clevis at RR=27% for load case 2.....150

Figure B.40 The von Mises stress distribution of clevis at RR=30% for load case 2.....150

Figure B.41 The von Mises stress distribution of main landing fitting at RR=2%.....151

Figure B.42 The von Mises stress distribution of main landing fitting at RR=4%.....151

Figure B.43 The von Mises stress distribution of main landing fitting at RR=6%.....152

Figure B.44 The von Mises stress distribution of main landing fitting at RR=8%.....152

Figure B.45 The von Mises stress distribution of main landing fitting at RR=10%.....153

Figure B.46 The von Mises stress distribution of main landing fitting at RR=12%.....153

Figure B.47 The von Mises stress distribution of support fitting at RR=4% for load case 1..154

Figure B.48 The von Mises stress distribution of support fitting at RR=8% for load case 1..154

Figure B.49 The von Mises stress distribution of support fitting at RR=12% for load case 1.....155

Figure B.50 The von Mises stress distribution of support fitting at RR=16% for load case 1.....155

Figure B.51 The von Mises stress distribution of support fitting at RR=20% for load case 1.....	156
Figure B.52 The von Mises stress distribution of support fitting at RR=24% for load case 1.....	156
Figure B.53 The von Mises stress distribution of support fitting at RR=4% for load case 2.....	157
Figure B.54 The von Mises stress distribution of support fitting at RR=8% for load case 2.....	157
Figure B.55 The von Mises stress distribution of support fitting at RR=12% for load case 2.....	158
Figure B.56 The von Mises stress distribution of support fitting at RR=16% for load case 2.....	158
Figure B.57 The von Mises stress distribution of support fitting at RR=20% for load case 2.....	159
Figure B.58 The von Mises stress distribution of support fitting at RR=24% for load case 2.....	159

CHAPTER 1

INTRODUCTION

1.1. OBJECTIVE

Structural optimization can be defined as maximizing or minimizing the objective function without breaking the design parameter rules. The main purpose of the optimization is designing in a way that can satisfy the requirement, while keeping the effort at minimum. The necessity of optimization is proved in the last few decades. When the nature is observed, all of the existing structures are optimized; otherwise they are not able to continue their existence. In optimization the formulation of problem should be well defined, otherwise the solution obtained can be unacceptable or inconsistent.

One of the most popular techniques for topology optimization is Evolutionary Structural Optimization (*ESO*). *ESO* is based on the simple concept of gradually removing inefficient material from the structure. Through this process, the resulting structure will evolve towards its optimum shape and topology. Theoretically, one is not capable to guarantee that such an evolutionary procedure would always produce the best solution (*global optimum*). However, the *ESO* technique provides a useful tool for engineers who are interested in exploring the structurally efficient forms and shapes during conceptual design stage of a project.

Via assistance of powerful and fast computer programs, structures can be investigated and analyzed more specifically. Finite element methods (*FEM*) are generally used in aerospace and automotive industries to create functional, economical and simple products by the help of decomposing into minor and known elements. As the number of elements and suitable algorithms are applied, convergence to real case is maximized.

1.2. METHODOLOGY

The main purpose of the study is to obtain the optimized structure of generic aircraft components under certain conditions. At first stage the bulk volume is formed and constraints, load conditions and supports of the component are specified by using MSC.PATRAN 2005. In

the next stage, structure is analyzed by MSC.NASTRAN 2005. Using analysis results, the optimization codes developed on MICROSOFT VISUAL BASIC 6.0 eliminates the unnecessary elements. The loop continues until the optimal solution is reached. Additionally the results are monitored by MSC.PATRAN 2005 as post processor. The results are compared with the existing aircraft components using CATIA V5 R19.

The result is the optimal solution of the aircraft component according to defined design parameters. Changing the design parameters will affect the final product.

1.3. OUTLINE

Chapter 2 expresses definition and basic concepts of various optimization methods, and includes a literature survey.

Chapter 3 defines the algorithm and comparison of code results with pre-defined solutions for check purposes.

Chapter 4 contains the optimization of four generic aircraft components, the lug, the clevis, the main landing fitting and power control equipment support, using evolutionary structural optimization method. The resulting optimized structures are compared with the existing aircraft components.

Chapter 5 reviews and concludes the study and presents future recommendations.

CHAPTER 2

OPTIMIZATION

Optimization can be briefly described as finding the best solution to the problem. Optimization is one of the major subjects of design which depends on not only on engineering but also on the universe. Possibly, for optimization, the most dominant and frequently used field is nature. All living elements of nature have been optimized since the beginning of life. The one that resist changing cannot continue to survive and become extinct. Nature should be carefully examined to realize the existence and importance of optimization. Human being is equipped with systems that operate with limited energy and maximum performance. Using optimization techniques the shape of apple or cherry are proved to have optimal shape of exposed to its own weight.

Simple mechanisms such as lever or pulley are fundamental illustrations that optimization has been performed using geometrical knowledge throughout history. The increasing demand on engineers to lower production costs to withstand competition has forced engineers to look for methods of decision making, such as optimization methods, to design and produce products both economically and efficiently. Almost all today's products are optimized according to certain parameters. The ultimate goal of all such decisions is either to minimize the effort required or to maximize the desired benefit.

2.1. STRUCTURAL OPTIMIZATION

Structural optimization can be defined as maximizing or minimizing the objective function without breaking the design parameter rules. Structural optimization logic is based on making an assembly of structures that sustain loads in best way. To be objective, the term "best" should be specified as in Figure 2.1. Weight, stiffness, critical load, stress, displacement or geometry can be selected to create "best" structure (Christensen and Klarbring, 2009). The design of the systems can be formulated as optimization problem where the performance is optimized satisfying all the constraints (Arora, 1989).

The development of the structural optimization dates back to eighteenth century. The importance of light weight designs is firstly comprehended in aerospace industry. Rapid

growth of raw material requirement, energy sources reduction and environmental impact compel engineers to create lightweight, efficient and low cost structures. Over last three decades, by the help of availability of high speed computers and rapid improvement in algorithms, engineers start to benefit from optimization techniques. Using the modern tools, time required for conceptual design can be reduced where thousands of design variables and constraints are included. More research and development activities are performed to extend optimization methods and create software packages which are reliable, easy and inexpensive (Huang and Xie, 2010).

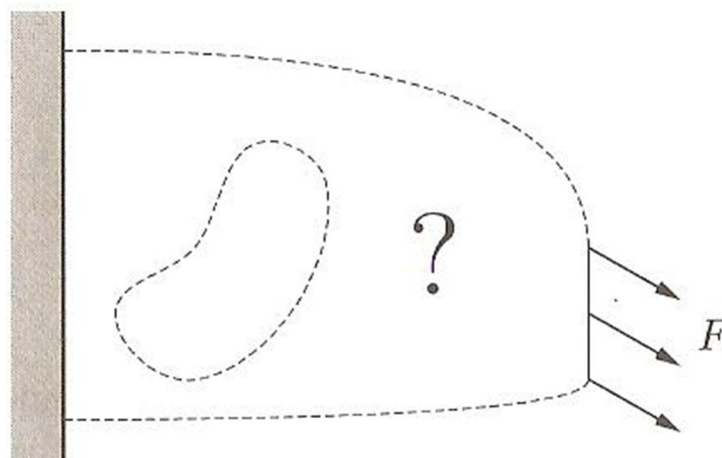


Figure 2.1 Finding the best structure to transmit the load F to the support. (Christensen and Klarbring, 2009)

The optimization problem has three fundamental elements which are

- Optimization variables (design variables) denoted by x ,
- Cost function (objective function) denoted by $f(x)$,
- Constraints expressed as equalities or inequalities denoted by $g_i(x)$ (Arora, 2007).

Parameters chosen to describe the design of a system are called *design variables*. *Constraints* are required for the definition of optimization problem because designer should not assign any value; otherwise the design is named as infeasible. An infeasible design does not meet one or more design requirements. Design variables should be selected properly, or else formulation may be incorrect or inconsistent. As the number of the design variables increases, design acquires more flexibility. Design variables should be independent as much as possible. One variable should take any numerical value independent from another variable (Arora, 1989).

Variables are usually denoted by a vector notation x . Design variables can be *continuous or discrete*. Continuous variables can take any value (i.e. real numbers) within a range whereas discrete variables such as material properties that are available can take isolated values (Haftka and Gürdal, 1992). Discrete variables are dominant during optimization generally. To illustrate discrete variables, standard material thicknesses or diameters of rods or tubes, material properties (elastic modulus, yield or ultimate strength, density etc.), integer numbers like number of bars, bolts are integer (Arora, 2007).

Cost function, in other words objective function, is the function whose goal is to maximize a quantity such as performance or minimize quantities such as weight or cost. Optimization with more than one objective function is called *Multicriteria Optimization*. For structural optimization problems, stress, displacement, weight, vibration frequency or buckling load are objective functions (Haftka and Gürdal, 1992). If all functions are linear then the optimization problem is named as *linear programming (LP) problem*. If the cost function is quadratic and constraints are linear then the problem is called *quadratic programming (QP) problem* (Arora, 2007).

Constraints are the design parameters that should be matched. Constraints can be in equality or inequality form. Inequality constraints create greater feasible design domain than equality constraints. Constraints can be either *linear or nonlinear*. Linear programming problems have only linear constraints, where problems generally have nonlinear constraint functions as well. Each constraint must be influenced by one or more design variables. Some of them are simple and have direct influence on optimum design; however some complex ones may be indirectly influenced by design variables are called implicit constraints (Arora, 1989).

Structural optimization methods can also be categorized into two, *analytical and numerical methods*. In analytical method, calculus and other mathematical theories are applied to the basic structures. They are more convenient however; they are not suitable for complicated structures. The structure is modeled via mathematical equations and the purpose is solving the equations exactly. They sometimes give unrealistic results or unpractical solutions. Problems solved with analytical methods are called *continuous problems* (Gallagher and Zienkiewicz, 1973). If the design variables are complicated then almost always the analytical methods cannot handle complex structural optimization problems, then numerical methods should be applied. The recent growth on the computer technology helps to develop the numerical methods. For the methodology, the initial selection is performed and iterative calculations are done without violating the constraints. According to the convergence criteria, if the

calculations yield smaller results than the error estimation, the problem is finalized and optimum solution is found. In real life applications, the design variables generally are not unbounded and continuous but discrete or integer and there are limits. Once the problem is clearly defined, numerical methods can easily be applied to the various distinct design variables (Rozvany *et al.*, 1995).

Engineers deal with difficulties in optimization designing efficient, cost effective and stiff structures. Today's sophisticated world compels engineers to create economical and compact designs. Design also includes analysis, presentation of results, simulation and optimization and an iterative process leads to final optimum design. In conventional design process, designer's skill and experience is vital and affects the results deeply. Conventional design process is necessary for making conceptual changes or adding specifications to the procedure. However, during detailed design the conventional design faces with treatment of complex constraints or inputs. In these cases, designer would have difficulty for decision to change the design variables, while satisfying the constraints. Even, conventional design process can cause uneconomical designs delaying project calendar. Computer aided design optimization (*CADO*) has been used for the assistance of computers in design process (Arora, 1989).

The optimum design process forces the designer to identify the design variables explicitly while minimizing the cost function and conforming the constraints. The problem should be mathematically well formulated. Optimum design process is more organized using the suitable algorithms to make decisions. The best approach would be to have an optimum design process assisted by the engineering experience and interaction. Hence, the design process can be automated using optimization techniques up to a certain point; however human creativity in optimization technique is essential (Arora, 1989).

2.2. COMPUTATIONAL ALGORITHMS

Engineering systems can be analyzed more rapidly and accurately by using computers. Design process is usually an iterative method that requires repeating the same calculations. Therefore computers are important and effective tools. Huge amount of data has been formed during calculations and these should be utilized or presented in a proper manner (Arora, 1989).

Optimization techniques have been widely used in many structural and mechanical systems. During solutions, problems are simplified, however simplification of problems may deviate the solution from the reality. As mentioned by Arora (2007), real world problems are complex,

computational tools should be improved to solve larger problems. Since the methods have matured during the last decade, new methodologies are being used. Suitable algorithms should be chosen to have more realistic results.

The optimization algorithms start from an initial design and continue with small steps to improve the value of the objective function. The search is terminated if the value of the objective function can no longer be updated without violating the constraints. Some optimization methods are terminated when the improvement of the objective function drops below a certain limit (Haftka and Gürdal, 1992).

A good optimization algorithm should have the following attributes;

- Robustness: The algorithm should converge to the local minimum point from any initial point.
- Generality: The algorithm should have equality and inequality constraints.
- Accuracy: The algorithm should converge to the optimum point as accurately as desired.
- Ease of use: The input should be minimized to let the algorithm to be used also by the inexperienced users.
- Efficiency: The algorithm should converge fast (Arora, 2007).

Different types of optimization algorithms available in literature are briefly discussed in the following sections.

2.2.1. GRADIENT-BASED ALGORITHMS

Gradient based algorithms are desired to solve for continuous variables and differential functions because gradients have been operated. They are executed on linear problems as well as nonlinear problems. At first stage the optimum point is estimated and improved by iteration. Taylor's series expansion for cost and constraint functions has been utilized for improvement. Modification in variables should be bounded properly to solve the problem by Sequential Linear Programming (*SLP*) successfully; however selection of limits is quite difficult in practice. Sequential Quadratic programming can also be used to define the step size (Arora, 2007).

Constrained problems can be altered to unconstrained problems for solution. The idea is to add the penalty term to the cost function. Penalty parameter is increased where the unconstrained function is minimized, however penalty parameters tend to infinity to find optimum solution. Another method has been established to find optimum solution, the penalty parameters are required to increase sufficiently large but finite value called Augmented Lagrangian Method (Arora, 2007).

2.2.2. DISCRETE VARIABLE ALGORITHMS

Continuous variable optimization problems have infinite number of feasible design domains however, discrete variable problems have only finite number of solutions that the optimum solutions have to reach. Finding optimum solution for a discrete variable problem is more difficult compared to a continuous variable problem hence, there is no optimality condition to guide the numerical search process. To find the best solution, discrete points should be listed. Basically there are two classes of methods for solving discrete variable problems which are enumeration method such as branch and bound algorithm and stochastic or evolutionary methods such as genetic algorithms and simulated annealing (Arora, 2007).

Branch and bound method is also known as implicit enumeration method. Firstly it has been formed for solving linear problems but also can be applied to nonlinear problems. The solution space can be represented by branches of an inverted tree. Each node of the tree represents a possible discrete solution. If the solution is infeasible, then the branch is truncated or other branches are searched for better solution. A node is said to be fathomed if no better solution is possible with further branching from that node. If the solution is feasible, it represents a new upper bound for the optimum, or fathomed (Arora, 2007).

Simulated annealing is a stochastic method that can be used to find the global minimum for mixed variable nonlinear problem. The objective function does not require being continuous or differentiable. Random points are created in a neighborhood of current best point. If the cost function or penalty function is smaller than the current best value then the point is accepted and best cost function is updated. The main deficiencies of the method are unknown rate at which the target level is to be reduced and uncertainty in total number of trials (Arora, 2007).

Round-off technique is a simple approach where the optimum solution is obtained by assuming all variables to be continuous. The variables are rounded-off to the nearest available discrete values to obtain discrete solution. The difficulty is to define whether the variables are

increased or decreased. The technique may not converge due to high nonlinearity or widely separated allowable discrete values (Arora, 2007).

2.2.3. GLOBAL SOLUTION ALGORITHMS

In practical applications it is vital to find the global optimum solutions rather than local minimum. The local minimum can also be the global minimum or not, and it is not possible to recognize this. Therefore, it is impossible to define a precise stopping criterion for computational algorithm for global optimization. The best solution obtained by algorithm after running for certain iterations or time is accepted as global solution of the problem. As the number of iterations increases, the possibility of gathering convergent solution increases. The challenge is to solve global optimization problem efficiently, as the number of design variables increases, computer time increases. Genetic algorithm and simulated annealing can also be used for global solutions. Global optimization methods are investigated in two main categories which are deterministic and stochastic methods. They are classified as whether stochastic procedures are applied for the solution or not. Covering method, zooming method, generalized descent method and tunneling method are basic deterministic methods (Arora, 2007).

Stochastic methods depend on random methods to find the global minimum point. They are used for deciding the stopping criteria and developing techniques to find the local minimum. Some stochastic methods determine all local minimums for the function. Multistart method, clustering method, controlled random search, acceptance-rejection methods and stochastic integration are some examples for stochastic methods (Arora, 2007).

2.2.4. MULTIOBJECTIVE OPTIMIZATION

Engineering design is a decision making process and requires critical decisions at every stage of the design. Multiobjective optimization techniques offer a formal methodology for effective design and choosing the best. Multiobjective optimization is a critical component of modern design process. Decision making is a challenging activity because the existence of conflicting requirements. When a beam is investigated and if the objective is to design the beam with minimizing the stress and mass, they are conflicting objectives because when the mass, i.e., cross section is decreased then the stress level is increased. Therefore a decision has to be made. If the mass objective is more important to designer than stress, it can be preferred to

design lower values of mass. Cars should have big cargo but then fuel efficiency has to be considered a trade-off should be made (Messac and Mullur, 2007).

Algorithms for solution of single objective optimization yield local minima for the cost function in the feasible set. If all local minima are found then the global minimum point is to be determined. However the problem does not possess a unique solution hence, the global minimum point does not minimize all the objectives simultaneously. The objectives can have conflicting characteristics, nevertheless using Palermo optimality optimal solution can be obtained. If one global optimum point minimizes all objective functions simultaneously, then it is called *utopia point*. If attaining utopia point is not possible then the closest point to the solution is called *compromise solution* (Arora, 2007).

Multiobjective optimization can be solved by weighted sum method. Each objective function is scaled by a weight factor. The relative value of weights generally reflects the relative importance of the objectives. If all the weights are omitted or set to one, then all objectives have the same contribution. Weighted global criterion can also be applied. To convert multiobjective optimization to single objective optimization problem lexicographic method, ϵ -constraint method or goal programming can be applied (Arora, 2007).

2.3. FINITE ELEMENT ANALYSIS

Bruce Irons, one of the pioneers of the finite element analysis (*FEA*) remarked that “*if there is an opportunity for improving the design, then somebody somewhere attempting to do so using Finite Elements*”. *FEA* has been used over 40 years and became a mature technique and special tool for improvement of the optimization process (Xie and Steven, 1997). It divides up a very complicated problem into small elements that can be solved in relation to each other. *FEA* solves finite number of algebraic equations. According to Xie and Steven (1997), *FEA* is a computational technique in which the structure is modeled as assembly of small elements. Elements have simple but different geometries such as triangle or quadrilateral shapes that are easy to analyze. *FEA* is a method that arises for structural stress analysis and broadens interest area to other fields such as heat transfer, fluid mechanics, acoustic and electromagnetic waves. *FEA* generates many simultaneous algebraic equations solved on a digital computer in an iterative manner. Complicated problems that are difficult or impossible to be solved by analytical methods can be solved by *FEA* approximately.

2.4. TYPES OF STRUCTURAL OPTIMIZATION

Depending on the geometrical feature, basically there are three main optimization characteristics; these are size optimization, shape optimization and topology optimization. These optimization types have different concepts which are presented in Figure 2.2.

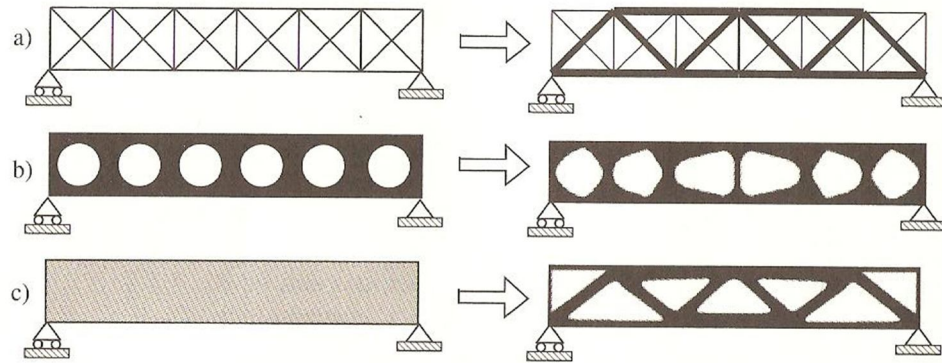


Figure 2.2 Initial design domains and optimized results of size, shape and topology optimization respectively (Bendsoe and Sigmund, 2004).

2.4.1. SIZE OPTIMIZATION

Size optimization is defining the optimum size and dimensions of the structure without changing the boundary or shape. The dimensions are optimized. The design domain and topology of the structure is fixed. Cross sectional area of truss member, thickness distribution of a sheet and material properties such as density, elastic modulus, and thermal conductivity are optimized without changing the mesh. This is the earliest and easiest approach for improving structural performance.

2.4.2. SHAPE OPTIMIZATION

Shape optimization is minimizing the objective function by changing or determining the boundary shape with satisfying the design requirements (Gallagher and Zienkiewicz, 1973). Christensen and Klarbring (2008) mentioned that connectivity of the structure is not changed by shape optimization and new boundaries are not formed. Lee (2007) stated that about 900 BC, the history of isoperimetric problem, the determination of the shape of a closure curve of given length and enclosing maximum area on a plane is also in the scope of a shape

optimization problem. In 1638, Galileo presents a logical definition for the shape of a cantilever beam for uniform strength as presented in Figure 2.3. Shape optimization techniques require special attention to define design variable and added constraints and to integrate Computer Aided Drawing (CAD) systems and optimizer. For solving the shape optimization problem, the boundary should be specified while minimizing the cost function and satisfying the constraints. Yet, shape optimization problem may have multiple solutions. It is difficult to provide continuous shape changes without violating mesh pattern during optimization. To eliminate mesh distortion or unacceptable designs, new constraints should be added to control the movement of each nodal coordinate by trial and error. Representation of geometric boundary, mesh generation and manipulation play important role on shape optimization.

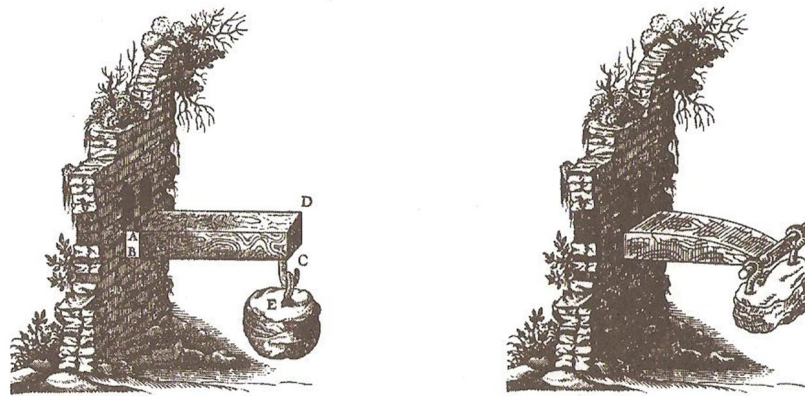


Figure 2.3 Shape optimization problem and solution proposed by Galileo in 1638 (Lee, 2007).

2.4.3. TOPOLOGY OPTIMIZATION

The aim of the topology optimization is to find the optimum layout of the structure, which best fits the requirements. There is no restriction on the final form of the structure relative to the initial form. This type of optimization has great advantages for determination of the conceptual design (Gallagher and Zienkiewicz, 1973). Christensen and Klarbring (2008) state that connectivity of the nodes is variable. According to Huang and Xie (2010) topology optimization of continuum structures is to find the optimal designs by determining the best locations and geometries of cavities in the design domain. Compared to the other types, topological optimization is the most challenging and economically most rewarded concept. Topology optimization gives freedom to designer to create high efficient conceptual designs

rather than limiting the boundaries of the structure. According to Bendsoe and Sigmund (2004), the purpose of the topology optimization is to find the optimal layout of the structure within a special region such as a satellite frame presented in Figure 2.4. The known quantities can be applied loads, possible support conditions, volume of the structure, and design restrictions such as location and size of prescribed holes or solid areas. The physical size, shape and connectivity of the structure are unknown.

In topological optimization the optimal placement of isotropic material in space is considered. The material points in space and void points should be determined. Then the geometry turns out to be black and white rendering of image.. This means intermediate values of artificial density function should be penalized in a manner analogous to other continuous optimization approximations of 0-1 problems. One possible popular and efficient method is Solid Isotropic Material with Penalization (*SIMP*) method (Bendsoe and Sigmund, 2004).

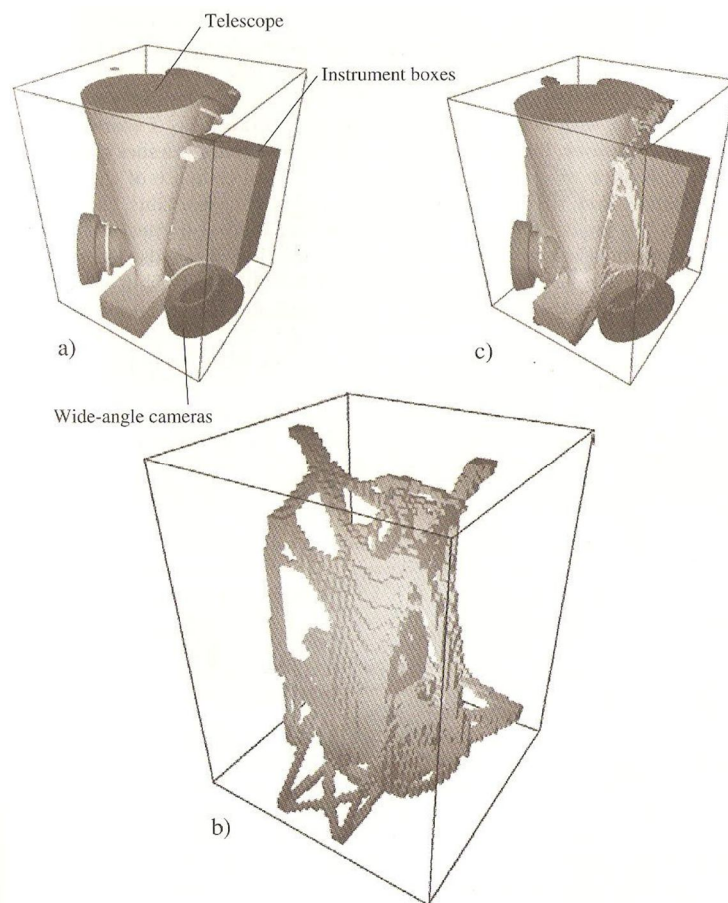


Figure 2.4 Topological optimization of a satellite frame. a) Design domain showing instruments around which frame is to be designed. b) Optimized topology c) Optimized topology with instruments (Bendsoe and Sigmund, 2004).

2.5. SOLID ISOTROPIC MATERIAL WITH PENALIZATION (SIMP) METHOD

The most popular way to introduce the notion of topology into the structural analysis of the topology optimization problem is through SIMP method. SIMP method was considered by Bendsoe (1989) and developed by Zhou and Rozvany (1991). The fundamental principle behind its use requires a density design variable dependent material constitutive law that penalizes intermediate density material in combination with an active volume constraint (Bruns, 2005). The SIMP method has been widely accepted in the area of topology optimization due to its conceptual simplicity and computational efficiency (Pasko *et al.*, 2008). The main idea of SIMP approach is that the system performance relies on cost/performance ratio which is disadvantageous for intermediate design variables. The penalization of intermediate design variables is introduced by substituting the dependence of objective function with weight coefficients raised by penalization parameter (Ambrósio and Eberhard, 2009). SIMP method creates a model that the elements are isotropic material with variable density. The elements are used to discretize the design domain and design variables are the relative densities of the elements. The intermediate densities are eliminated and material distribution having formed or non-formed structures are obtained. It has been widely used because the algorithm is effective and simple (Huang and Xie, 2010).

Density $\rho(x)$ is the design function. If the design has zero or one at all points, the design is a black and white design and performance can be evaluated with correct physical model. Experience show that optimization does the actual result in such designs if ρ is chosen sufficiently big, to obtain true 0-1 designs, ρ should be 3 or larger (Huang and Xie, 2010).

2.6. HOMOGENIZATION METHOD

Homogenization method is a structural optimization technique that many microscale voids are created to form a porous medium that makes a linearly elastic structure. Optimization is performed by defining the optimal porosity of the medium identified with a design domain. If the region contains only void, that means there is no material there, on the other hand if the region consists of no porosity, a solid structure should be placed over there. Porous medium is generated by distributing the material and void (Suzuki and Kikuchi, 1991). Introducing the material density, ρ , the infinite number of infinitely small voids can be distributed through the material, i.e. constructing a composite structure; topology problem can be converted to sizing

problem. The $\rho = 0$ expression refers to void and $\rho = 1$ refers to the solid material at micro level (Bendsoe, 1995). The voids are optimally distributed and structure is formed to achieve the objective function. Optimization problem can be solved both for minimizing the main compliance or volume of voids. The volume of the whole design domain, Ω , and the volume of solid distributed design domain, Ω_s , is specified as notation. For simplicity, for plane stress problems, the voids can be assumed as rectangle. Rectangle holes are preferred because they can create complete void if $a = b = 1$, complete solid if $a = b = 0$ and porous microstructure if $0 < a < 1$ and $0 < b < 1$ as shown in Figure 2.5. Circle voids are not preferred because they cannot form a complete void. Elliptic structures can also be used (Suzuki and Kikuchi, 1991).

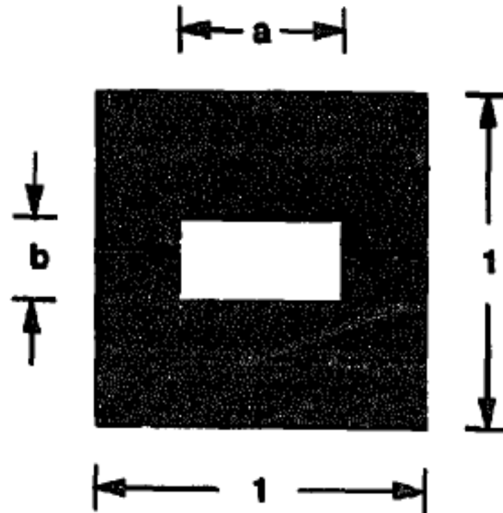


Figure 2.5 A unit cell describing the microstructure with a rectangle void (Suzuki and Kikuchi, 1991).

The density of the material is a function of design variables which reveals the size and the geometry of holes at micro level. The formation of the material distribution method, for generating optimal continuum structures involves the introduction of a composite consisting of the base material with periodically repeated micro voids. The microstructures distributed on the material are infinitely small and infinitely many. The angle of rotation of the material axes will have direct influence on the compliance of the structure. For any material with a specified linearly elastic material, including microscopic voids, should have intermediate density value and provide strictly less proportional rigidity. There is a strong relationship between unit cell formation and effective material properties. The density of the optimal structure is expected to

have values between 0 and 1. The optimal rotation of an orthotropic material is not only important for the solution of optimization problem, but also significant in the design of laminates and composites (Bendsoe, 1995). Microstructures can also have orientation different than the previous structure. In low density case, the second order microstructure yields better results, however the material constants are hard to be derived if Poisson's ratio is not zero. First order microstructure gives out result for any Poisson's ratio. Since holes are rectangular in the unit cell for porous medium, orientation of voids, θ , have important role for stress analysis. Anisotropic elasticity tensor depends on the orientation of microscale holes. The sizes of rectangular voids and orientation are design parameters for optimization problem. If a , b , and θ are functions of the position x of an arbitrary point of a macroscale domain of a linearly elastic porous structure, Ω , in two dimensional Euclidean space R^2 , then $a = a(x)$, $b = b(x)$, $\theta = \theta(x)$. Figure 2.6 shows a schematic setting of varying microstructures, a homogenized elasticity tensor $E^H(x)$ is computed to solve macroscopic stress analysis problem of a porous structure (Suzuki and Kikuchi, 1991).

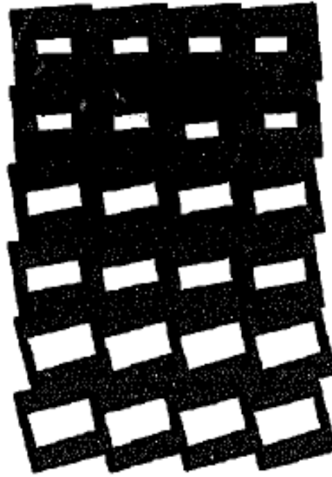


Figure 2.6 Assumption of continuous change in microstructures (Suzuki and Kikuchi, 1991).

Homogenization method introduces micro-perforated composite to avoid ill-conditioned optimization problems. The relationship has been formed between the microstructure parameters and material properties by creating voids on the structures. The structural distribution is derived from parameters of the microstructure; however resulting structure does not have meaning since the microstructure has no definite length scale (Huang and Xie, 2010).

2.7. LEVEL SET METHOD

Other than taking material properties as design variables, level set method deals with boundary variations. Internal and external boundaries are design variables for level set method. Boundaries are represented by level set function and propagated by the level set equations. The interfaces can be separated or merged using level set method, which offers a tool for shape and topology optimization. Firstly, the method is developed for the boundaries allowed to move according to the stress concentration. A level set method is employed for tracking the motion of the structural boundaries under a speed function and handling the presence of potential topological changes. Level set method can also be applied on the frequency optimization problem as performed by Osher and Santosa (2001). Functional gradients are used to calculate the velocity of the level set and deal with optimization problem with geometrical constraints. The theories and algorithms are developed and applied for the solution of more general problems. Boundary based method that handles with topology changes, have promising potential. The solution method of level set equations show diversity. Radial basis functions are used to discretize the level set function which the dependence on space and time are separated and converted from PDE into ODE. Instead of solving level set equation, Radial basis functions (*RBF's*) can also be applied for the parameterization of the level set method. Level set equation, discretized by the RBF's is substituted into the shape derivative formulation. Level set function can be updated by varying parameters according to design sensitivities (Xing, 2009).

A piecewise constant level method is also implemented for optimization problems. In this method, piecewise density function is defined over a design domain. This function acts as a link between level set function and objective function. New holes can be formed using this method. Level set equations are hyperbolic PDE's. Galarkin finite elements solution may create instability problems. Therefore stabilized finite element methods should be applied for the solution of hyperbolic PDE's. Petrov-Galarkin method is performed to approximate Hamilton-Jacobi equation for treatment of the cracks. For another solution technique Eikonal equations are introduced. There are generally two stages in a level set based structural optimization procedure: the stress analysis stage and the boundary evolution stage involving level set methods. In most applications, level set of method is applied with finite difference method (*FDM*). This method works well for simple geometries, however; complex geometries and boundaries may create difficulties. Finite element method should be applied with level set method (Xing, 2009).

2.8. EVOLUTIONARY STRUCTURAL OPTIMIZATION

One of the most popular techniques for topology optimization is Evolutionary Structural Optimization (ESO). ESO method was firstly developed by Xie and Steven (1992) in the early 1990's and has since been continuously developed to solve wide range of topology optimization problems (Huang and Xie, 2010). The method gives out reliable results while the algorithm is easy to understand for engineering situations. ESO concept can be applied to stress based, stiffness/displacement based, frequency based and buckling load based problems with single or multiple environments (Xie and Steven, 1997). ESO is based on the simple concept of gradually removing inefficient material from the structure. Through this process, the resulting structure will evolve towards its optimum shape and topology. Theoretically, one cannot guarantee that such an evolutionary procedure would always produce the best solution. However, the ESO technique provides a useful tool for engineers who are interested in exploring the structurally efficient forms and shapes during conceptual design stage of a project (Huang and Xie, 2010).

Stiffness is one of the major issues that are required to be dealt with during design process of buildings and bridges. Structure should be stiff enough that maximum deflection or displacement should not exceed a prescribed limit. The strain energy of the structure can be defined as;

$$C = 1/2 \cdot [P]^T \cdot [u] \quad (2.1)$$

where C is strain energy of the structure, P is load vector and u is displacement vector in equation (2.1). The strain energy is also known as *mean compliance*. Strain energy must be minimized to maximize the overall stiffness as strain energy is the inverse measure of overall stiffness. The sensitivity number of the i^{th} element, α_i , can be calculated by such equation;

$$\alpha_i = 1/2 \cdot [u^i]^T \cdot [K]^i \cdot [u^i] \quad (2.2)$$

where $[K]$ is global stiffness matrix at equation (2.2). The sensitivity number indicates the change in the strain energy as a result of removing i^{th} element. Elements having lowest value of sensitivity number should be removed to minimize the main compliance and maximize the stiffness then increase in the main compliance will be minimal. The removal continues until prescribed limit for strain energy is reached. The sensitivity number for equation (2.2) is always positive. If a limit is imposed on the j^{th} displacement component, the change of the

specified displacement component by removing the i^{th} element of the structure, α_{ij} , can be either positive or negative that the displacement component can change both in opposite directions. The elements which have the smallest absolute value for α_{ij} should be removed to minimize the change in displacement component. The optimization steps for stiffness can be summarized as follows;

- I. Discretize the structure using a fine mesh of finite elements
- II. Solve static equilibrium equation, $[K][u] = [P]$, for specified load where $[K]$ is the overall stiffness matrix of the structure, $[u]$ is the displacement vector and $[P]$ is the load vector.
- III. Calculate the sensitivity number of each element using equation (2.2)
- IV. Remove the elements having lowest sensitivity numbers.
- V. Repeat steps II to IV until prescribed strain energy of the structure is reached.

The main aim is to design the lightest structure while satisfying the stiffness or displacement constraint (Xie and Steven, 1997).

During optimization, while the high strength material has been continuously developed and structural elements are becoming thinner, the structures are prone to buckling problem. Optimization is performed by shifting materials from stronger points to weaker points to achieve better buckling performance. The weight of the structure does not change however the structure may endure higher buckling load. The load carrying capacity of a slender member under compression is usually determined by buckling load. Optimization technique is applied by maximizing the buckling load carriage capacity of the structure while keeping the weight constant (Xie and Steven, 1997). Rong *et al.* (2000) improves a method for ESO method against buckling and propose maximizing the critical buckling load of structure of constant weight. Firstly, the sensitivity number of the first eigenvalue or first multiple eigenvalues are obtained. A set of optimum criteria for closely-spaced eigenvalues and repeated eigenvalues are established, based on the sensitivity numbers of the first multiple eigenvalues to increase the buckling load factor effectively. Three portal, three member space and box frame is investigated. The results demonstrate that the proposed method is valid and effective and is suitable for various complex cases of practical structures. It can be readily implemented in any of the existing finite-element codes (Rong *et al.* 2000).

The evolutionary procedure for buckling optimization is presented as (Xie and Steven, 1997);

- I. Discretize the structure using a fine mesh of finite elements.
- II. Solve the eigenvalue problem.
- III. Calculate the sensitivity numbers for each element.
- IV. Increase the cross sectional area of elements which have the highest positive sensitivity number, α_i^+ , values and decrease the cross sectional area of the same number of elements which have the lowest negative sensitivity number, α_i^- , values.
- V. Repeat step II to IV until buckling load factor cannot be increased any further.

The natural frequency design is of great significance in many engineering fields such as aeronautical and automotive. Excessive response will be caused if the structural frequency is close to the excitation frequency (Yang *et al.* 1999a). Xie and Steven (1997) mention that it is often necessary to shift the fundamental frequency or several of lower frequencies of the structure away from the frequency range of the dynamic load in order to avoid severe vibration. The sensitivity number is formulated as an indicator of the contribution of the element removal or addition to the frequency change. As an optimum is reached by gradually removing and adding elements, the weight requirement can be satisfied explicitly in algorithms. The frequency-related function is focused and chosen as the objective function in formulating the mathematical statement (Yang *et al.* 1999a).

There has been extensive research focused on structural optimization with frequency constraints. Grandhi (1993) performs most of the developments in this area. Frequency optimization has been restricted by changing the size of the beams or thickness of the plates in these studies. Applications for simultaneous shape and topology optimization (Diaz and Kikuchi, 1992; Ma *et al.* 1993; Tenek and Hagiwara 1993; Ma *et al.* 1995) of general structural dynamic systems have noticeable success which is applied by homogenization method. ESO concept, gradually removing material, can easily be extended and effectively used for frequency optimization. The great advantage of ESO method to others is its simplicity, compared with any structural optimization method (Xie and Steven, 1997).

Three types of design objectives are considered based on (Yang *et al.* 1999a);

- I. Maximizing a single frequency, the i^{th} eigenvalue,
- II. Maximizing the multiple frequencies.
- III. Satisfying the set of specified frequencies.

Finite element analysis based optimization techniques require to regenerate meshes if the final structure changes dramatically however the ESO method does not need to create mesh again. Another way for removing the element is reducing the elastic modulus or thickness to a very small value. Hinton and Sieng (1995) reduce elastic modulus by multiplying by a factor of 10^{-5} . However due to large difference of thickness or elastic moduli among the materials, the global stiffness matrix may become ill-conditioned; therefore numerical error may occur. Additionally, the unnecessary elements which are not removed are still being calculated. The number of equations to be solved does not change; the computer time cannot be decreased as the structure evolves. Consequently the more preferred way is to eliminate the low stress value elements, instead of keeping them (Xie and Steven, 1997).

An optimization model can be set in a way that these parts are not removed or changed during evolutionary process. These regions are named as non-design domain. Material properties can be same or different from those of other regions, however the elements in the non-design domain are not allowed to be removed even the stress level is low (Xie and Steven, 1997).

In real cases, the structures are exposed to different load cases at different times. Each load acts on the structure at different times, namely *multiple load case*. The structure should be designed so that, the requirements should be satisfied for all load cases. The bicycle has been optimized using ESO method for different conditions such as starting, speeding, rolling and braking by Medved (1995). The material is only removed from boundaries. Design of a bearing pedestal is investigated by Xie and Steven (1997), using ESO method. The result is validated when the solution of the Rasmussen *et al.* (1992) is examined having solution of homogenization method. When the moving loads are investigated in bridges, it can be approximated as multiple load case. The traffic load can be changed into point load applied on finite number and equal spaced locations at different time intervals (Xie and Steven, 1997). Optimum design of a bridge with a moving load is performed in Chapter 3. An element can be removed from the structure if it satisfies rejection criterion for all load cases.

If the structure support changes it is called *multiple support environment*. For example, an aircraft is supported by distributed air pressure in flight and supported by hoisting point when on ground. A car is supported by suspension during the driving and supported by lifting point for repairing. These are examples for multiple supports. When the structure is held in different ways, each support environment has different global stiffness matrix and is needed to be solved separately. The computational cost for extra support environment is much more when compared with multiple load case (Xie and Steven, 1997).

Çiftçi (2006) studies in both stress and displacement based ESO method for different topologies. In his study, he develops a code which discretizes the design domain into small elements, produces nodes and connects them in MATLAB software. Afterwards FORTRAN code, solves the global matrix equations, calculates the displacement and stress values of elements. Using such information, low stressed or stiffness value elements according to stress or displacement based analysis are removed from the structure. The outputs are visualized using MATLAB software. The results are compared with existing solutions in literature for verifying the code and then novel, three dimensional optimized structures are obtained. Another study was conducted by Taşkınoğlu (2006) using genetic algorithm method. Genetic algorithm is the probabilistic optimization method, since the fittest has the highest probability to remain and produces offspring. The objective function is to obtain the lightest structure regarding the integrity of the structure. The genetic algorithm is processed using FORTRAN software. NASTRAN software is utilized for finite element solver as in my study. Some test problems are performed to practice the genetic algorithm and results are compared with the ones in literature. Chen (2008) also performs study genetic algorithm in shape topology optimization for well-known 2-D plane stress problems, flat plate with hole, cantilever beam and bracket. The outputs are compared with the existing results in literature.

Xie and Steven (1997) perform ESO method on two bar frame. The solution is evaluated in Chapter 3. The optimization is performed by choosing the, Initial Rejection Ratio (RR_0) and Evolutionary Rate (ER) both as 1%. As the rejection ratio increases more inefficient material is removed from the structure. After certain RR value, the gap between the minimum and maximum stresses is reduced and steady state is reached that is no elements are removed from the structure. When the maximum stress change is calculated, there is 33% increase in stress however; the total volume of the structure is reduced more than 90% of its initial volume. The stress increase is compensated with the great decrease in weight (Xie and Steven, 1997).

Liang *et al.* (1999) study on optimal selection of topologies for the minimum weight design of continuum structures subject to stress constraints using performance index (PI). The proposed performance index has been used in ESO procedure to monitor the optimization process and to identify the optimal topology of various structures with stress and height constraints. The magnitude of load has significant impact on final design but not on the optimal topology (Liang *et al.* 1999).

Ren *et al.* (2005) present a new approach that the excavation shape is optimized using ESO

method with stress constraint. Finding the optimal shape for an excavation based on stress distribution has practical significance in increasing stability and lowering support costs. (Ren *et al.* 2005).

For another illustration, Michell truss, least weight truss for the situation of vertical load acting in the middle of two fixed supports. The Michell solution is based on truss solution where members are connected with pin joints and all members are of uniform cross sectional area, however; the ESO is obtained as continuum model and the members can have different cross sectional areas. ESO suggest the structure to have larger cross sectional areas on the arches than the spokes. The volume has been reduced by 73%, while the maximum stress has only increased by 0.8% (Xie and Steven, 1997). Steven *et al.* (2000) summarize some of the ESO research of pin and rigid jointed frames with or without multiple load conditions.

Querin (1997) seeks to find the optimal shape of an object hanging in the air under its own weight. The top of the stalk is fixed. The only loading on object is its own weight due to gravity. RR_0 and ER are 0.05 %. After performing ESO method for shape optimization, the cherry or apple shape solutions are acquired. Similar results are achieved for different iterations. The initial design domain and ESO results are presented in Figure 2.7 (Xie and Steven, 1997).

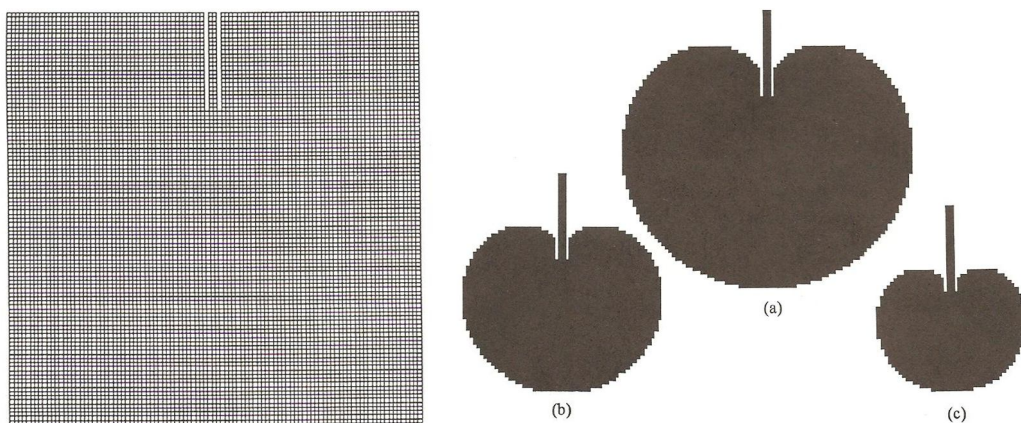


Figure 2.7 Initial design domain and ESO results for different iterations of an object hanging in the air with own weight (Xie and Steven, 1997).

Burry *et al.* (2005) work on optimization of Antoni Gaudi's Sagrada Familia church in Barcelona. Gaudi tries to obtain only compression designs for masonry buildings. The elements having highest level of tensile stress were removed iteratively to find the optimal

shape of masonry structure and resultant structure is planned to have predominantly compression stress. It is not possible to obtain a design purely in compression. The initial design domain is formed from the sketches of Passion Façade. The final geometry should carry the gravity load most efficiently under boundary supports. Gaudi uses optimal structural forms knowledge and lower column supports branching upper columns. This shape is simply a bone or shell, natural load carrier. Burry *et al.* (2005) reveals that the optimal shape for compression load capacity is two narrow necks at the bottom and the top. Figure 2.8 is the original drawing of Passion Façade and Figure 2.9 reveals that the ESO results are very similar to Gaudi's monument.

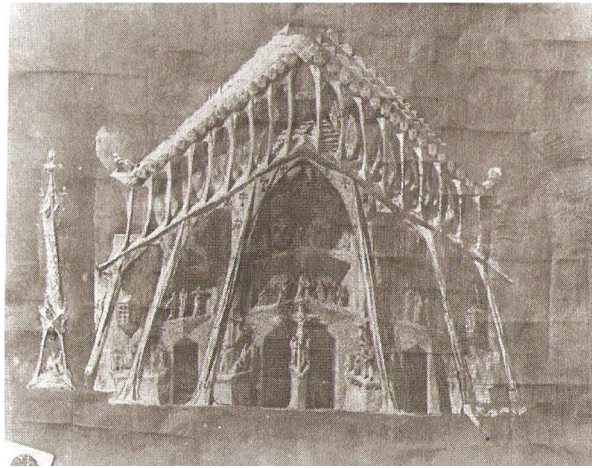


Figure 2.8 Photograph of Gaudi's original drawing for Passion Façade (Burry *et al.*, 2005).

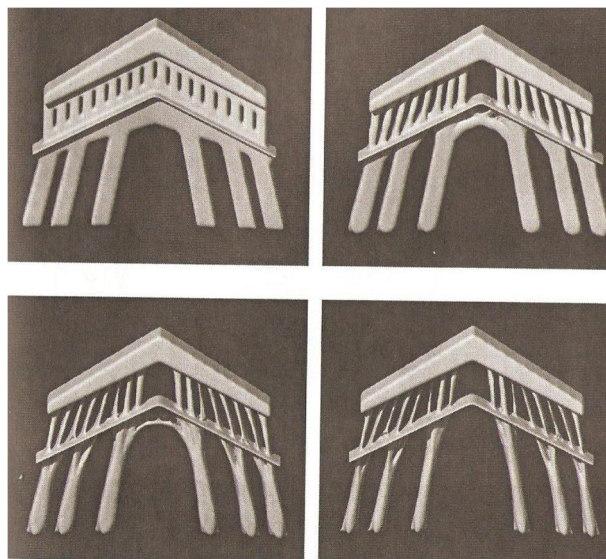


Figure 2.9 Evolution of Passion Façade (Burry *et al.*, 2005).

Ansola *et al.* (2006) proposed a new methodology for Evolutionary Structural Optimization for topological optimization of continuum structures subjected to self-load. Traditional calculation of the sensitivity number used in the ESO procedure does not lead to the optimum solution. Therefore, it is necessary to correct the computation of the element sensitivity numbers in order to achieve the optimum design. An original correction factor to compute the sensitivities and enhance the convergence of the algorithm is proposed. Some examples are illustrated to validate the approach for self-loading conditions.

Xie and Steven (1997) work on cantilever beam case, which the left hand side of the beam is fixed. The vertical displacement is measured as 0.33mm due to application of force on free end. As the prescribed limit for displacement is increased to 0.5, 0.75 and 1 mm, the volumes of the designs are decreased to 56.87%, 39.37% and 30.0% of the initial design respectively.

Guan *et al.* (2003) study on ESO method with stress and displacement constraint for different bridge types such as arched, tie-arched, cable stayed and suspension. Two performance index formulas are developed to determine the efficiency of the topology design. Cable supported bridges are optimized with frequency constraint incorporating the nibbling technique. The applicability, simplicity and effectiveness of ESO method are validated through its application in the optimum design of various types of bridges.

For the Michell type structure, Xie and Steven (1997) apply ESO method. The force is exerted on the free end and also a circular non-design domain exists. The displacement of the loaded point in vertical direction is 2.87 mm. The displacement limits is increased to 5, 7 and 9 mm, the volumes of the designs are decreased to 47.45%, 36.26% and 29.26% of the initial design respectively (Xie and Steven, 1997).

Kwak and Noh (2006) introduces a new method for determination of strut and tie models in reinforced concrete (RC) using ESO method. Conventional methods can hardly offer useful RC elements due to complicated loading conditions ESO method can find out the optimum topology using truss elements. Optimization criterion is based on minimizing the elastic strain energy of the structure. The method is advantageous that the procedure is less sensitive to the mesh size and requires less computer time and the method introduced more efficient designs.

The optimization of a support beam for a civil aircraft produced by Messerschmitt-Bölkow-Blohm has now become a classical problem in topology optimization (Zhou and Rozvany, 1991). A vertical load is applied on the middle and the maximum

deflection should not exceed 9.4 mm under specified load. Solution is performed by Xie and Steven (1997) the volume of ESO design equals to 50.33 % of initial design (Xie and Steven, 1997).

A square plate is simply supported on the four edges and loaded at the center by a point load. The initial out of plane displacement at the center is 1.16 mm. The limit of the displacement is 1.6 mm. The ESO solution achieved by Xie and Steven (1997) is similar to the solution of Atrek (1989), Tenek and Hagiwara (1994). Hinge lines are formed between the central part and four corners (Xie and Steven, 1997).

Xie and Steven (1997) perform ESO method for frequency optimization on a short beam that is clamped on both sides. At the first example, fundamental frequency of the beam is increased and at the second example, second frequency of the beam is increased. Both results are compared with the literature and the new designs of the short beam are very close to what Tenek and Hagiwara (1993) obtained using homogenization method. For another illustration Xie and Steven (1997) work on a plate fixed at two corners on its diagonal. Again the procedure is applied, maximizing a single frequency; the results are almost identical to Tenek and Hagiwara's (1993) results obtained by homogenization method. Using ESO method the first frequency is increased by 39.0% by removing the 50% of the initial volume. However when the single frequency is maximized, the other frequencies may drop which is undesired or at least should be delayed. Instead of maximizing the single frequency, multiple frequencies are to be maximized. Using ESO method the first three frequencies is increased by 35.5%, 19.1% and 29.3% respectively by removing the 50% of the initial volume. Xie and Steven (1997) study on a square plate that the three sides of the plate are clamped. The first object is to increase fundamental frequency, by removing 8% of the initial volume, 14.3% frequency increment is satisfied. The second object is to decrease fundamental frequency, removing 8% of the initial volume. 92.0% decrement is satisfied due to slim neck connecting the top and bottom parts, making the structure much more flexible. For the third study, the change of first frequency is kept in minimum, removing 8% of the initial volume, 6.7% frequency decrement is performed (Xie and Steven, 1997).

2.9. BI-DIRECTIONAL EVOLUTIONARY STRUCTURAL OPTIMIZATION

The Evolutionary Structural optimization (ESO) based on removing of inefficient material from a full sized domain whereas the Bi-directional Evolutionary Structural Optimization

(*BESO*) starts from an initial domain and progress the resultant structure by adding or subtracting the material simultaneously. One material can be removed impulsively at any iteration during ESO process; therefore permanent and irreversible hole can be produced. *BESO* method (Yang *et al.* 1999b; Querin *et al.* 2000; Liu *et al.* 2000) is introduced to debug the removed element. It is a SLP based approximate optimization method followed by the Simplex algorithm. More recently a new *BESO* algorithm has been introduced by Huang *et al.* (2006). When uniform mesh is considered, the variation of the main compliance can be calculated by equation (2.2), same formulation in ESO method, however if mesh is non-uniform, the effect of the element volume, V_i , should be considered. In such case the sensitivity number, α_i , is replaced by elemental strain energy density, α_i^e , in equation (2.3): (Huang and Xie, 2010)

$$\alpha_i^e = \frac{1}{2} \cdot [u_i]^T \cdot [K_i] \cdot [u_i] / V_i \quad (2.3)$$

According to Huang *et al.* (2007), the procedure is controlled by removal ratio of the volume (RRV), the ratio of variation of volume to the current volume. α_{th}^e , is the elemental threshold sensitivity number. In *BESO* algorithm, solid elements which satisfy the equation (2.4) are removed. On the other hand void elements which satisfy the equation (2.5) are added. The cycle of finite element analysis and element removal or addition is repeated until the objective weight (W^*) is achieved.

$$\alpha_i^e > \alpha_{th}^e \quad (2.4)$$

$$\alpha_i^e \leq \alpha_{th}^e \quad (2.5)$$

BESO can initiate from any initial design whereas ESO should start from full sized domain. The compliance values of the final shape are almost the same if different initial design are chosen, however computer time varies (Huang *et al.* 2007).

Huang *et al.* (2007) perform some illustrations to compare ESO and *BESO* methods. First example is Michell type structure which is fixed from both ends. Second a design domain, pressurized at the top is studied. Top surface is a non-design domain and 10% initial volume is selected. The third illustration is a car park, again the pressure is applied at the top surface and design and non-design domains are selected. All examples are run by same computer for different RRV values using ESO and *BESO* method. For small RRV values in ESO solution, almost the same compliance values are obtained. For ESO, small RRV is required, because ESO requires removing small amount of material at each iteration not to damage the integrity

therefore small number of RRV is preferred. In BESO technique high RRV values can be used however large RRV values can cause singularity problem. RRV value change creates great diversity for ESO solution on computer time; nevertheless, it has small effect on computer time on BESO technique. For BESO solution, it will be a better practice to choose the initial guess domain geometrically close to the final shape to save computer time. ESO solution is highly controlled with RRV value. Higher RRV value causes less iteration but more compliance. BESO method solutions depend on not only RRV, but also maximum allowable value for performance error, τ , and initial design. Total number of iterations in ESO method is much more compared with BESO technique. BESO method creates smoother topology that is easy to manufacture.

Michell type structure is studied by Yang *et al.* (1999b) for prescribed weight 30% and 50% for case 1 and case 2 respectively. The two cases are solved using ESO and BESO methods. Case 1 requires more computer time than case 2 to remove more unit. ESO method needs more computer time and iterations than BESO method for the two cases. BESO is more efficient than ESO, when the optimum topology covers only small area compared with full domain.

Huang and Xie (2009) utilize the material interpolation scheme, BESO method with penalization parameter arises. The results show that the optimal designs from the present BESO method are independent on the degree of penalization. Numerical examples show the resulted topologies are similar to those obtained by SIMP and continuation methods. The value of the objective function is much lower than that of SIMP method and very close to that of the continuation method (Huang and Xie, 2009).

Yang *et al.* (2005) investigate the ESO and BESO methods in solving the topology optimization of continuum structures with a constraint on the global stiffness. They focus on problems considering design dependent loads, self-weight and surface loads. BESO can be computationally more efficient than ESO for a large FE problem, and it has the flexibility to balance the computing time and solution quality (Yang *et al.* 2005).

Rong *et al.* (2007) introduces a new methodology, topology optimization method mixed with continuum and discrete elements. By the help of finite element analysis, stress sensitivity numbers are obtained. Based on the BESO method, an optimality criterion considering element stress levels, relative difference quotients has been established and then a modified BESO procedure has been proposed and implemented. The example results reveal that proposed method is valid and efficient (Rong *et al.* 2007).

2.10. GENETIC ALGORITHMS

Genetic algorithms (*GA*) are derived technique from biology and rely on the principle of Darwin's theory of survival of the fittest. When a population of biological creatures is allowed to evolve over generations, individual characteristics that are useful for survival tend to be passed on the future generations, because individuals carrying them get more chances to breed. Those individual characteristics in biological populations are stored in chromosomal strings. The mechanics of natural genetics is based on operations that result in structured yet randomized exchange of genetic information between chromosomal strings of reproducing parents and consists of reproduction, crossover and mutation of the chromosomal strings (Haftka and Gürdal, 1992). *GA*'s are in the category of the stochastic search methods. In the methods, a set of alternative points, called the population, at iteration, called generation, is used to generate a new set of points. Combinations of the most desirable characteristics of current members of the population are used which results in points better than the current ones. Average fitness of successive set of points improves giving better values for the fitness function. Fitness is cost function or penalty function for constrained problems. The fitness value is calculated for each member of the population. An advantage of this approach is that the derivatives of the functions are not needed (Arora, 2007).

GA's work with a population of strings, chromosomes. This aspect of the *GA*'s are responsible for capturing near global solutions, by keeping many solution points that may have the potential of being close to the local or global minima, in the pool during search process rather than choosing a point early in the process and running the risk of getting stuck at local minimum (Haftka and Gürdal, 1992). *GA*'s are very useful for problems with discontinuous cost and constraint functions because the gradients of the functions are not needed for finding approximate optimal solutions (Goldberg 1989).

The quality of the individual in a *GA*, is often based upon the objective fitness of the individual, which is evaluated using the value of the objective functions as well as satisfaction of the constraints. The object fitness of the individual is scaled using penalties that are function of the degree to which the constraints are violated. The phenotypic or genotypic representation of the individuals within a genetic algorithm is most often a chromosome of binary digits. In keeping with biologic analog, each binary digit can be thought of as a gene. Individuals need not be represented in the form of binary string chromosomes. In fact, binary string single chromosomes can make search difficult because neighboring solutions can have very significant differences in their binary string representations. Obtaining high precision

solutions can also result in very long binary strings. Long binary strings also imply larger population sizes (Foley, 2007).

2.10.1. SELECTION

The primary goal of the selection is to find those chromosomes, that are good and those that are not so good within the population. The algorithm is expected to create the additional copies of good solutions and allow the “not so good” solutions to simply vanish. More highly fit strings receive higher number of offspring. The challenge in developing selection mechanism or selection operators for evolutionary algorithms is to facilitate exploration, while maintaining exploitation for good solutions. Various selection mechanisms have been developed to meet this challenge. There are many different selection schemes such as the tournament selection or rank based selection. The roulette wheel is the easiest system to implement. In other words, the slice of the wheel for an individual with better objective fitness will be larger than a lower quality individual. Therefore, the probability of the better individual being chosen for the mating pool is higher. If individuals within the population begin to have objective fitness magnitudes that greatly overshadow others, their slice of the roulette wheel can become exceedingly large to the point where certain individuals take over the subsequent population. Scaling objective fitness is one way to inhibit or slow take over by dominant individuals (Foley, 2007).

2.10.2. CROSSOVER

Crossover is a process by which two candidate solutions to the optimization problem are combined to create one or more new potential solutions. Crossover can also be named as recombination. These new solutions contain aspects of both parent solutions and assuming the parents has “high quality” genetic material, the offspring which solutions selected to form new solutions. It takes two chromosomes and swaps part of their genetic information to produce new chromosomes. This operation is similar to sexual reproduction in nature. Crossover operator is used to exchange the characteristics of the chosen members of the population. There are several types of crossovers that include single crossover also known as one-point crossover, two-point crossover, and uniform crossover among others. The selection mechanism carries out the task of identifying solutions to become members of mating pool (Foley, 2007).

Single point crossover begins with the identification of the parent strings. A point along the string is chosen and the segment of the parent chromosome to the right or left of the crossover point is exchanged to create new candidate designs (Foley, 2007).

The second crossover mechanism is multipoint crossover. The two crossing sites are chosen at random and the center segment of the parent chromosomes are exchanged. This crossover operator has a higher probability of creating offspring that do not have common genes with the parent strings. As the design variable numbers increase, more than two crossing sites may be required to carry out crossover that adequately searches the design space. Uniform crossover is the final mechanism commonly used. This crossover operator is added by simply moving bit-by-bit along the chromosomes and flipping a two sided coin. If the toss results in heads, the bits are exchanged. It should be noted that there is no guarantee that the crossover mechanism employed will result in a better candidate solution (Foley, 2007).

2.10.3. MUTATION

Mutation is the process by which an individual in the offspring population is selected at random and is mutated through exchanging bits in the individual chromosomes. Mutation seeks to generate diversity in the population and therefore, explore the design space. By generating diversity, mutation helps the genetic algorithm avoid being trapped in local minimums in objective space (Foley, 2007). According to Haftka and Gürdal (1992), it is possible to have population with multiple copies of the same string. In the worst scenario, it is possible to have the entire pool to be made of same string. Mutation prevents this uniformity. As a result, mutation is sometimes thought of as a global search mechanism, while crossover is sometimes thought to be a local search mechanism. Mutation can create better or worse solutions. There is no guarantee to improve the candidate with mutation (Foley, 2007).

Because crossover and mutation can result in candidate solutions that are worse than the best solution resident in the mating pool, genetic algorithms often maintain the best solution from a previous population through a mechanism called elitism. Elitism takes the best solutions from one generation and simply carries them over the next generation (Foley, 2007).

The convergence criteria can be defined as limiting the maximum number of generation. When the number of generations reaches to a predefined value then the optimization process terminated. Another common criterion is based on the percentage of identical solutions in the population. If the percentage of identical solutions are higher or equal to the predefined percentage value then the optimization process is terminated. A criterion based on no

improvement tolerance can also be used in GA's. This criterion checks for the number of generations with no improvement in the best solution obtained and it terminates the optimization process based on the predefined tolerance (Taşkınoğlu, 2006).

Genetic algorithm is first applied by Holland (1975), and the concept is said to be derived from Rechenberg (1965). After 1990's genetic algorithm has been widely used for structural optimization problems (Jenkins 1991; Hajela and Lin 1992; Rajeev and Krishnamoorthy 1997; Hayalioglu 2000; Antonio 2002). Genetic algorithm is applied to truss topology optimization problems by Jenkins (1991) and Ohsaki (1995). Grierson and Pak (1993) apply GA to truss optimization problems where the topology and cross sectional properties are encoded using binary strings. Lemonge *et al.* (2009) optimize shape and cross sectional areas of latticed domes using a genetic algorithm with constraints on the number of different cross-sections to reduce construction cost (Ohsaki 2011).

GA is also widely used for optimization of lamina composites. Hajela and Lin (1991) optimize the stacking sequence of a composite beam with dampers. Marcelin *et al.* (1995) developed a multiobjective GA for design of composite beams. Kogiso *et al.* (1994) present a binary tree approach for checking duplicate solutions as well as an operator for local improvement of composite laminates. Kameshki and Saka (2001) and, Hayalioglu and Degertekin (2005) use genetic algorithms for optimizing frames with semi-rigid connections, where the types of connections are fixed. In contrast, Kameshki and Saka (2003) also optimize the types of the semi-rigid connections. Kocer and Arora (1999) compare the performances of GA and simulated annealing for optimization of transmission towers. Yun and Kim (2005) reveal that GA is very useful for design under constraints on inelastic responses, for which the sensitivity coefficients of responses are difficult to obtain (Ohsaki 2011).

CHAPTER 3

PROGRAM FOR EVOLUTIONARY STRUCTURAL OPTIMIZATION AND VALIDATION

3.1. EVOLUTIONARY STRUCTURAL OPTIMIZATION

The Evolutionary Structural Optimization (ESO) method for stress based formulations is performed to obtain the resultant structure. Nature progresses with the principle, “*rarely used elements vanish, whereas frequent used elements develop.*” Nature removes the unnecessary objects throughout the world existence. Bones are optimized such that unnecessary portions are removed, besides the topology does not permit to form stress concentration regions. Bones are also broken not to carry excess load to the neighbor structure. ESO method works with the same principle of nature. From a bulk structure, the unstressed elements are removed subsequently to acquire the optimal shape. Finite element method occupies great role on solution method. The stress level in any part of a structure can be determined by conducting a finite element analysis. Bulk structure is decomposed into well-known small elements to calculate von Mises stress value. Von Mises stress can be used to control the stress based removal.

A reliable indicator of inefficient use of material is the low values of stress in some parts of the structure. Ideally the stress in every part of the structure should be close to the same, safe level. The low stressed material is assumed to be under-utilized and is therefore removed subsequently. The removal of material can be conveniently undertaken by deleting elements from the finite element model. The stress level of each element is determined and if the von Mises stress level of element, σ_e^{vm} , is below the current rejection ratio, (RR_i) , when compared with the maximum von Mises stress level of the whole element, σ_{max}^{vm} , the element is deleted (Huang and Xie, 2010):

$$\sigma_e^{vm} / \sigma_{max}^{vm} < RR_i \quad (3.1)$$

Cycle of finite element and element removal is repeated until the steady state is reached. At this stage, evolutionary rate, ER , is added to the rejection ratio (Huang and Xie, 2010):

$$RR_{i+1} = RR_i + ER \quad (3.2)$$

Else the optimization process can be performed up to the certain limit for rejection ratio. The result may not give out the best result however the final shape may give a clue about improved solutions for shape and topology. Two parameters, Evolutionary Rate, ER , and Initial Rejection Ratio, RR_0 , are need to be described. Usually RR_0 & $ER = 1\%$ values are selected; however for some special cases much lower values should be used. After making some trials on new model, suitable values can be estimated (Xie and Steven, 1997).

The evolutionary procedure for stress optimization can be summarized as follows (Huang and Xie, 2010);

- I. Discretize the structure using a fine mesh of finite elements.
- II. Carry out finite element analysis for the structure.
- III. Remove element which have stress levels below the certain limit.
- IV. Increase rejection ratio.
- V. Repeat step II to IV until desired optimum is obtained.

Apart from rejection ratio, volumetric removal can be used for convergence criterion. Certain percentage of elements are removed for each iteration such as 2% and optimized result can be obtained after the removal of 50% of the initial element number.

3.2. PROGRAM ALGORITHM

The program code is written using MICROSOFT VISUAL BASIC software. MSC. PATRAN has modules for different optimization algorithms, however; instead of purchasing module of MSC. PATRAN, using interface code in MICROSOFT VISUAL BASIC, same task can be performed with open source data presented in Appendix A. Besides additional lines can be added to code to personalize according to the requirements.

The bulk structure is created, loading and boundary conditions are defined using MSC.PATRAN. FEM is built using three dimensional solid isometric hexahedron or tetrahedron elements. Design (where elements that do not carry necessary load may be removed) and non-design (none of the elements may be removed) domains are selected. MSC.PATRAN software creates “bdf” file that contains all information about elements,

connectivity, nodes and locations, constraints and degree of freedom of the support nodes, magnitude and direction of forces. MSC.NASTRAN reads the “bdf” file, performs finite element solution and creates “f06” file that includes, nodal and central von Mises stresses and mean pressure values, displacement vectors of the nodes, grid point force balance and singularity tables. The elements are gathered and arranged in ascending order with the assistance of MICROSOFT VISUAL BASIC code. The elements which are below the stress limit are identified and element number row is not copied to new “bdf” file (i.e. that element is deleted from the model). After using MSC.NASTRAN, new “f06” file is formed and this cycle continues until the prescribed final rejection ratio is reached where the program is terminated. Meanwhile, significant information such as, time, stress and element numbers are recorded. The Microsoft Visual Basic code is presented in Appendix A. The interaction of MICROSOFT VISUAL BASIC with MSC.NASTRAN, MSC.PATRAN and CATIA, and, the flowchart of the code developed are summarized in Figures 3.1 and 3.2 respectively;

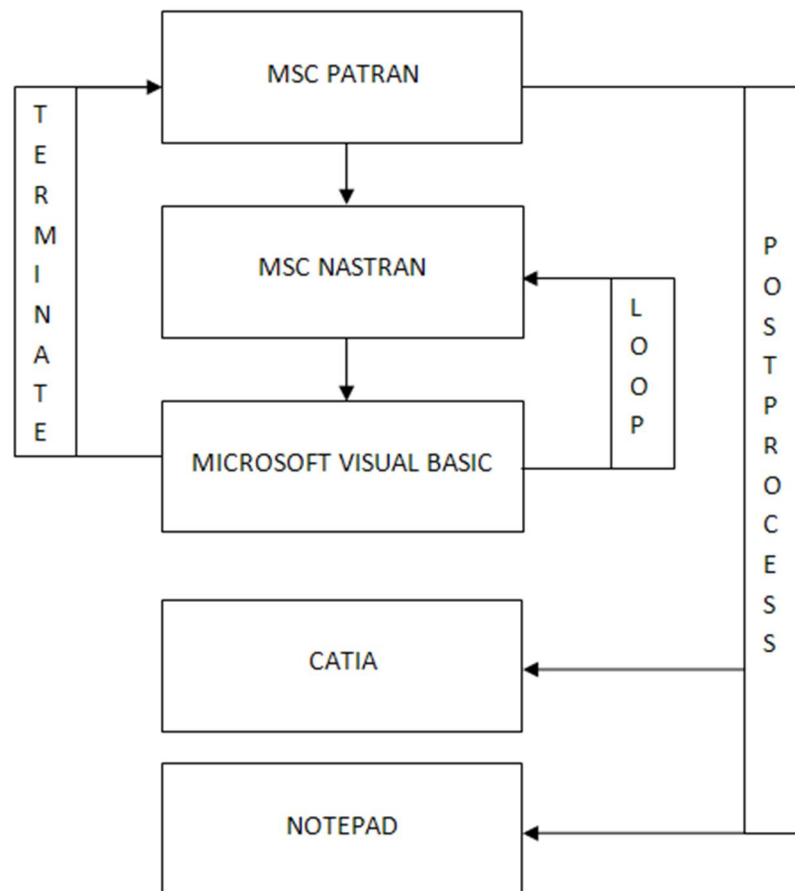


Figure 3.1 Flow chart of the program interactions.

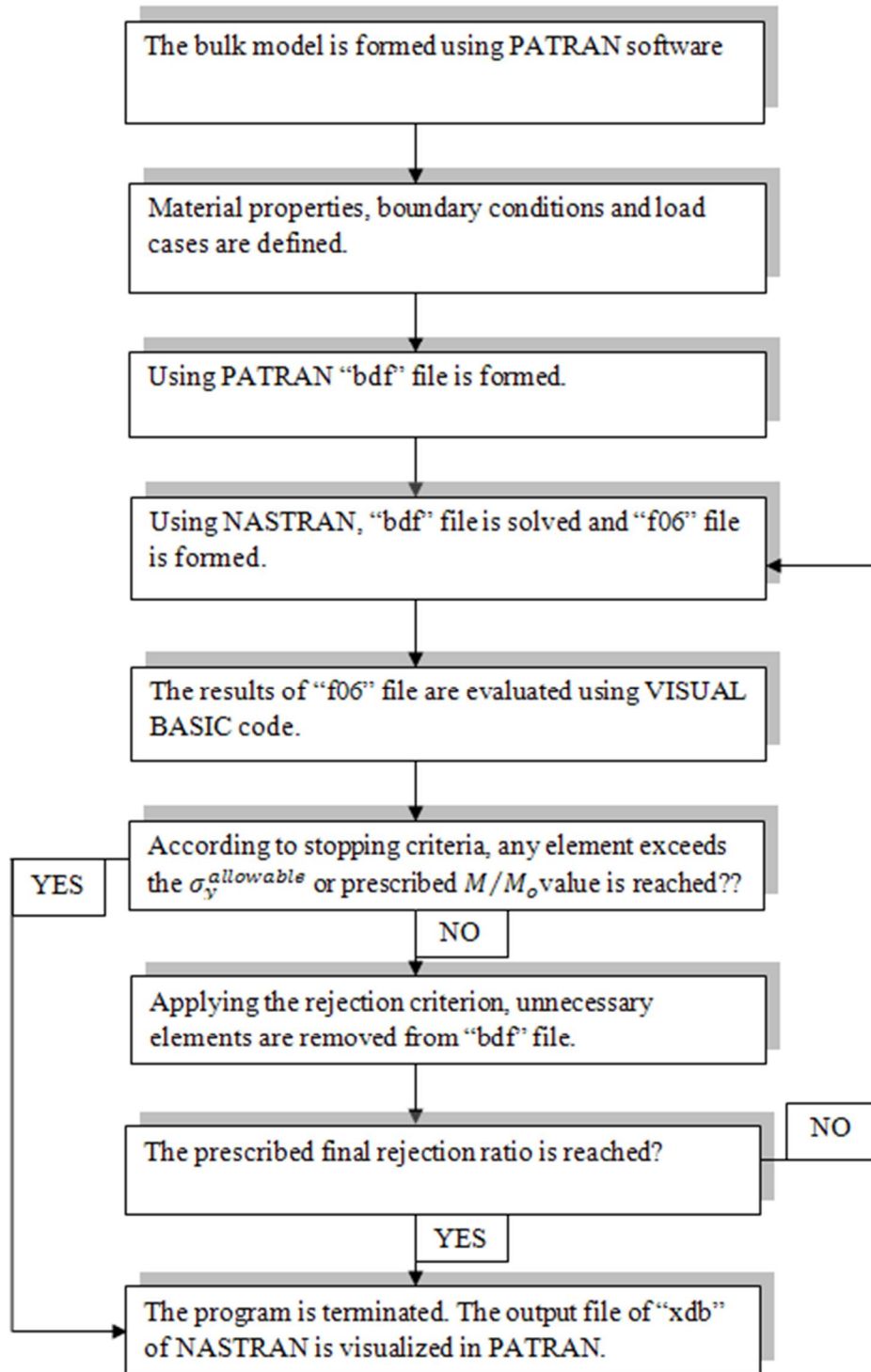


Figure 3.2 General flow chart of the program.

3.2.1. BUILDING THE “BDF” FILE

At first step bulk geometry is constructed using points and lines. This geometry should include the entire design domain to evaluate all the elements. Then FEM model should be constructed using mesh command. In program either isometric hexahedron or tetrahedron solid mesh can be selected. After the definition of global edge length, suitable mesh formation is completed. At Load/BCs section, the magnitude and direction of forces or pressure is specified and support location and degree of freedom is selected. The force and support information can be defined for only nodes; therefore suitable nodes should be identified. The code is programmed as to work both in single and multiple load case. For multiple load case, the code requires to build a “bdf” file showing all the load cases in one file. Special code “*param, bailout, -1*” is added to avoid to terminate of the program by ill condition case. The code assigns the stress value as zero to elements which are detached from the bulk structure; therefore, these elements are immediately removed at the next iteration as the stress value is set as zero.

Material section is chosen at the next step. The material is treated as isotropic, linear elastic and material properties such as Poisson’s ratio (ν) and elastic modulus (E) are expressed. The whole structure is homogenous and isotropic, however to define some elements as non-design domain, second group of material is created and grouped. Design and non-design domains are separated at properties section. First property belongs to design domain elements and second property is for non-design domain. The code is regulated as the elements on the second property are stationary and should not be removed. To illustrate, critical region elements, support or load application node elements are non-design domain.

3.2.2. “F06” CREATION AND INTERFACE CODE

MSC.NASTRAN is used as solver which calculates the von Mises stress, mean pressure and displacement values and forms “f06” file after forming “bdf” file in MSC.PATRAN. The interface code, using MICROSOFT VISUAL BASIC software, performs the algorithm of ESO method. For single load case, some input values are required such as initial rejection ratio, evolutionary rate and final rejection ratio. Besides, multiple load case requires the number of load cases as an input. Additionally, the maximum allowable stress of the material is demanded. The elements which exceed the maximum allowable stress are noted to log file to inform the user. At first step, the code reads the von Mises stress of the central elements and sort the values in ascending order. The von Mises stress value of each element is divided by the

maximum von Mises stress value of the whole structure for the formulation of ESO method. The elements having stress ratio smaller than the rejection ratio are specified and these elements which do not belong to non-design domain, are removed from “bdf” file. The non-design domain elements are kept regardless of von Mises stress value. Therefore, new “bdf” file is formed at the end of each iteration. New “bdf” file is solved by MSC.NASTRAN at the next iteration and new “f06” file is created. All “f06” and “bdf” files are kept by changing files name for further investigations. However, for large number of elements in multiple cases, the “f06” files can reach up to 1 gigabyte, therefore not to create storage problems “f06” files can be deleted if desired by activating single command line. At this point, rejection ratio is increased by evolutionary rate, which is defined as input. The maximum stress value of the structure tends to increase without considering local decreases due to nature of the structure. As the rejection ratio ascends, the stress limit between “unnecessary” and “necessary” of elements are increased. Log file generated may be viewed using NOTEPAD to follow the evaluation of the structure, pop ups after the program termination. Log file specifies program initiation time, iteration number, the number of elements removed, the removed elements and stress values, the elements number, stress values and load case exceeding the yield strength of the specified material for each iteration, maximum stressed element and stress value at each load case, current removal ratio, the number of remaining elements, iteration and program termination time.

3.2.3. REJECTION AND STOPPING CRITERION

The optimization process works in iterative manner and should be terminated after removing a certain amount of element. The most frequent solution is using rejection ratio and increase the value with evolutionary rate, until a specified number is reached. In program, initial and final rejection ratio and evolutionary rate are demanded as inputs. The stress values of elements at each load cases are calculated and enumerated for multiple load case problems, the elements are removed if and only if the element is below the rejection ratio for all load cases. Volumetric removal can be applied for single load case for an alternative solution. This method removes certain percentage of material having smallest stress values for each iteration, until total element removal reaches to a certain amount.

The program is terminated before reaching the final rejection ratio if the stress value of an element exceeds the allowable stress limit for any load case. As an alternative method, the program can be terminated if the desired ratio of elements is removed compared with initial model. The flowchart of the rejection and stopping criterion is illustrated in Figure 3.3.

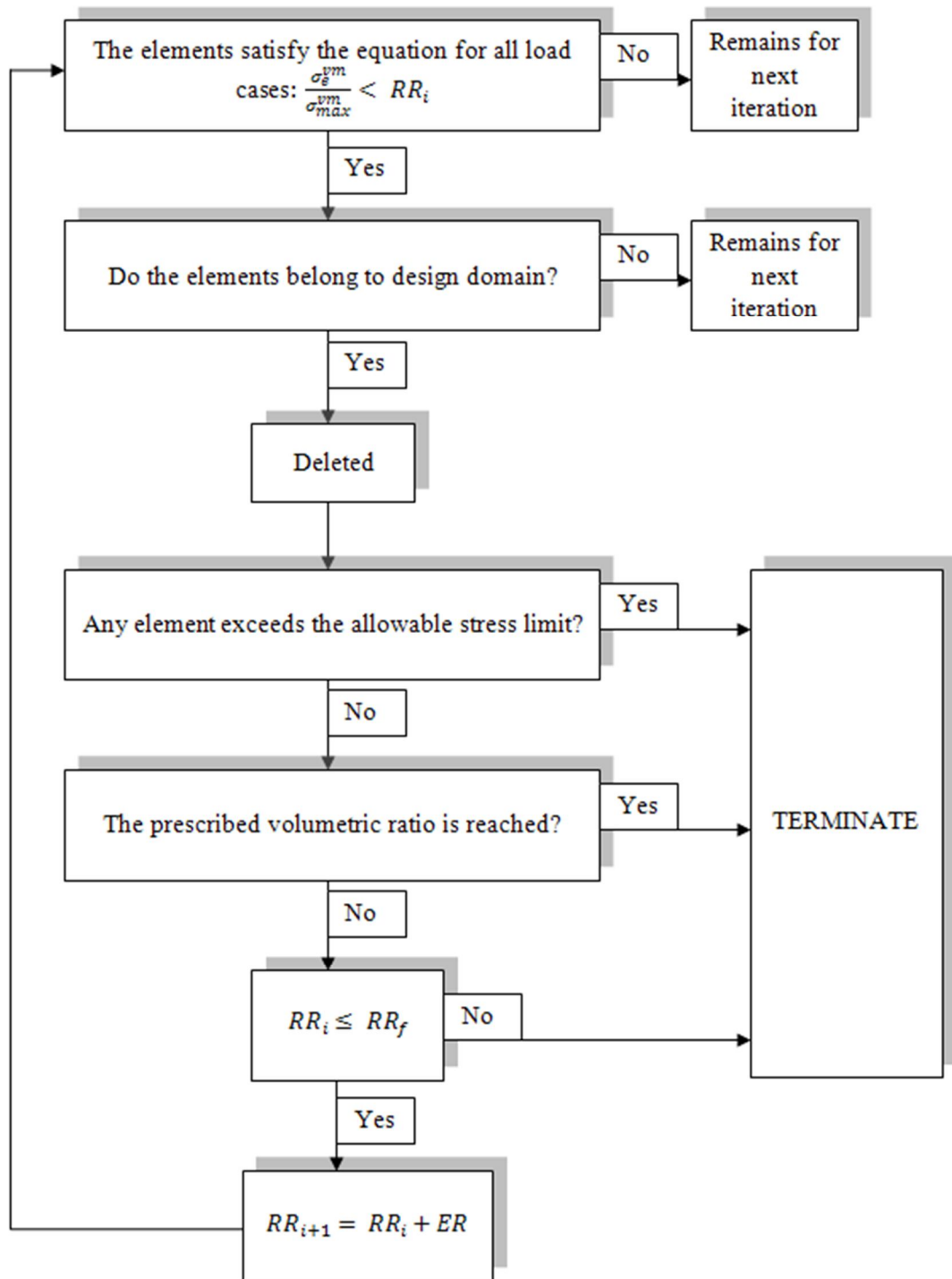


Figure 3.3 Rejection and stopping criterion of the program.

3.2.4. POST PROCESSING

After achieving the optimum solution, the result is monitored using MSC.PATRAN. The “bdf” file is opened; afterwards the “xdb” file that includes von Mises stress value is attached

to the geometry. The stress results of optimum structure of each element can be visualized by color palette in results section in MSC.PATRAN. The highly stressed regions are evaluated. The resultant geometry is transferred to the CATIA V5 R19, CAD software to compare the optimum structure with the existing aircraft design. Certain modifications and comments should be conducted by comparing the two structures.

3.2.5. PROGRAM MANUAL

Program running performance and stability depends on how the program is run and the conditions have great impact on the working principle of the code. There are some regulations that should be verified to acquire the exact solution. These rules can be summarized as follows;

- The folder that includes program should be on the root of directory of drive C or D. It is highly recommended to create the folder at directory where MSC.NASTRAN software exists, because of the continuous data transfer of code with software. Also folder name should contain only alphabetic and numerical characters. Space character in folder directory would create running problems in MSC.
- “bdf” file should be named as “loop.bdf”. The program creates “loop.f06” file as MSC.NASTRAN output file firstly. Then, for every iteration, the “bdf” and “f06” files are kept with iteration number such as “loop1.bdf” and “loop1.f06” for traceability. MSC.NASTRAN software also creates a log file “loop.log”, “f04” file “loop.f04” and “loop.xdb”. “xdb” files contain various information about loads and supports which can be monitored using MSC.PATRAN software. “xdb” files are essential, especially when the “f06” files cannot be explored or even opened due to occupying great storage area. “bdf” files monitor geometry using MSC.PATRAN software.
- After locating four files, “Form1.frm”, “Project1.vbp”, “Project1.vbw” and “loop.bdf” file, the program is run and menu appears. On the menu, according to the optimization problem, single or multiple load case is selected. Single load case requires four inputs, initial rejection ratio, evolutionary rate, final rejection ratio, maximum allowable stress (in MPa unit) and desired M/M_o where multiple case

demands one more which is the number of load cases as indicated on Figure 3.4 and Figure 3.5 respectively.

The screenshot shows a window titled "Form1" with a blue title bar. At the top, there are two radio buttons: "Single" (which is selected) and "Multiple". Below this, there are five input fields, each followed by a percentage sign (%):
1. "INITIAL REJECTION RATIO (RRi)"
2. "Evolutionary Rate (ER)"
3. "FINAL REJECTION RATIO (RRf)"
4. "ENTER THE YIELD STRENGTH"
5. "Enter desired M/Mo" (with a red note below it: "Write 0 not to apply M/Mo")
At the bottom center, there is a "Run" button.

Figure 3.4 Program interface for single load case input.

The screenshot shows a window titled "Form1" with a blue title bar. At the top, there are two radio buttons: "Single" and "Multiple" (which is selected). Below this, there are six input fields, each followed by a percentage sign (%):
1. "INITIAL REJECTION RATIO (RRi)"
2. "Evolutionary Rate (ER)"
3. "FINAL REJECTION RATIO (RRf)"
4. "ENTER THE YIELD STRENGTH"
5. "Enter desired M/Mo" (with a red note below it: "Write 0 not to apply M/Mo")
6. "Enter the number of load cases"
At the bottom center, there is a "Run" button.

Figure 3.5 Program interface for multiple load case input.

- MICROSOFT VISUAL BASIC software accepts comma, instead of dot in decimal representation. Dot in decimal is neglected by MICROSOFT VISUAL BASIC software.
- Maximum stress in each load case, current removal ratio, elements having stress higher than yield strength and stress values, number of elements removed and remaining elements and computer time are processed to log file to acquire more information for removal elements from the structure. Text file can be utilized to obtain detailed information about each iteration named as “logfile.txt”. Also by editing the inactive codes, more information such as elements and stress order can be achieved. User can have an idea of steady state by revealing the overstressed material.

3.3. PROGRAM VALIDATION

Subsequent to the code generation, the code outputs should be validated and debugged using the well-known examples in the literature. Two bar frame, Michell type structures, bridge with moving load, beam exposed to pure torsion are the most frequent and convincing stress based examples. The equivalent inputs such as Initial Rejection Ratio (RR_o) and Evolutionary Rate (ER) are employed. The output of the code and figures in the reference are compared and the similarities and deviations from results are discussed.

3.3.1. TWO BAR FRAME

A well-known structural optimization problem is two bar frame subjected to a single load F applied on a certain horizontal length $L = 10\text{ m}$. For definite F and L values, optimal length can be found as $2L$ with analytical solution. A rectangular design domain, slightly greater size in vertical length, is defined to cover the final design to prove this fact. The design domain is supported from left side and shear load 1000 N is applied center of the right side of the domain as indicated in Figure 3.6. Design domain is discretized into $25 \times 60 \times 1$, 1500 elements. Solid cubic element, with dimensions 0.4 m while material properties are $E=100\text{GPa}$ and $\nu=0.3$ are utilized (Huang and Xie, 2010).

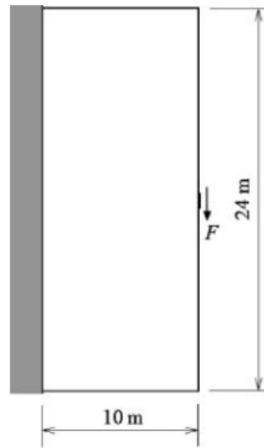


Figure 3.6 Design domain of the two bar frame (Huang and Xie 2010).

The code is initiated with $RR_o = 1\%$ and ER is set as 1% . The results adopted from literature and code outputs are compared for different RR values such as 3% , 6% , 9% , 12% , 15% , 18% , 21% , 24% and 30% from Figure 3.7 to 3.15 respectively, which show the different stages of evolutionary history. Black areas represent the remaining elements where, the small dots demonstrate the initial finite element analysis model. As the rejection ratio increases, more inefficient elements are removed, and the final product reveals with expected geometry in analytical solution.

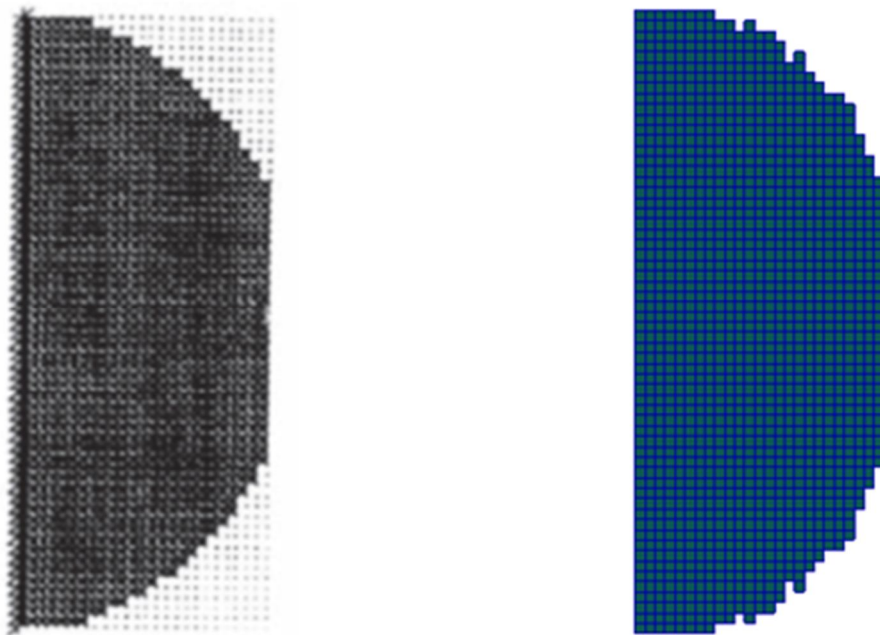


Figure 3.7 Result of two bar for $RR=3\%$ (Huang and Xie 2010) and optimized structure.

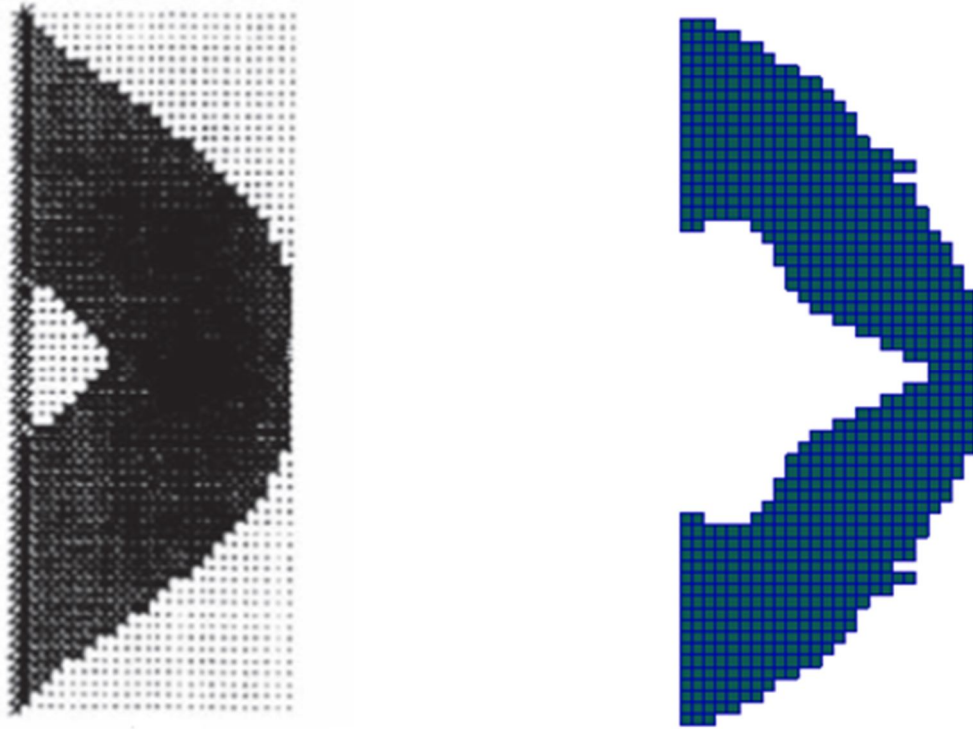


Figure 3.8 Result of two bar for $RR=6\%$ (Huang and Xie 2010) and optimized structure.

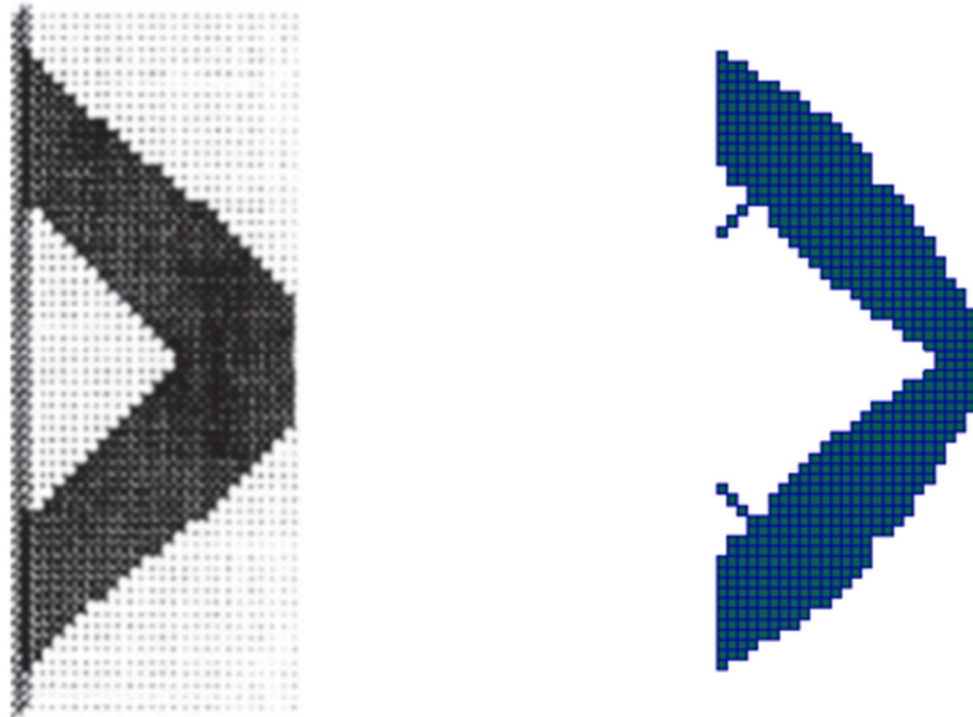


Figure 3.9 Result of two bar for $RR=9\%$ (Huang and Xie 2010) and optimized structure.

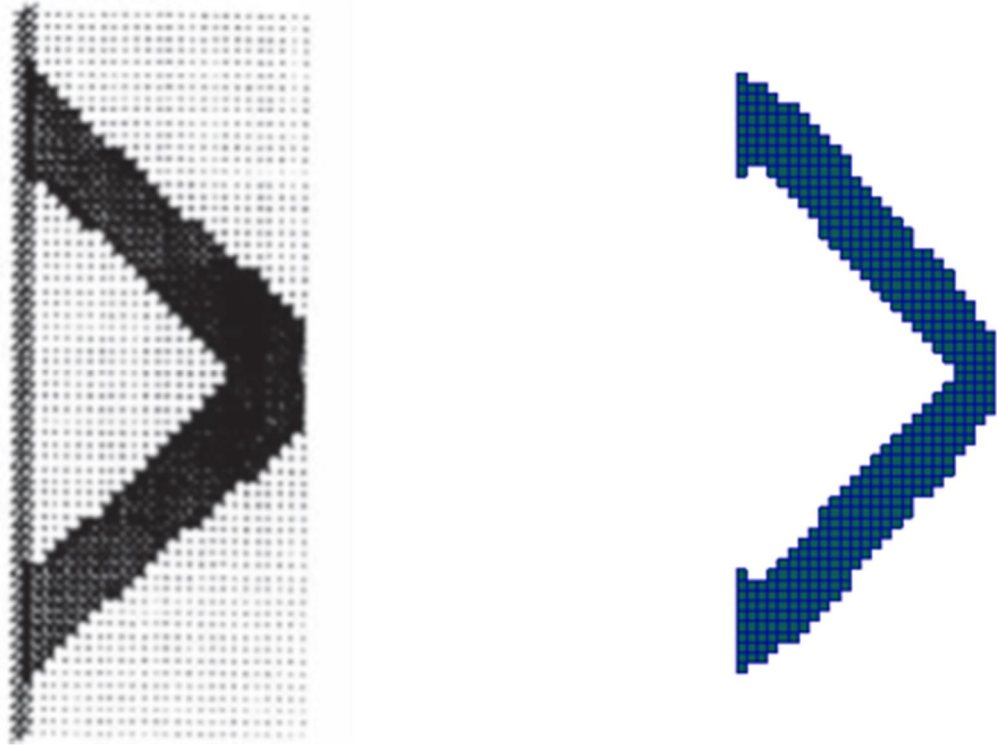


Figure 3.10 Result of two bar for $RR=12\%$ (Huang and Xie 2010) and optimized structure.

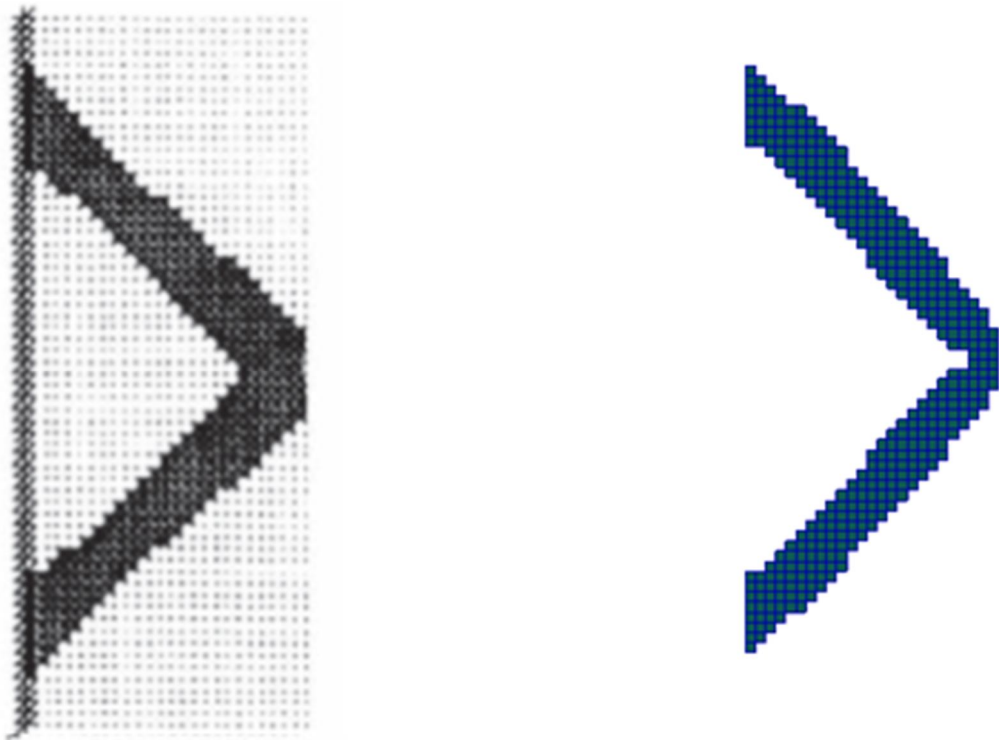


Figure 3.11 Result of two bar for $RR=15\%$ (Huang and Xie 2010) and optimized structure.

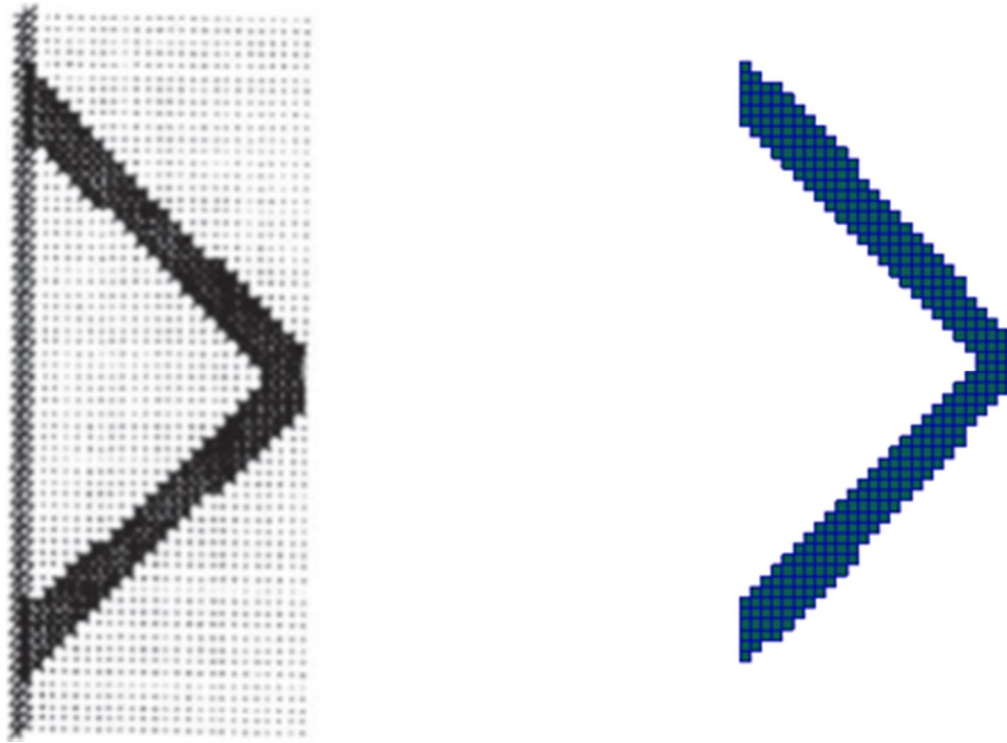


Figure 3.12 Result of two bar for $RR=18\%$ (Huang and Xie 2010) and optimized structure.

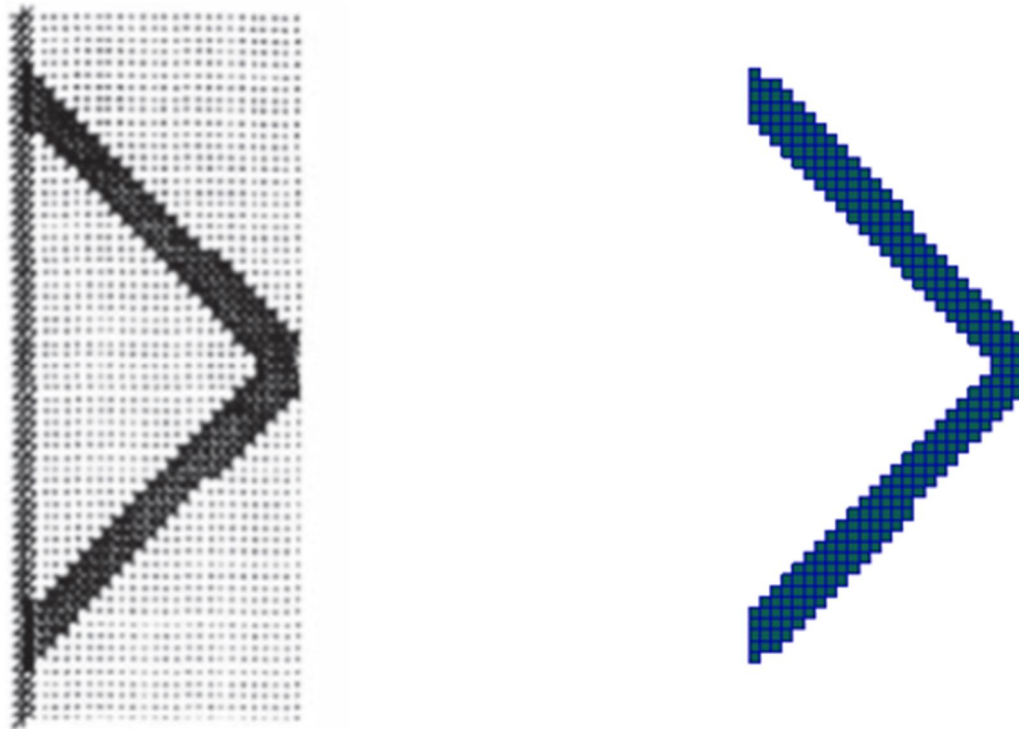


Figure 3.13 Result of two bar for $RR=21\%$ (Huang and Xie 2010) and optimized structure.

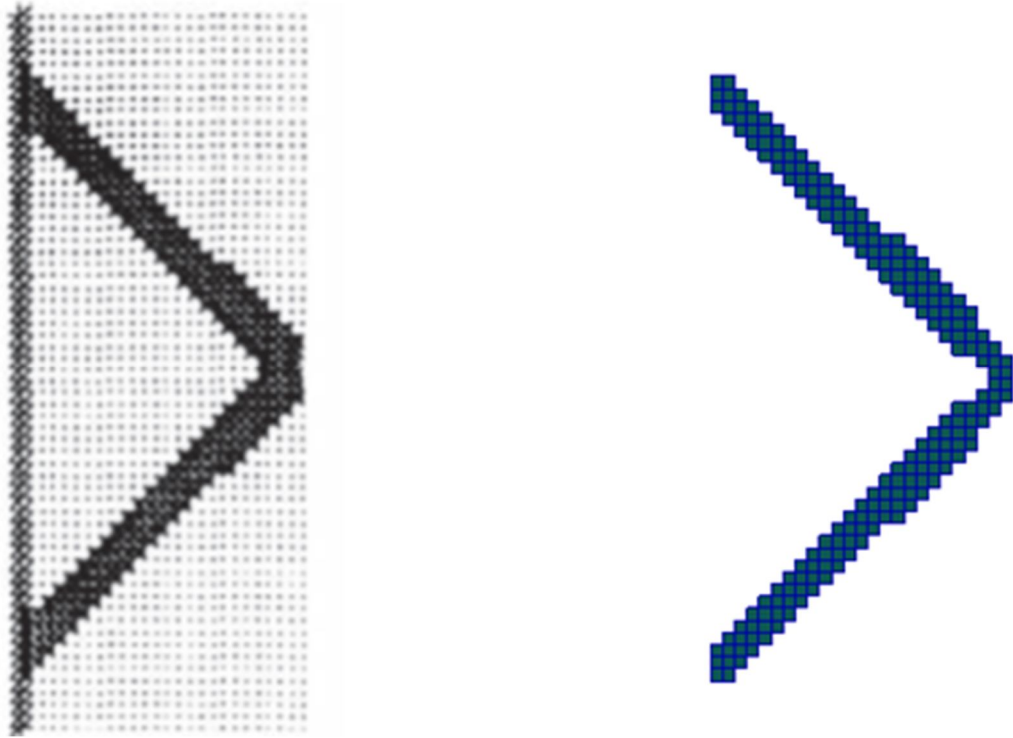


Figure 3.14 Result of two bar for $RR=24\%$ (Huang and Xie 2010) and optimized structure.

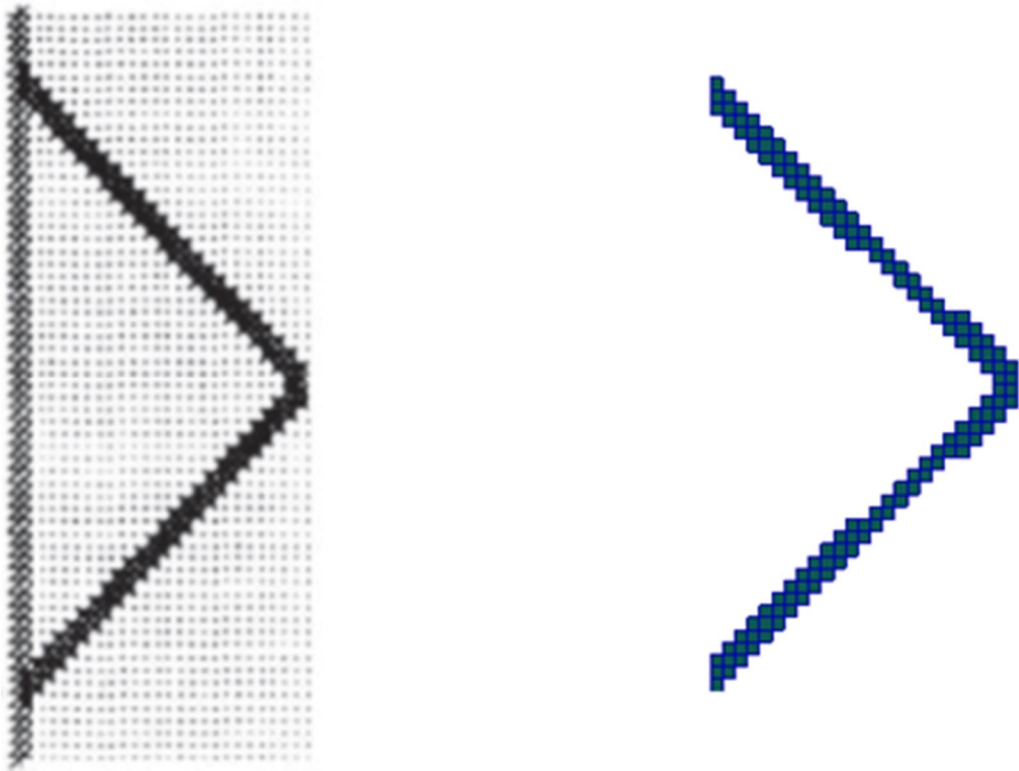


Figure 3.15 Result of two bar for $RR=30\%$ (Huang and Xie 2010) and optimized structure.

The time versus iteration number in Figure 3.16 reveals that as the number of remaining elements decreases, iteration time reduces. Because of reducing number of elements the number of computations decreases.

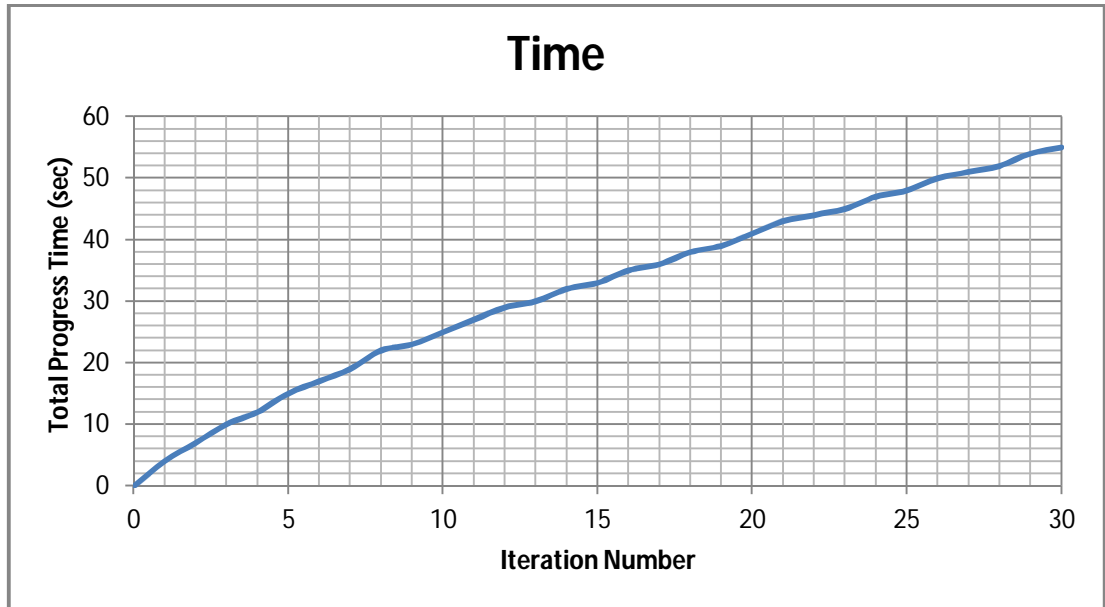


Figure 3.16 Total progress time vs. iteration numbers for two bar frame optimized structure.

The volume ratio versus iteration number in Figure 3.17 shows that the volume reduction increases at various iterations. The maximum von Mises stress value is plotted in Figure 3.18. It is not surprising that maximum von Mises stress level of the structure has sharp increase during large scale element removals such as at 5th and 15th iteration. On the other hand, maximum von Mises stress increases drastically at 23th and 24th iterations, whereas the element removal is not huge. As the iteration number increases, small number of element removal may lead to rapid increase in stress level.

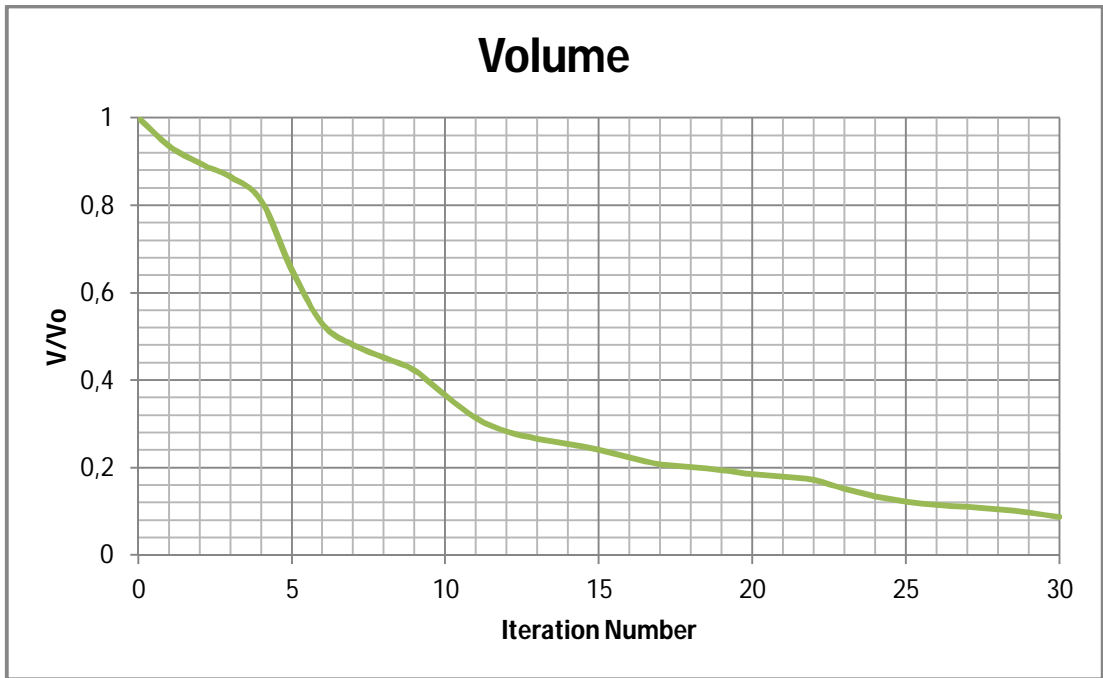


Figure 3.17 Volume reduction vs. iteration numbers for two bar frame optimized structure.

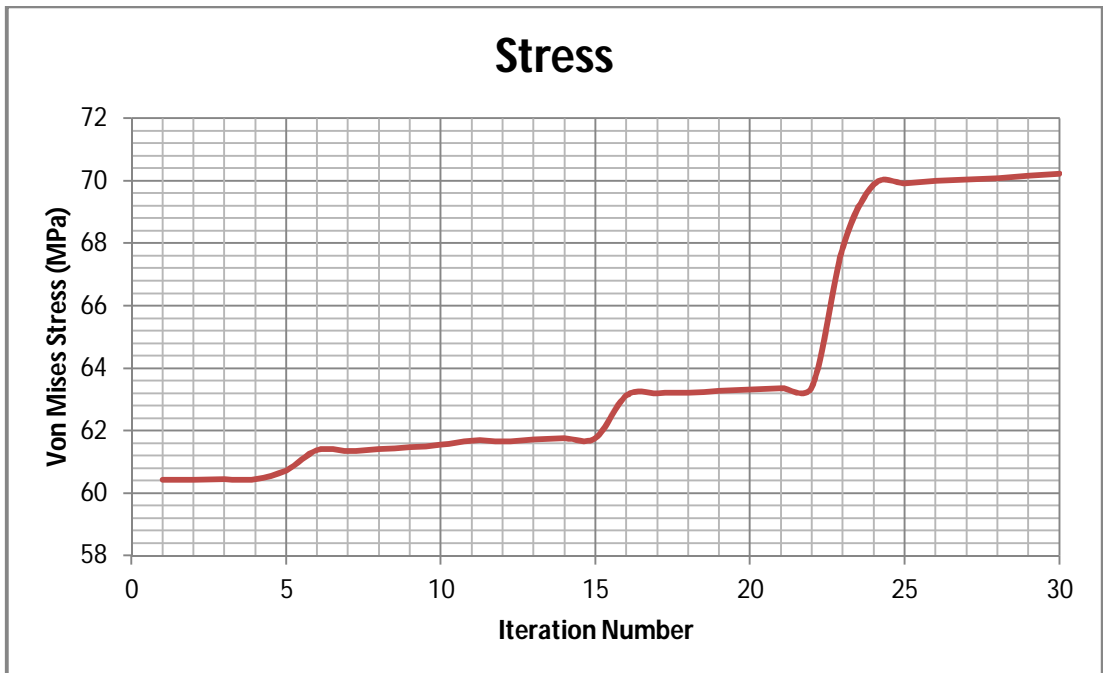


Figure 3.18 Maximum von Mises Stress vs. iteration numbers for two bar optimized structure.

3.3.2. MICHELL TYPE STRUCTURES WITH TWO FIXED SUPPORTS

Another well-known structural optimization problem is Michell type structures. A rectangular design domain having length $H = 5\text{ m}$ and length $L = 2H$. Michell truss is the lightest truss for the situation of vertical load acting in the middle of two fixed supports as in Figure 3.19. Two corners at the bottom are controlled for translational movements (Huang and Xie, 2010).

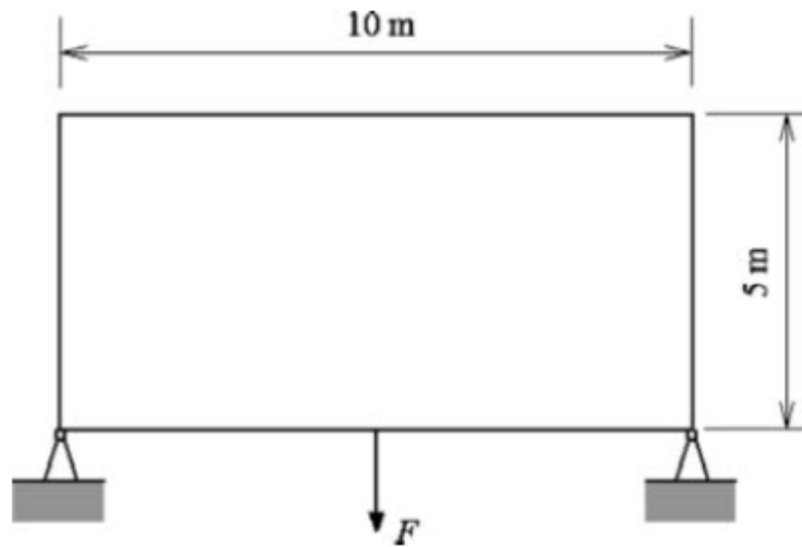


Figure 3.19 Design domain of Michell type structure with two fixed support. (Huang and Xie 2010)

Design domain is discretized into $50 \times 25 \times 1$, 1250 elements. Solid cubic element, with dimensions 0.1 m while material properties are $E=100\text{GPa}$ and $\nu=0.3$. The vertical F load is 1000N. The code is initiated with $RR_0 = 1\%$ and ER is set as 0.5%. The results adopted from literature and generated by the proposed code are compared for different RR values such as 5%, 10%, 15%, 20% and 25% which shows the different stages of evolutionary history in Figure 3.20 to 3.24 respectively.

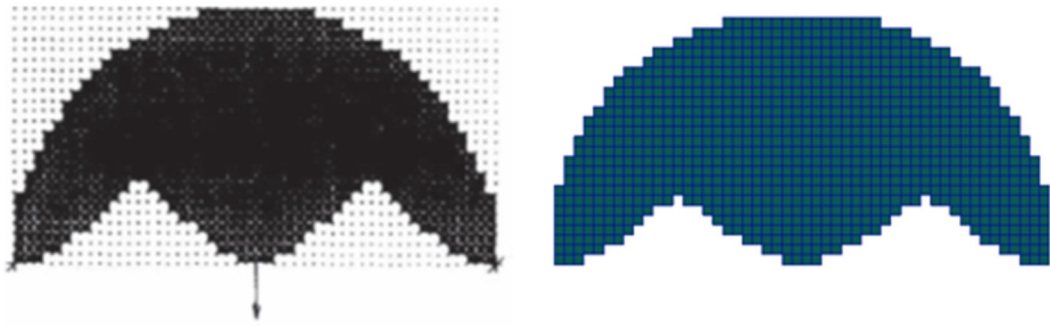


Figure 3.20 Result of Michell truss with two fixed supports for $RR=5\%$ (Huang and Xie 2010) and optimized structure.



Figure 3.21 Result of Michell truss with two fixed supports for $RR=10\%$ (Huang and Xie 2010) and optimized structure.



Figure 3.22 Result of Michell truss with two fixed supports for $RR=15\%$ (Huang and Xie 2010) and optimized structure.

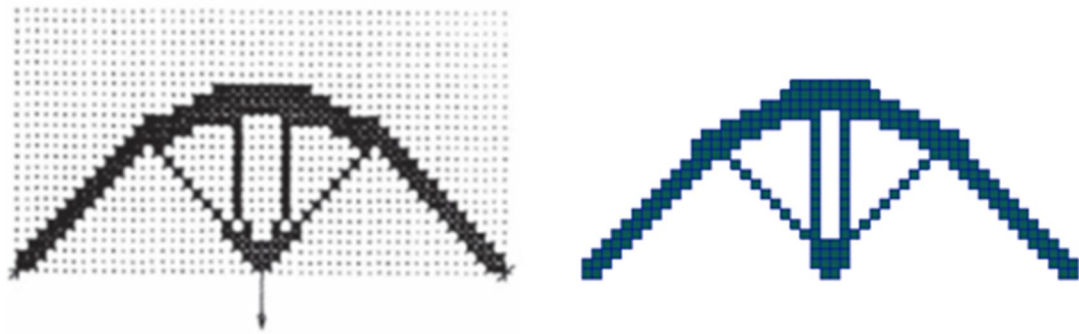


Figure 3.23 Result of Michell truss with two fixed supports for RR=20% (Huang and Xie 2010) and optimized structure.

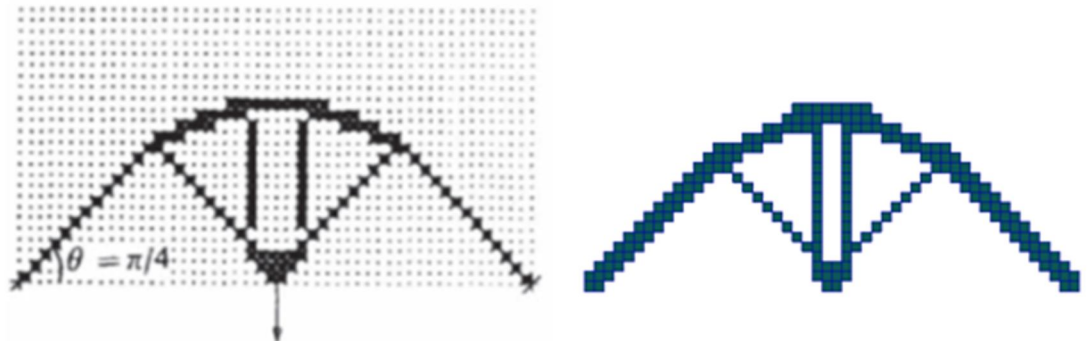


Figure 3.24 Result of Michell truss with two fixed supports for RR=25% (Huang and Xie 2010) and optimized structure.

The total progress time vs. iteration number of Michell truss with two fixed supports expressed in Figure 3.25 that remaining elements and iteration time are inversely proportional. As the number of elements decreases, the iteration takes slightly less time.

The element reduction in Figure 3.26 has almost no effect on maximum von Mises stress; even though the volume reduction rate is high. After 25th iteration, the stress increase initiated. The highest von Mises stress increment occurs after 47th iteration as in Figure 3.27, since 30% of the volume has removed.

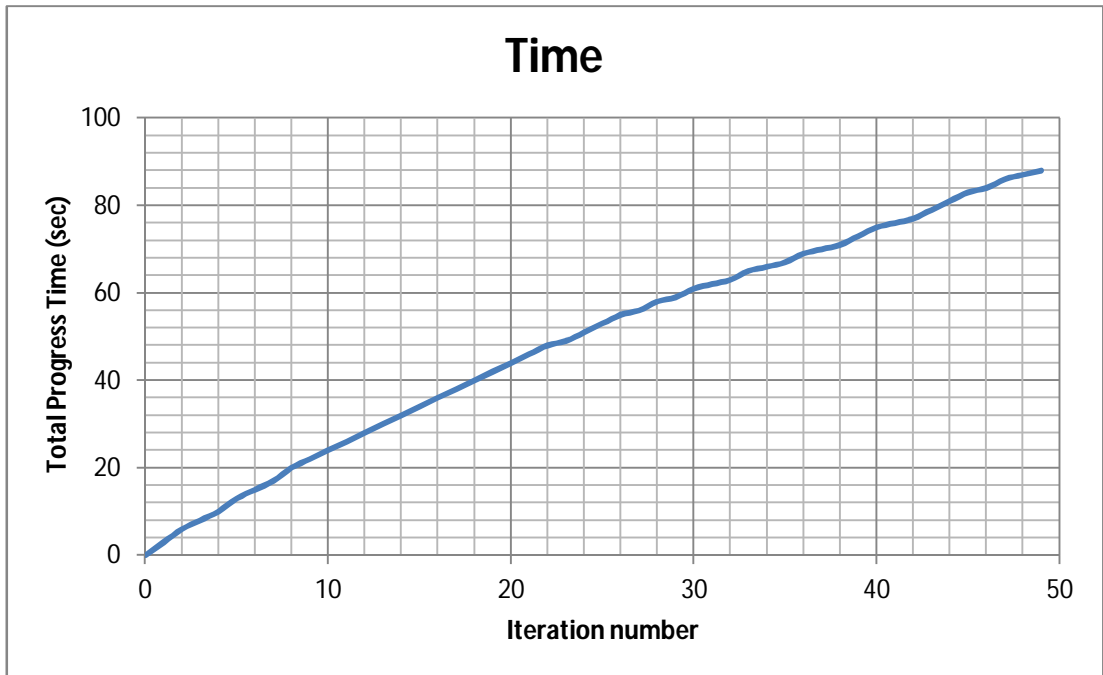


Figure 3.25 Total progress time vs. iteration numbers for Michell truss with two fixed supports optimized structure.

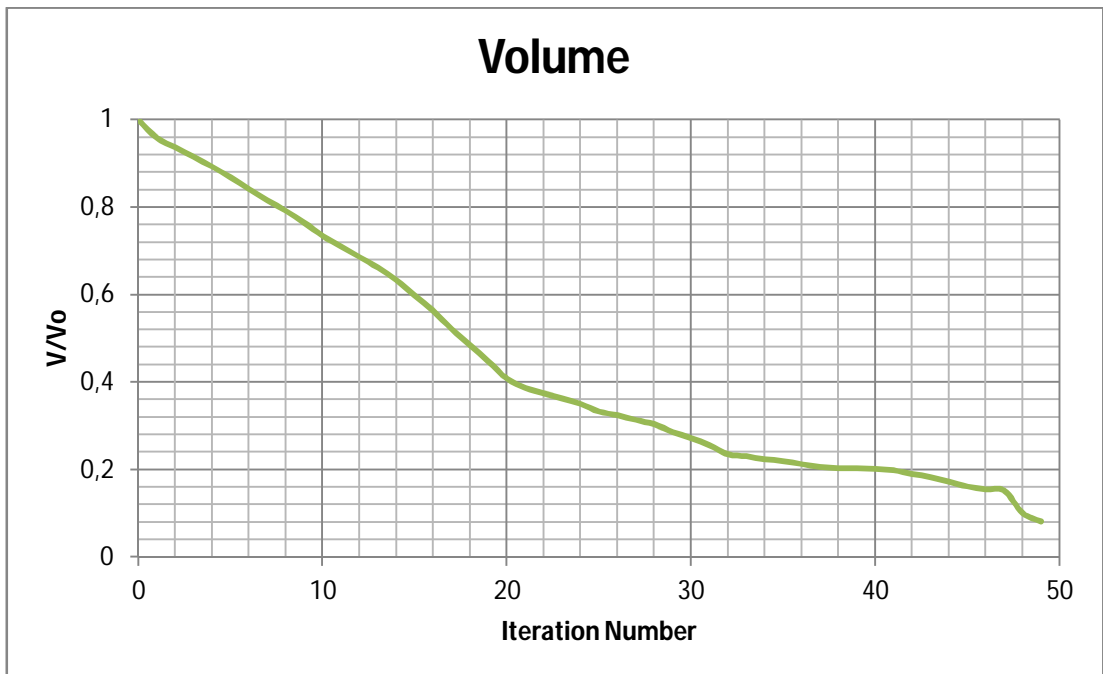


Figure 3.26 Volume reduction vs. iteration numbers for Michell truss with two fixed supports optimized structure.

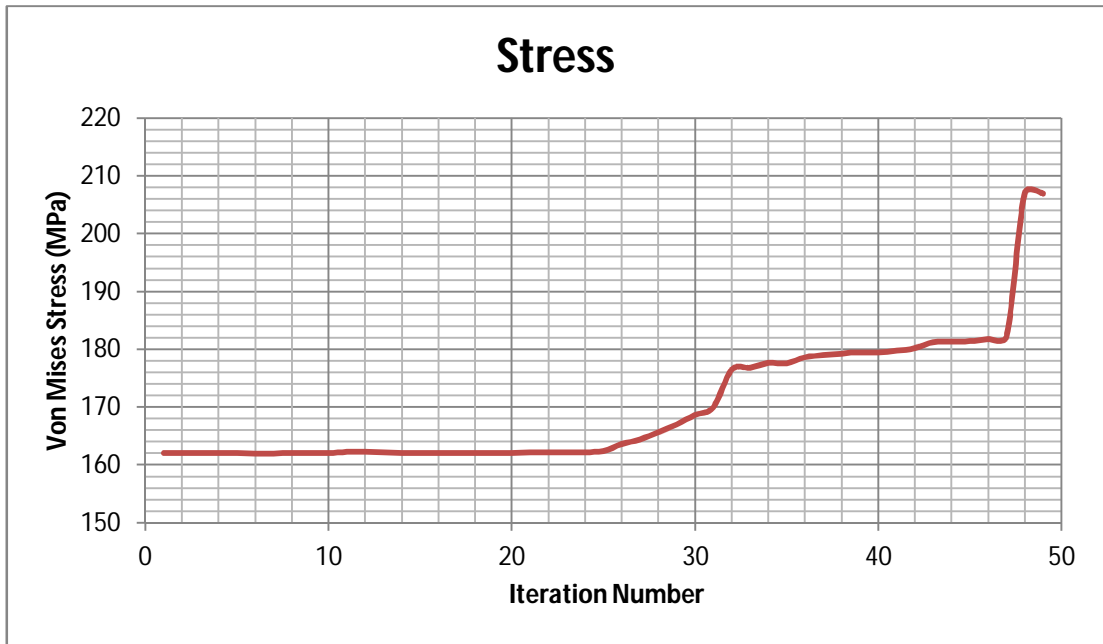


Figure 3.27 Maximum von Mises Stress vs. iteration numbers for Michell truss with two fixed supports optimized structure.

3.3.3. MICHELL TYPE STRUCTURES WITH A ROLLER AND FIXED SUPPORT

The same Michell type structure is computed however other than two fixed supports, one roller and one fixed support is used. The results adopted from literature and code is performed with volumetric approach in Figure 3.28, 3.29 and 3.30.

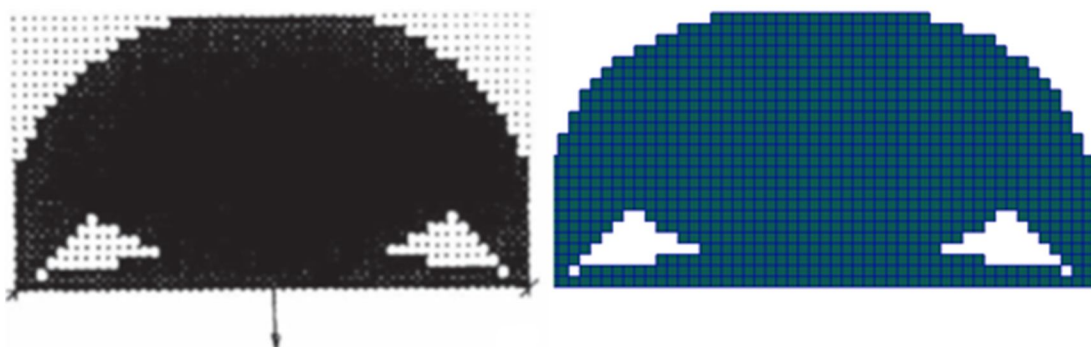


Figure 3.28 Result of Michell truss with a roller and fixed support with volumetric approach (Huang and Xie 2010) and optimized structure.

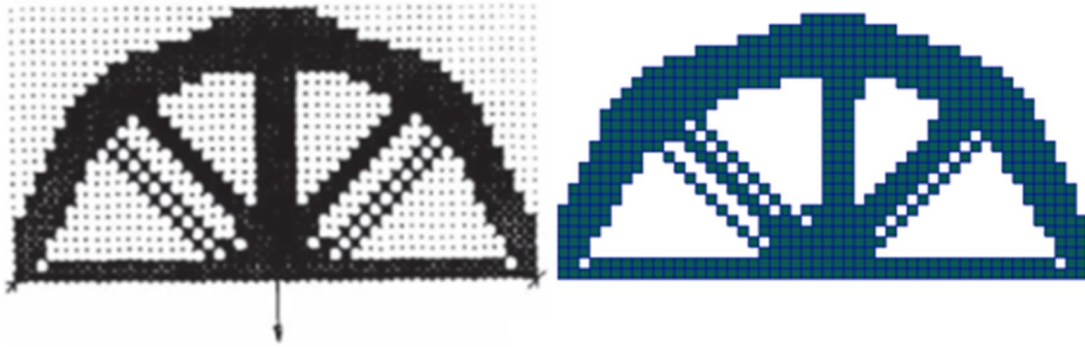


Figure 3.29 Result of Michell truss with a roller and fixed support with volumetric approach (Huang and Xie 2010) and optimized structure.

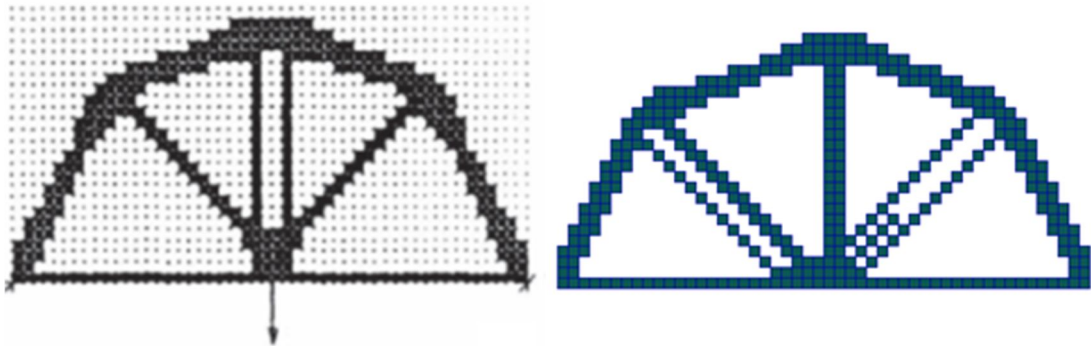


Figure 3.30 Result of Michell truss with a roller and fixed support with volumetric approach (Huang and Xie 2010) and optimized structure.

The iteration time is almost constant due to reduction in number of removed elements in Figure 3.31. The volumetric approach operates as, the number of remaining elements are divided into a specified removal number so that, the number of removed elements decreases in every iteration and creates an exponential curve for volume reduction in Figure 3.32. The maximum stress level has an increase attitude; however, the curve performs unexpected oscillations at last iterations shown in Figure 3.33. The oscillation magnitude is small when compared with stress values.

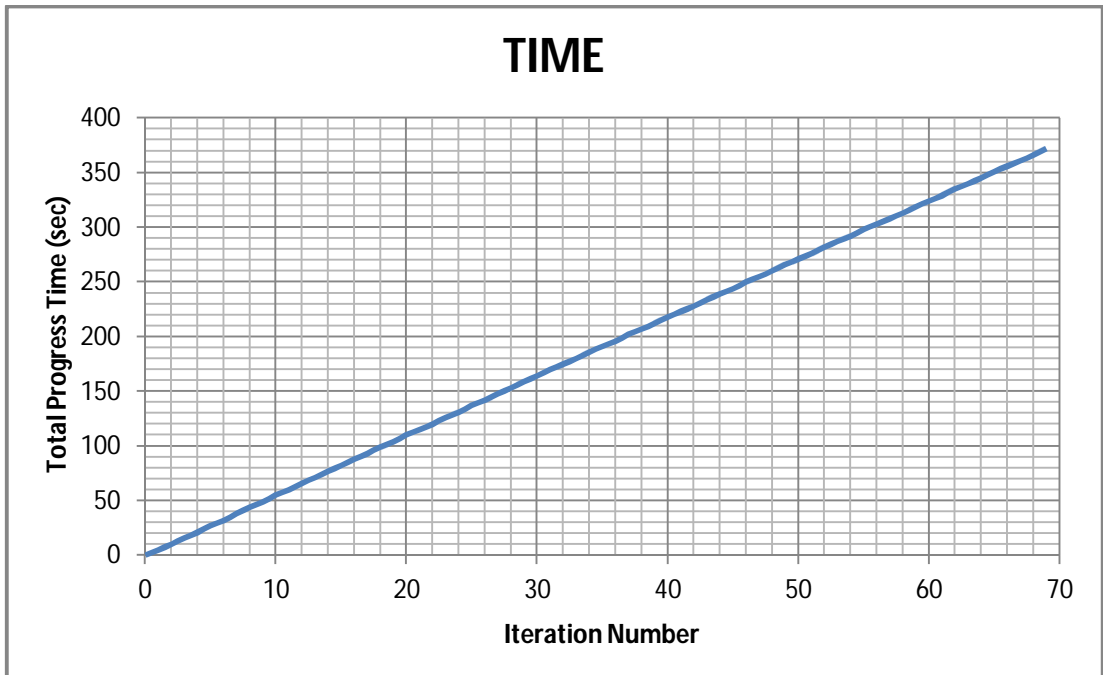


Figure 3.31 Total progress time vs. iteration numbers for Michell truss with a roller and fixed support optimized structure.

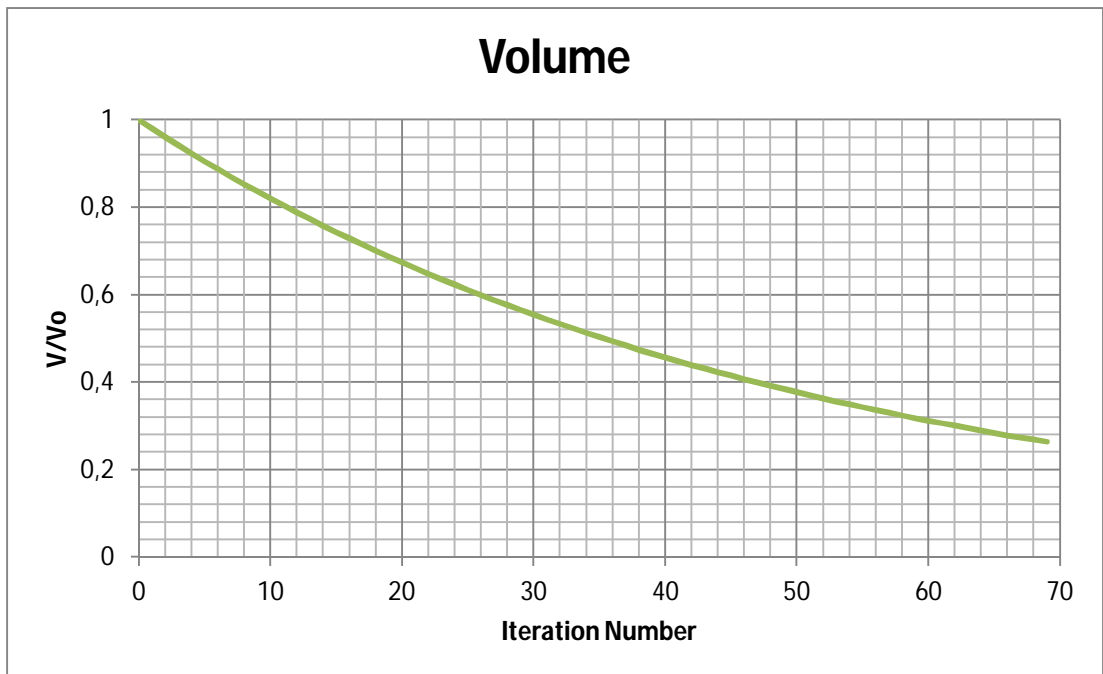


Figure 3.32 Volume reductions vs. iteration numbers for Michell truss with a roller and fixed support optimized structure.

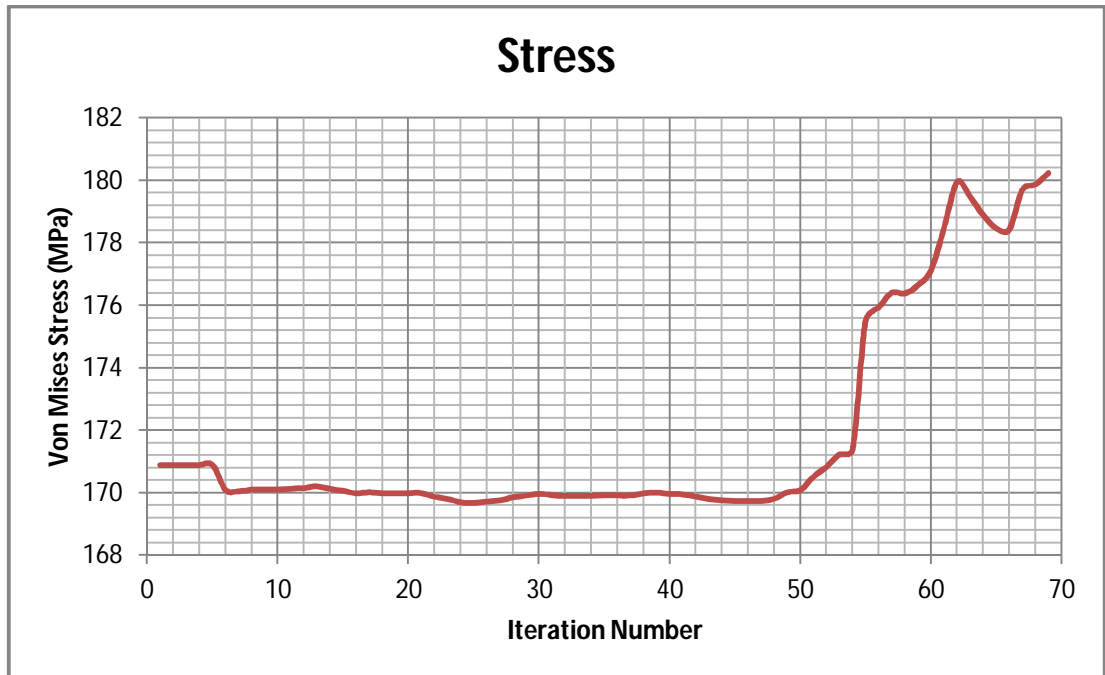


Figure 3.33 Maximum von Mises Stress vs. iteration numbers for Michell truss with a roller and fixed support optimized structure.

3.3.4. BRIDGE WITH A MOVING LOAD

The bridge is optimized according to the traffic and vehicle load passing from one side to another. The continuous moving load can be approximated as finite number of load cases. At each load case the vehicle load is applied with the same magnitude whereas, the load is exerted at different time intervals. The point load is moving from left to right on the top surface. Nine load cases with equal distance are specified. The path vehicles moves at the top and four bridge supports are designated as non-design domain. The bridge is discretized into 60 X 40 X 1 solid cubic elements as in Figure 3.34 (Xie and Steven, 1997).

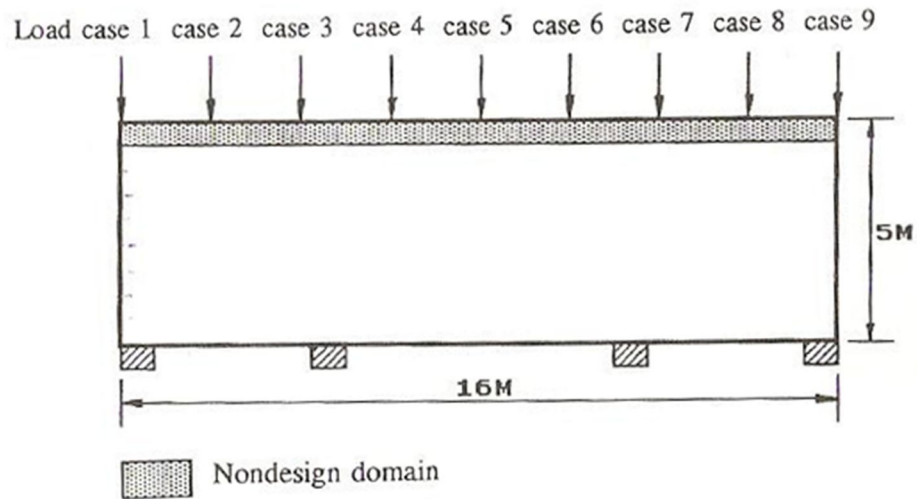


Figure 3.34 Initial model of the bridge with loading and boundary conditions (Xie and Steven 1997).

Applying the ESO method, RR_o 1% and ER 1% are chosen. When the rejection ratio reaches 10%, the result at Figure 3.35 is obtained. The result bears a striking resemblance to classical arch bridges.

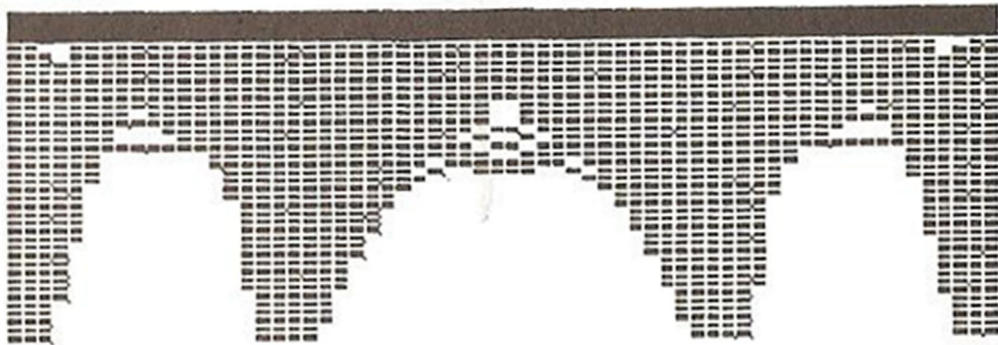


Figure 3.35 Optimal design for the bridge with nine load cases (Xie and Steven 1997).

The resultant topology of the code shown in Figure 3.36 and reference shows same diversity may occur due to different level of maximum stress element. Total progress time vs. iteration number forms almost a straight line, that is, iteration time does not vary and there is no significant maximum von Mises stress value change during iterations. Volume reduction does not exceed 30% of the initial element number.

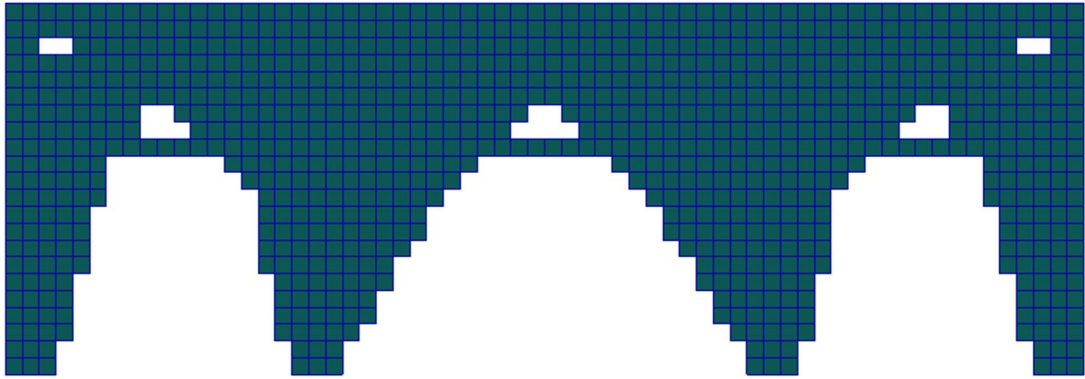


Figure 3.36 The optimum geometry at Rejection Ratio 12%.

3.3.5. TORSION BEAM

Any moment vector that is collinear with the axis of a mechanical element is called *torque vector*, a mechanical element which is subjected to such a moment is said to be *torsion*. For a circular shaft, the shear stress is zero at the center and maximum at the outer surface. Radius is directly proportional with torsion magnitude.

A beam specimen is subjected to pure torsion 1 kN.m from one end, and other end is supported to prevent all degree of freedom movements such as located into a wall like structure. The specimen is created from 20X20X120, 48000 solid cubic elements having square profile in Figure 3.38. The first and last square structure at load application and support are accepted as non-design elements as in Figure 3.37. The topological optimization results are obtained as expected. The portion at the center is removed because of low stress values, also edges of square are deleted as presented in Figure 3.40. Hollow structure at each section except the loading and support sections are formed at rejection ratio 62% in Figure 3.39. The single load case optimization with 48000 elements takes about 2.5 hours.

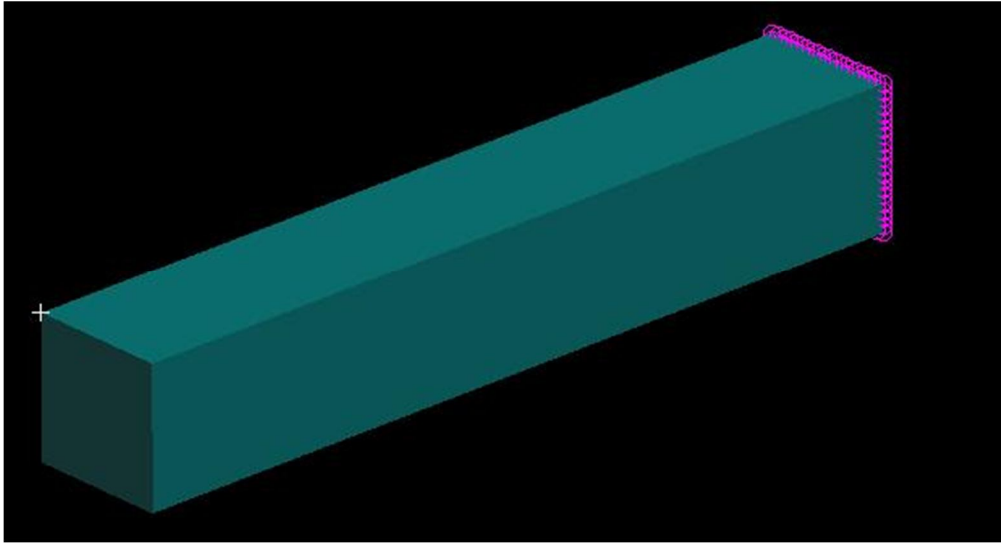


Figure 3.37 The design domain, colored as green, the support is colored as pink.

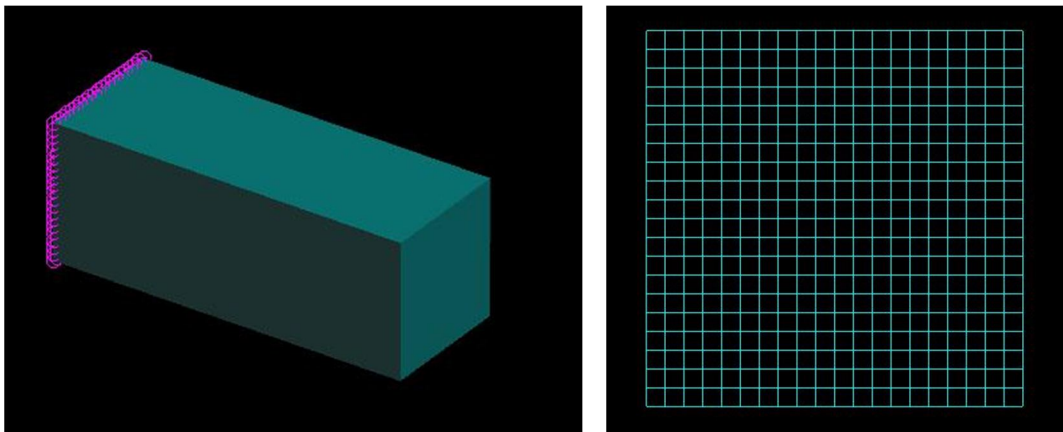


Figure 3.38 The design domain is solid rectangular beam with square profile. Left figure is the section cut of design domain.

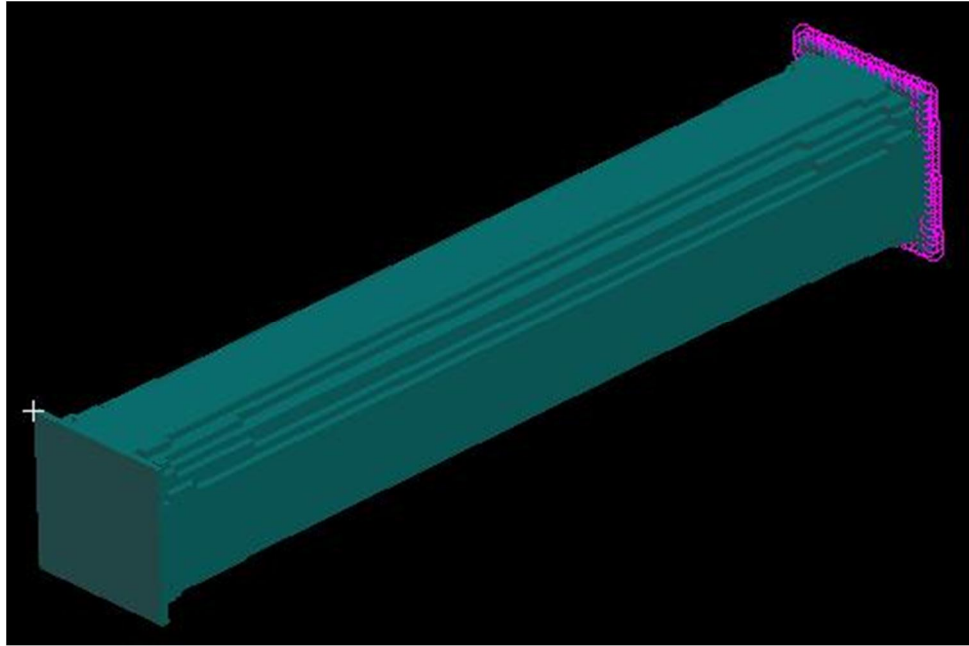


Figure 3.39 The code output at Rejection Ratio % 62.

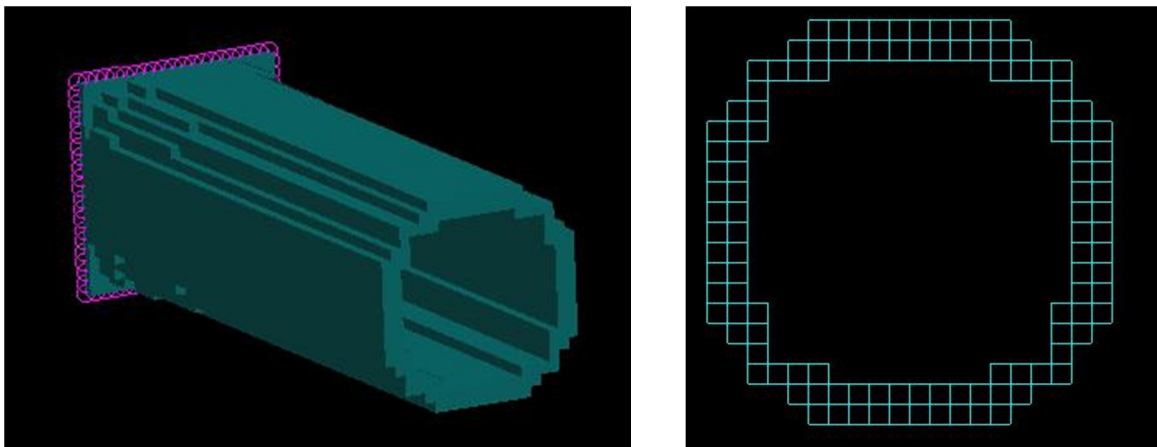


Figure 3.40 The hollow shape is constant in all sections except loading and support transient regions. Left figure corresponds to section cut.

The oscillations in Figure 3.41 are unexpected, however; the general trend of the plot is to decrease as the iteration number increases. The volume reduction ratio is expected to decrease as the iteration number increases, however; the slope increases in Figure 3.42. This may occur since the magnitude of stress levels is close, which most of the elements vanish at later stages. The sudden increases in maximum von Mises stress levels in Figure 3.43 support the idea.

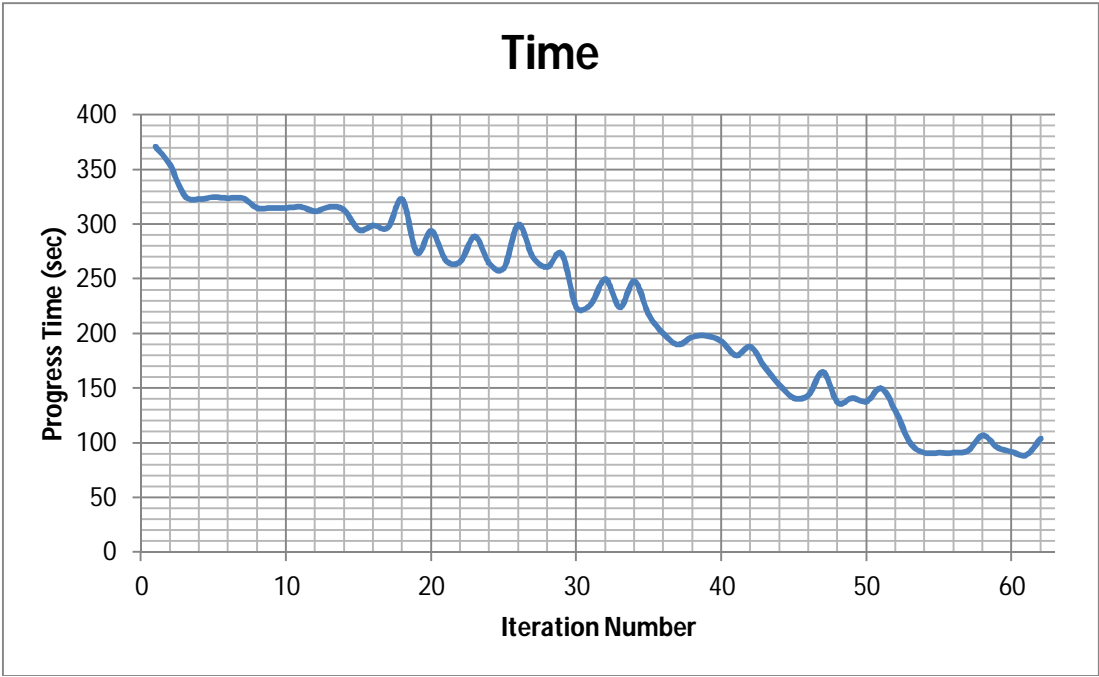


Figure 3.41 Total progress time vs. iteration numbers for torsion beam.

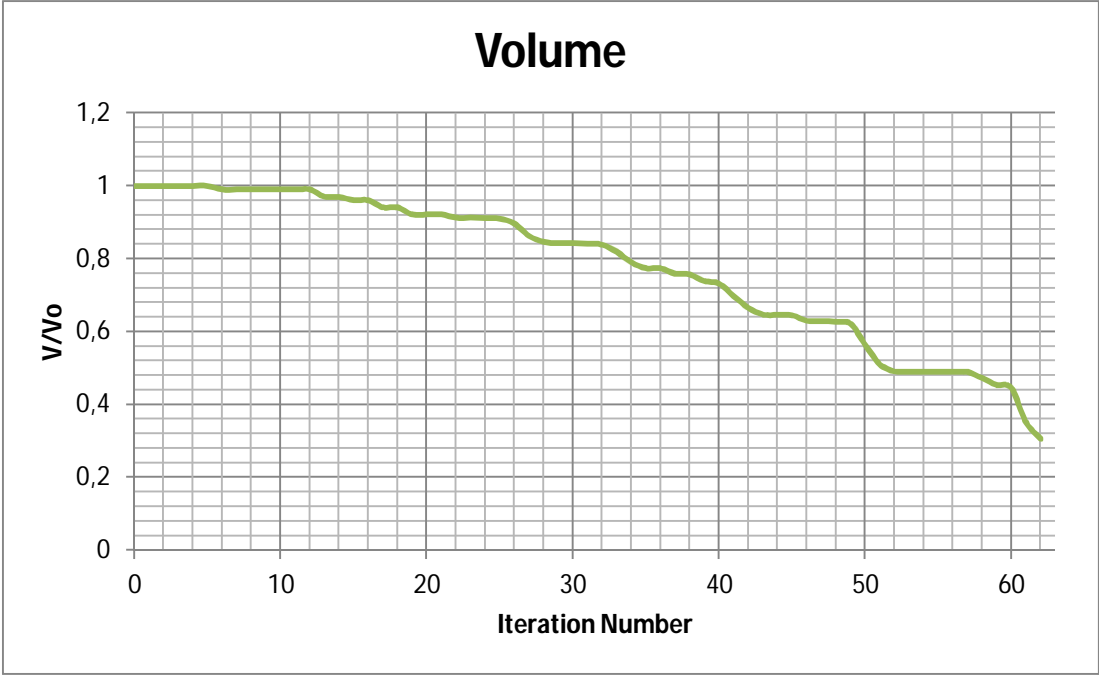


Figure 3.42 Volume reduction vs. iteration numbers for torsion beam.

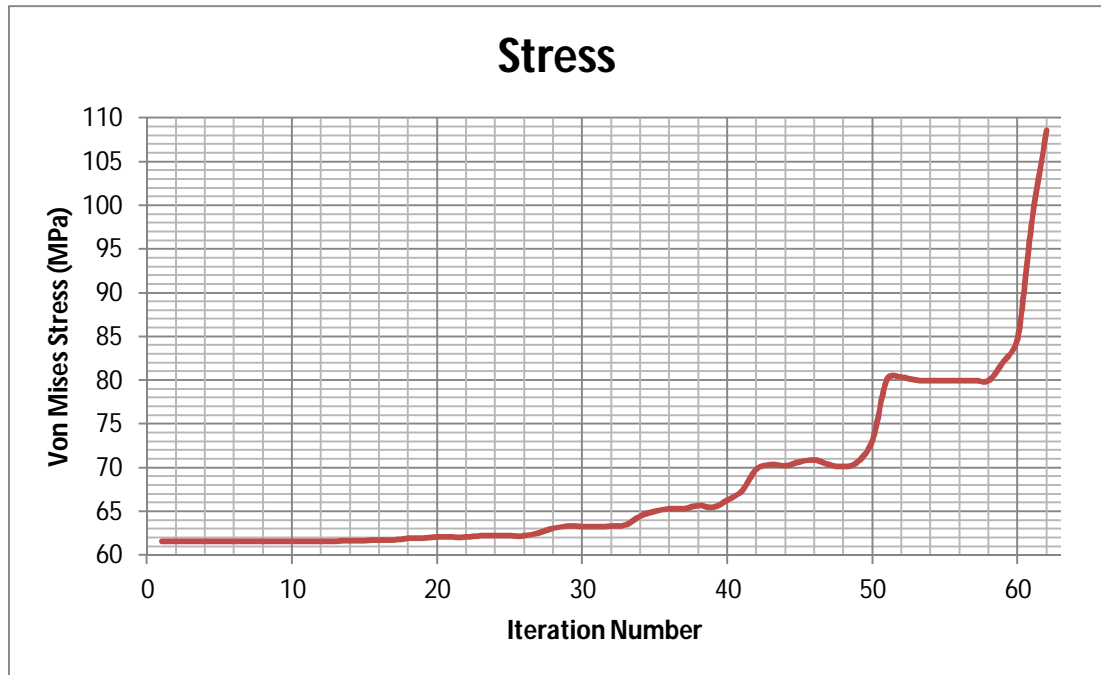


Figure 3.43 Maximum von Mises Stress vs. iteration numbers for torsion beam.

3.4. RESULTS AND DISCUSSION

The optimization process converges and the results of codes and literature are similar which reveals the confidence of the codes for ESO method. However there are some differences. In some results symmetry cannot be formed. Topological differences may arise as the numerical solution is applied. The three examples in the books are 2-D problems and four node plane stress elements are utilized. The code process is based on 3-D problems with eight nodes solid cubic elements which may cause possible errors. The force cannot be applied directly on a point, due to geometry divided into two and applied. Also ESO method has two approaches as indicated before, stress and volumetric method. Volumetric approach damages the symmetry as the number of removed elements is exact, that is the elements having same stress level, and one can be removed where the other element remains. These methods may give out different results. Stress method is advantageous to create symmetrical models however; if the stress levels are quite similar, not to conduct with stability problem, volumetric approach can be applied. Removing a large number of elements in iteration may lead to instability. Each and every iteration small portions of element removal is suggested.

CHAPTER 4

OPTIMIZATION OF GENERIC AIRCRAFT COMPONENTS

The aircraft components which are optimized by ESO method are lug, clevis, main landing fitting and power control equipment support.

4.1. ENVIRONMENT OF LUG AND CLEVIS

Lug is a T shaped structure and clevis resembles a fork that operates together in harmony. Lug and clevis are joined with connection bolt. Spherical plain bearing is inserted into the lug cavity. In addition, two bushings are seated to the two arms of the clevis to reduce wear effects. Suitable nut and washers are selected to complete the lug-clevis connection. The assembly is presented in Figure 4.1 and Figure 4.2 respectively.

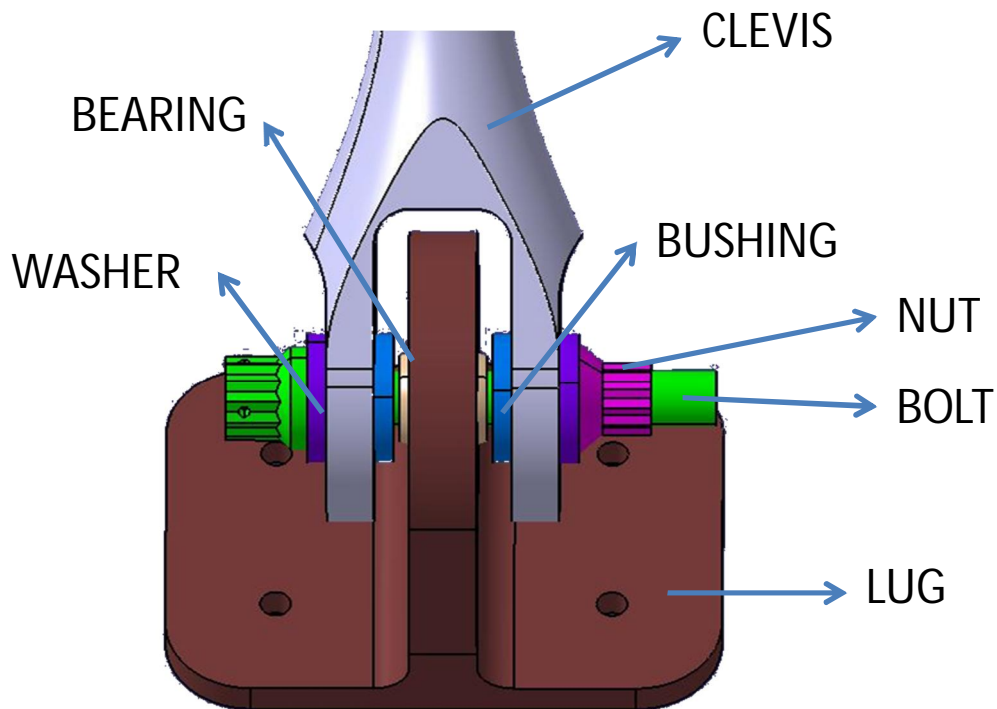


Figure 4.1 The front view of the lug, clevis assembly.

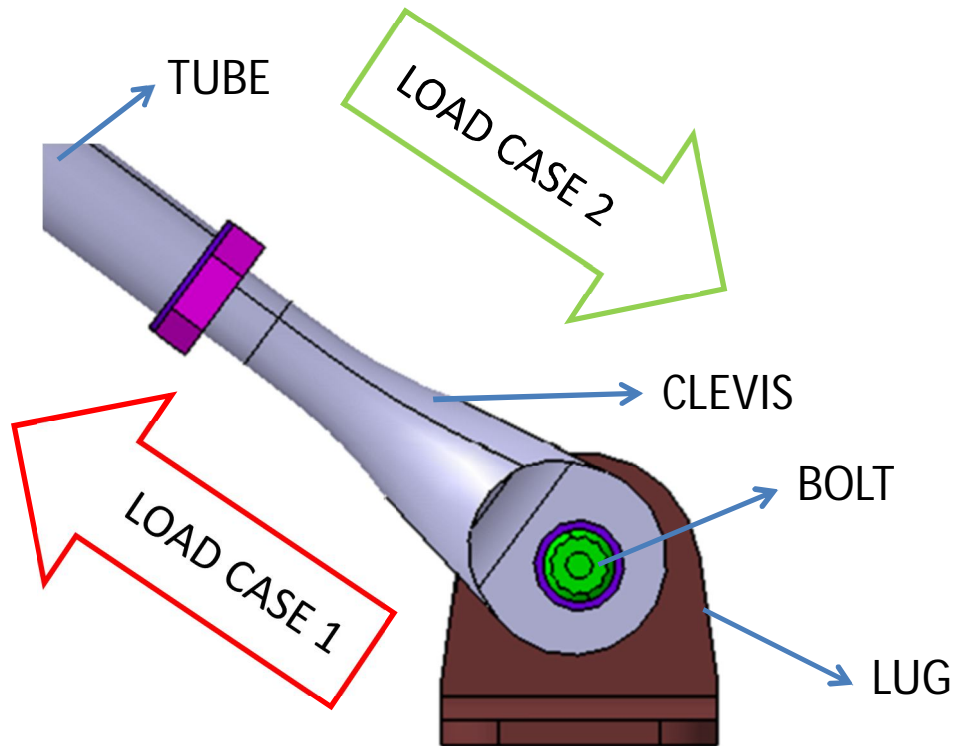


Figure 4.2 The left view of the lug, clevis connection and load case assembly.

Lug is mounted to the ground structure with solid rivets. Spacing of the rivets is predetermined using riveting standards. Clevis is assembled to a tube with thread connection. Clevis has outer thread whereas the tube has inner thread. Due to form of the tube and structural integrity, the lug, clevis and tube assemble is assumed to carry loads only along the tube direction and not able to carry bending moment or shear.

The assembly is functioned to support the instrument panel. Instrument panel is the structure in cockpit, which houses the equipment of aircraft. The load that assembly should carry can be calculated using the free body diagram of the environmental structure shown in Figure 4.3. The dashed lines represent 4 load directions. In purple line, line 1, central gravity of the whole instrument panel is located. Line 2, is the direction which includes optimized generic aircraft components. Line 3 and Line 4 are other support directions. d_2 , d_3 , d_4 are perpendicular lines from central gravity of instrument panel to force directions 2, 3 and 4 respectively.

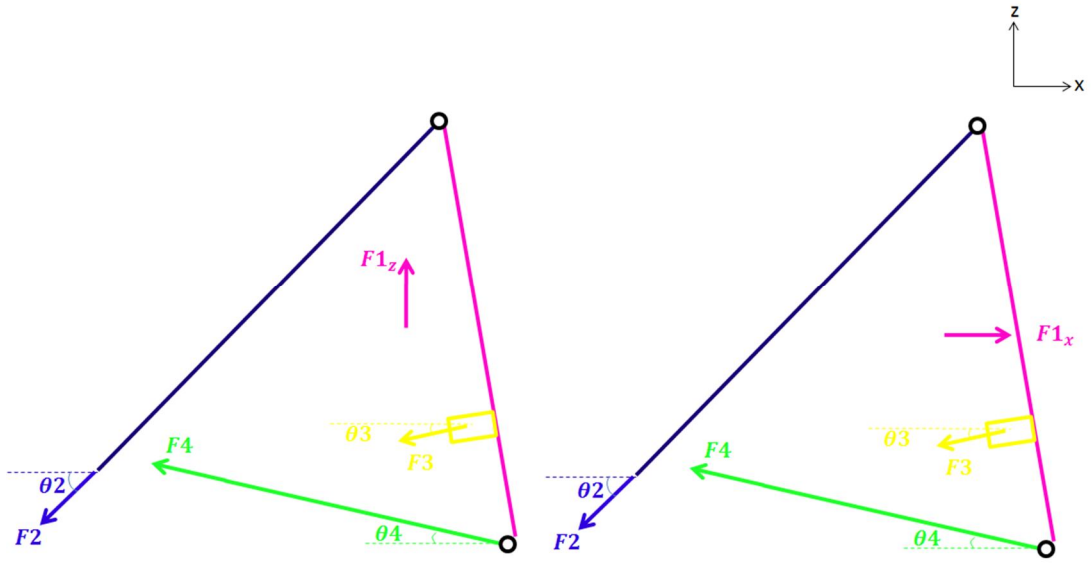


Figure 4.3 The free body diagram of the instrument panel for Load Case 1 and Load Case 2 respectively.

The support points are symmetrical therefore only one side of the panel is investigated. The two maximum acceleration values of aircraft in critical maneuvers are considered. Therefore two load cases are obtained. As the load and accelerations are known, only three unknowns remain that forms a statically determine problem. The equations above are solved simultaneously for both load cases and the desired forces obtained;

$$F1_x - F2 \times \cos \theta_2 - F3 \times \cos \theta_3 - F4 \times \cos \theta_4 = 0 \quad (4.1)$$

$$F1_z - F2 \times \sin \theta_2 - F3 \times \sin \theta_3 + F4 \times \sin \theta_4 = 0 \quad (4.2)$$

$$F2 \times d2 - F3 \times d3 - F4 \times d4 = 0 \quad (4.3)$$

$$F2_{LC1} = 2522 \text{ N} \quad (4.4)$$

$$F2_{LC2} = 1475 \text{ N} \quad (4.5)$$

The value of formulation 4.4 and 4.5 are named as load case 1 and load case 2 respectively and the directions are specified in Figure 4.2. The material is selected as Aluminum 7075 T7451 with yield strength of 440 MPa. The elastic modulus (E) is 72 GPa and Poisson's ratio (ν) is 0.33. A safety factor of 1.5 is selected. As a result, the maximum allowable stress is formulated in (4.6);

$$\sigma_e^{max} = \sigma_e^y / n = 440 / 1.5 = 293.3 \text{ MPa} \quad (4.6)$$

4.2. LUG

Lug has a T shaped geometry hence two sides of the lug should be occupied by clevis arms. Besides some constraints such as the wall thickness of lug should be employed. The spherical plain bearing has specific width and diameter; therefore the wall thickness and bearing hole of lug has already been defined. Also diameter of rivets and rivet spacing is a constraint; consequently the holes are not optimization variables. The existing lug in aircraft has 4 rivet holes; however, during optimization procedure the design domain of lug includes 8 rivet holes. As the unnecessary elements are removed, the necessary rivets are discovered. The geometry is elongated due to angle difference of load directions and lug surface; therefore the outer geometry of the lug is also optimized. The initial half and full model of the lug are shown in Figure 4.4. The lug is symmetrical therefore one side of the lug is modeled and solved. The constraint along the normal of symmetry plane is applied to the wall of the model neighboring the omitted volume, which is shown in Figure 4.5.

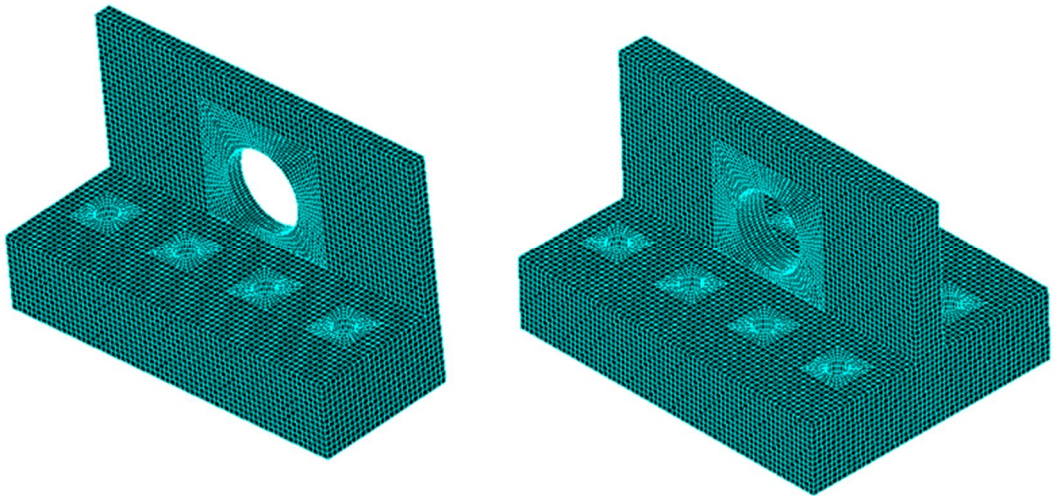


Figure 4.4 The half and full model of lug.

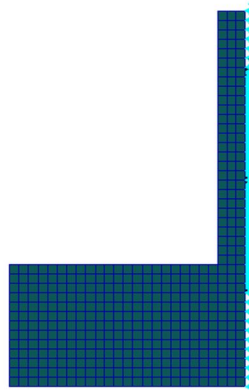


Figure 4.5 The half model is constraint from the symmetry plane

The program operates not only with three dimensional solid hexahedron mesh but also tetrahedron mesh. Areas around the holes are discretized separately from the bulk model not to create connectivity problems of the nodes. Also the model is controlled by MSC.PATRAN using Elements-Verify-Boundaries route. All 8 nodes of a hexahedron element are connected to the neighbor nodes. The initial half model including design and non-design domains contains 29784 elements and 37231 nodes. As the number of elements is halved by preferring half model, the stiffness matrix is narrowed and the compute time is decreased. Besides the results are not symmetrical in full model due to numerical errors, therefore half model is chosen. The number of elements for full model is 59568.

The load case 1 and load case 2 forces were applied on the bearing contact surfaces with a sinusoidal distribution along the angular direction as presented in Figure 4.6. The load direction has the maximum stress, as moving apart from load direction, the stress is reduced to zero.

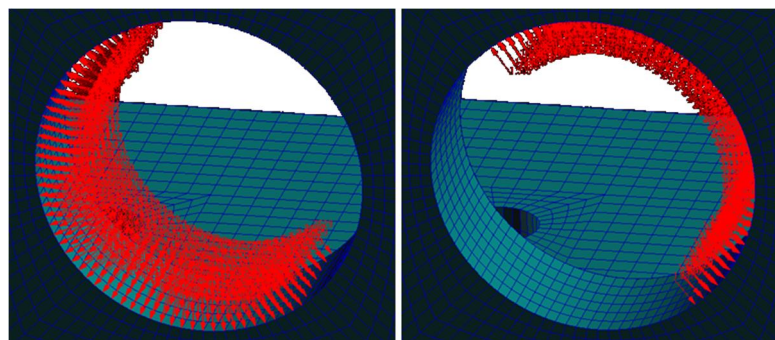


Figure 4.6 The load distribution in bearing hole for load case 1 on the left and for load case 2 on the right.

Sinusoidal load distribution is frequent approach. Lazovic *et al.* (2008) employs sinusoidal load distribution for bearing load transfer. Solidworks software utilizes sinusoidal distribution for bearing load. Strand H., (2005) refers to sinusoidal distribution among other types. Before this approach, MPC (Multipoint Constraints) was performed. MPC concept loads all selected nodes equally, resulting even tensile contact forces as well, which is not a valid assumption. The nodes, located near to load direction, should be exposed to higher stress. Hertz contact theory is an analytical model for defining the stress distribution and applied when two structures are in spherical or cylindrical contact. Pereira *et al.* (2010), Tian-quan (1991) state that this theory is performed in limited conditions when the dimension of the deformed contact is very small compared with radius of elements. In our case, contact area is greater than the radius of the bearing. Johnson (1982) declare that ratio of half contact area to radius of elements up to 0.3 can employ Hertz contact theory. It is 1.24 in our case; therefore Hertz contact theory is not applicable for bearing stress distribution.

The lug is mounted to the ground structure with rivets. Load 1 and Load 2 forms different support areas therefore two support regions are created. Design domain forms 13 mm thickness, which is not realistic for riveting; therefore it is assumed to have 2 mm thickness for riveting. This assumption is validated in results section that overstressed region is not formed. The nodes facing with rivets are marked as support points, shown in Figure 4.7.

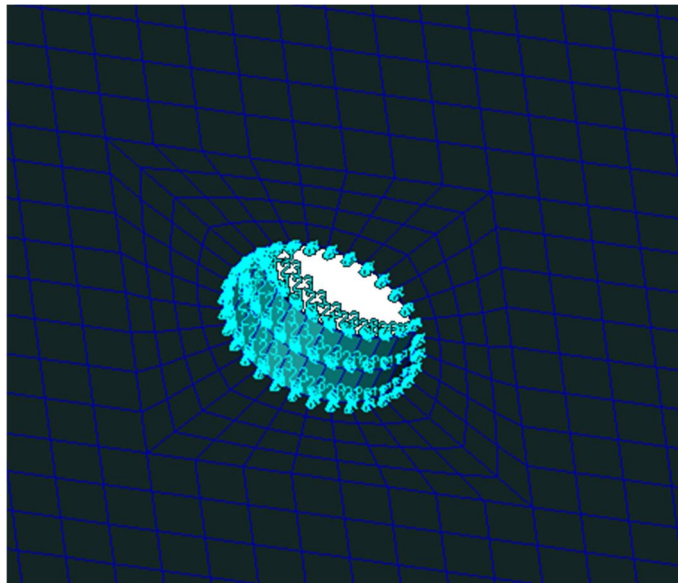


Figure 4.7 Support nodes around the rivet.

The applied loads should create certain regions exposed to tension or compression at the bottom of the lug with mating structure. The compression nodes are also considered as support points due to forming of contact area shown in Figure 4.8 and 4.9. The tension and compression nodes at the bottom are essential since they also reveal which rivets are in tension or compression. The regions do not vary for iterations; therefore they are valid through the optimization process.

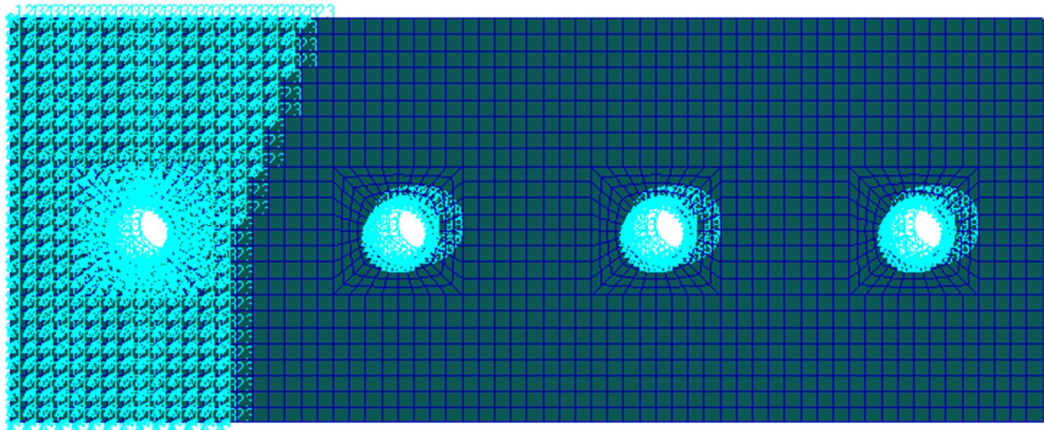


Figure 4.8 The contact elements and compression rivets at the bottom of lug in load case 1.

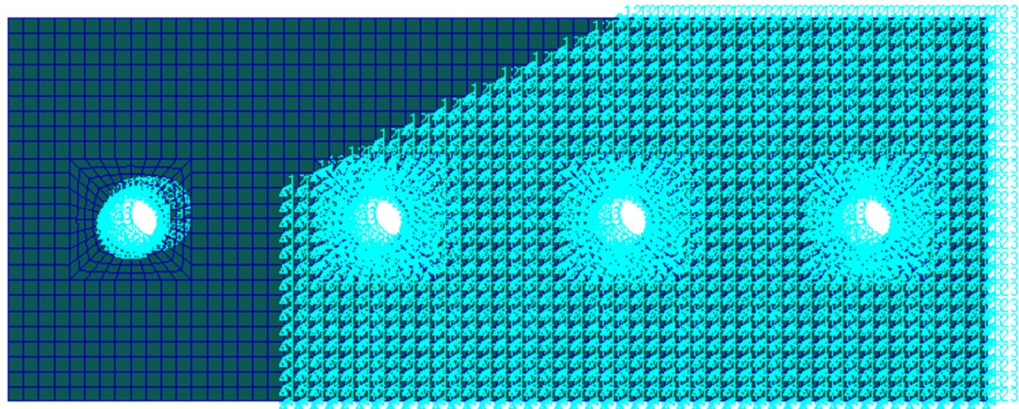


Figure 4.9 The contact elements and compression rivets at the bottom of lug in load case 2.

The nodes in tension region try to move apart; however due to riveting, the rivet heads create additional reinforcement as in Figure 4.10. These nodes are also selected for support. Rivet head will occupy a volume in design domain that has to be removed as in Figure 4.11.

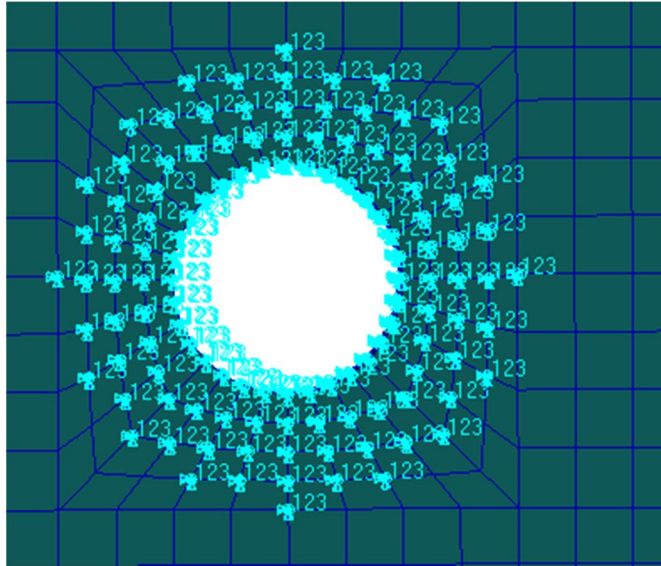


Figure 4.10 The support points of rivet head in tension regions.

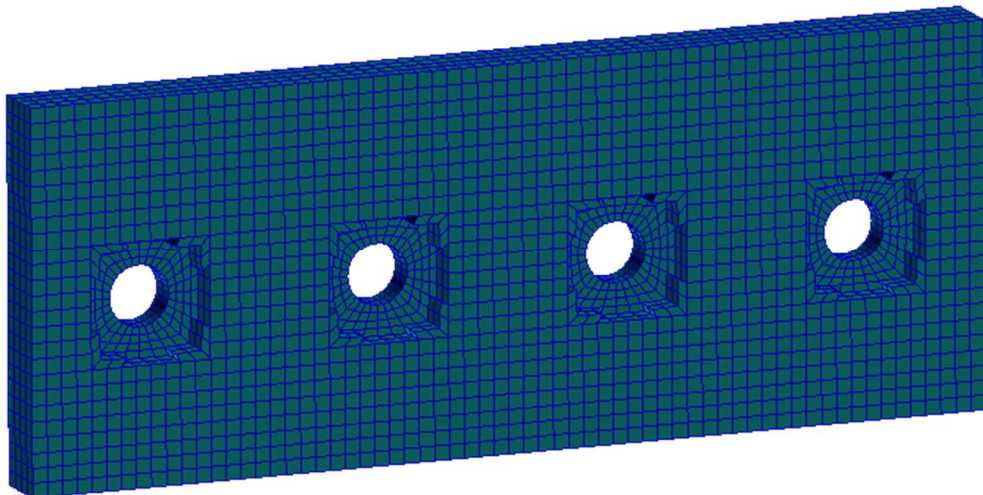


Figure 4.11 Rivet head spacing.

Figure 4.12 and 4.13 show the design and non-design domain of the bulk structure. Design domain is represented with red color, whereas non design domain is white. The three element thickness around bearing hole is protected. Even the von Mises stress level is low; they are kept due to bearing. Also four rivets and rivet seat areas nearest to the load direction are reserved.

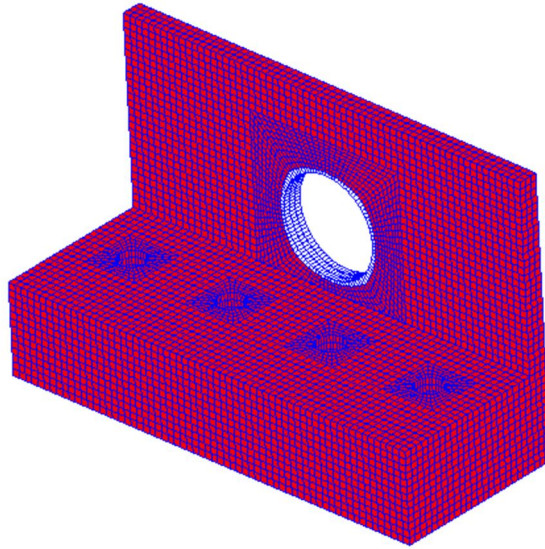


Figure 4.12 The design and non-design domain of bearing.

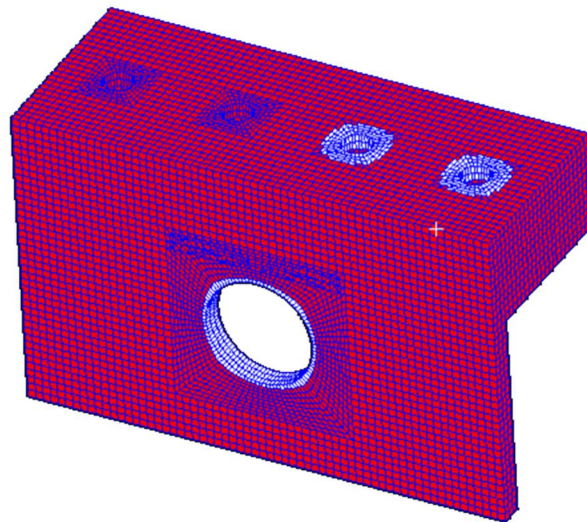


Figure 4.13 The design and non-design domain of rivets.

The initial rejection ratio, RR_0 , and evolutionary rate, ER , is chosen as 0.25% to avoid stability problems. The number of load cases is 2 and allowable stress, σ_e^{max} is 293 MPa. The optimized result is obtained at 103th iteration, i.e. rejection ratio, RR , 25.75%. The final half geometry contains 3150 elements, i.e., 6300 elements for full domain. The optimized shape of the lug is presented in Figure 4.14.

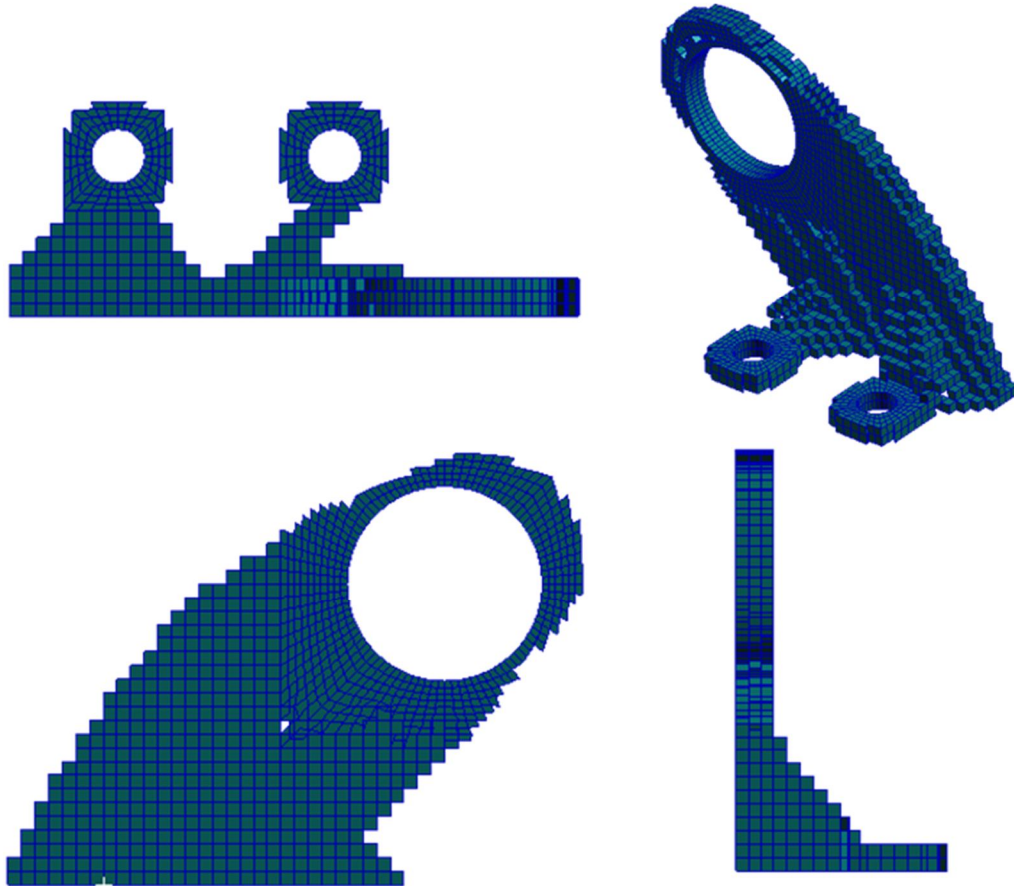


Figure 4.14 The front, top, right side and isometric view of the optimized lug.

The iterations took 5 hours 8 minutes and 11 seconds on an Intel Core 2 Duo T9550 4 Gigabyte RAM computer. Total progress time vs. iteration number is monitored in Figure 4.15. 1st iteration took more than 12 minutes whereas 103th iteration took about 20 seconds. Number of elements has great effect on iteration time. After 80th iteration, iteration time fluctuates. Total progress time can be decreased by choosing greater RR_0 or ER value. Besides modeling of symmetrical volume decreases the computer time compared with whole model.

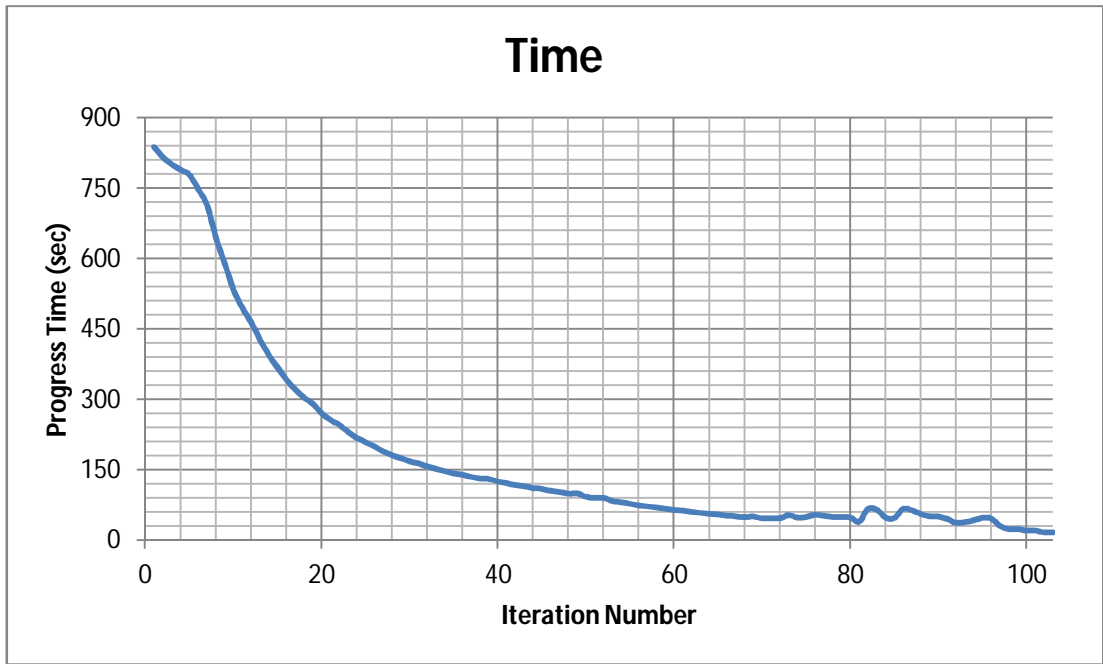


Figure 4.15 Total progress time vs. iteration numbers for optimized lug.

89.4% of the initial volume is removed. The volume reduction graph is shown in Figure 4.16. The volume reduction rate decreases as the iteration number increases as expected.

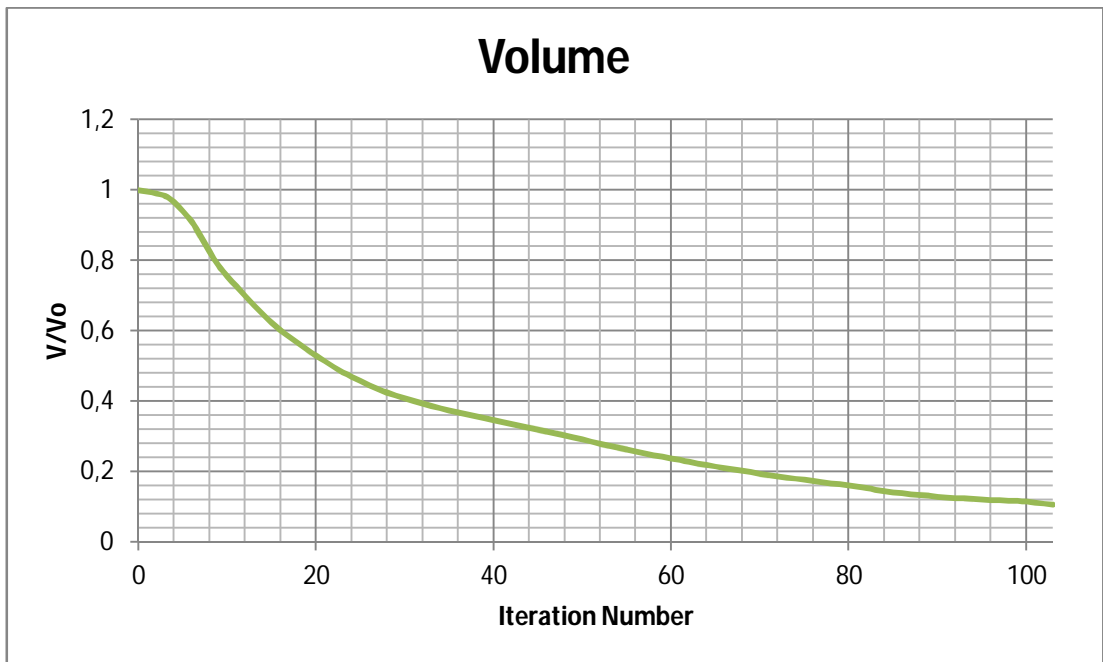


Figure 4.16 Volume reduction vs. iteration numbers for optimized lug.

The optimized lug maximum von Mises stress is monitored in Figure 4.17. The maximum stress in load case 1 changes rapidly; however the maximum stress in load case 2 almost stationary. Since stress application region of load case 1 are removed rapidly whereas stress application region of load case 2 does not vanish.

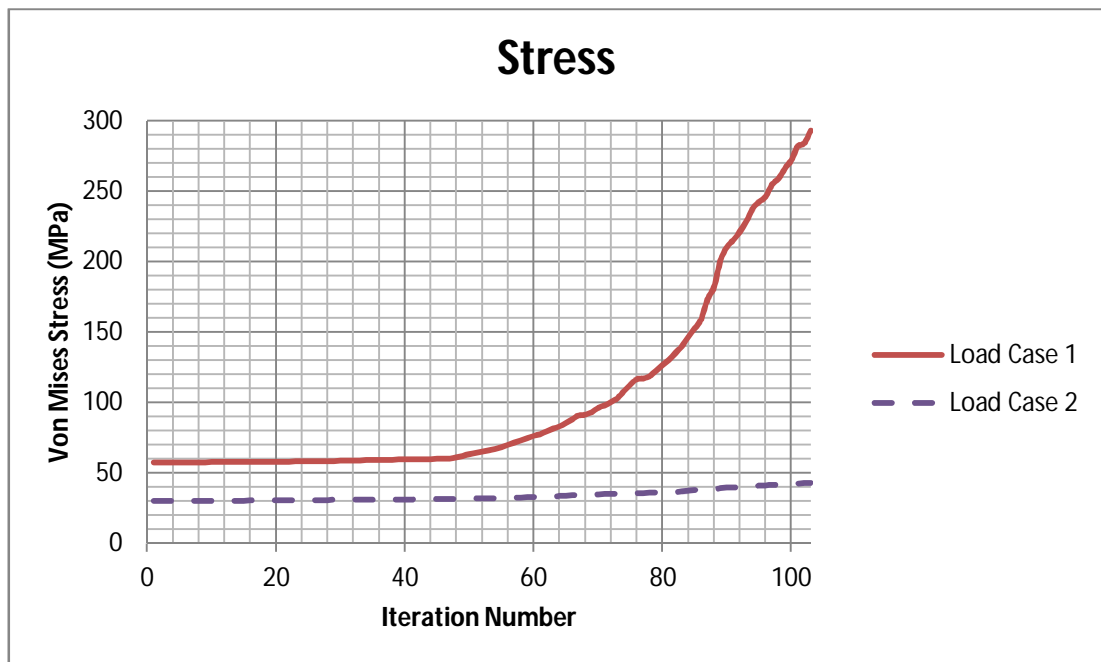


Figure 4.17 Maximum von Mises Stress vs. iteration numbers for optimized lug.

For post processing of the optimized lug, “xdb” file is attached on the “bdf” file using MSC.PATRAN in Analysis- Access Results- Attach xdb- Select Result File section. Then apply Result tab, choose object as Fringe, select desired Result Case to obtain the von Mises stress distribution of the optimized lug. Same load and boundary conditions are applied to existing design. The stress spectrums of optimized lug and existing design are matched to compare the stress distribution change regions easily and to increase visualization. The stress distribution of lug in load case 1 for existing design and optimized topology is shown in Figure 4.18 and 4.19 respectively. The maximum von Mises stress of lug for load case 1 is increased from 151 MPa to 293 MPa, i.e., 94% increase.

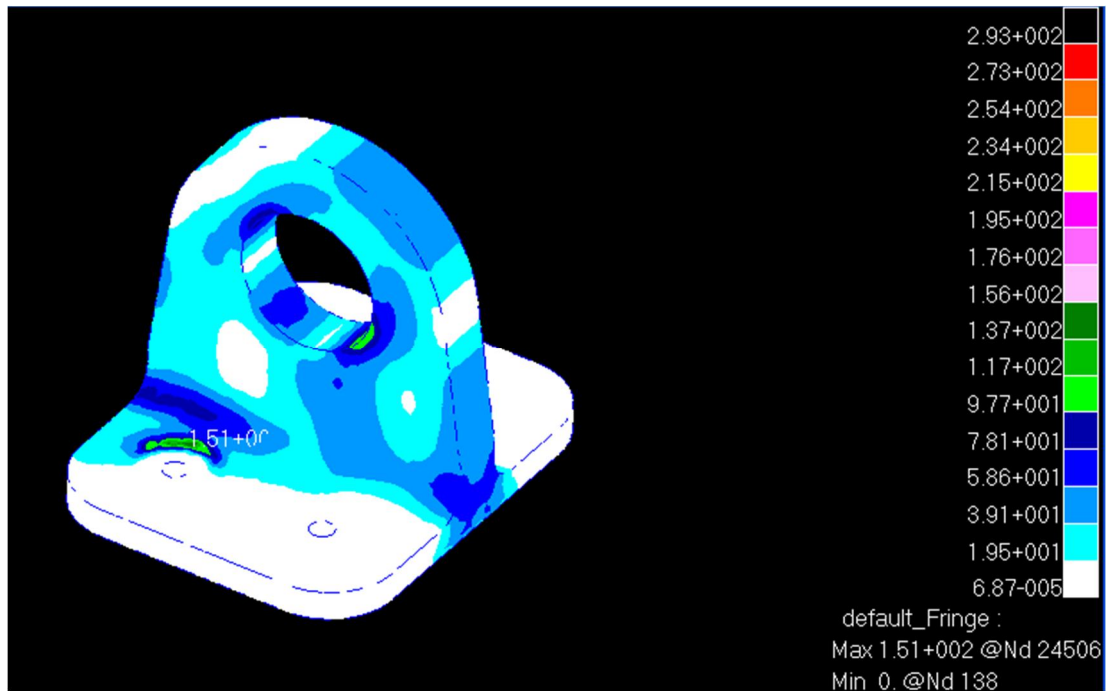


Figure 4.18 The von Mises stress distribution of existing design lug for load case 1.

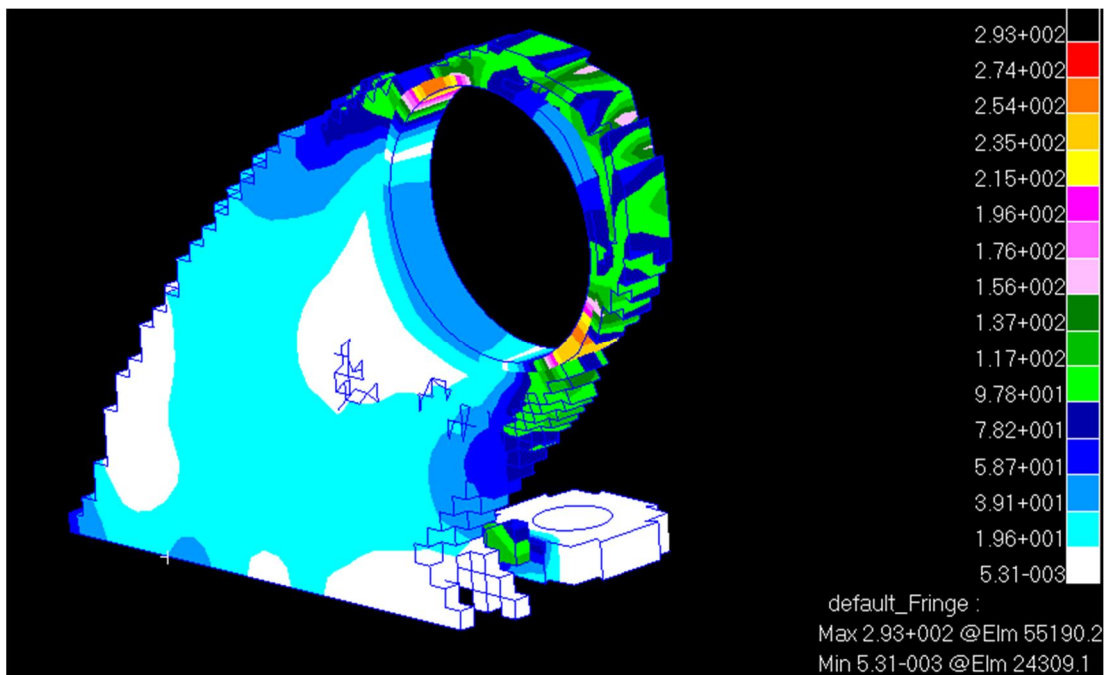


Figure 4.19 The von Mises stress distribution of optimized lug for load case 1.

The stress distribution of lug in load case 2 for existing design and optimized topology is shown in Figure 4.20 and 4.21 respectively. The maximum von Mises stress is decreased from 59 MPa to 43 MPa, i.e. 27.1% decrease.

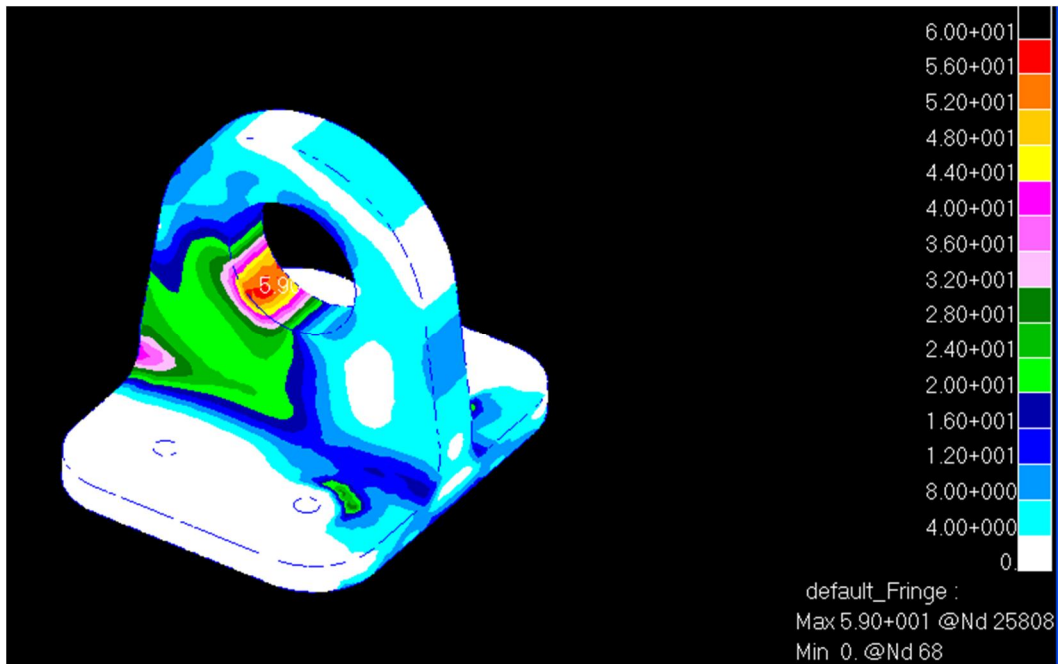


Figure 4.20 The von Mises stress distribution of existing design lug for load case 2.

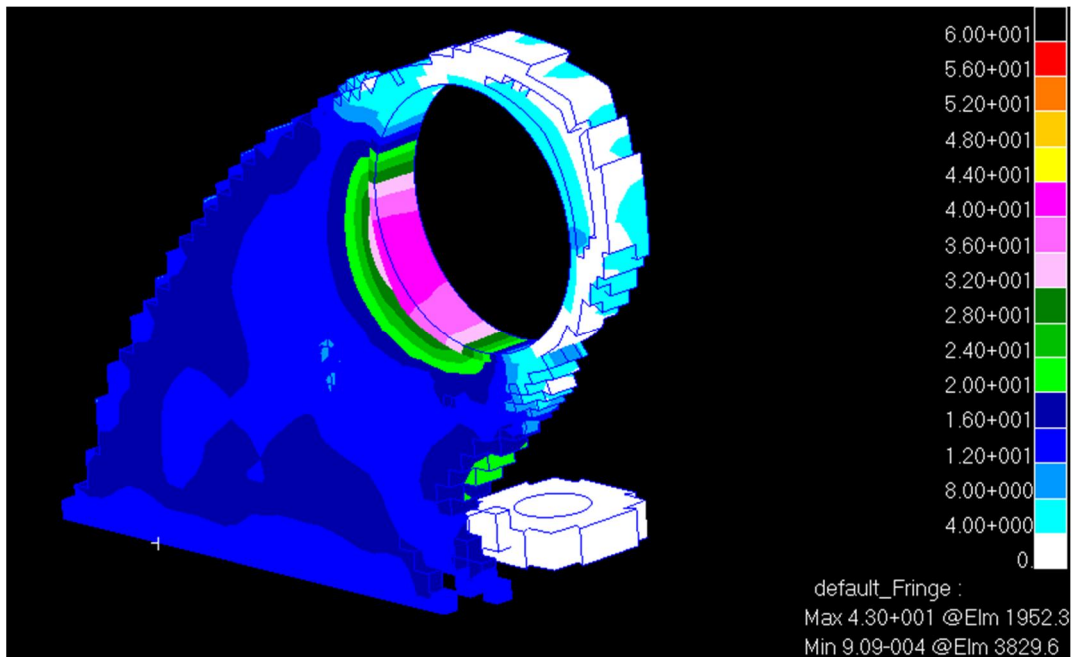


Figure 4.21 The von Mises stress distribution of optimized lug for load case 2.

Two lugs, optimized and existing design lugs are compared topologically in Figure 4.22. The optimized lug occupies different area than existing design, since an elongated initial domain is to be defined. The optimized lug takes form according to load direction. The orientation of optimized lug has almost the same angle with load direction. Lug bearing thickness is a

geometrical constraint, therefore same thicknesses are acquired. Besides, rivet positions and spacing are constraint due to mating component on aircraft. As the load direction is closer to the back rivets, more elements are placed at the back side whereas fewer elements are utilized at front side. Unnecessary elements and regions can be visualized easily by comparing the lugs. The regions between the rivets and side areas around the rivets, zones not closer to the load directions, elements around the bearing thickness and areas connecting rivets to the structure can be removed to obtain weight reduction. Mass of the lug decreased from 23.9 g to 10.9 g, 54.4% reduction in weight. The evaluation of the optimized lug is presented in Appendix B from Figure B.1 to B20.

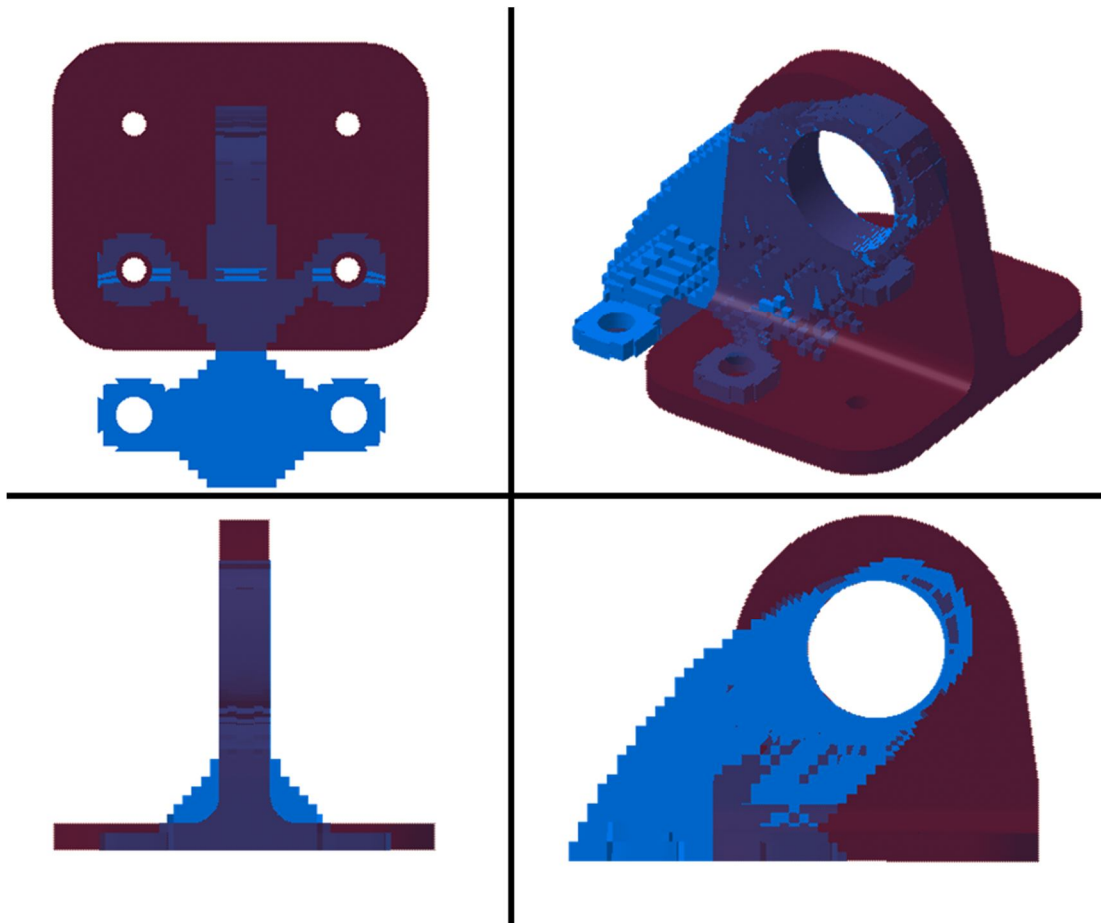


Figure 4.22 Top, front, right side and isometric view of existing design and optimized lug. Existing design is red, optimized topology is blue.

4.3. CLEVIS

Clevis is fork like structure that covers the two faces of lug. The initial design domain is formed with two arms and rod end for tube connection. The clevis is threaded into a tube, thread standards are selected; therefore the clevis end has a geometrical constraint and stated as non-design domain. Bushings are seated into the clevis to reduce the effect of wear with bolt and to protect the clevis integrity. The elements inside the hole are in contact with bushing; therefore these elements are also portion of non-design domain. The spacing between clevis arms are defined according to lug width which was predetermined due to bearing geometry and required spacing between bushing and bearing. Thus this region is a geometrical constraint. The initial half and full design domains which are formed using geometrical constraint is shown in Figure 4.23. The load and boundary conditions are symmetrical therefore; the half of the bulk volume is modeled and solved. Same constraints are applied to clevis for symmetrical model.

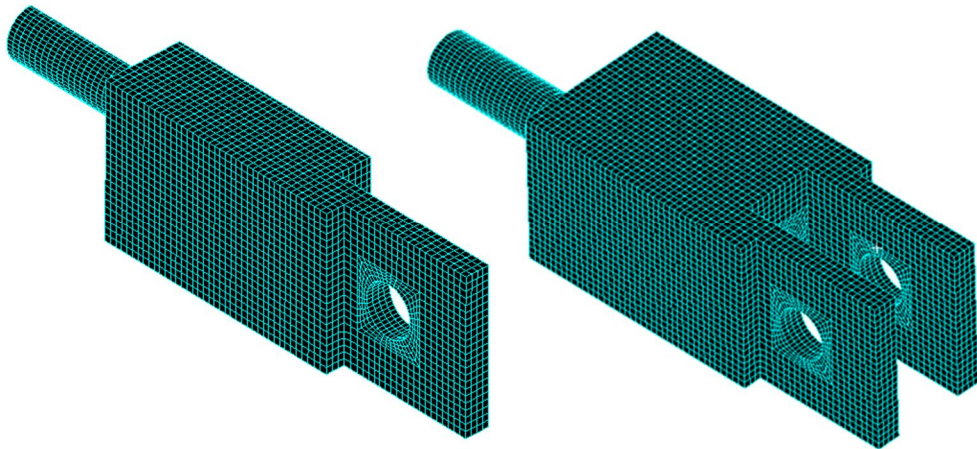


Figure 4.23 The half and full bulk model of clevis.

The holes create node connectivity problems during mesh, whether three dimensional solid hexahedron mesh is utilized. The regions around holes are meshed independently and after creating initial design domain, node connectivity should be controlled as performed for lug. The initial geometry includes 19761 hexahedron elements and 24144 nodes. The half bulk model is chosen to decrease the process time compared to full model. Also the numerical errors that break the symmetry can be avoided using half model. The number of elements for full model is 39522.

The load is distributed sinusoidal around the bushing holes with the same principle of lug. The reaction load of lug at load direction is maximum and approaches to zero, as deviating from load direction as presented in Figure 4.24. The direction of force is parallel to clevis structure, therefore only compression and tension occurs in clevis arms. Reaction force is assumed to split into two arms equally as the geometry is symmetrical. The clevis end is threaded to the tube therefore the elements at the top, facing with inner side of the tube are support points shown in Figure 4.25.

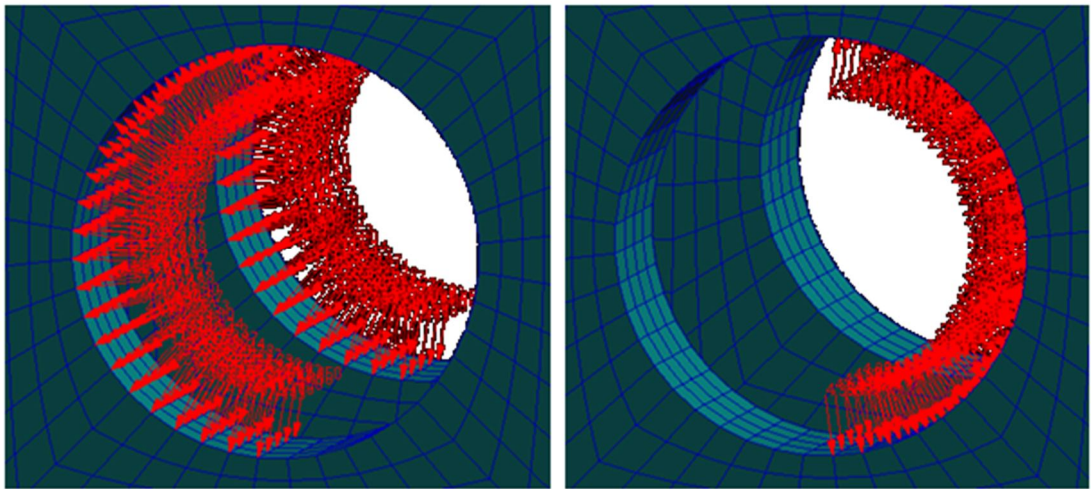


Figure 4.24 The load distribution in bushing holes for load case 1 on the left and for load case 2 on the right.

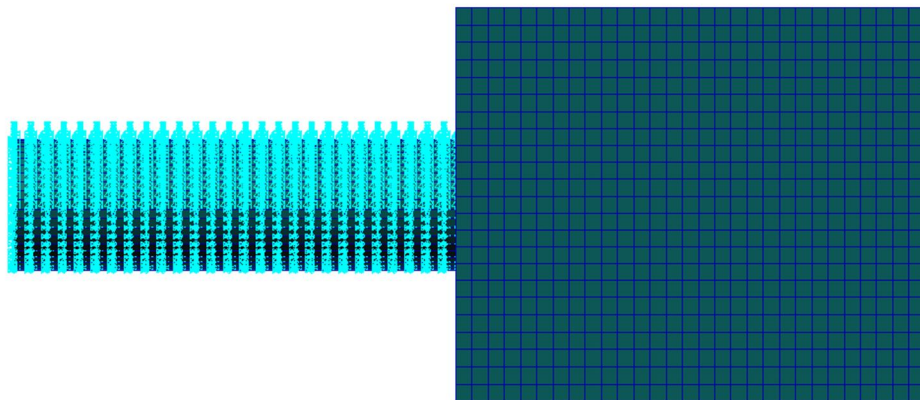


Figure 4.25 The support elements of the clevis end.

The design and non-design domain in initial geometry are shown in Figure 4.26. Red color represents design domain, whereas white color is non-design domain. One element thickness around the bushing hole and clevis end is protected.

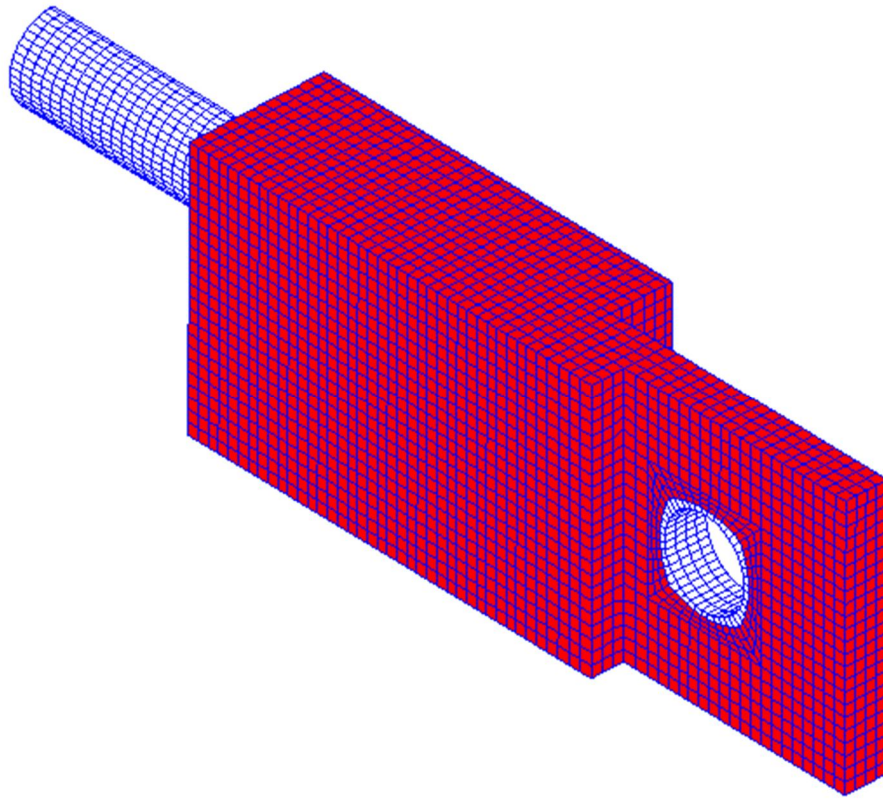


Figure 4.26 The design and non-design domain of clevis

The initial rejection ratio, RR_0 , and evolutionary rate, ER , is chosen as 0.25%. The number of load cases is 2 and allowable stress, σ_e^{max} is 293 MPa as input. The optimized result is obtained at 125th iteration, i.e. rejection ratio, RR , 31.25%. The final geometry contains 8602 elements, 5158 is non-design domain. The views of the optimized clevis are presented in Figure 4.27 and 4.28.

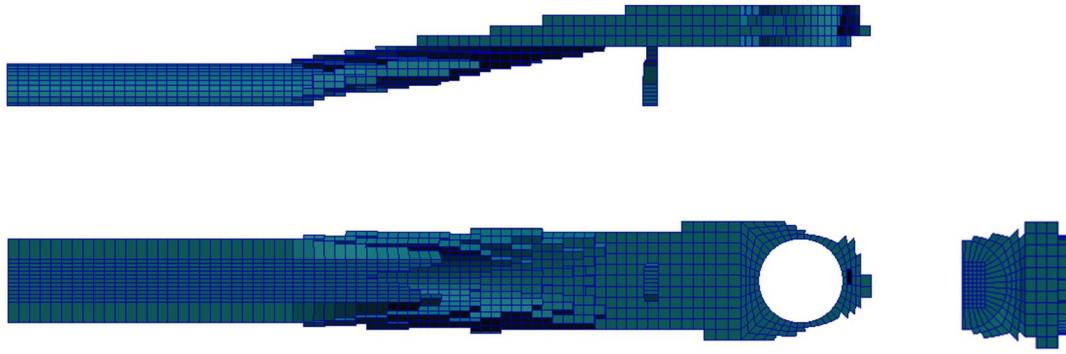


Figure 4.27 The front, top, right view of the optimized clevis.

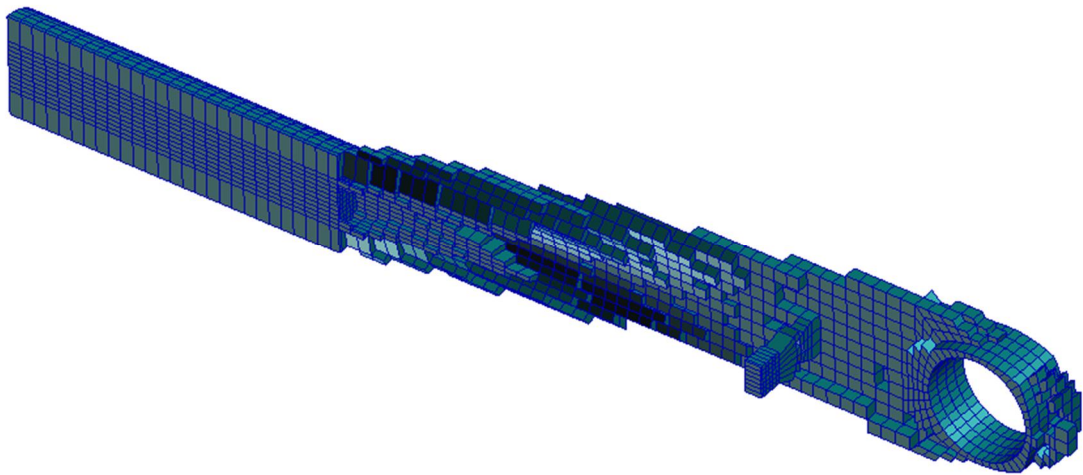


Figure 4.28 The isometric view of the optimized clevis.

The iterations took 3 hours 56 minutes and 31 seconds on an Intel Core 2 Duo T9550 4 Gigabyte RAM computer. Total progress time vs. iteration number is monitored in Figure 4.29. 1st iteration duration is 6 minutes whereas 104th iteration takes less than 30 seconds, the process time decreases drastically. Iteration time is highly related with number of elements. As the number of elements decreased in further iterations, iteration duration decreases.

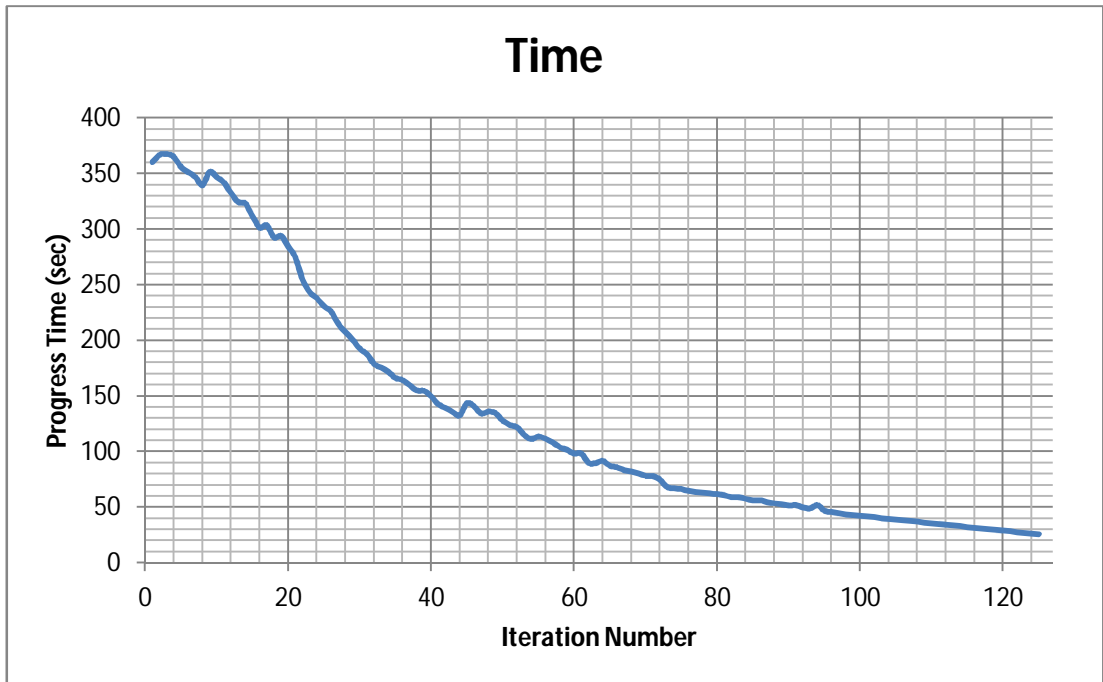


Figure 4.29 Total progress time vs. iteration numbers for optimized clevis.

78.2 % of the initial volume and 90 % of the initial design domain is removed. The volume reduction graph is shown in Figure 4.30. The volume reduction rate decreases as the iteration number increases as expected.

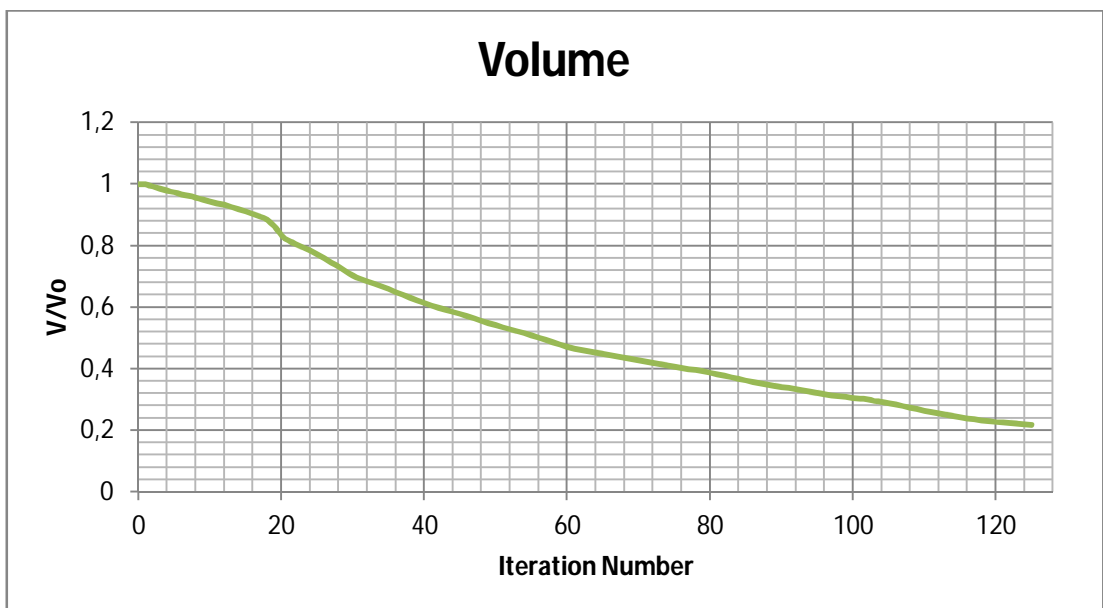


Figure 4.30 Volume reduction vs. iteration numbers for optimized clevis.

Maximum von Mises stress of elements and iteration number is presented in Figure 4.31. The maximum stress at load case 1 is greater than the maximum stress at load case 2; however as the elements around the bushing hole is removed maximum stress at load case 2 increases more rapid than load case 1.

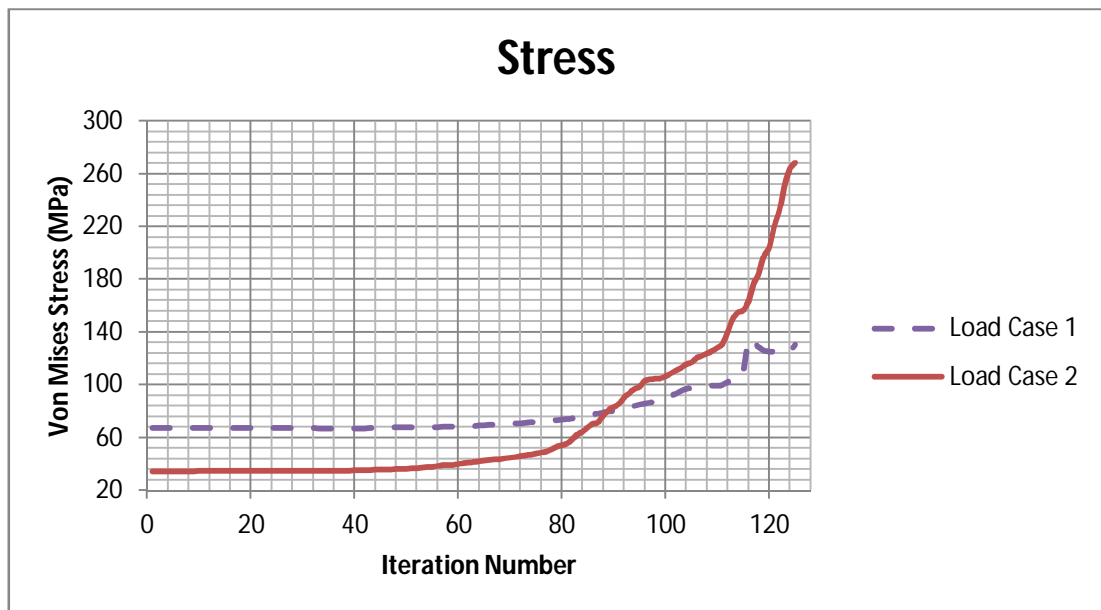


Figure 4.31 Maximum von Mises Stress vs. iteration numbers for optimized clevis.

For post processing of the optimized clevis same procedures with lug is conducted. Same load and boundary conditions are applied to existing design. The stress distribution of lug in load case 1 for existing design and optimized topology is shown in Figure 4.32 and 4.33 respectively. The maximum von Mises stress of clevis for load case 1 is increased from 78 MPa to 130.6 MPa, i.e., 67.4% increase.

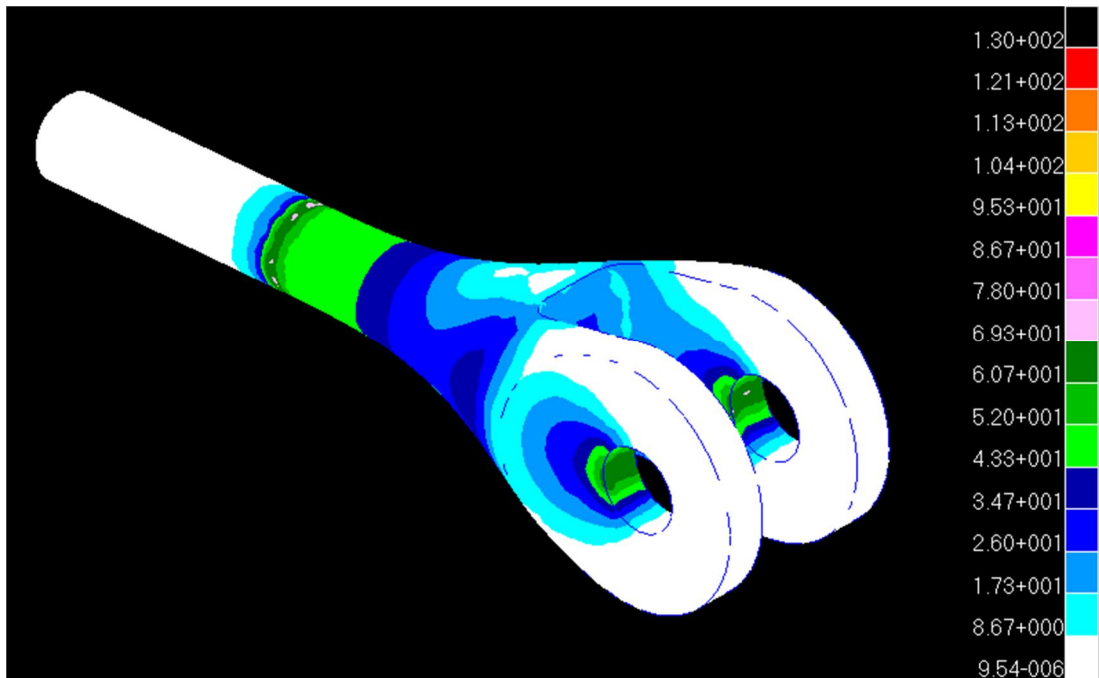


Figure 4.32 The von Mises stress distribution of existing design clevis for load case 1.

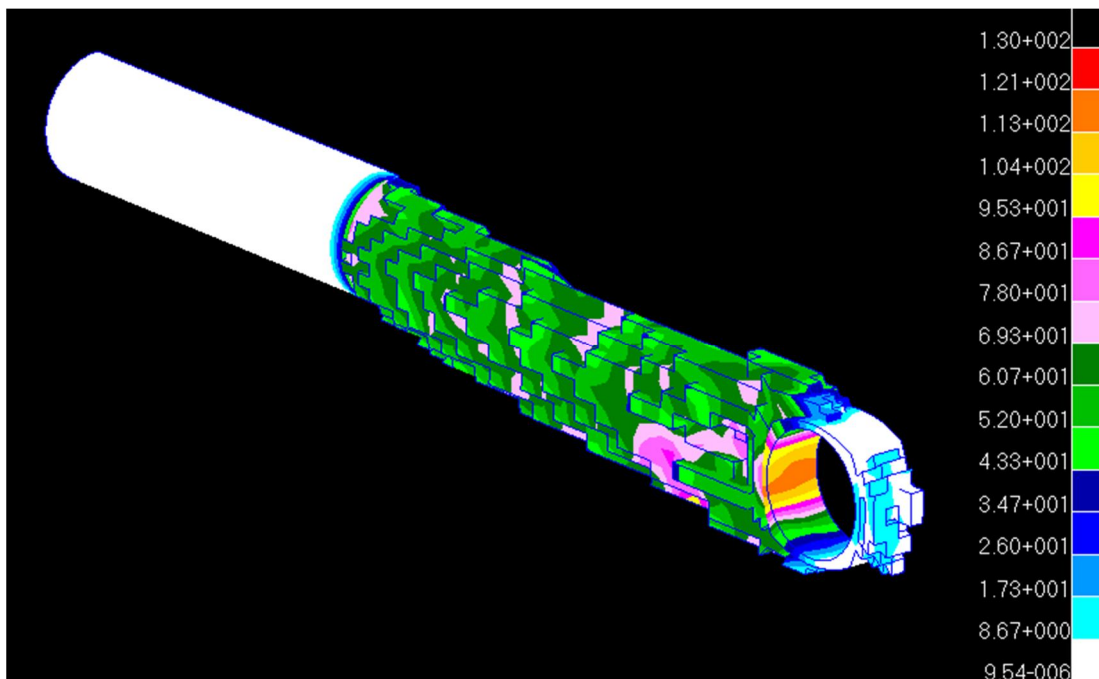


Figure 4.33 The von Mises stress distribution of optimized clevis for load case 1.

The stress distribution of clevis in load case 2 for existing design and optimized topology is represented in Figure 4.34 and 4.35 respectively. The maximum von Mises stress of clevis for load case 2 is increased from 45.6 MPa to 268 MPa, i.e. 487.7% increase.

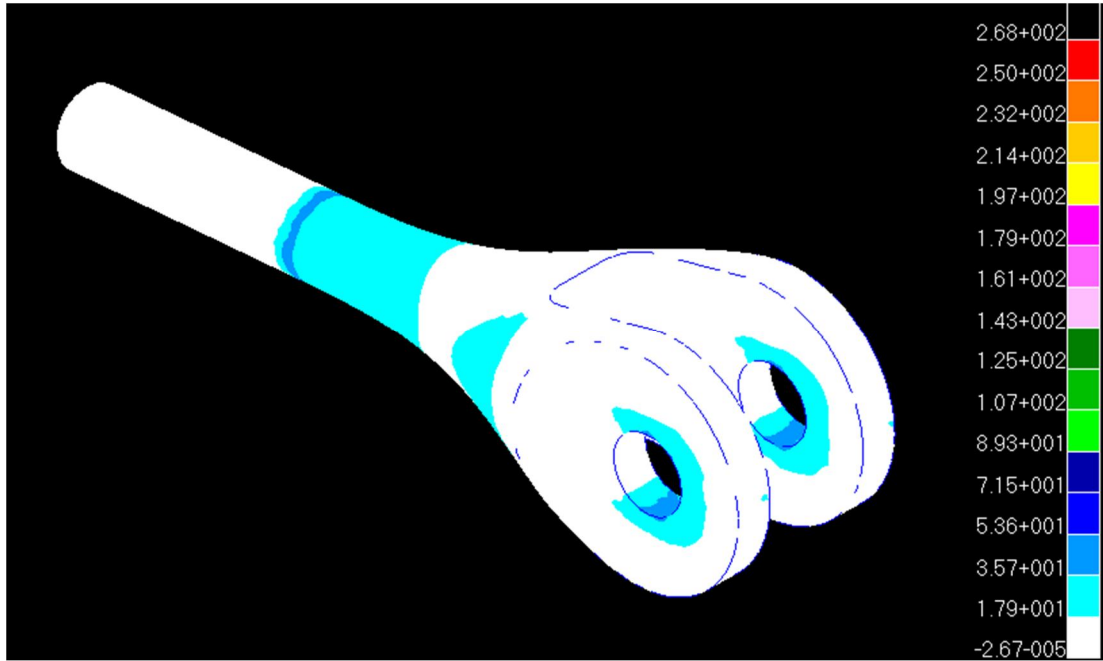


Figure 4.34 The von Mises stress distribution of existing design clevis for load case 2.

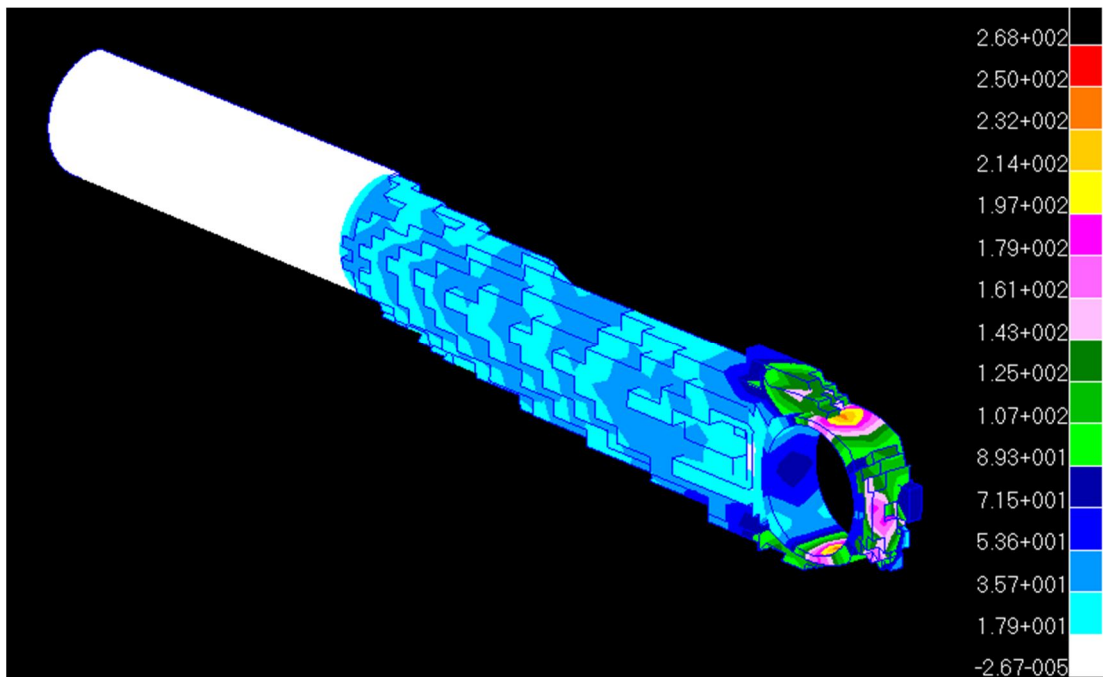


Figure 4.35 The von Mises stress distribution of optimized clevis for load case 2.

Two clevis, optimized and existing design lugs are compared topologically in Figure 4.36. Bushing hole diameter and bushing length is predefined. The tube geometry is fixed; therefore these areas are defined as non-design domain. These elements cannot be removed even the

stress values are low at clevis end. The low stress elements in design domain are removed and during comparison, unnecessary regions can be visualized. Bending is not applied; therefore the width of the clevis arm can be reduced. The optimized geometry suggests changing the transition geometry of clevis arm to clevis end. Instead of concave, convex geometry is formed. Mass of the clevis decreased from 24.8 g to 11.7 g, 52.8% reduction in weight. The design domain of existing design is 21 g to 7.9 g 62.4% decrease in weight. The evaluation of the optimized clevis is presented in Appendix B from Figure B.21 to B.40.

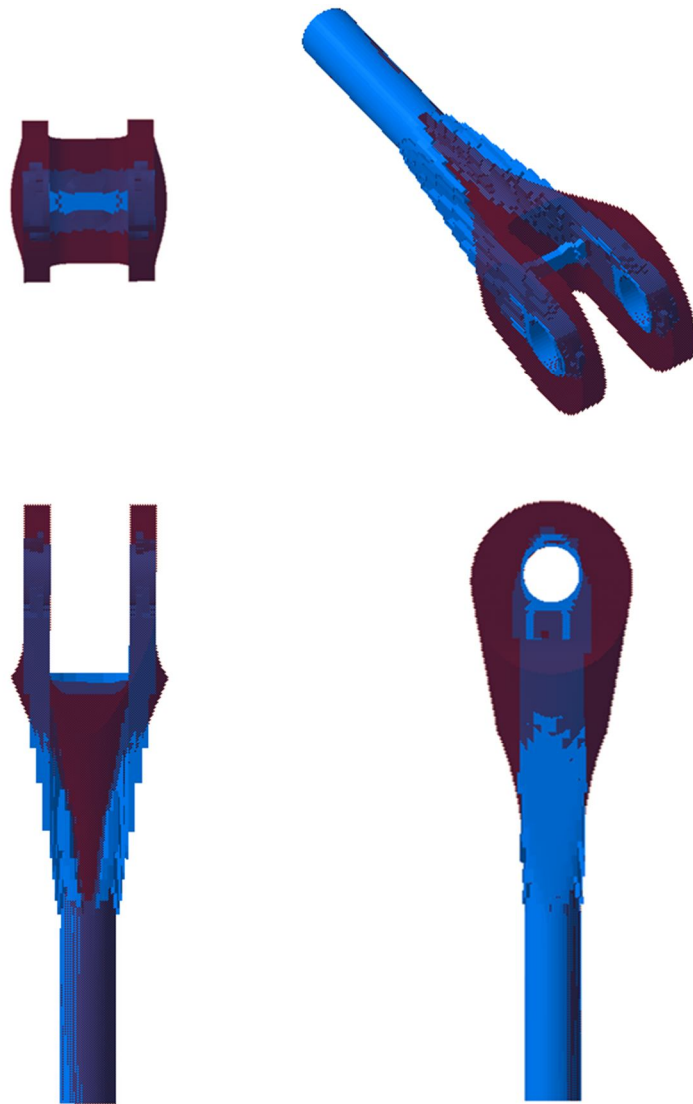


Figure 4.36 Top, front, right side and isometric view of existing design and optimized clevis. Existing design is red, optimized topology is blue.

4.4. MAIN LANDING FITTING

Landing system is a primary structure of an aircraft which is functional during landing and parking on the ground. Two main and a nose landing assemblies form the landing system of the aircraft. Nose landing assembly is located at the front fuselage whereas two main landing assemblies are placed at right and left wings. Main landing assemblies are positioned between rear and main spar since there is high load bearing ability and it is connected to structure via fittings. The landing gear main fitting is a part of main landing assembly, designed to carry the relatively high landing forces. Aircraft wheel is connected to trailing arm which is attached to the torque link and piston. Main landing assembly is actuated by a piston. The landing assembly folds into the body after take-off and is opened before landing by the piston. Mooring ring connects the aircraft to ground at parking position. Brake system is utilized to form hydraulic pressure for tire brakes. Electrical connections power the landing lights. Figure 4.37 presents the main landing fitting and other components of the assembly.

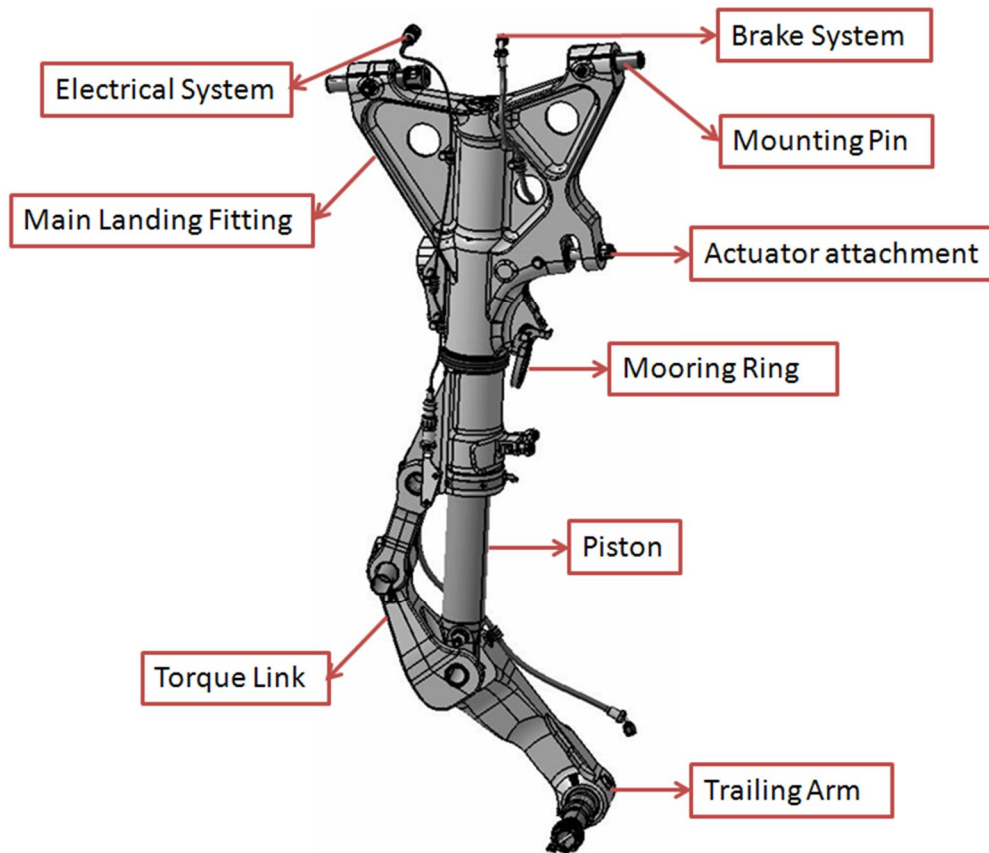


Figure 4.37 Components of main landing assembly.

Main landing fitting is the essential load carrier of the main landing assembly which is loaded through torque link, actuator attachment and piston. Landing light creates additional load on the fitting, though minor compared to forces applied by the torque link and the actuator. The fitting is connected to aircraft via mounting pins. The schematic representation of load and boundary conditions are presented in Figure 4.38.

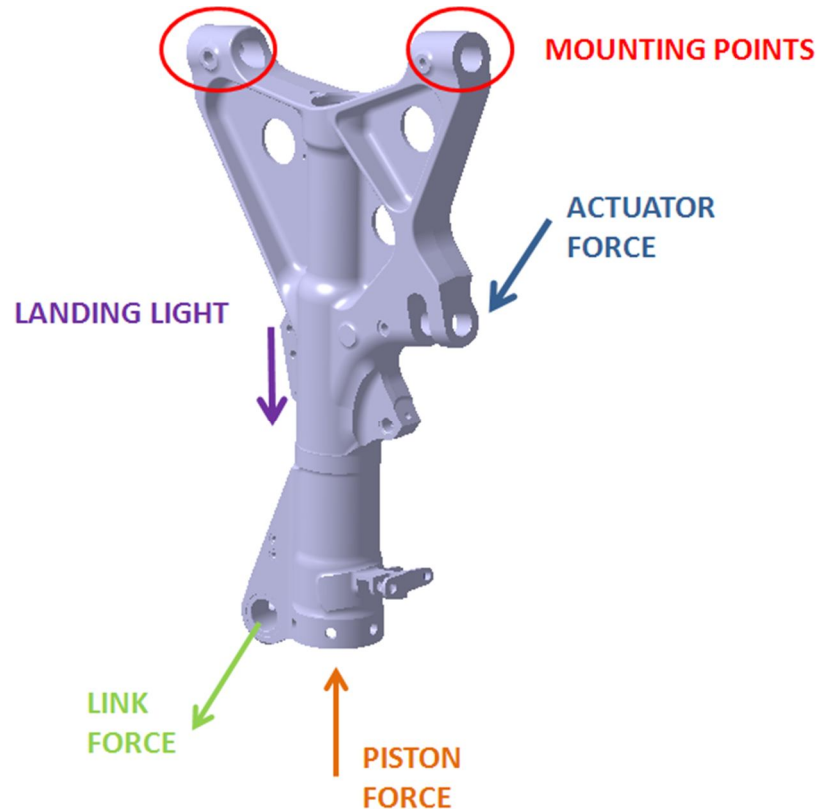


Figure 4.38 The load and boundary conditions of the main landing fitting.

The connection concept of main landing fitting and actuator rod end are similar to lug and clevis connection. The bearing is seated into actuator end and the load is transferred via bolt to sleeve and flanged bushing. Bushings are located in the main fitting for load carriage. The connection is shown in Figure 4.39. Actuator transmits force along its longitudinal direction. Torque link and main landing fitting is attached through connection pin. Secure pin is located to avoid translational movements and disassembly of torque link and main landing fitting. Two flanged bushings transfer the load from torque link to connection pin as shown in Figure 4.40. The landing light case is connected to main landing fitting via three rivets with rivet locations predetermined.

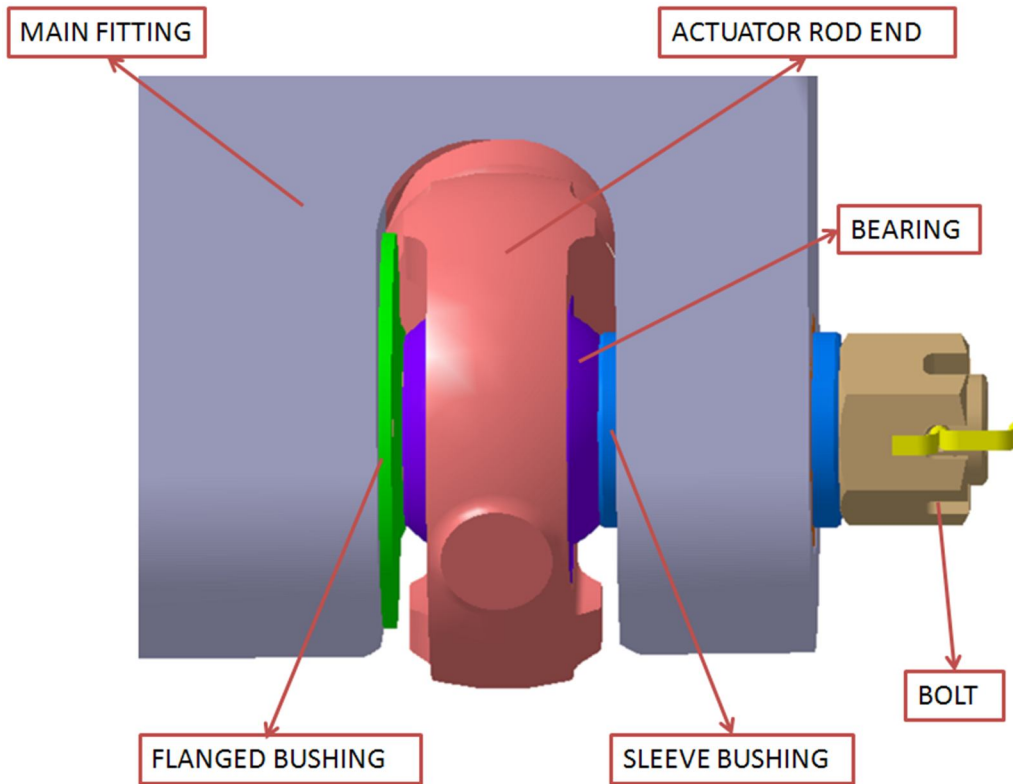


Figure 4.39 The connection of main landing fitting and actuator rod end.

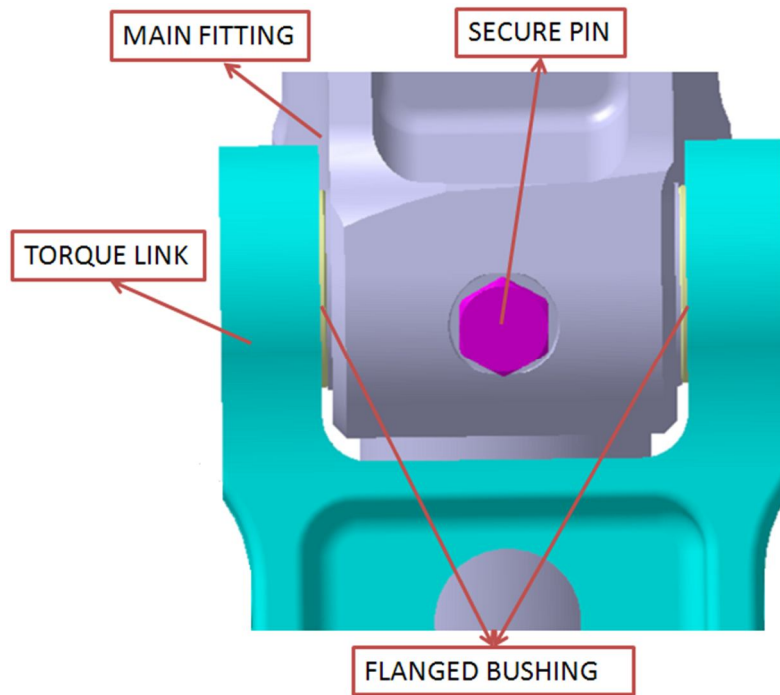


Figure 4.40 The connection of main landing fitting and torque link.

The material of the main landing fitting is Aluminum 7075 T7451. The maximum allowable stress was presented in Eq. 4.6. The initial model is formed by covering all volume of the part. The piston housing, mounting points, mooring lug and other geometries are thickened and applied to model. The thickness of the whole component has geometrical limit since the main fitting should fit into a certain volume after takeoff. Final “V” shape is modeled as a rectangular prism to reveal the load path of the fitting. The lug which is sheltering the mooring ring, is widened to observe the transition geometry of rectangular prism to cylinder housing. The geometry near torque link is preserved since a predefined routing is attached. The non-design domain that should not be modified are;

- Housing the piston
- Mounting area
- Torque link, actuator and landing light load elements
- Lug sheltering mooring ring
- Routing holder lug.

The force exerted elements are kept since the bushing or rivet is seated on these elements. The optimization is performed for a single load case which is the emergency landing where the forces are very high compared to all other landing scenarios. The initial model of the main landing fitting is shown at Figure 4.41. As the initial model of the component is more complex than the lug and the clevis tetrahedron mesh is selected. Tetrahedron mesh does not require meshing area around the holes separately. The bulk model of the fitting includes 225949 elements and 43874 nodes.

The major forces of the main landing fitting exerted from torque link and actuator are modeled as sinusoidal pressure distribution in MSC.NASTRAN since the stress level observed along the direction of forces is maximum and decrease with the deviation from the load direction and vanishes at perpendicular sides. Sinusoidal pressure distribution is more realistic and successful in modeling while load is transferred from one component to other via bushings in Figure 4.42. Actuator operates longitudinally therefore the reaction force is applied along the direction of actuator. As the center of gravity of landing light and the case are known, the weight is distributed to predefined rivet holes of structure via Multi Point Constraint (MPC) in Figure 4.43. Piston force is distributed to housing with the same principle. Each purple line directs to a load carrier node from center of gravity. Main landing fitting is supported by pins at the top of the structure shown at Figure 4.44.

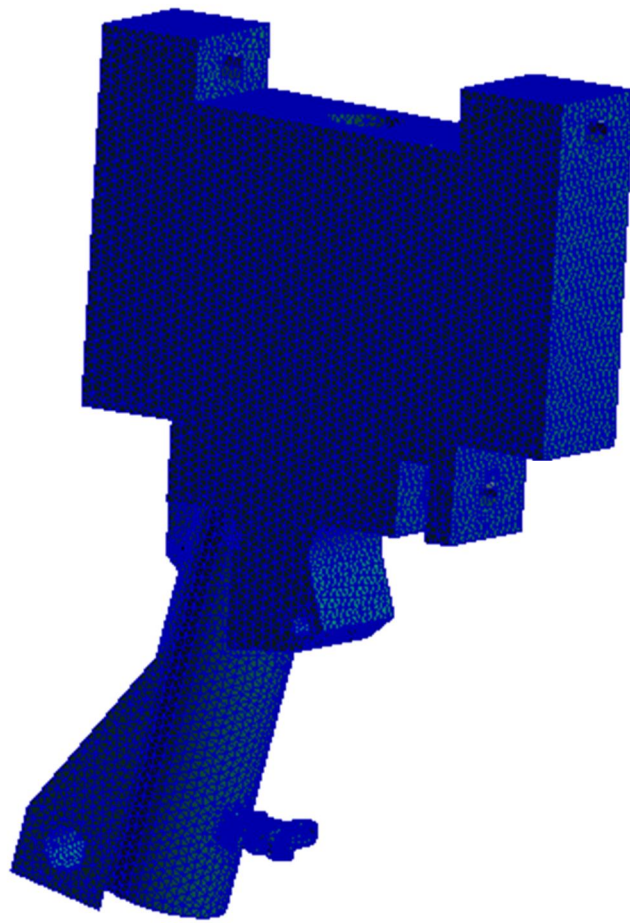


Figure 4.41 The bulk model of main lading fitting.

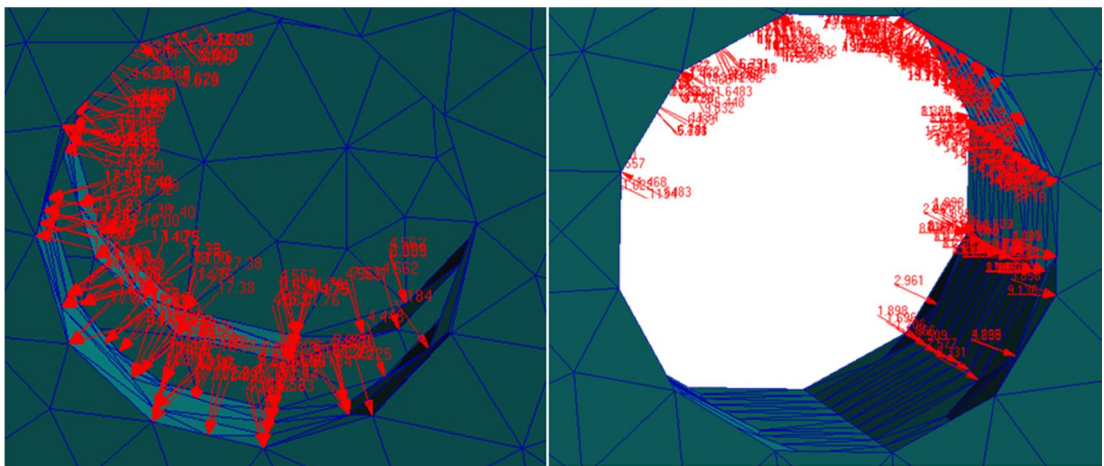


Figure 4.42 The sinusoidal load distribution in bushing holes via actuator on the left and via torque link on the right.

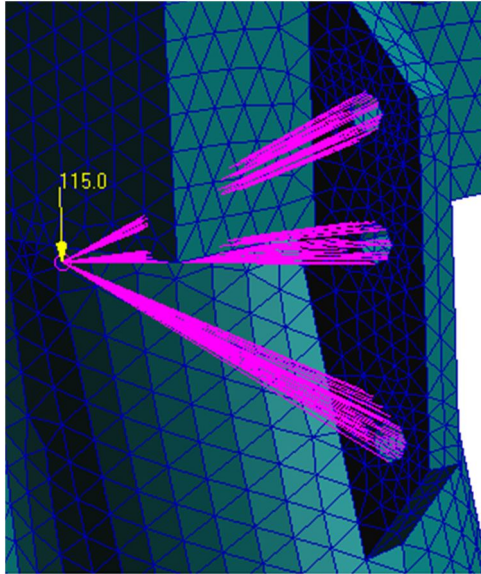


Figure 4.43. The MPC force distribution from CG of landing light to rivet holes.

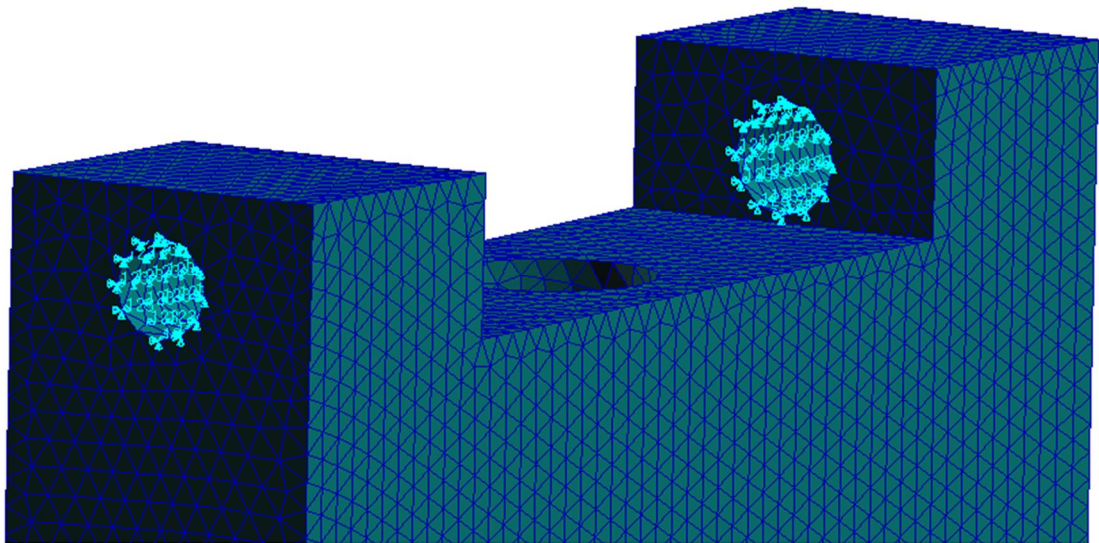


Figure 4.44. The support elements of main landing fitting.

The design and non-design domain in initial geometry are shown in Figure 4.45. Red color represents design domain, whereas white color is non-design domain. Bushing seated areas, structures required for electrical or hydraulic routing are labeled as non-design domain which should be retained regardless of the von Misses stress level.

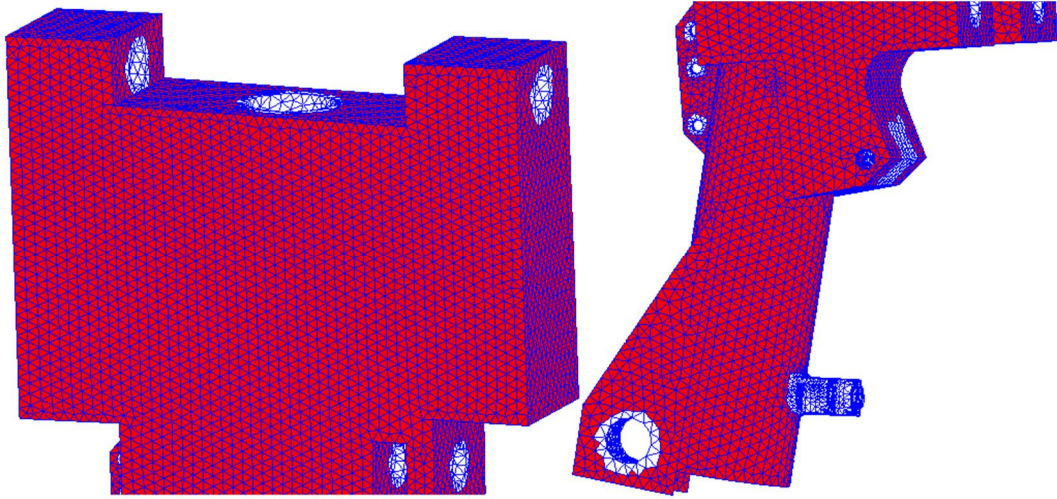


Figure 4.45. Design and non-design domain of main landing fitting.

The initial rejection ratio, RR_0 , and evolutionary rate, ER , is chosen as 0.25% to prevent instability problems. For single load case, allowable stress, σ_e^{max} is 293 MPa as input. The optimized result is obtained at 64th iteration, i.e. rejection ratio, RR , 14%. The final geometry contains 69376 elements, 21344, 30.8% of the whole structure is non-design domain. The views of the optimized main landing fitting are presented in Figure 4.46, 4.47 and 4.48.

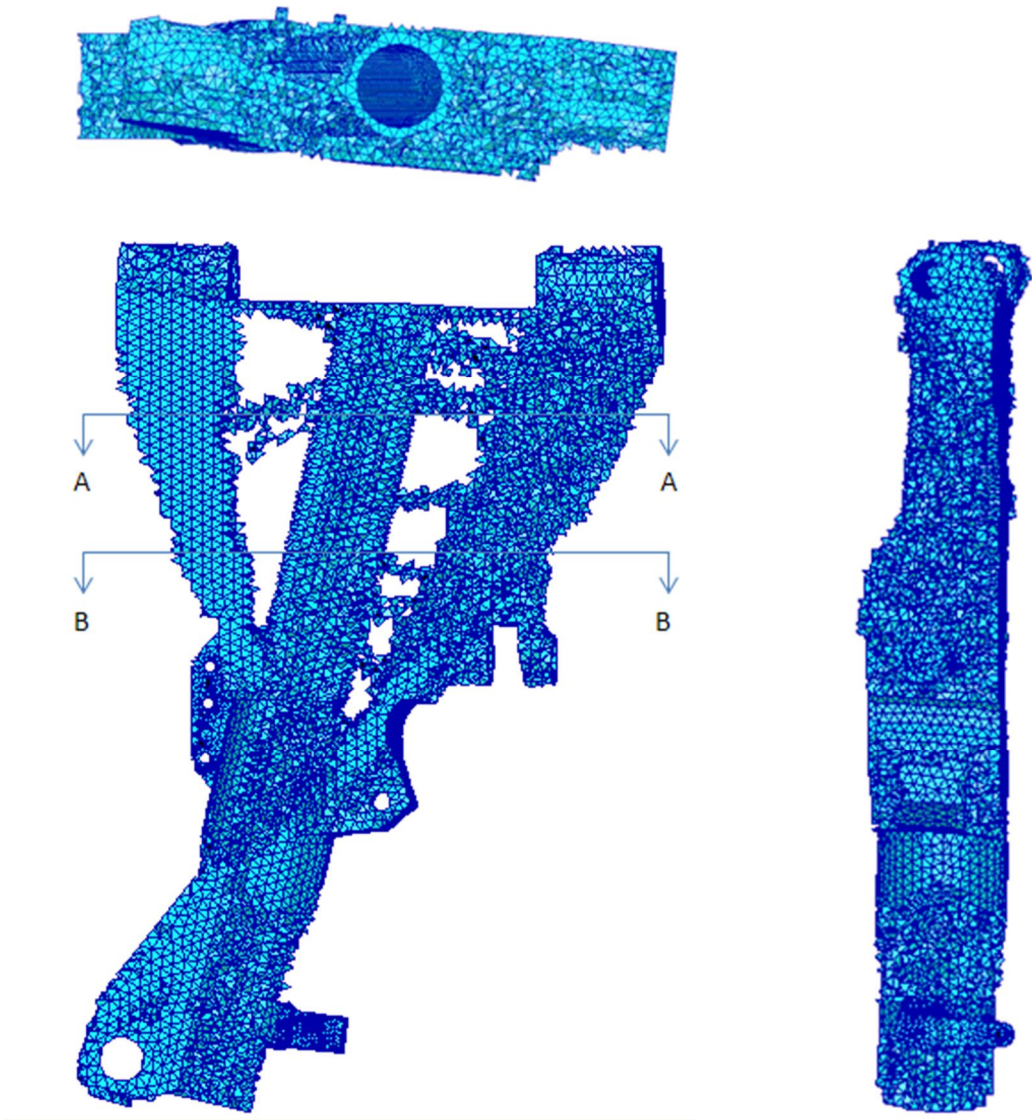


Figure 4.46 The front, top, right view of the optimized main landing fitting.

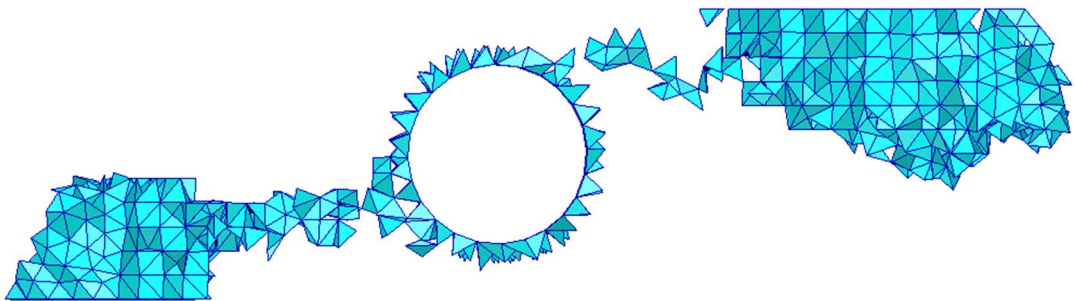


Figure 4.47 Section A-A of the Figure 4.46.

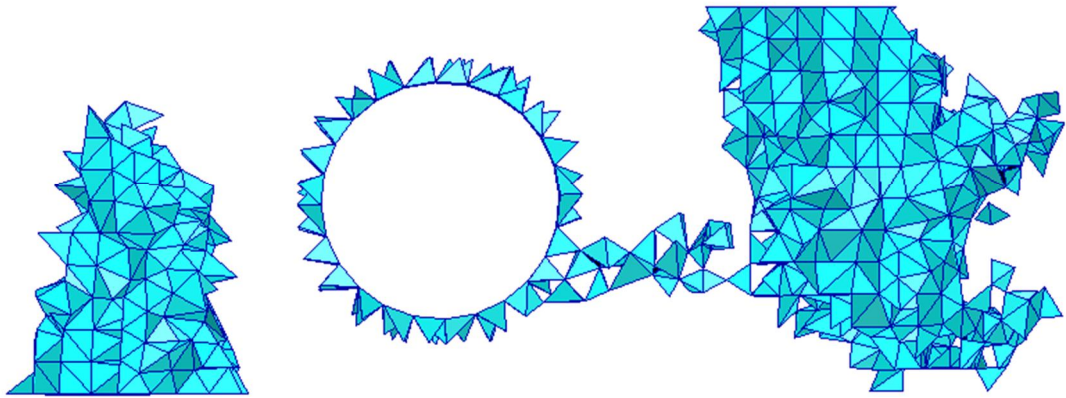


Figure 4.48 Section B-B of the Figure 4.46.

The optimization process continues for 4 days 11 hours 15 minutes and 20 seconds on an Intel Core 2 Duo T9550 4 Gigabyte RAM computer. Total progress time vs. iteration number graph is sketched in Figure 4.49. 1st iteration takes is 4 hours 35 minutes and 5 seconds whereas 56th iteration takes only 35 minutes and 41 seconds. Iteration time is highly related with element number. As the number of elements is decreased in further iterations, iteration duration reduces.

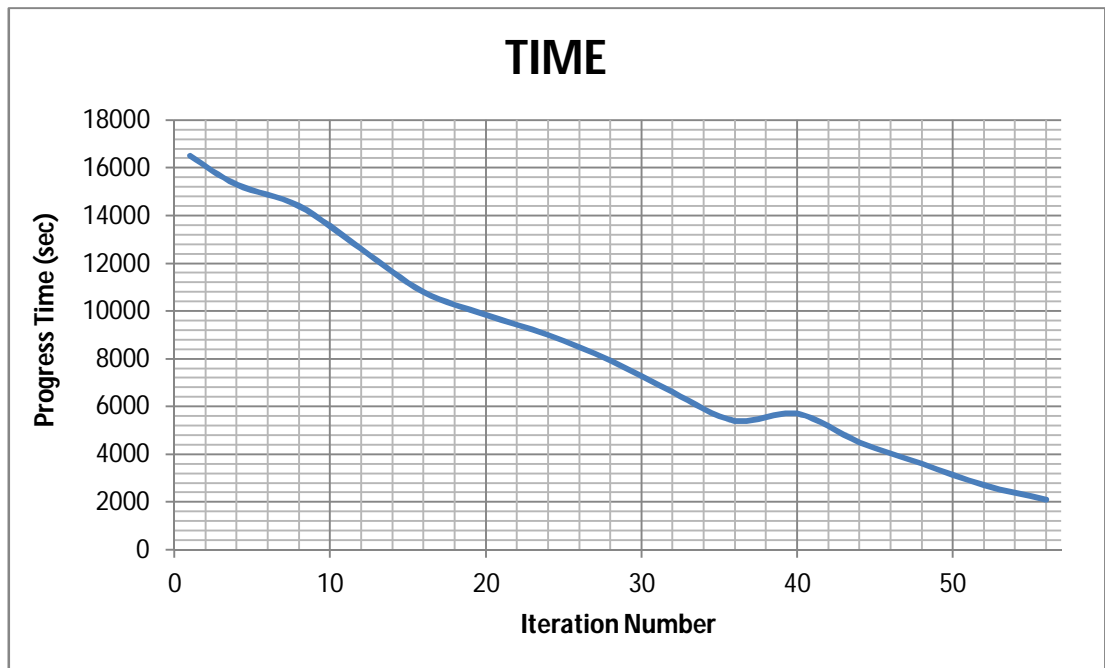


Figure 4.49 Total progress time vs. iteration numbers for optimized main landing fitting.

69.3 % of the initial volume and 76.5% of the initial design domain is removed. The volume reduction graph is shown in Figure 4.50. The volume reduction rate decreases as the iteration number increases as expected; however, more elements than the previous iterations are removed at the last steps due to the high level of rejection ratio. The optimization is terminated to avoid instability problems.

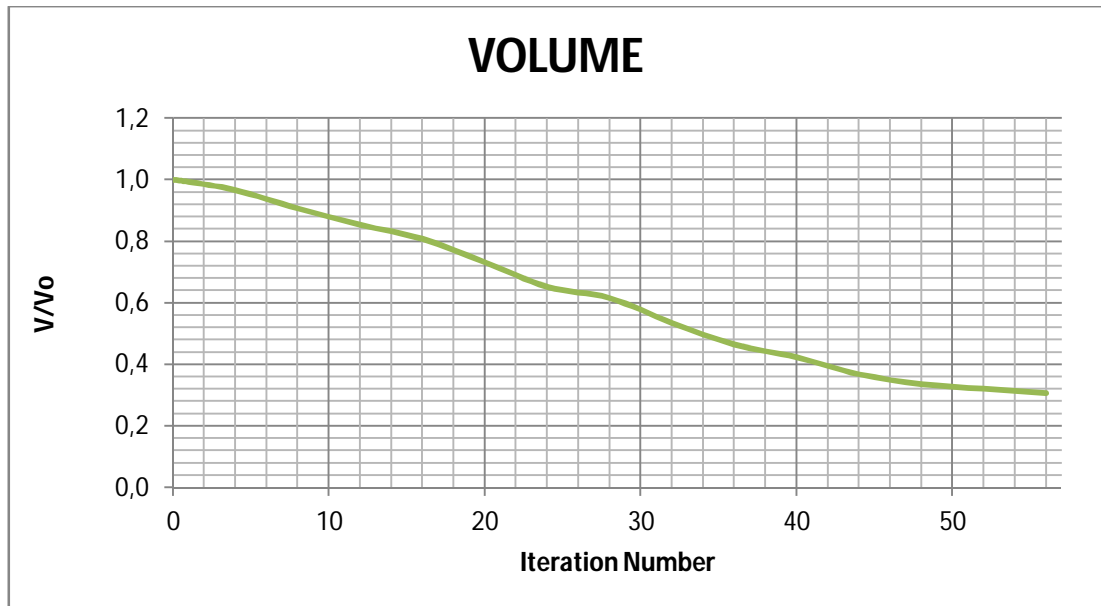


Figure 4.50 Volume reduction vs. iteration numbers for optimized main landing fitting.

Maximum von Mises stress of elements and iteration number is presented in Figure 4.51. The maximum von Mises stress increases as the number of elements decreases. High numbers of element removal during very first iterations, have little effect on the maximum stress level; however, as the number of elements and structure stiffness decreases, structure responds to element removals become more sensitive and maximum stress level increases more rapidly. The volume reduction at final iterations is almost the same amount with initial iterations, nevertheless, maximum stress increases rapidly, even the maximum stress level is virtually stationary at first iterations. The maximum stress has tendency to increase, whereas stress level reveals minor drops after some iterations. Load path changes or geometry of tetrahedral mesh may cause such a behavior.

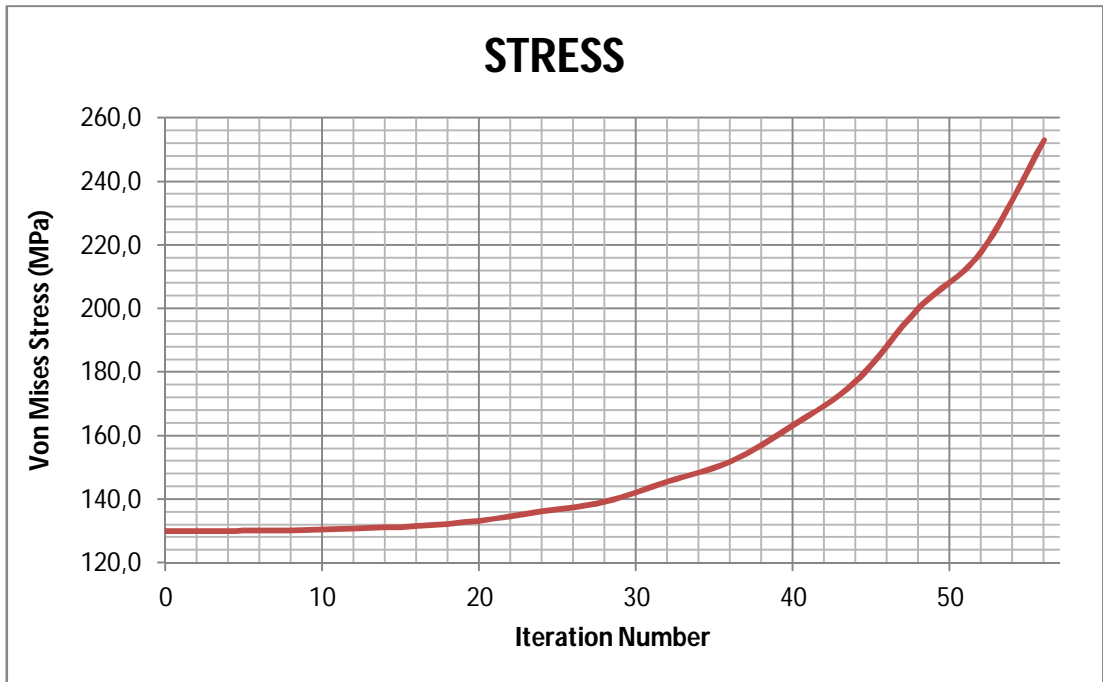


Figure 4.51 Maximum von Mises Stress vs. iteration numbers for optimized main landing fitting.

Same load and boundary conditions are applied to the existing design to compare the maximum stress level and stress distribution. The stress distribution of main landing fitting for existing design and optimized topology are shown in Figure 4.52 and 4.53 respectively. The maximum von Mises stress of main landing fitting is decreased from 276 MPa to 253 MPa, i.e., 8.3 % decrease. The displacement values of main landing fitting for existing design and optimized topology are shown in Figure 4.54 and 4.55 respectively. The maximum displacement decreased from 1.37 mm to 1.1 mm, 19.7 % decrease.

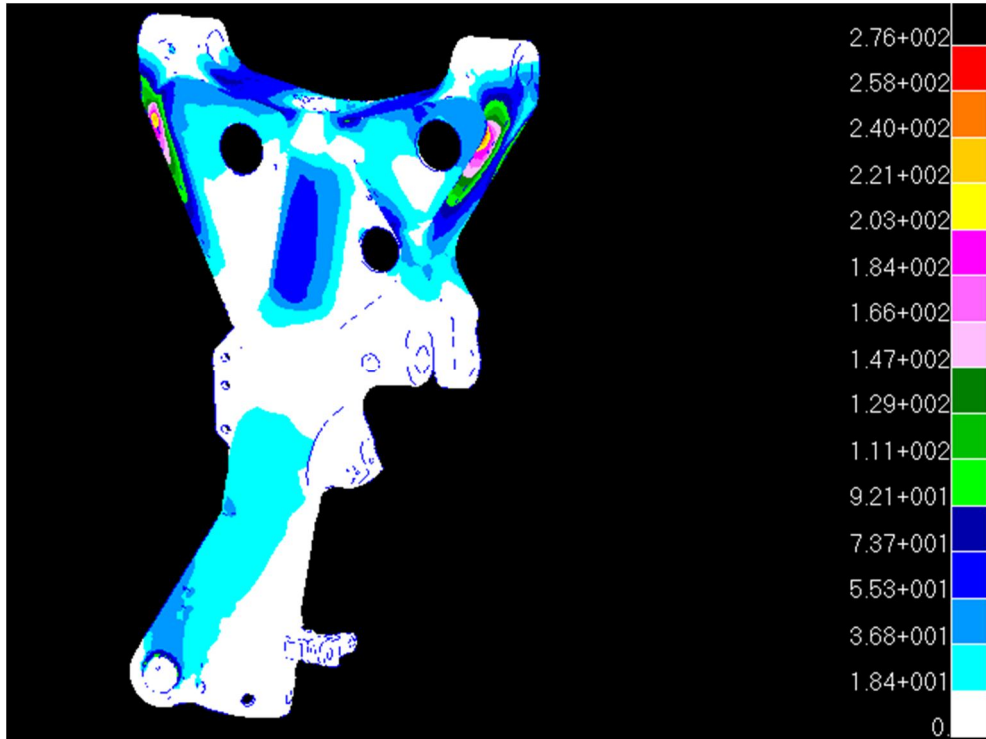


Figure 4.52 The von Mises stress distribution of existing design main landing fitting.

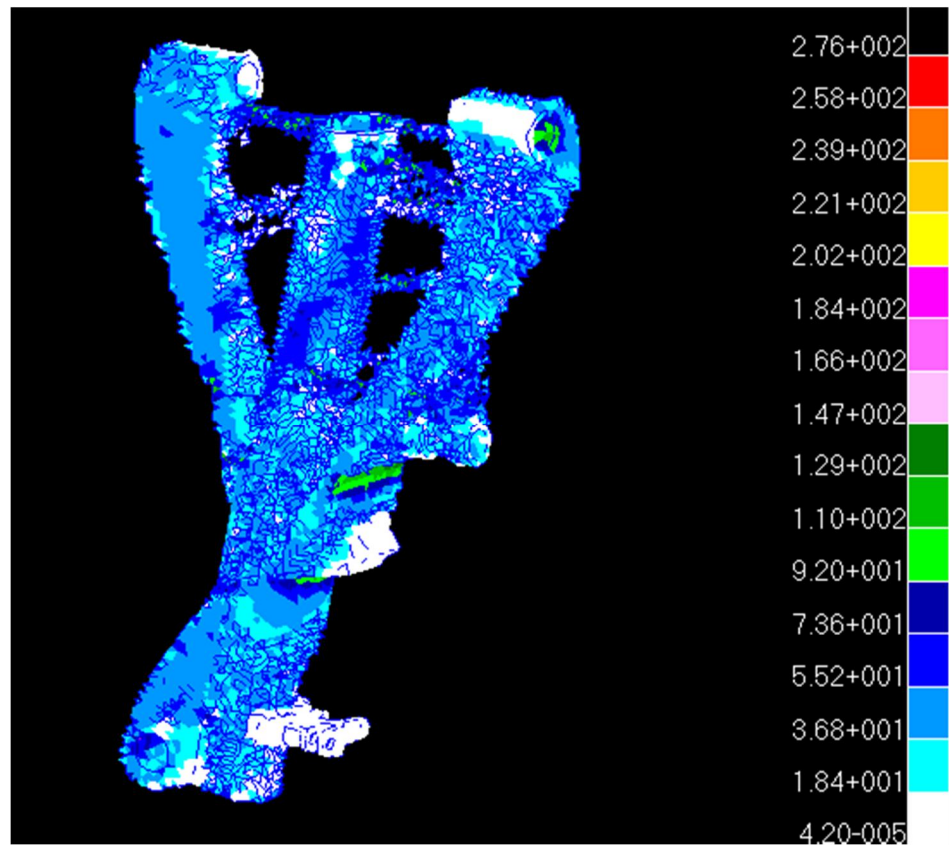


Figure 4.53 The von Mises stress distribution of optimized main landing fitting.

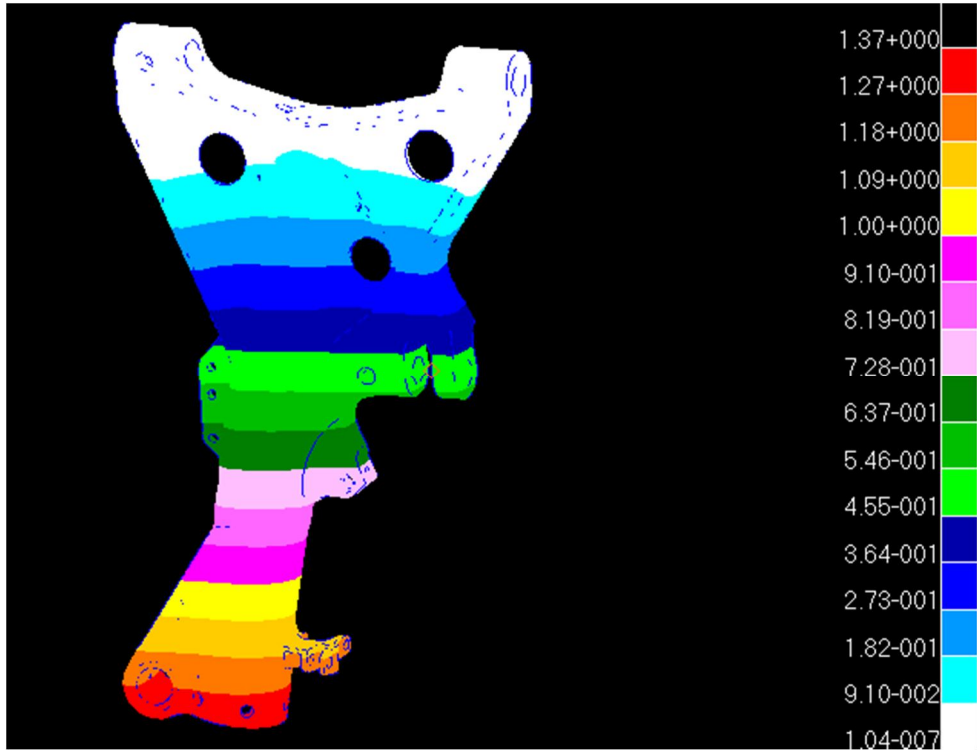


Figure 4.54 The total displacement distribution of existing design main landing fitting.

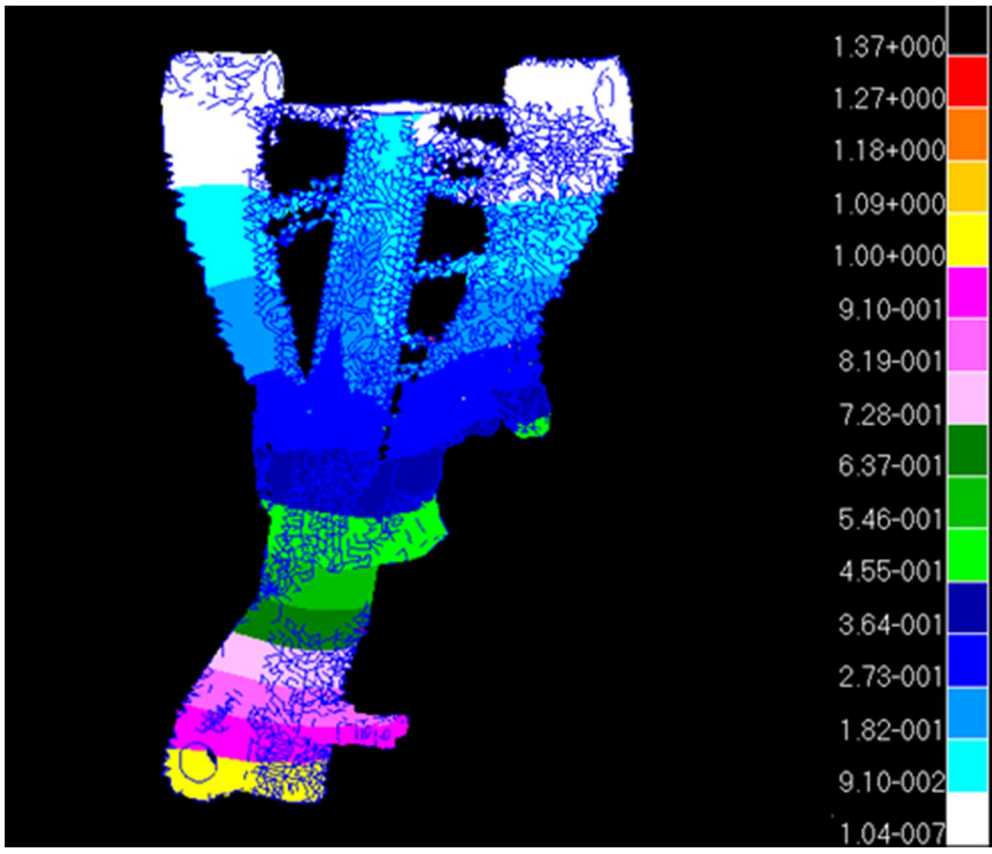


Figure 4.55 The total displacement distribution of optimized main landing fitting.

Existing design and optimized main landing gear are compared topologically in Figure 4.56 and 4.57. The structure is bent due to effect of actuator loading, supporting points perform the minimal displacement, and as departed from the support points displacement increases and maximizes around the piston holder. Similar displacement distribution and values are gathered. Optimized geometry is quite different from the existing design. The greatest von Mises stress arises at the edge of the existing design between support points and actuator lug. Optimized geometry also reveals the similar behavior, creates bridge structures from piston housing to main structure. Neck like structure forms at the surround of the mooring ring which are highly stressed regions. The elements are frequent at the side of actuator fitting and rare at the opposite side due to loading. The actuator and piston forces are relatively higher than link forces. The lug exposed to link forces has bulk geometry at initial design, eventually; the lug evolves to a “C” section at final geometry, same with the existing design. Mass of the main landing fitting decreases from 9.62 kg to 7.94 kg, 17.5 % reduction in weight. The evolution of the optimized main landing fitting is presented in Appendix B from Figure B.41 to B.46.

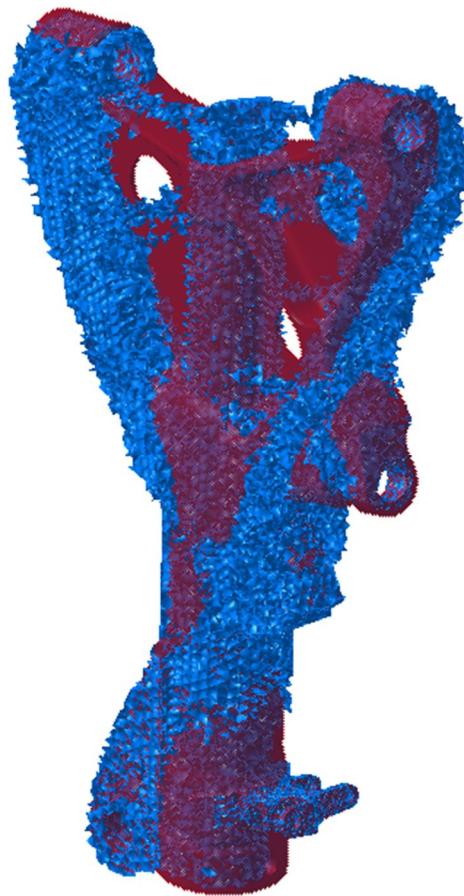


Figure 4.56 Isometric view of existing design and optimized main landing fitting. Existing design is red, optimized topology is blue.

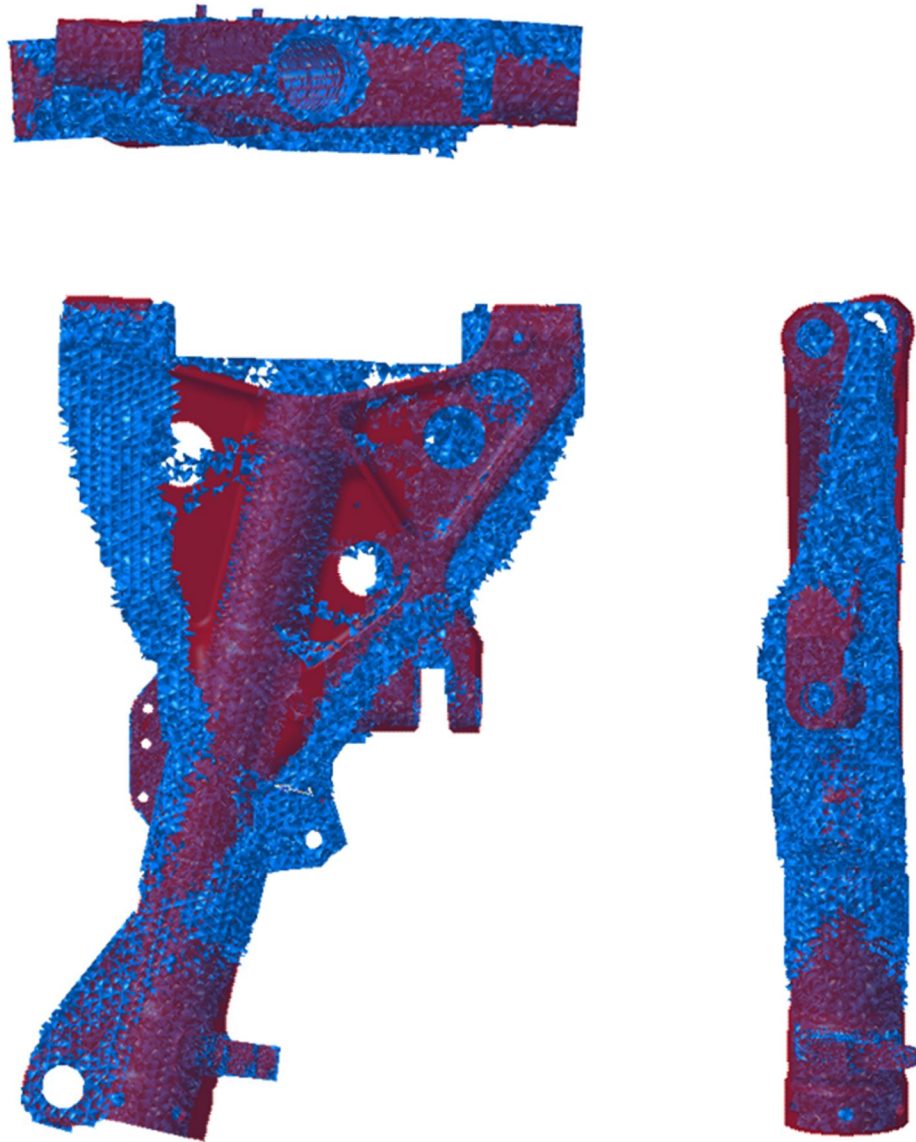


Figure 4.57 Top, front and right side views of existing design and optimized main landing fitting.

4.5. POWER CONTROL EQUIPMENT SUPPORT

Power control equipment is located in the front fuselage, connected to the border between front and center fuselage, firewall. Main function of power control equipment is to distribute electrical power through its multiple connectors. The system installation brackets on the equipment are designed to attach the equipment to firewall via support fittings. The equipment and system installation brackets are shown in Figure 4.58. The support fittings are optimized and optimum topology is formed. System installation brackets have definite rivet holes distribution where the support fittings are fastened. Support fittings should be attached to firewall on other side.

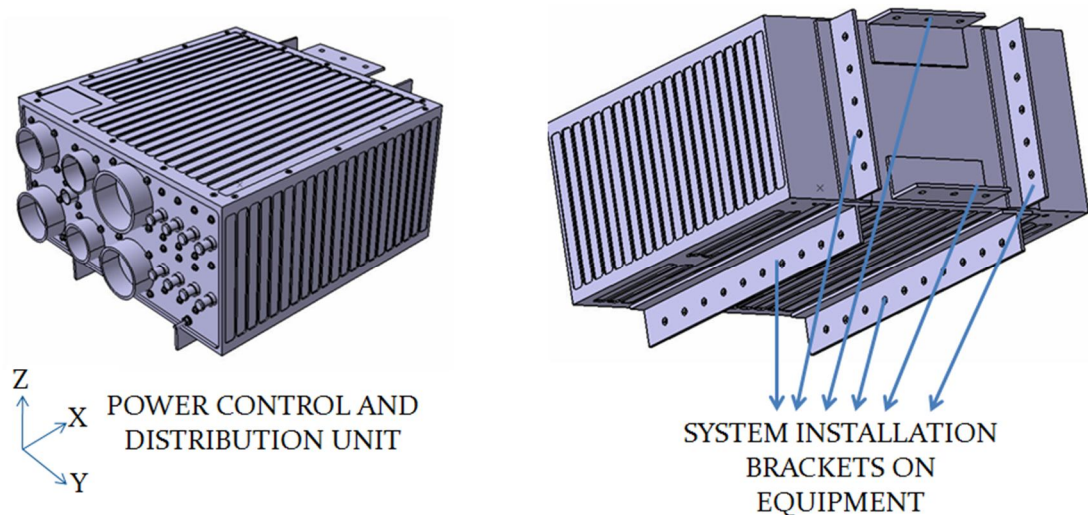


Figure 4.58 Power control and distribution unit and system installation brackets.

The weight of the equipment is 9.53 kg. The support fittings are optimized for two different load cases. For the first load case, the dominant acceleration is along z-direction and for the second case the acceleration is along x-direction. The loads on the power control and distribution unit for two load cases are;

$$F1 = 675 N \quad (4.6)$$

$$F2 = 312 N \quad (4.7)$$

There are four types and total eight support fittings on aircraft to connect the equipment to the firewall which are shown in Figure 4.59.

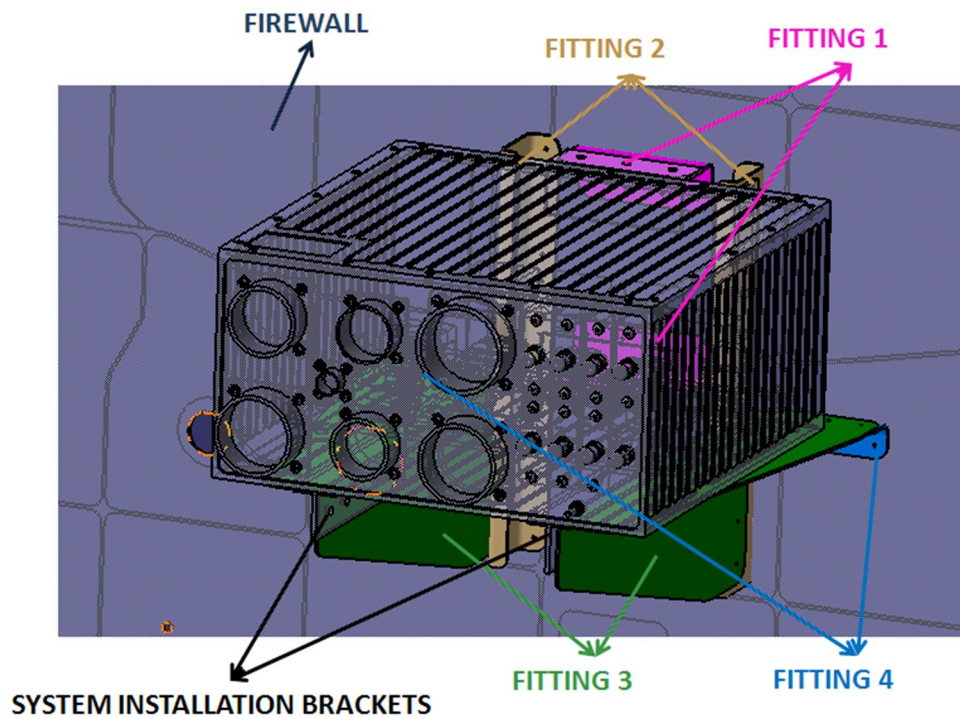


Figure 4.59 Power control unit and support fittings connected to firewall.

The initial bulk geometry occupies all the support fittings volume to reveal the optimal topology having geometry of rectangular prism. As the initial design domain has simple geometry, the volume is discretized into hexahedron meshes and system installation brackets volume is excluded from the initial geometry in Figure 4.60. The model includes 277118 elements and 632808 nodes. The material of support fittings is Aluminum 7075 T7451; therefore same material properties and maximum allowable stress with lug-clevis can be used. The support fittings and system installation brackets are fastened using rivets. The purple lines in Figure 4.61 represent the load distribution to rivet locations from center of gravity of power control unit via MPC. As the support fittings are attached to system installation brackets, one thickness of plate is defined on both sides of brackets are defined as non-design domain to avoid element removal due to low stress level. The plates are physically required for assembly process. The support fittings connect to the aircraft structure via firewall, therefore all surfaces, facing with firewall, are described as mounting points, whereas the elements in contact with firewall are also part of design domain. The elements can be removed to obtain load path of the system and shown in Figure 4.61 with turquoise color. The design and non-design domain in initial geometry are shown in Figure 4.62 which is a section view for clear explanation. Red color represents design domain, whereas white color is non-design domain.

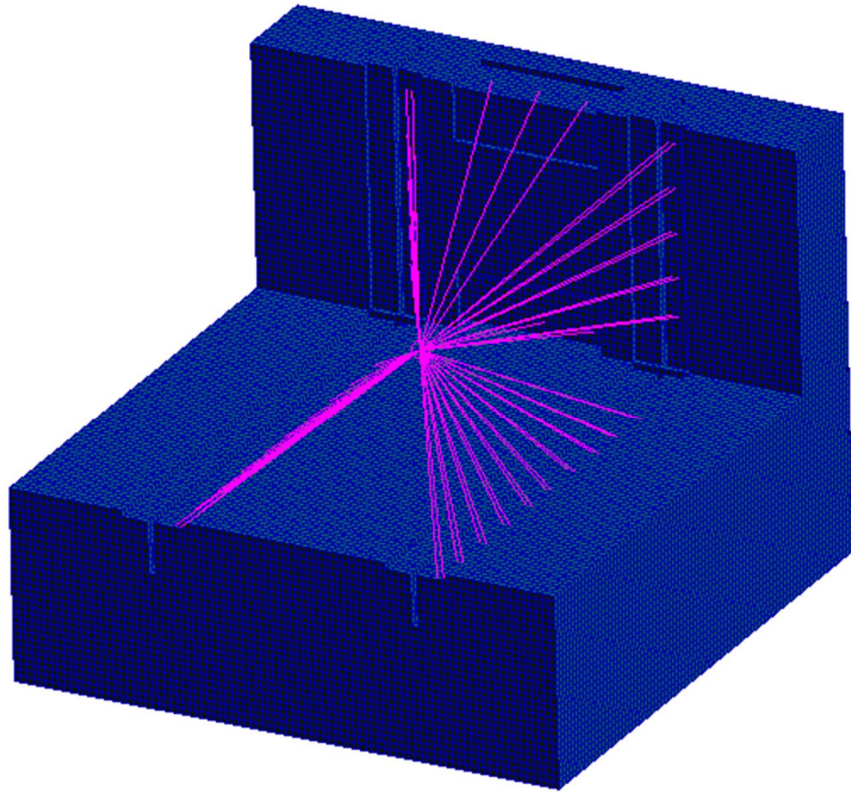


Figure 4.60 The bulk model of equipment support fitting and MPC of equipment.

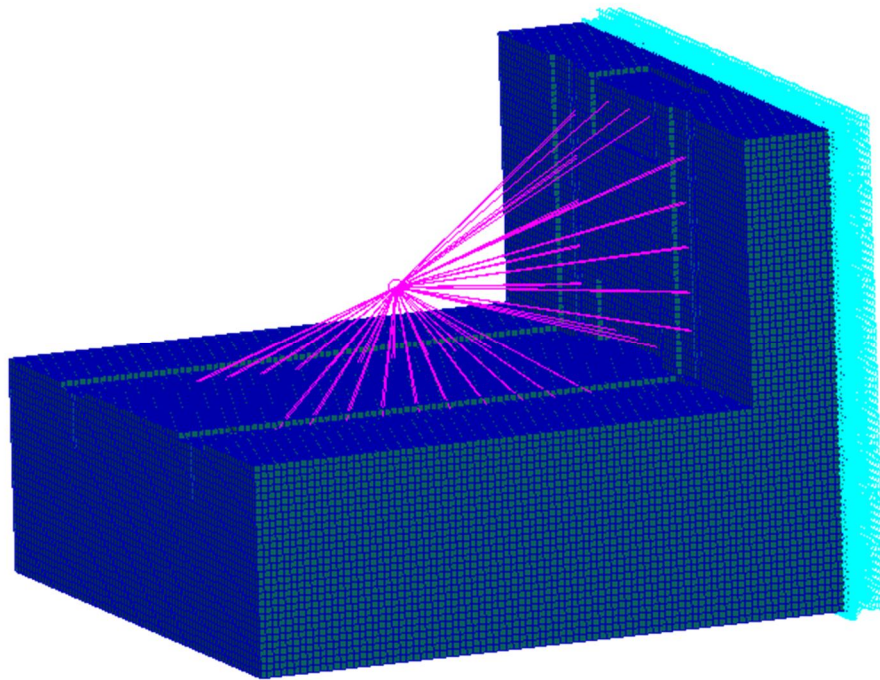


Figure 4.61 The boundary elements of the support fittings.

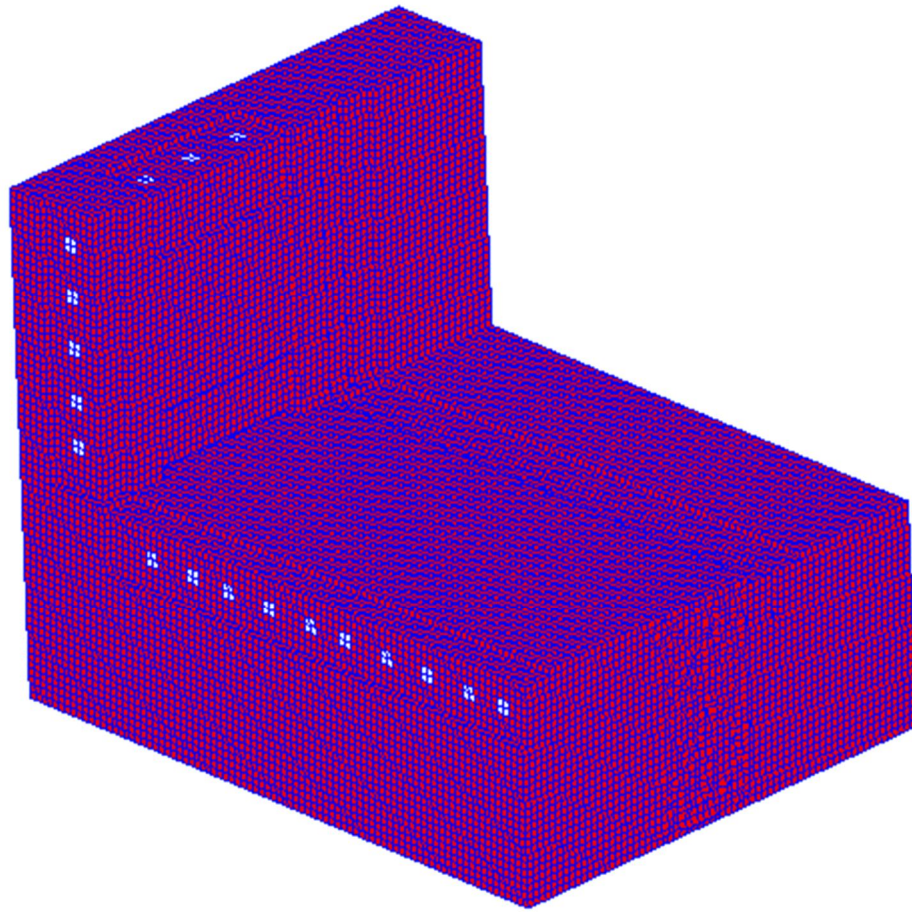


Figure 4.62 The design and non-design domain of support fittings.

The initial rejection ratio, RR_0 , and evolutionary rate, ER , is chosen as 1%. The number of load cases is 2 and allowable stress, σ_e^{max} is 293 MPa as an input. The optimized result is obtained at 28th iteration, i.e. rejection ratio, RR , 28%. The final geometry contains 8869 elements, 264 of them belong to the non-design domain. The views of the optimized support fittings are presented in Figure 4.63. The center of gravity location of the equipment is not at the center but 87 mm to the right of the mid-plane therefore the resultant topology is unsymmetrical as expected. Besides force distribution of geometrically symmetrical locations are dissimilar.

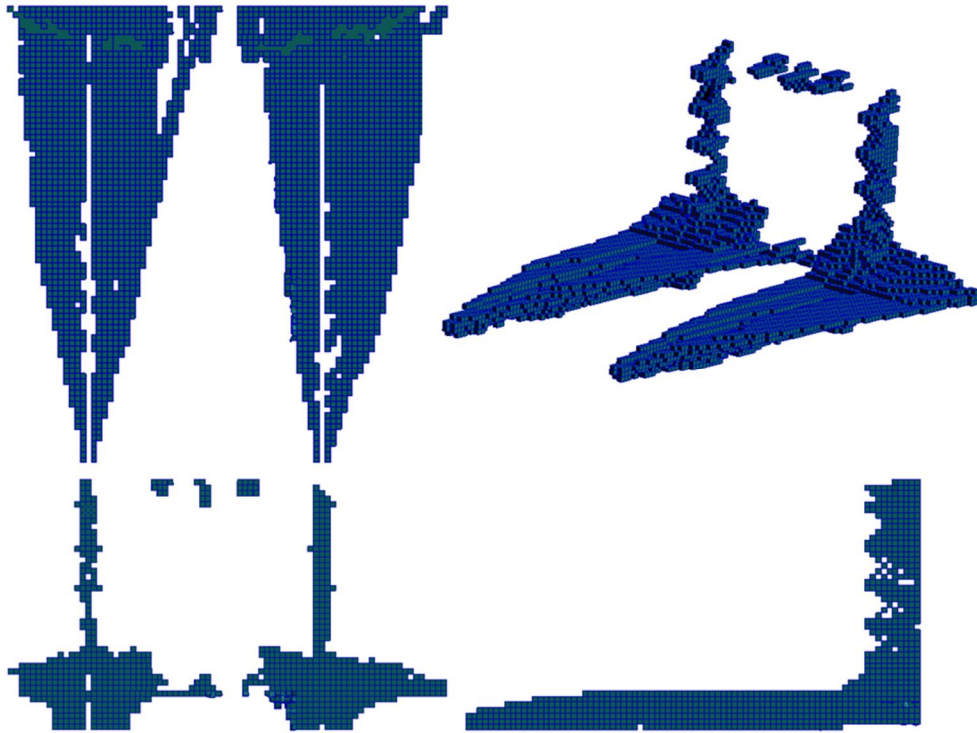


Figure 4.63 The front, top, right view of the optimized support fitting.

The optimization process takes 3 days 14 hours 22 minutes and 57 seconds on an Intel Core 2 Duo T9550 4 Gigabyte RAM computer. Total progress time vs. iteration number is presented in Figure 4.64. 1st iteration completed in 15 hours 59 minutes and 53 seconds whereas 28th iteration takes only 10 minutes and 12 seconds.

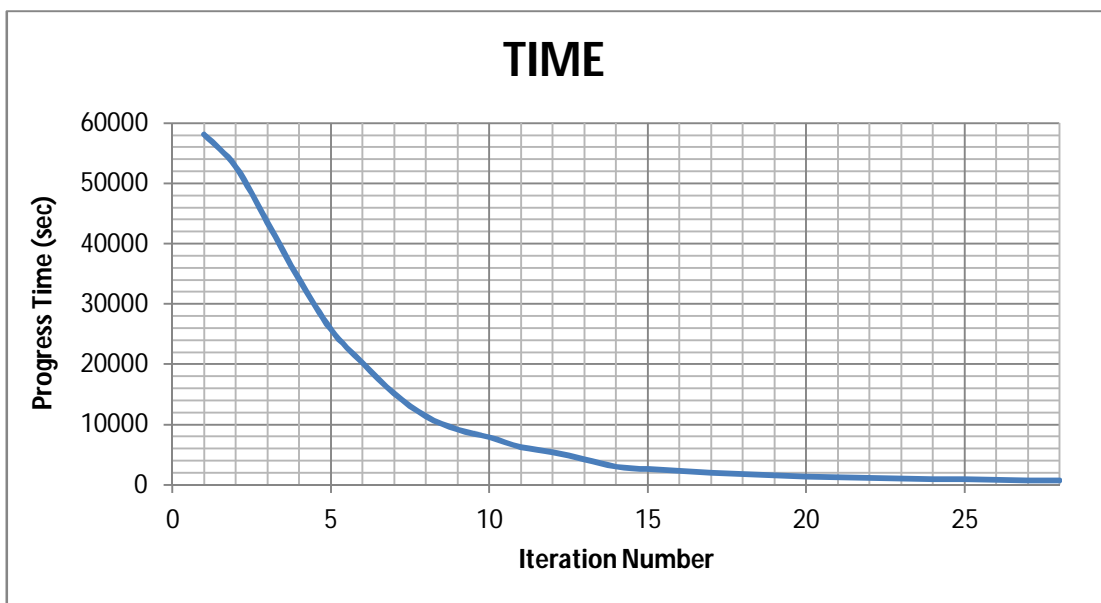


Figure 4.64 Total progress time vs. iteration numbers for optimized support fittings.

96.1 % of the initial volume and 96.2 % of the initial design domain are removed. The volume reduction graph is shown in Figure 4.65. The volume reduction rate decreases as the iteration number ascends; nevertheless, more elements are removed than the previous iterations at the last steps due to the high level of rejection ratio. The optimization is finalized to avoid instability problems. Besides, removal of vast majority of the elements and enormous number of nodes affect the stability of problem. After 13th iteration, MSC.NASTRAN cannot solve the system. Therefore, the nodes without elements are removed. Afterwards MSC.NASTRAN operates properly and analysis the structure.

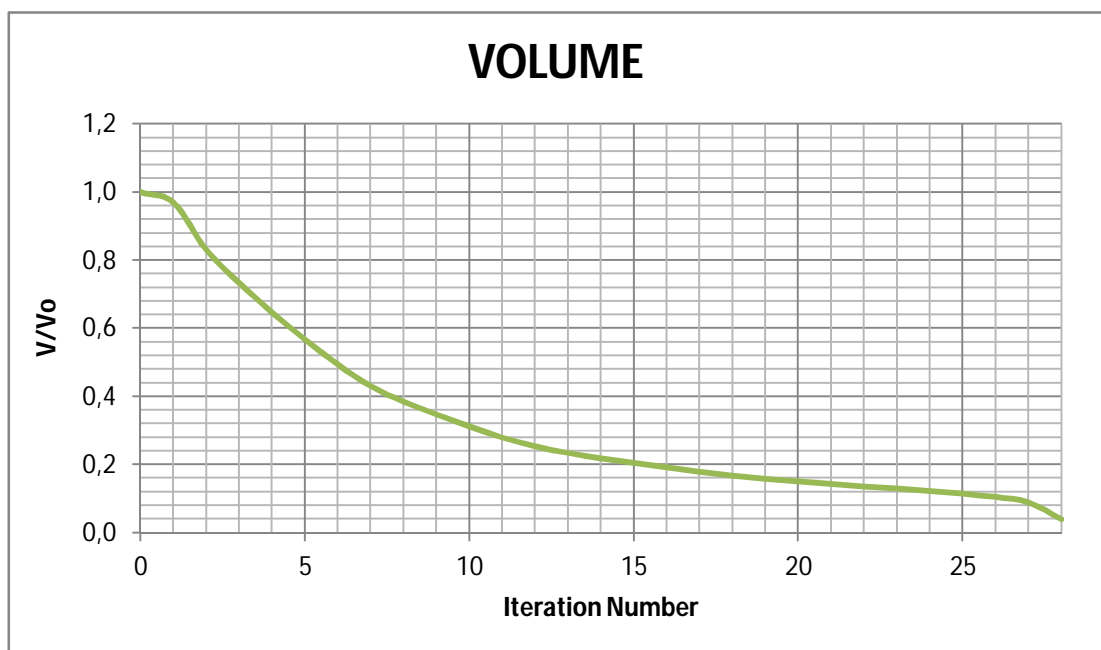


Figure 4.65 Volume reduction vs. iteration numbers for optimized support fitting.

Maximum von Mises stress versus iteration number is presented in Figure 4.66. The maximum stress level increment is proportional to the number of elements decrement. The element removal at first and last stages is almost equal; nevertheless, the stress level remains nearly same at first iterations and changes drastically at final iterations. As the number of elements decreases, structure develops more susceptible to maximum stress level increments.

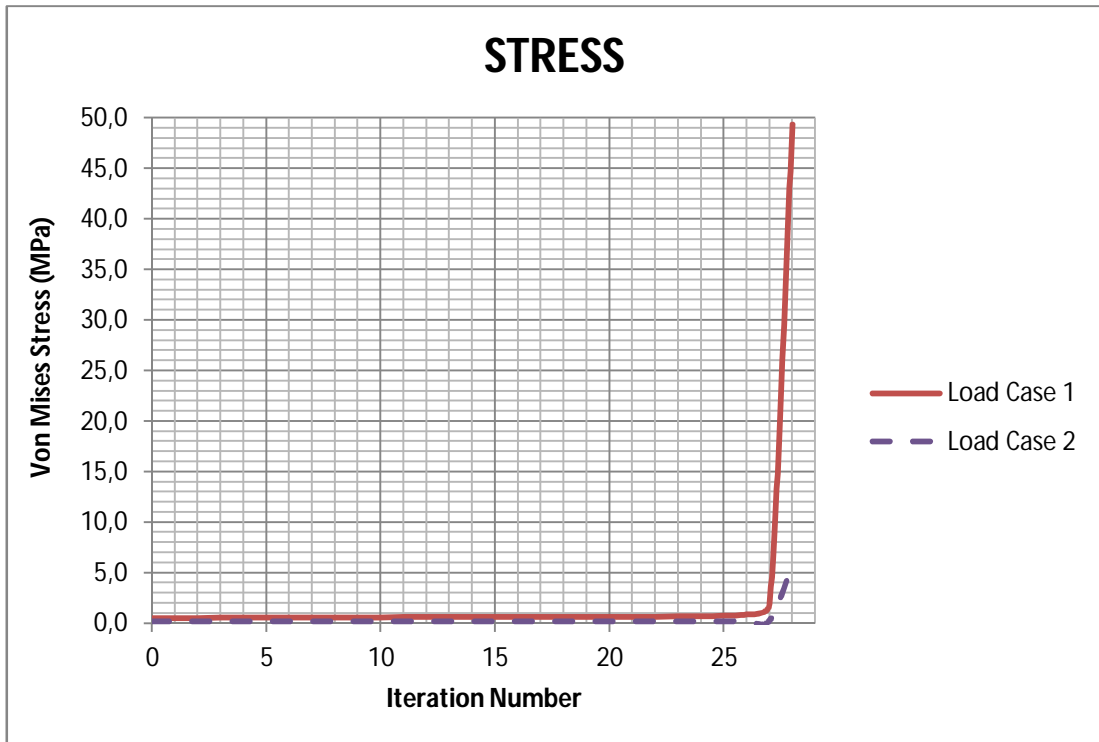


Figure 4.66 Maximum von Mises Stress vs. iteration numbers for optimized support fitting.

Same load and boundary conditions are applied to the existing design to compare the maximum stress level and stress distribution. The von Mises stress distribution of support fitting in load case 1 for existing design and optimized topology are shown in Figure 4.67 and 4.68 respectively. The maximum von Mises stress of support fitting is decreased from 117 MPa to 58.6 MPa, i.e., 49.9 % decrease.

The von Mises stress distribution of support fitting in load case 2 for existing design and optimized topology are shown in Figure 4.69 and 4.70 respectively. The maximum von Mises stress of support fitting is decreased from 14.6 MPa to 7.6 MPa, i.e., 47.9 % decrease.

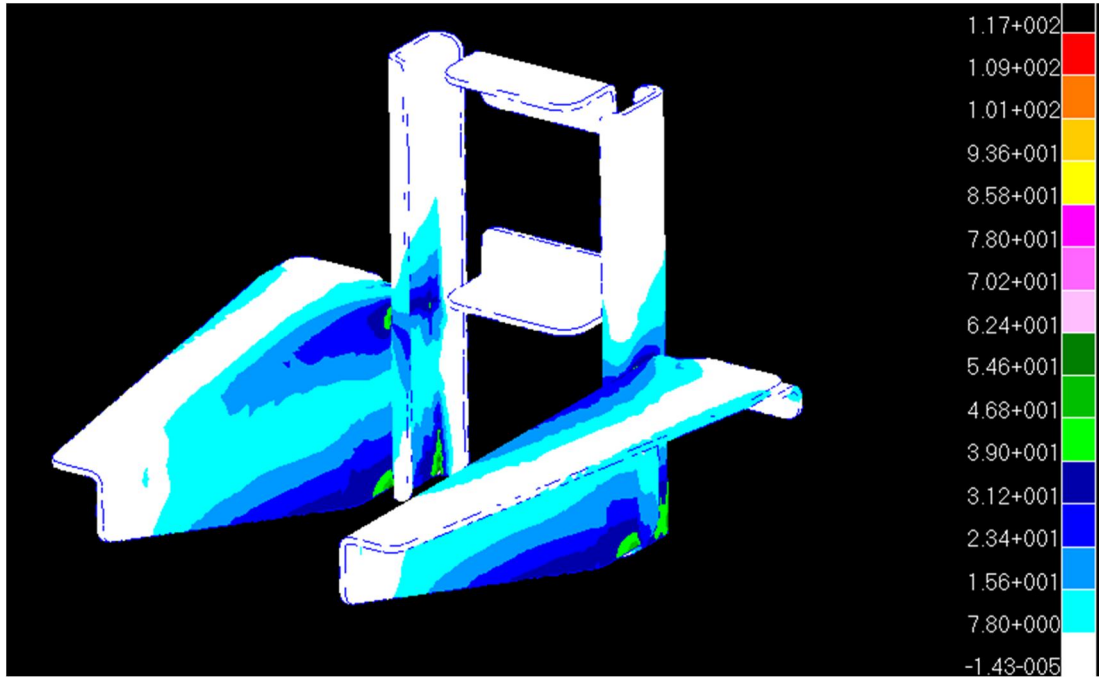


Figure 4.67 The von Mises stress distribution of existing design support fitting for load case 1.

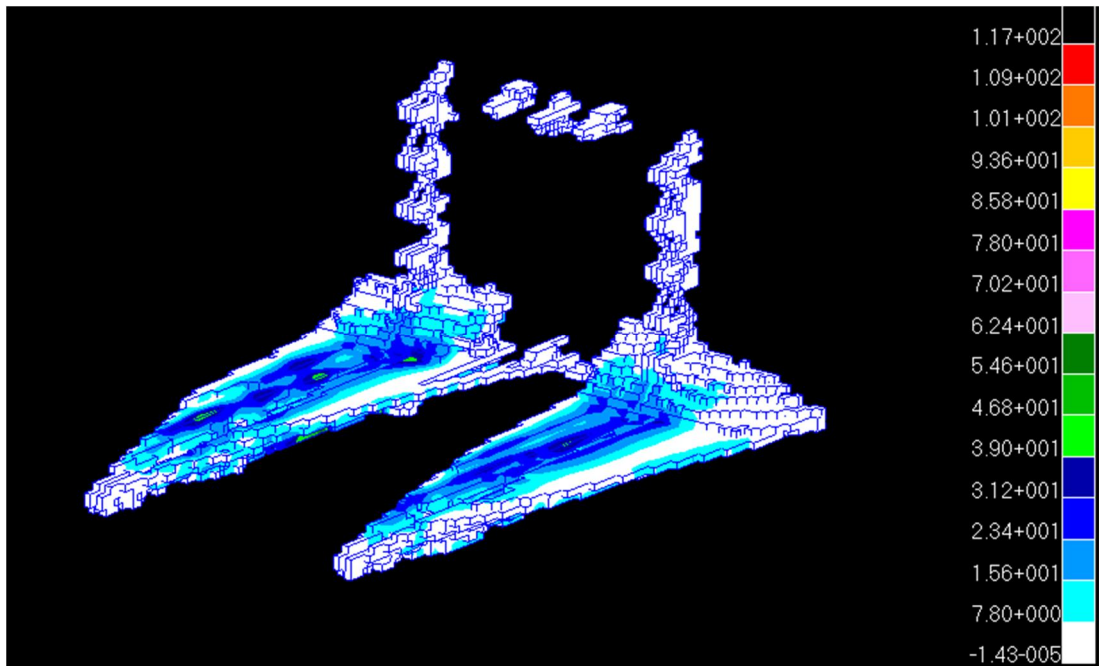


Figure 4.68 The von Mises stress distribution of optimized support fitting for load case 1.

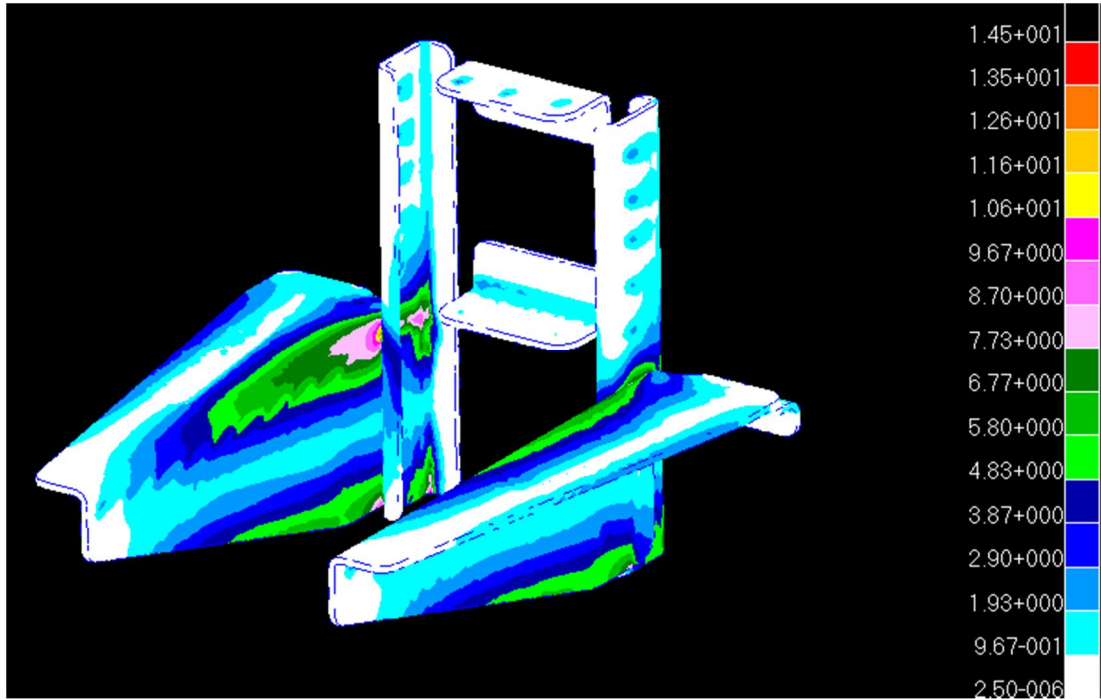


Figure 4.69 The von Mises stress distribution of existing design support fitting for load case 2.

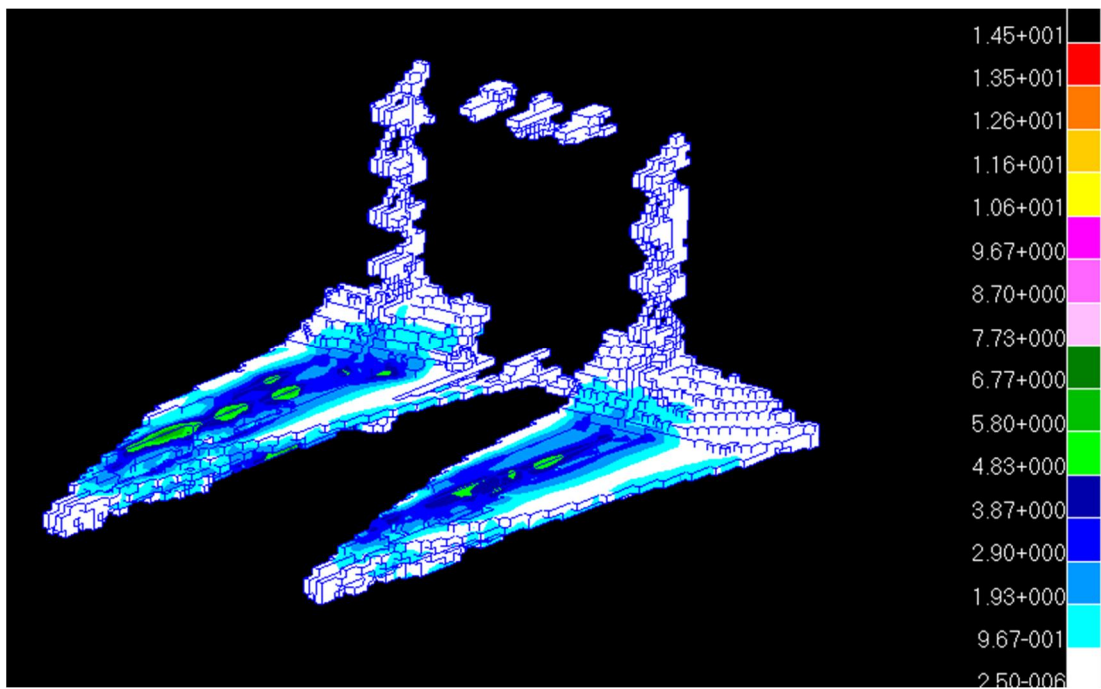


Figure 4.70 The von Mises stress distribution of optimized support fitting for load case 2.

Existing design and optimized power control equipment support are compared topologically in Figure 4.71 and 4.72. The elements of power control and distribution unit seated on rivet location are defined as non-design domain. Fitting 1, and 2 are in low stressed regions, therefore most of the initial design domain are removed and the web of fitting 3 is shortened. Instead of such structure, a new topology formed connecting fittings 3. It is unnecessary to elongate the fitting 2 along negative z direction. Besides the flange of fitting 4 forms along negative z direction, according to the resultant topology, flange should be along positive z direction. Flanges on the fittings are mostly used for assembly and they are low stressed regions. Resultant topology cannot be directly applied to aircraft structure; nevertheless, it has great benefit on revealing the load path of the structure and hints for correct geometry. Mass of the support fitting decreases from 1.66 kg to 1.53 kg i.e., 7.8% reduction in weight. The evolution of the optimized main landing fitting is presented in Appendix B from Figure B.47 to B.58.

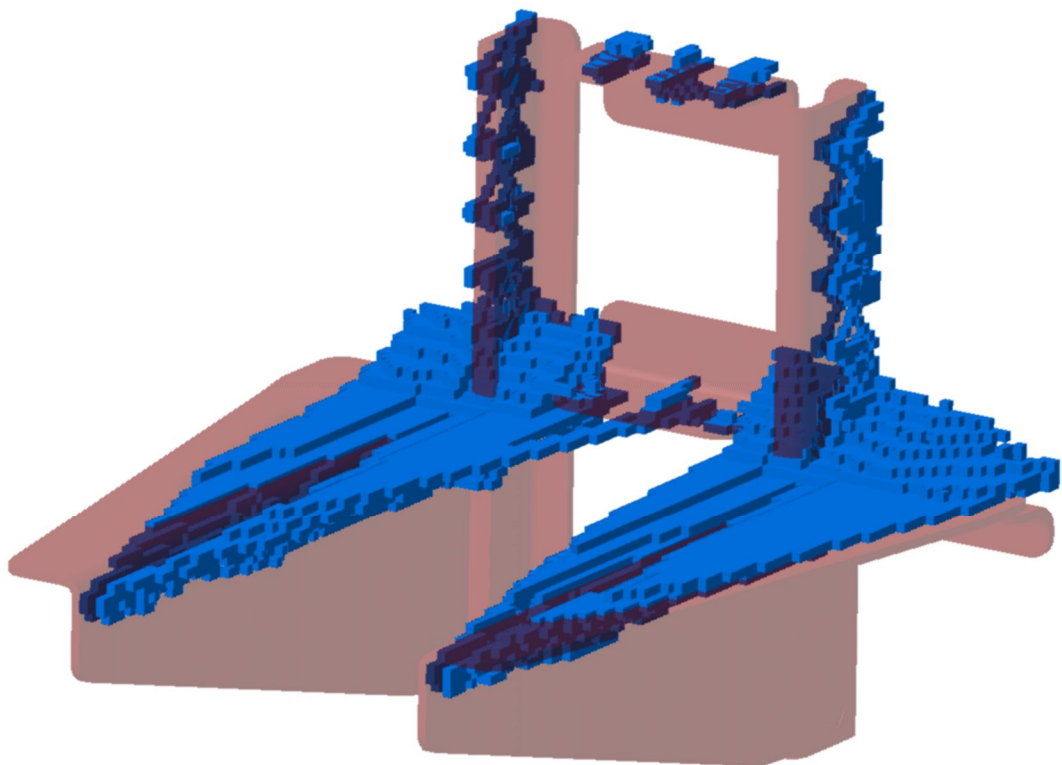


Figure 4.71 Isometric view of existing design and optimized support fitting. Existing design is red, optimized topology is blue.

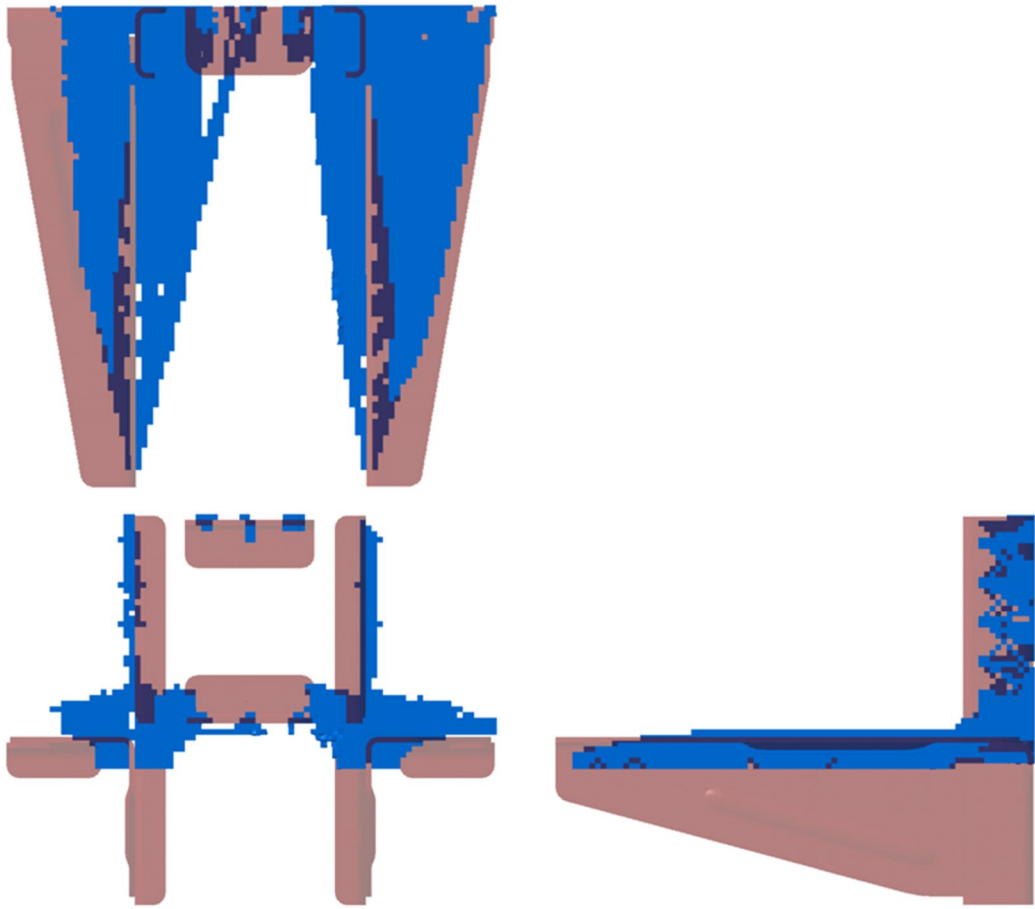


Figure 4.72 Top, front and right side views of existing design and optimized support fitting.

CHAPTER 5

DISCUSSION AND CONCLUSION

The aim of this study is to optimize generic aircraft components using stress based Evolutionary Structural Optimization (ESO) method. This method removes the material with low stress levels from an initial geometry to acquire the optimum topology by leaving material that carries load (therefore higher stress levels) by an iterative way utilizing finite element analysis. ESO algorithm is simple and easy to apply on finite element analysis; therefore, it has been widely used in conceptual design in diverse disciplines such as construction, architecture, design (e.g. mechanical and aerospace) engineering. Optimization methods shorten design period and reduce cost and weight effectively and in a systematic manner. The weight reduction in aircraft industry increases the performance of aircraft. Constrains and objective functions need to be defined similar to real world conditions so that optimized results obtained would be useable. Direct implementation of the results may create impossible or infeasible to manufacture products; however it helps to discover the force carrying and relatively low stressed regions in the design.

5.1. DISCUSSION

In this study, four generic aircraft components which are lug, clevis, main landing fitting and power distribution and control support fitting are optimized using stress based ESO.

Small initial rejection and evolution number extend the program execution time, thus avoids the risk of irreversible removal of some material that might be useful in transferring load. Initial and evolutionary rate should be selected compromising instability risk and program execution time. During the first few iterations, since the number of elements are high the iteration time is longer however as the elements are removed, the number of remaining elements reduce and iteration time gets considerably shorter. Total process time is highly related with the number of iterations.

The number of elements and maximum von Mises stress are highly related. As the total number of elements is decreased, maximum von Mises stress in the remaining elements increases. Small decreases in maximum stress, compared to increase trend of stress during

optimization, may occur since the load paths of structure changes as the elements are removed or precision of numerical solution is not good enough. Finer mesh or slower element removal can be applied to avoid fluctuation of stress level.

The topologies are optimized according to pure mechanical considerations such as load and boundary conditions, geometrical constraints, physical necessities, nonetheless; the concepts such as aesthetics, geometrical smoothing, manufacturability and cost are not considered.

Lug initial domain is chosen as longer than the component, since load direction is not perpendicular but has acute angle with lug base. The expectation is that, the elements close to the load direction is highly stressed and exist in design domain, nevertheless; the elements distant from load direction are removed. The rivets distant from load direction vanish. The topology of the lug oriented along the load direction which validates the claim. Load direction is closer to the back rivets therefore; the number of connection elements at the back rivets is greater than the number of connection elements at the front rivets. Furthermore, the grip length of rivet is assumed to be 2 mm; rivet head layer is selected using this assumption. The structures around the rivet are not highly stressed therefore assumption is valid.

Clevis is loaded through the tube, whether the tube geometry is excluded and force direction is not exerted along clevis end, moment forms and the increment in width of the clevis arm is observed for optimized topology. The optimized topology suggests a convex geometry instead of concave transition between clevis rod and arms. Besides the connection between clevis rod and arms are optimized as hollow instead of filled geometry.

Link, piston and light forces are planar, yet, the actuator force creates bending on main landing fitting. The intensity of elements is much more at the vicinity of actuator lug due to actuator force. The link force lug has a "C" section as the existing design. Optimized geometry creates a great void at the top and forms stiffeners towards piston housing, near to mounting points. A single load case is applied for the solution, emergency landing case, which forces exerted on the link, piston and actuator are relatively much higher than other load cases. The topology optimized for emergency landing case would definitely succeeds in other loading conditions such as wind effect during actuation before landing or parking position.

For power control equipment support, the optimized structure is not symmetrical in zx-direction since; the center of gravity is located 87 mm to the right of the axis. Besides, force distribution of geometrically symmetrical locations is dissimilar. The flanges are functioned

for connecting the system to firewall, however; as the stress level at these regions is low, they are removed. The fitting 3 is optimized with smaller web and flange; nevertheless, new topology between symmetrical fitting 3 is added. Fitting 2 is shortened.

5.2. LIMITATIONS OF CURRENT STUDY

The optimization process is performed using load and boundary conditions and has certain limitations such as initial design domain, geometrical constraints. The initial design domain should cover all the volume for possible load paths. Initial design domain is not a limitation if Bi-directional Evolutionary Structural optimization method is applied. The holes have certain thickness such as lug, since the bearing width is predefined. Also rivet spacing in lug and support fitting are carried from the mating component. Clevis tube thread standard is defined therefore the diameter of clevis end is a geometrical constraint.

5.3. RECOMMENDATIONS FOR FUTURE WORK

Code processes only stress based optimization, after additional algorithms, code can be updated to perform displacement based or frequency based optimization. Multi objective optimization can be performed using a weight function. Constrains for manufacturability, aesthetics etc. may be included as well.

In special cases some elements may be grouped and removed once if every element is in low stress region for each load cases. The sheet metal has uniform thickness; the elements on the same thickness level are grouped to form a smooth surface.

The code was processed for three dimensional meshes, tetrahedron and hexahedron meshes, the code can be arranged for axisymmetric or two dimensional plane stress or plane strain problems as well.

REFERENCES

- Ambrósio, J.A.C., Eberhard, P. (2009), “Advanced Design of Mechanical Systems: From Analysis to Optimization” Springer Wien New York, pp. 311-314.
- Ansola, R., Canales, J., Tarrago, J.A. (2006), “An Efficient Sensitivity Computation Strategy for the Evolutionary Structural Optimization (ESO) of Continuum Structures Subjected to Self-Weight Loads. “Finite Elements in Analysis and Design, Vol. 42, pp. 1220-1230.
- Arora, J.S. (1989), “Introduction to Optimum Design”, McGraw-Hill, 2nd edition, pp. 1-56.
- Arora, J.S. (2007), “Optimization of Structural and Mechanical Systems”, World Scientific, pp. 1-34.
- Atrek, E. (1989), “Shape: A Program for Shape Optimization of Continuum Structures”. Xie, Y.M., Steven, G.P. (Eds) “Evolutionary Structural Optimization”, Springer, London.
- Bendsoe, M.P. (1995), “Optimization of Structural Topology, Shape and Material”, Springer, Berlin, pp. 1-29.
- Bendsøe, M.P. (1989), “Optimal shape design as a material distribution problem.” Bruns, T.E. (Eds) “A Reevaluation of the SIMP Method with Filtering and an Alternative Formulation for Solid-Void Topology Optimization” Structural and Multidisciplinary Optimization, Vol. 30, pp. 428-431.
- Bruns, T.E. (2005), “A Reevaluation of the SIMP Method with Filtering and an Alternative Formulation for Solid-Void Topology Optimization” Structural and Multidisciplinary Optimization, Vol. 30, pp. 428-431.
- Burry, J., Felicetti, P, Tang, J.W., Burry, M.C., Xie, Y.M. (2005), “Dynamic structural modeling – a collaborative design exploration” Huang, X., Xie, Y.M. (Eds) “Evolutionary Topology Optimization of Continuum Structures”, Wiley, 1st edition, pp.173-187.
- Chen, W.H. (2008) “A Genetic Algorithm For 2D Shape Optimization” Master of Science in Mechanical Engineering, Middle East Technical University.
- Christensen, P.W., Klarbring, A. (2009), “An Introduction to Structural Optimization”, Springer, pp. 1-8.
- Çiftçi, E. (2006), “Evolutionary Algorithms in Design” Master of Science in Mechanical Engineering, Middle East Technical University.
- Diaz, A.R., Kikuchi, N. (1992), “Solutions to Shape and Topology Eigenvalue Optimization Problems Using Homogenization Method.”, Xie, Y.M., Steven, G.P. (Eds) “Evolutionary Structural Optimization”, Springer, London.
- Foley, C.M. (2007), “Optimization of Structural and Mechanical Systems”, “Structural Optimization Using Evolutionary Computation” World Scientific, pp. 59-119.
- Gallagher, R.H., Zienkiewicz, O.C. (1973), “Optimum Structural Design”, John Wiley & Sons, pp. 1-31.

- Goldberg, D.E., (1989), “Genetic Algorithms in Search, Optimization and Machine Learning”, Addison-Wesley, New York.
- Grandhi R.V. (1993), “Structural Optimization with Frequency Constraints.” – a review.”, Xie, Y.M., Steven, G.P. (Eds) “Evolutionary Structural Optimization”, Springer, London.
- Grierson, D.E., Pak, W.H. (1993), “Optimal sizing, geometrical and topological design using a genetic algorithm.” Ohsaki, M. (Eds), “Optimization of Finite Dimensional Structures”, CRC Press, pp. 122-130.
- Guan, H., Chen, Y.J., Loo, Y.C., Xie, Y.M., Steven, G.P. (2003), “Bridge Topology Optimization with Stress, Displacement and Frequency Constraints.” Computers and Science, Vol. 81, pp. 131-145.
- Haftka, R.T., Gurdal, Z. (1992), “Elements of Structural Optimization”, Third ed., Kluwer Academic Publishers, Boston, pp. 1-23, 145-152.
- Hajela, P, Lin, C.-Y. (1991). “Optimal design of viscoelastically damped beam structures.” Ohsaki, M. (Eds), “Optimization of Finite Dimensional Structures”, CRC Press, pp. 122-130.
- Hayalioglu, M.S., Degertekin, S.O. (2005), “Minimum cost design of steel frames with semi-rigid connections and column bases via genetic optimization.”, Ohsaki, M. (Eds), “Optimization of Finite Dimensional Structures”, CRC Press, pp. 122-130.
- Hinton, E., Sienz, J. (1995), “Fully Stressed Topological Design of Structures using an Evolutionary Procedure.”, Xie, Y.M., Steven, G.P. (Eds) “Evolutionary Structural Optimization”, Springer, London.
- Holland, J. H. (1975), “Adaptation in Natural and Artificial Systems”, Ohsaki, M. (Eds), “Optimization of Finite Dimensional Structures”, CRC Press, pp. 122-130.
- Huang, X., Xie, Y.M. (2009), “Bi-Directional Evolutionary Topology Optimization of Continuum Structures with One or Multiple Materials.”, Computer Mechanics, Vol. 43, pp.393-401.
- Huang, X., Xie, Y.M. (2010), “Evolutionary Topology Optimization of Continuum Structures”, Wiley, 1st edition, pp. 1-38, 51-63, 173-187.
- Huang, X., Xie, Y.M., Burry, M.C. (2006). “A New Algorithm for Bi-Directional Evolutionary Structural Optimization”, Huang, X., Xie, Y.M., Burry M.C. (Eds) “Advantages of Bi-Directional Evolutionary Structural Optimization (BESO) Over Evolutionary Structural Optimization (ESO)”Advances in Structural Engineering, Vol. 10, No. 6, pp. 727-737.
- Huang, X., Xie, Y.M., Burry M.C. (2007), “Advantages of Bi-Directional Evolutionary Structural Optimization (BESO) Over Evolutionary Structural Optimization (ESO)”Advances in Structural Engineering, Vol. 10, No. 6, pp. 727-737.
- Jenkins, W. M. (1991), “Towards structural optimization via the genetic algorithm.”, Ohsaki, M. (Eds), “Optimization of Finite Dimensional Structures”, CRC Press, pp. 122-130.
- Johnson, K.L (1982). “One Hundred Years of Hertz Contact”, Institution of Mechanical Engineers, Vol.196, pp. 363-378.

- Kameshki, E. S., Saka, M. P. (2003) "Genetic algorithm based optimum design of nonlinear planar steel frames with various semi-rigid connections." Ohsaki, M. (Eds), "Optimization of Finite Dimensional Structures", CRC Press, pp. 122-130.
- Kwak, H.G., Noh, S.H. (2006), "Determination of Strut and Tie Models Using Evolutionary Structural Optimization ." Engineering Structures, Vol. 28, pp. 1440-1449.
- Lazovic, T., Ristivojevic, M., Mitrovic, R. (2008) "Mathematical Model of Load Distribution in Rolling Bearing" FME Transactions, Vol. 36, pp. 189-196
- Lee T.H. (2007), "Optimization of Structural and Mechanical Systems", "Shape Optimization", World Scientific, pp. 149-159.
- Lemonge, A.C.C., Barbosa, H.J.C., Fonseca, L.G. (2009). "A genetic algorithm for configuration and sizing optimization of dome structures including cardinality constraints." Ohsaki, M. (Eds), "Optimization of Finite Dimensional Structures", CRC Press, pp. 122-130.
- Liang, Q.Q., Xie, Y.M., Steven, G.P. (1999), "Optimal Selection of Topologies for the Minimum-Weight Design of Continuum Structures with Stress Constraints" Journal of Mechanical Engineering Science, Vol. 213 pp. 755-762.
- Liu, J.S., Parks, G.T., Clarkson, P.J. (2000), "Metamorphic Development: a New Topology Optimization Method for Continuum Structures" Huang, X., Xie, Y.M., Burry M.C. (Eds) "Advantages of Bi-Directional Evolutionary Structural Optimization (BESO) Over Evolutionary Structural Optimization (ESO)" Advances in Structural Engineering, Vol. 10, No. 6, pp. 727-737.
- Ma, Z.D., Kikuchi, N., Cheng, H.C., Hagiwara, I. (1993), "Topology and Shape Optimization Methods for Structural Dynamic Problems.", Xie, Y.M., Steven, G.P. (Eds) "Evolutionary Structural Optimization", Springer, London.
- Marcelin, J. L., Trompette, P., Dornberger R. (1995), "Optimization of composite beam structures using a genetic algorithm." Ohsaki, M. (Eds), "Optimization of Finite Dimensional Structures", CRC Press, pp. 122-130.
- Medved, J.J., (1995), "Design and Optimization of a Carbon Monocoque Bicycle Frame", Xie, Y.M., Steven, G.P. (Eds) "Evolutionary Structural Optimization", Springer, London.
- Messac, A., Mullur, A.A. (2007), "Optimization of Structural and Mechanical Systems", "Multiobjective Optimization: Concepts and Methods", World Scientific, pp. 121-123.
- Ohsaki, M. (2011), "Optimization of Finite Dimensional Structures", CRC Press, pp. 122-130.
- Osher, S.J., Santosa F. Level (2001) "Level set methods for optimization problems involving geometry and constraints: I. Frequencies of a two-density inhomogeneous drum." Xing, X. (Eds), "A Finite Element Based Level Set Method for Structural Topology Optimization", Doctor of Philosophy in Automation and Computer-Aided Engineering, Chinese University of Hong-Kong. (UMI Number: 3392251)
- Pasko, A., Adzhiev, V., Cominos, P. (2008), "Heterogeneous Objects Modeling And Applications: Collection Of Papers On Foundations And Practice" Springer, pp. 201-208.
- Pereira, C.M., Ramalho, A.L., Ambrosio, J.A. (2011), "A Critical Overview of Internal and External Cylinder Contact Force Model", Nonlinear Dynamics, Vol. 63, pp. 681-697.

- Querin O.M., (1997), “Evolutionary Structural Optimization, Formulation and Implementation, PhD thesis, Xie, Y.M., Steven, G.P. (Eds) “Evolutionary Structural Optimization”, Springer, London.
- Querin, O.M., Young, V., Steven, G.P. and Xie, Y.M. (2000). “Computational Efficiency and Validation of Bi-Directional Evolutionary Structural Optimization”, Huang, X., Xie, Y.M., Burry M.C. (Eds) “Advantages of Bi-Directional Evolutionary Structural Optimization (BESO) Over Evolutionary Structural Optimization (ESO)” *Advances in Structural Engineering*, Vol. 10, No. 6, pp. 727-737.
- Rasmussen, J., Lund, E., Birker, T. (1992), “Collection of examples: CAOS optimization system” Xie, Y.M., Steven, G.P. (Eds) “Evolutionary Structural Optimization”, Springer, London.
- Ren, G., Smith, J.V., Tang, J.W., Xie, Y.M. (2005), “Underground Excavation Shape Optimization using an Evolutionary Procedure” *Computers and Geotechnics*, Vol. 32, pp. 122-132.
- Rong, J.H., Xie, Y.M., Yang, X.Y., (2001), “An Improved Method for Evolutionary Structural Optimization Against Buckling” *Computers and Structures*, Vol. 79, pp. 253-263.
- Rong, J.H., Jiang, J.S., Xie, Y.M. (2007), “Evolutionary Structural Topology Optimization for Continuum Structures with Structural Size and Topology Variables” *Advances in Structural Engineering*, Vol. 10, No. 6, pp. 681-695.
- Rozvany, G.I.N., Bendsøe, M.P., Kirsch, U. (1995), “Layout Optimization of Structures”, *Applied Mechanics Review*, Vol. 48, No. 2.
- Shigley, J.E., Mischke, C.R., Budynas, R. (2004) “Mechanical Engineering Design” Mc Graw Hill, 7nd edition, pp. 75.
- Strand, H. (2005) “Design Testing and Analysis of Journal Bearings for Construction Equipment”, *Doctoral Thesis in Machine Design*, Royal Institute of Technology, pp. 10-15.
- Steven, G., Querin, O., Xie, M., (2000), “Evolutionary Structural Optimization (ESO) for Combined Topology and Size Optimization of Discrete Structures.”, *Computer Methods in Applied Mechanics and Engineering*, Vol. 188, pp. 743-754.
- Suzuki, K., Kikuchi, N. (1991), “A Homogenization Method for Shape and Topology Optimization”, *Computer Methods in Applied Mechanics and Engineering*, Vol. 93, pp. 291-318.
- Taşkınoğlu, E.E. (2006), “A Genetic Algorithm for Structural Optimization”, *Master of Science in Mechanical Engineering*, Middle East Technical University.
- Tenek, L.H., Hagiwara, I. (1993), “Static and Vibration Shape and Topology Optimization using Homogenization and Mathematical Programming”, Xie, Y.M., Steven, G.P. (Eds) “Evolutionary Structural Optimization”, Springer, London.
- Tenek, L.H., Hagiwara, I. (1994), “Optimal Rectangular Plate and Shallow Shell Topologies using Thickness Distribution or Homogenization” Xie, Y.M., Steven, G.P. (Eds) “Evolutionary Structural Optimization”, Springer, London.

Tian-quan, Y. (1991), "The Exact Integral Equation of Hertz Contact Theory", *Applied Mathematics and Mechanics*, Vol. 12, No. 2, pp. 181-185.

Xie, Y.M., Steven, G.P. (1997), "Evolutionary Structural Optimization", Springer, London, pp. 1-48, 63-92.

Xing, X. (2009), "A Finite Element Based Level Set Method for Structural Topology Optimization", Doctor of Philosophy in Automation and Computer-Aided Engineering, Chinese University of Hong-Kong. (UMI Number: 3392251)

Yang, X.Y., Xie, Y.M., Steven, G.P. (2005), "Evolutionary Methods for Topology Optimization of Continuous Structures with Design Dependent Loads." *Computers & Structures*, Vol.83, pp. 956-963.

Yang, X.Y., Xie, Y.M., Steven, G.P. and Querin, O.M. (1999a)," Topology Optimization for Frequencies Using an Evolutionary Method", *Journal of Structural Engineering*, pp. 1432-1438

Yang, X.Y., Xie, Y.M., Steven, G.P. and Querin, O.M. (1999b), "Bidirectional Evolutionary Method for Stiffness Optimization", *AIAA Journal*, Vol. 37, No. 11, pp. 1483-1488.

Zhou, M., Rozvany, G.I.N., (1991), "Topological, geometrical and generalized shape optimization." Bruns, T.E. (Eds) "A Reevaluation of the SIMP Method with Filtering and an Alternative Formulation for Solid-Void Topology Optimization" *Structural and Multidisciplinary Optimization*, Vol. 30, pp. 428-431.

APPENDICES

A. MICROSOFT VISUAL BASIC INTERFACE CODE

The interface code, which evaluates the stress values and defines the unnecessary elements for single and multiple load case are presented below:

```
Dim waste As String
Dim matrix1(555000, 2) As Double
Dim matrix3(555000, 2) As Double
Dim matrix4(555000, 2) As Double
Dim matrix6(555000, 2) As Double
Dim nofelements As Double
Dim matprop As String
Dim matprop1 As Double
Dim matprop2 As Double
Dim totalelements As Double
Dim x As Double
Dim y As Double
Dim t As Double
Dim iteration As Double
Dim s As Double
Dim k As Double
Dim cut1 As String
Dim cut2 As String
Dim cut3 As String
Dim cut4 As String
Dim cut5 As String
Dim loop1 As Double
Dim delelements As Double
Dim max As Double
Dim min As Double
Dim maxelement As Double
Dim err As Double
Dim rej_ratio As Double
Dim nofdelements As Double
Dim current_rej_ratio As Double
Dim a As Double
Dim nofloadcase As Double
Dim corryield As Double
Dim voll As Double
'-----
' TO STOP CODE PROGRESS WITHOUT SLEEP COMMAND DURING NASTRAN COMMAND
Private Declare Sub Sleep Lib "kernel32" (ByVal dwMilliseconds As Long)
Private Declare Sub ExitProcess Lib "kernel32" (ByVal uExitCode As Long)
Private Declare Function CloseHandle Lib "kernel32" (ByVal hObject As Long) As Long
Private Declare Function GetExitCodeProcess Lib "kernel32" (ByVal hProcess As Long, lpExitCode As Long) As Long
Private Declare Function OpenProcess Lib "kernel32" (ByVal dwDesiredAccess As Long, ByVal bInheritHandle As Long,
ByVal dwProcessId As Long) As Long
Public Function ShellX(ByVal PathName As String, Optional ByVal WindowStyle As Integer = vbMinimizedFocus, Optional
ByVal Events As Boolean = True) As Long
'Declarations:
Const STILL_ACTIVE = &H103&
Const PROCESS_QUERY_INFORMATION = &H400&
Dim ProcId As Long
Dim ProcHnd As Long
'Get process-handle:
ProcId = Shell(PathName, WindowStyle)
ProcHnd = OpenProcess(PROCESS_QUERY_INFORMATION, True, ProcId)
'wait for process end:
Do
If Events Then DoEvents
GetExitCodeProcess ProcHnd, ShellX
```

```

Loop While ShellX = STILL_ACTIVE
'clean up:
CloseHandleProcHnd
End Function
'-----
'START OF MULTI LOAD CASE CODE

Private Sub Command1_Click()
Command1.Enabled = False
'-----
'PROGRESS OF NASTRAN
Dim xx As Long
Dim strDosBatchFullPath As String
strDosBatchFullPath = "C:\MSC.Software\MSC.Nastran\bin\nastran.exe msgbell=no scr=yes " & "loop.bdf"
xx = ShellX("C:\MSC.Software\MSC.Nastran\bin\nastran.exe msgbell=no scr=yes " & "loop.bdf", WindowStyle)
'-----
'CREATING LOG FILE FOR TRACEABILITY
Dim check3
check3 = "logfile" & ".txt"
Open check3 For Append As #3
Print #3, "LOGFILE FOR EVOLUTIONARY STRUCTURAL OPTIMIZATION"
Print #3, " "
Print #3, "          M.ATACAN AVGIN / 1392018 "
Print #3, " "
Print #3, "THE PROGRAM HAS INITIATED AT " & Format(Time, "hh:mm:ss") & " "
iteration = 1
exit1:
If (iteration > 0) Then
For t = 0 To 2
x = 0
y = 0
'-----
' F06 FILE ARE SEARCHED FOR STRESS VALUES
If (iteration = 1) Then
a = 1
current_rej_ratio = Text2.Text / 100
Open "loop.f06" For Input As #1
Else
Dim check2
check2 = "loop" & iteration - 1 & ".f06"
Open check2 For Input As #1
End If
matprop = 0
Do
Line Input #1, name1
If (matprop1 = 1) Then
waste = Mid(name1, 5, 13)
If (Trim(waste) = "MSC.NASTRAN") Then
matprop = 0
matprop1 = 0
End If
End If
If (matprop = 1) Then
If (matprop2 = 1) Then
waste = Mid(name1, 2, 24)
If (Trim(waste) = "CENTER") Then
waste = Mid(name1, 118, 129)
matrix1(x, y) = Trim(waste)
y = 0
x = x + 1
matprop2 = 0
End If
End If
waste = Mid(name1, 7, 9)
If (Trim(waste) <> "") Then
matrix1(x, y) = Trim(waste)
matprop2 = 1
y = y + 1
End If
End If
'-----
' STRESS VALUES ARE FOUND AND COPIED
waste = Mid(name1, 2, 12)
If (Trim(waste) = "ELEMENT-ID") Then

```

```

matprop = 1
matprop1 = 1
End If
Loop While Not EOF(1)
Close #1
'-----
' TO DELETE EX F06 FILE
Kill "C:\uni\*.f06"
'-----
NUMBER OF LOAD CASE IS READ AS INPUT
totalelements = x
nofloadcase = Text4.Text
nofelements = x / nofloadcase
'-----
'STOPPING CRITERIA FIR VOLUMETRIC CONSTRAINT
If (Volume.Text = 0) Then
vol1 = 0
ElseIf (iteration = 1) Then
vol1 = nofelements * (1 - (Volume.Text / 100))
End If
'-----
TO WRITE ALL ELEMENTS IN ELEMENT NUMBER ORDER
Print #3, " "
Print #3, " "
For x = 0 To totalelements - 1
Print #3, matrix1(x, 0), "      " & matrix1(x, 1)
Next x
Print #3, " "
Print #3, " "
'-----
THE ELEMENTS ARE ARRANGED FOR STRESS VALUES IN ASCENDING ORDER
Dim list_1 As Double
Dim list2 As Double
For i = 0 To nofloadcase - 1
list_1 = nofelements * (i + 1)
list2 = nofelements * i
For x = list2 To list_1 - 1
For y = x + 1 To list_1 - 1
If (matrix1(x, 1) > matrix1(y, 1)) Then
waste = matrix1(y, 0)
s = matrix1(y, 1)
matrix1(y, 0) = matrix1(x, 0)
matrix1(y, 1) = matrix1(x, 1)
matrix1(x, 0) = waste
matrix1(x, 1) = s
End If
Next y
Next x
Next i
'-----
'ELEMENTS HAVING STRESS HIGHER THAN YIELD IN EACH CASE ARE DECLARED FOR CHECK IF ANY.
For i = 0 To nofloadcase - 1
list_1 = nofelements * (i + 1)
list2 = nofelements * i
max = matrix1(list_1 - 1, 1)
corryield = Text5.Text * 1000000
If (corryield < max) Then
Print #3, " "
Print #3, "THE ELEMENTS HIGHER THAN YIELD STRESS AT LOAD CASE "& i + 1 & " ARE;"
Print #3, " "
Print #3, "ELEMENT NO      VON MISSES STRESS (MPa)"
Else
End If
For x = list2 To list_1 - 1
If (corryield < matrix1(x, 1)) Then
Print #3, matrix1(x, 0), "      " & matrix1(x, 1) / 1000000
End If
Next x
Next i
Next x
'-----
PROGRAM TERMINATION IF STRESS OF EVEN ONE ELEMENT IS GREATER THAN YIELD STRESS
If (corryield < max) Then
iteration = 0

```

```

GoTo exit1
End If
Next i
'-----
' TO WRITE ALL ELEMENTS IN STRESS ORDER
'Print #3, ""
'Print #3, " "
'Print #3, " "
'Print #3, " ALL ELEMENTS IN STRESS ORDER IS;"
For x = 0 Tototalelements - 1
'Print #3, matrix1(x, 0), "      " & matrix1(x, 1)
Next x
'Print #3, " "
'Print #3, " "
Dim lowstress As Double
lowstress = 0
'iteration = 0
'-----
'ELEMENTS ON DIFFERENT LOAD CASES ARE SEPERATED. AND BELOW THE REJECTION RATIO FORM
ANOTHER MATRIX.
For i = 0 Tonofloadcase - 1
list_1 = nofelements * (i + 1)
list2 = nofelements * i
max = matrix1(list_1 - 1, 1)
maxelement = matrix1(list_1 - 1, 0)
matrix6(i, 0) = maxelement
matrix6(i, 1) = max
nofdelements = 0
For x = list2 To list_1 - 1
min = matrix1(x, 1)
rej_ratio = min / max
If (rej_ratio < current_rej_ratio) Then
matrix4(lowstress, 0) = matrix1(x, 0)
matrix4(lowstress, 1) = matrix1(x, 1)
lowstress = lowstress + 1
'nofdelements = nofdelements + 1
Else
Exit For
End If
Next x
Next i
'-----
'UNNECESSARY ELEMENTS ARE LISTED AT LISTBOX.
For x = 0 Tolowstress
>List1.AddItem (matrix4(x, 0))
>List1.AddItem (matrix4(x, 1))
Next x
'-----
'UNNECESSARY ELEMENTS FOR EACH ITERATION IS DEFINED.
Dim lowstress1 As Double
lowstress1 = 0
Dim nofdelements1 As Double
nofdelements1 = 0
For x = 0 Tolowstress - 1
For y = x + 1 Tolowstress - 1
If (matrix4(x, 0) = matrix4(y, 0)) And (matrix4(x, 0) <> 0) Then
nofdelements1 = nofdelements1 + 1
If (nofdelements1 = nofloadcase - 1) Then
matrix3(lowstress1, 0) = matrix4(x, 0)
matrix3(lowstress1, 1) = matrix4(x, 1)
lowstress1 = lowstress1 + 1
GoTo jump:
End If
End If
Next y
jump:
nofdelements1 = 0
Next x
'-----
'STOPPING CRITERIA FIR VOLUMETRIC CONSTRAINT
delements = lowstress1
If (vol1 <> 0) Then
If ((nofelements - delements) < vol1) Then
iteration = 0

```

```

GoTo exit1
End If
End If'-----
'CHECK FOR FINAL REJECTION RATIO.
Dim final_rej_ratio As Double
final_rej_ratio = Text1.Text / 100 - 0.0005
If (current_rej_ratio >= final_rej_ratio) Then
If (a = 1) Then
GoTo jump2
End If
iteration = 0
GoTo exit1
jump2:
a = 0
End If
'-----
'TO PRINT DELETE ELEMENTS IF NOT AT NON DESIGN.
'Print #3, " DELETED ELEMENTS IN ELEMENT ORDER IS WITHOUT REGARDING NON DESIGN DOMAIN;"
'For x = 0 To lowstress1 - 1
'Print #3, matrix3(x, 0), "      " & matrix3(x, 1)
'Next x
'-----
'NEW BDF FILE IS FORMED.
If (iteration = 1) Then
Open "loop.bdf" For Input As #1
Else
Dim check0
check0 = "loop" & iteration - 1 & ".bdf"
Open check0 For Input As #1
End If
Dim check1
check1 = "loop" & iteration & ".bdf"
Open check1 For Append As #2
'-----
'REQUIRED INFORMATION IS PRINTED ON LOG FILE
Print #3, ""
For i = 0 To nloadcase - 1
Print #3, "MAXIMUM VON MISES STRESS OF THE LOAD CASE " & i + 1 & " IS " & matrix6(i, 1) / 1000000 & " MPa ON
ELEMENT " & matrix6(i, 0) & "."
Next i
Print #3, " "
Print #3, "THE CURRENT REMOVAL RATIO IS "&current_rej_ratio * 100 &" %."
Print #3, " "
Print #3, "ELEMENT NO      VON MISSES STRESS (MPa)"
'-----
'UNNECESSARY ELEMENTS ARE REMOVED FROM BDF LINE BY LINE.
For x = 0 To Todelements - 1
For y = x + 1 To Todelements - 1
If matrix3(x, 0) > matrix3(y, 0) Then
s = matrix3(y, 0)
k = matrix3(y, 1)
matrix3(y, 0) = matrix3(x, 0)
matrix3(y, 1) = matrix3(x, 1)
matrix3(x, 0) = s
matrix3(x, 1) = k
k = 0
s = 0
End If
Next y
Next x
'-----
'UNNECESSARY ELEMENTS ARE MONITORED IN LISTBOX.
For x = 0 To Todelements - 1
List1.AddItem (matrix3(x, 0))
List1.AddItem (matrix3(x, 1))
Next x
'-----
'CONTINUE OF REMOVAL OF UNNECESSARY ELEMENTS FROM BDF FILE
Dim kkk As Double
kkk = 0
Do
Line Input #1, name1
cut1 = Mid(name1, 1, 6)
cut6 = Trim(cut1)

```

```

cut1 = cut6
If (cut1 = "CTETRA") Then
loop1 = 0
End If
If (loop1 = 1) Then
loop1 = 0
ElseIf ((cut1 = "CHEXA") Or (cut1 = "CTETRA")) Then
cut2 = Mid(name1, 8, 10)
cut3 = Trim(cut2)
cut4 = Mid(name1, 18, 8)
cut5 = Trim(cut4)
If (iteration > 0) Then
GoTo record
record1:
Else
record2:
Print #2, name1
End If
Else
Print #2, name1
End If
Loop While Not EOF(1)
If (iteration < 0) Then
record:
For x = 0 Todelements - 1
If (matrix3(x, 0) > cut3) Then
GoTo record2
End If
If cut3 = matrix3(x, 0) And cut5 = 1 Then
loop1 = 1
Print #3, matrix3(x, 0), "      " & matrix3(x, 1) / 1000000
kkk = kkk + 1
GoTo record1
'Else
'GoTo record2
End If
Next x
GoTo record2
End If
Close #1
Close #2
Dim str As String
'-----
'REQUIRED INFORMATION IS PRINTED ON LOG FILE
Print #3, " "
Print #3, kkk&" ELEMENTS ARE REMOVED. THE NUMBER OF REMAINING ELEMENTS IS "& (todelements /
nofloadcase) - kkk& "."
Print #3, " "
'-----
'PROGRESS OF NASTRAN
str = "loop" & iteration & ".bdf"
Dim strDosBatchFullPath2 As String
strDosBatchFullPath2 = "C:\MSC.Software\MSC.Nastran\bin\nastran.exe msgbell=no scr=yes " & str
xx = ShellX("C:\MSC.Software\MSC.Nastran\bin\nastran.exe msgbell=no scr=yes " & str, WindowStyle)
'-----
'REQUIRED INFORMATION IS PRINTED ON LOG FILE
Print #3, "THE ITERATION " & iteration & " IS COMPLETED AT " & Format(Time, "hh:mm:ss") & "."
Print #3, "-----"
'-----
'CURRENT REJECTION RATIO IS CALCULATED.
iteration = iteration + 1
Dim current_rej_ratio1, current_rej_ratio2 As Double
current_rej_ratio1 = current_rej_ratio
current_rej_ratio2 = Text3.Text / 100
current_rej_ratio = 0
current_rej_ratio = (current_rej_ratio1 + current_rej_ratio2)
'-----
'IF CURRENT REJECTION RATIO REACHES TO FINAL, PROGRAM TERMINATED.
t = t - 1
If (current_rej_ratio > final_rej_ratio + 0.005) Then
iteration = 0
GoTo exit1
End If
Next t

```

```

Else
'-----
'REQUIRED INFORMATION IS PRINTED ON LOG FILE
Print #3, " "
Print #3, "THE PROGRAM IS TERMINATED AT "&Format(Time, "hh:mm:ss") & ". "
Close #3
'-----
'FINAL LOG FILE POP-UPS.
Shell "C:\windows\NOTEPAD.EXE " & "logfile.txt", vbNormalFocus
Command1.Enabled = True
End If
End Sub
'-----
'START OF SINGLE LOAD CASE CODE
Private Sub Command2_Click()
Command2.Enabled = False
'-----
'PROGRESS OF NASTRAN
Dim xx As Long
Dim strDosBatchFullPath As String
strDosBatchFullPath = "C:\MSC.Software\MSC.Nastran\bin\nastran.exe msgbell=no scr=yes " & "loop.bdf"
xx = ShellX("C:\MSC.Software\MSC.Nastran\bin\nastran.exe msgbell=no scr=yes " & "loop.bdf", WindowStyle)
'-----
'CREATING LOG FILE FOR TRACEABILITY
Dim check3
check3 = "logfile" & ".txt"
Open check3 For Append As #3
Print #3, "LOGFILE FOR EVOLUTIONARY STRUCTURAL OPTIMIZATION"
Print #3, " "
Print #3, "          M.ATACAN AVGIN / 1392018 "
Print #3, " "
Print #3, "THE PROGRAM HAS INITIATED AT "&Format(Time, "hh:mm:ss") & ". "
iteration = 1
exit1:
If (iteration > 0) Then
For t = 0 To 2
x = 0
y = 0
'-----
' F06 FILE ARE SEARCHED FOR STRESS VALUES
If (iteration = 1) Then
a = 1
current_rej_ratio = Text2.Text / 100
Open "loop.f06" For Input As #1
Else
Dim check2
check2 = "loop" & iteration - 1 & ".f06"
Open check2 For Input As #1
End If
matprop = 0
Do
Line Input #1, name1
If (matprop1 = 1) Then
waste = Mid(name1, 5, 13)
If (Trim(waste) = "MSC.NASTRAN") Then
matprop = 0
matprop1 = 0
End If
End If
If (matprop = 1) Then
If (matprop2 = 1) Then
waste = Mid(name1, 2, 24)
If (Trim(waste) = "CENTER") Then
waste = Mid(name1, 118, 129)
matrix1(x, y) = Trim(waste)
y = 0
x = x + 1
matprop2 = 0
End If
End If
waste = Mid(name1, 7, 9)
If (Trim(waste) <> "") Then
matrix1(x, y) = Trim(waste)
matprop2 = 1

```

```

y = y + 1
End If
End If
'-----
' STRESS VALUES ARE FOUND AND COPIED
waste = Mid(name1, 2, 12)
If (Trim(waste) = "ELEMENT-ID") Then
matprop = 1
matprop1 = 1
End If
Loop While Not EOF(1)
Close #1
'-----
' TO DELETE EX F06 FILE
'Kill "C:\uni\*.f06"
totalelements = x
'-----
'STOPPING CRITERIA FIR VOLUMETRIC CONSTRAINT
If (Volume.Text = 0) Then
vol1 = 0
ElseIf (iteration = 1) Then
vol1 = totalelements * (1 - (Volume.Text / 100))
End If
'-----
TO WRITE ALL ELEMENTS IN NUMBER ORDER
To write all elements in element order"
'Print #3, " "
'Print #3, " "
For x = 0 Tototalelements - 1
'Print #3, matrix1(x, 0), "      " & matrix1(x, 1)
Next x
'Print #3, " "
'Print #3, " "
'-----
THE ELEMENTS ARE ARRANGED FOR STRESS VALUES IN ASCENDING ORDER
For x = 0 Tototalelements - 1
For y = x + 1 Tototalelements - 1
If (matrix1(x, 1) > matrix1(y, 1)) Then
waste = matrix1(y, 0)
s = matrix1(y, 1)
matrix1(y, 0) = matrix1(x, 0)
matrix1(y, 1) = matrix1(x, 1)
matrix1(x, 0) = waste
matrix1(x, 1) = s
End If
Next y
Next x
'-----
'ELEMENTS HAVING STRESS HIGHER THAN YIELD IN EACH CASE ARE DECLARED FOR CHECK IF ANY.
max = matrix1(totalelements - 1, 1)
corryield = Text5.Text * 1000000
If (corryield < max) Then
Print #3, ""
Print #3, "THE ELEMENTS HIGHER THAN YIELD STRESS ARE;"
Print #3, " "
Print #3, "ELEMENT NO      VON MISSES STRESS (MPa)"
Else
End If
For x = 0 Tototalelements - 1
If (corryield < matrix1(x, 1)) Then
Print #3, matrix1(x, 0), "      " & matrix1(x, 1) / 1000000
End If
Next x
'-----
PROGRAM TERMINATION IF STRESS OF EVEN ONE ELEMENT IS GREATER THAN YIELD STRESS
If (corryield < max) Then
iteration = 0
GoTo exit1
End If
'-----
TO WRITE ALL ELEMENTS IN STRESS ORDER
Print #3, ""
To write all elements in stress order"
Print #3, " "

```

```

'Print #3, " "
'Print #3, " ALL ELEMENTS IN STRESS ORDER IS;"
'For x = 0 Tototalelements - 1
'Print #3, matrix1(x, 0), "      " & matrix1(x, 1)
'Next x
'Print #3, " "
'Print #3, " "
'-----
'CONTINUE OF THE ELEMENTS ARE ARRANGED FOR STRESS VALUES IN ASCENDING ORDER
max = matrix1(totalelements - 1, 1)
maxelement = matrix1(totalelements - 1, 0)
nofdelements = 0
'For x = 0 Tototalelements - 1
min = matrix1(x, 1)
rej_ratio = min / max
If (rej_ratio < current_rej_ratio) Then
matrix3(x, 0) = matrix1(x, 0)
matrix3(x, 1) = matrix1(x, 1)
nofdelements = nofdelements + 1
Else
Exit For
End If
'Next x
'-----
'UNNECESSARY ELEMENTS AND ALL ELEMENTS ARE MONITORED IN LISTBOX.
'For x = 0 Tototalelements - 1
>List1.AddItem (matrix1(x, 0))
>List1.AddItem (matrix1(x, 1))
'Next x
'For x = 0 Tototalelements - 1
>List2.AddItem (matrix3(x, 0))
>List2.AddItem (matrix3(x, 1))
'Next x
'-----
'STOPPING CRITERIA FIR VOLUMETRIC CONSTRAINT
delements = nofdelements
If (vol1 <> 0) Then
If ((totalelements - delements) < vol1) Then
iteration = 0
GoTo exit1
End If
End If
'-----
'CHECK FOR FINAL REJECTION RATIO.
Dim final_rej_ratio As Double
final_rej_ratio = Text1.Text / 100 - 0.0005
If (current_rej_ratio >= final_rej_ratio) Then
If (a = 1) Then
GoTo jump2
End If
iteration = 0
GoTo exit1
jump2:
a = 0
End If
'-----
'TO PRINT DELETE ELEMENTS IF NOT AT NON DESIGN.
'Print #3, " DELETED ELEMENTS IN ELEMENT ORDER IS WITHOUT REGARDING NON DESIGN DOMAIN;"
'For x = 0 Tonofdelements - 1
'Print #3, matrix3(x, 0), "      " & matrix3(x, 1)
'Next x
'-----
'NEW BDF FILE IS FORMED.
If (iteration = 1) Then
Open "loop.bdf" For Input As #1
Else
Dim check0
check0 = "loop" & iteration - 1 & ".bdf"
Open check0 For Input As #1
End If
Dim check1
check1 = "loop" & iteration & ".bdf"
Open check1 For Append As #2
'-----

```

```

REQUIRED INFORMATION IS PRINTED ON LOG FILE
Print #3, " "
Print #3, "MAXIMUM VON MISES STRESS OF THE WHOLE STRUCTURE IS "& max / 1000000 &" MPa ON ELEMENT "
&maxelement& "."
Print #3, " "
Print #3, "THE CURRENT REMOVAL RATIO IS "&current_rej_ratio * 100 &" %."
Print #3, " "
Print #3, "ELEMENT NO      VON MISES STRESS (MPa)"
'-----
'UNNECESSARY ELEMENTS ARE REMOVED FROM BDF LINE BY LINE.
For x = 0 Todelements - 1
For y = x + 1 Todelements - 1
  If matrix3(x, 0) > matrix3(y, 0) Then
    s = matrix3(y, 0)
    k = matrix3(y, 1)
    matrix3(y, 0) = matrix3(x, 0)
    matrix3(y, 1) = matrix3(x, 1)
    matrix3(x, 0) = s
    matrix3(x, 1) = k
  k = 0
  s = 0
End If
  Next y
Next x
'-----
'UNNECESSARY ELEMENTS ARE LISTED IN LISTBOX.
For x = 0 Todelements - 1
>List1.AddItem (matrix3(x, 0))
>List1.AddItem (matrix3(x, 1))
Next x
'-----
'CONTINUE OF REMOVAL OF UNNECESSARY ELEMENTS FROM BDF FILE
Dim kkk As Double
kkk = 0
Do
Line Input #1, name1
cut1 = Mid(name1, 1, 6)
cut6 = Trim(cut1)
cut1 = cut6
If (cut1 = "CTETRA") Then
loop1 = 0
End If
If (loop1 = 1) Then
loop1 = 0
ElseIf ((cut1 = "CHEXA") Or (cut1 = "CTETRA")) Then
cut2 = Mid(name1, 8, 10)
cut3 = Trim(cut2)
cut4 = Mid(name1, 18, 8)
cut5 = Trim(cut4)
If (iteration > 0) Then

GoTo record
record1:
Else
record2:
Print #2, name1
End If
Else
Print #2, name1
End If
Loop While Not EOF(1)
If (iteration < 0) Then
record:
For x = 0 Todelements - 1
If (matrix3(x, 0) > cut3) Then
GoTo record2
End If
If cut3 = matrix3(x, 0) And cut5 = 1 Then
loop1 = 1
Print #3, matrix3(x, 0), "      " & matrix3(x, 1) / 1000000
kkk = kkk + 1
GoTo record1
Else
GoTo record2

```

```

End If
Next x
GoTo record2
End If
Close #1
Close #2
Dim str As String
'-----
'REQUIRED INFORMATION IS PRINTED ON LOG FILE
Print #3, " "
Print #3, kkk&" ELEMENTS ARE REMOVED. THE NUMBER OF REMAINING ELEMENTS IS "&totalements - kkk& "."
Print #3, " "
'-----
'PROGRESS OF NASTRAN
str = "loop" & iteration & ".bdf"
Dim strDosBatchFullPath2 As String
strDosBatchFullPath2 = "C:\MSC.Software\MSC.Nastran\bin\nastran.exe msgbell=no scr=yes " &str
xx = ShellX("C:\MSC.Software\MSC.Nastran\bin\nastran.exe msgbell=no scr=yes " &str, WindowStyle)
'-----
'REQUIRED INFORMATION IS PRINTED ON LOG FILE
Print #3, "THE ITERATION " & iteration & " IS COMPLETED AT " & Format(Time, "hh:mm:ss") & "."
Print #3, "-----"
'-----
'CURRENT REJECTION RATIO IS CALCULATED.
iteration = iteration + 1
Dim current_rej_ratio1, current_rej_ratio2 As Double
current_rej_ratio1 = current_rej_ratio
current_rej_ratio2 = Text3.Text / 100
current_rej_ratio = 0
current_rej_ratio = (current_rej_ratio1 + current_rej_ratio2)
t = t - 1
If (current_rej_ratio>final_rej_ratio + 0.005) Then
iteration = 0
GoTo exit1
End If
Next t
Else
'-----
'REQUIRED INFORMATION IS PRINTED ON LOG FILE
Print #3, " "
Print #3, "THE PROGRAM IS TERMINATED AT "&Format(Time, "hh:mm:ss") & "."
'-----
'FINAL LOG FILE POP-UPS.
Close #3
Shell "C:\windows\NOTEPAD.EXE " & "logfile.txt", vbNormalFocus
Command2.Enabled = True
End If
End Sub
'-----
'THE INTERFACE OF INPUT FOR SINGLE LOAD CASE
Private Sub Form_Load()
Option1.Value = True
Text4.Visible = False
Label7.Visible = False
Command2.Visible = True
Command1.Visible = False
End Sub
Private Sub Option1_Click()
Option2.Value = False
Text4.Visible = False
Label7.Visible = False
Command2.Visible = True
Command1.Visible = False
End Sub
'-----
'THE INTERFACE OF INPUT FOR MULTIPLE LOAD CASE
Private Sub Option2_Click()
Option1.Value = False
Text4.Visible = True
Label7.Visible = True
Command2.Visible = False
Command1.Visible = True
End Sub

```

B. THE EVALUATION OF THE AIRCRAFT COMPONENTS

The optimal evaluation of the aircraft components, the lug, the clevis, main landing fitting and fitting support is presented in Appendix B.

B.1. THE EVALUATION OF LUG

The optimization steps of lug are presented from Figure B.1 to B.20. As mentioned in Chapter 4, the RR_o and ER are 0.25% and figures are inserted for each 10th iteration at each load case respectively. (i.e., $RR = 2.5\%$, 5%, 7.5%, 10%, 12.5%, 15%, 17.5%, 20%, 22.5%, 25%) Figure B.1 to B.10 present load case 1 and B.11 to B.20 present load case 2. Same von Mises spectrum is utilized with the Figure 4.19 and 4.20 for clarity.

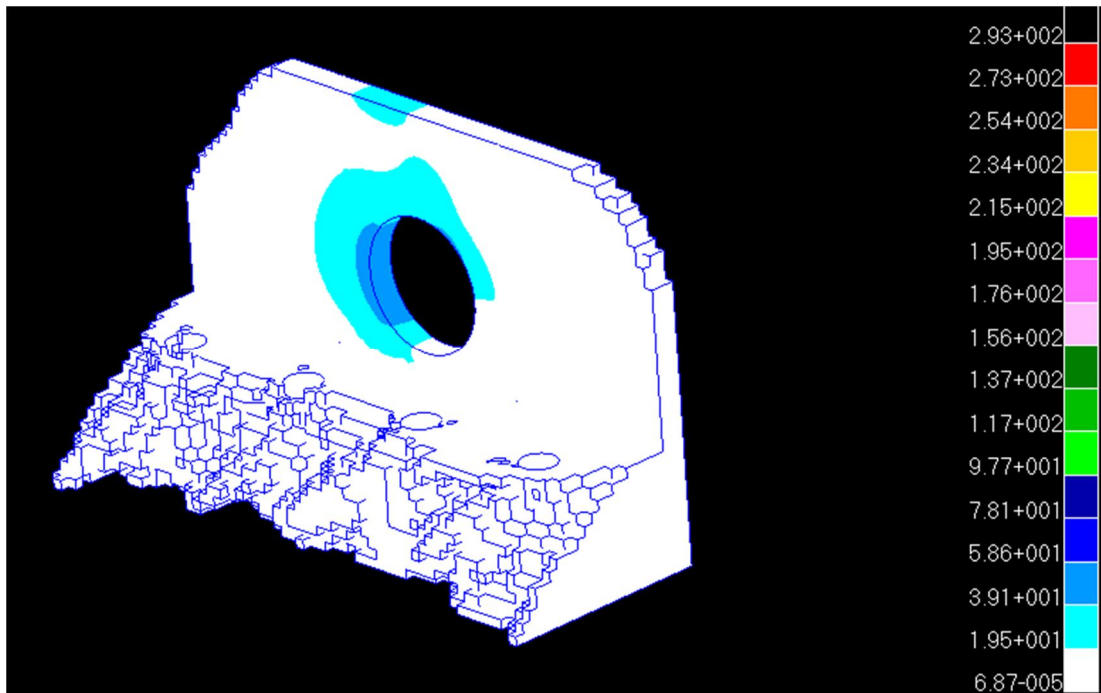


Figure B.1 The von Mises stress distribution of lug at RR=2.5% for load case 1.

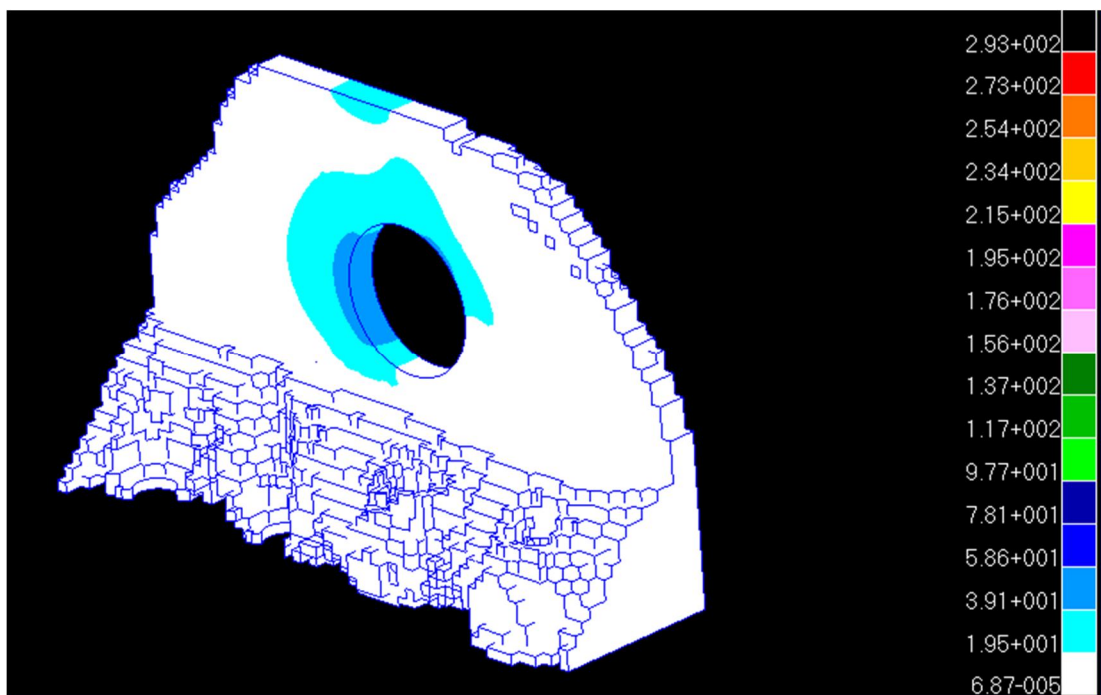


Figure B.2 The von Mises stress distribution of lug at RR=5% for load case 1.

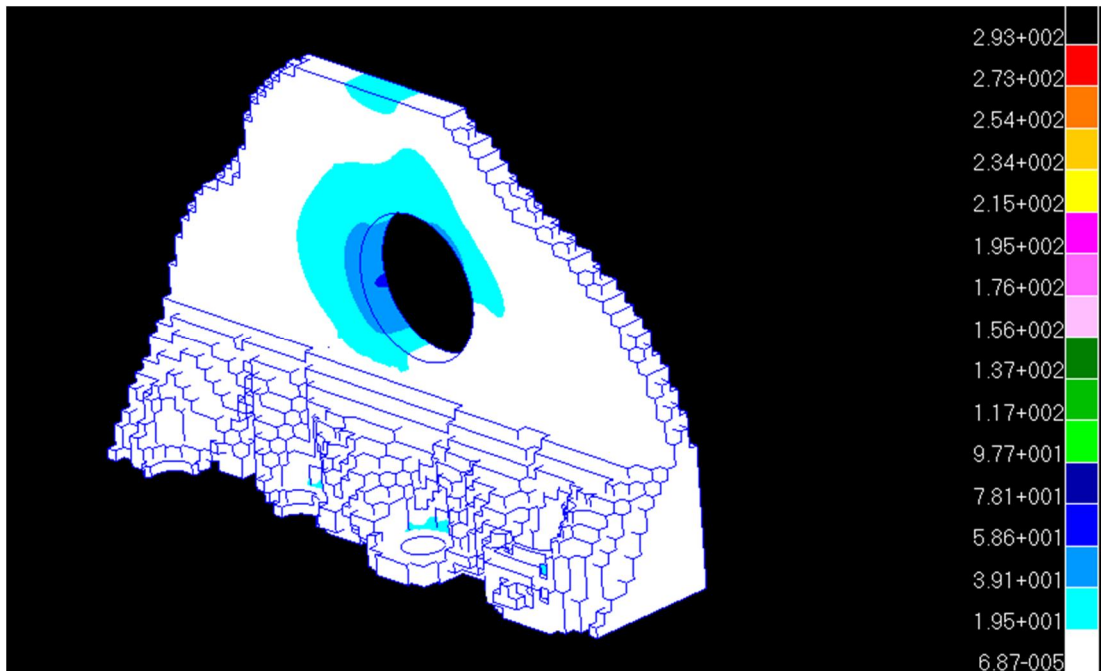


Figure B.3 The von Mises stress distribution of lug at RR=7.5% for load case 1.

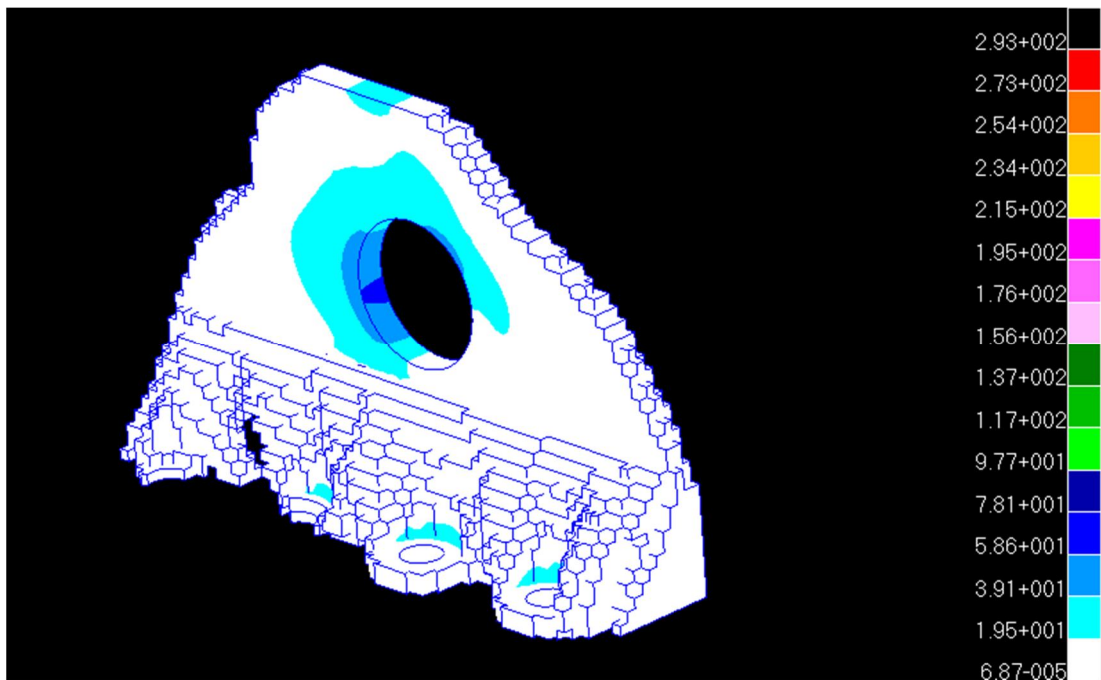


Figure B.4 The von Mises stress distribution of lug at RR=10% for load case 1.

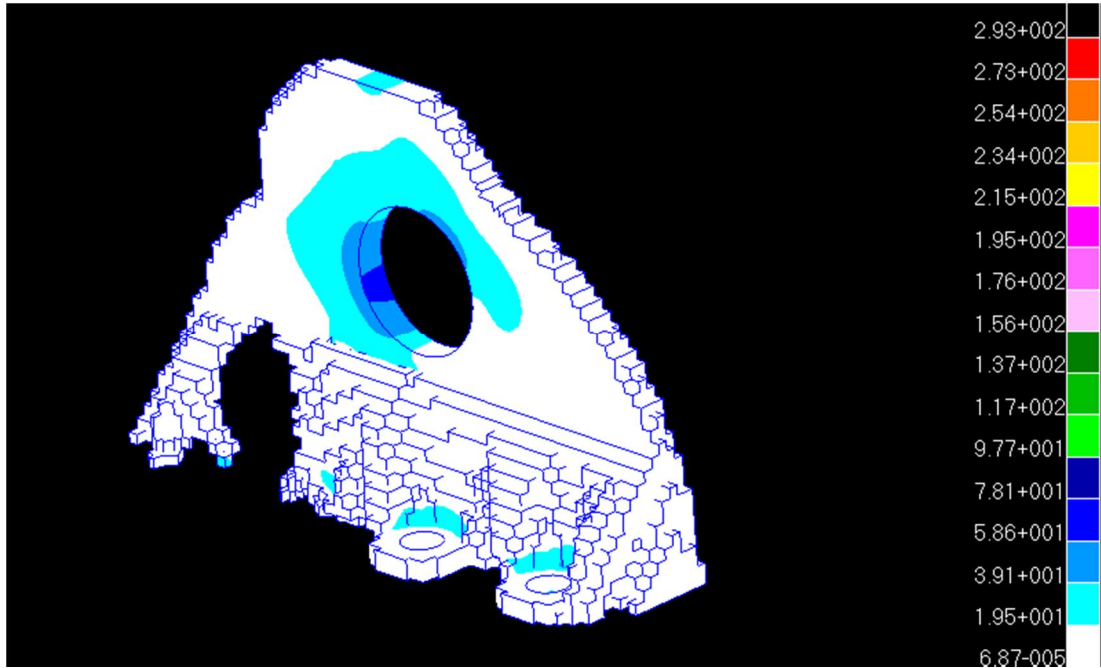


Figure B.5 The von Mises stress distribution of lug at RR=12.5% for load case 1.

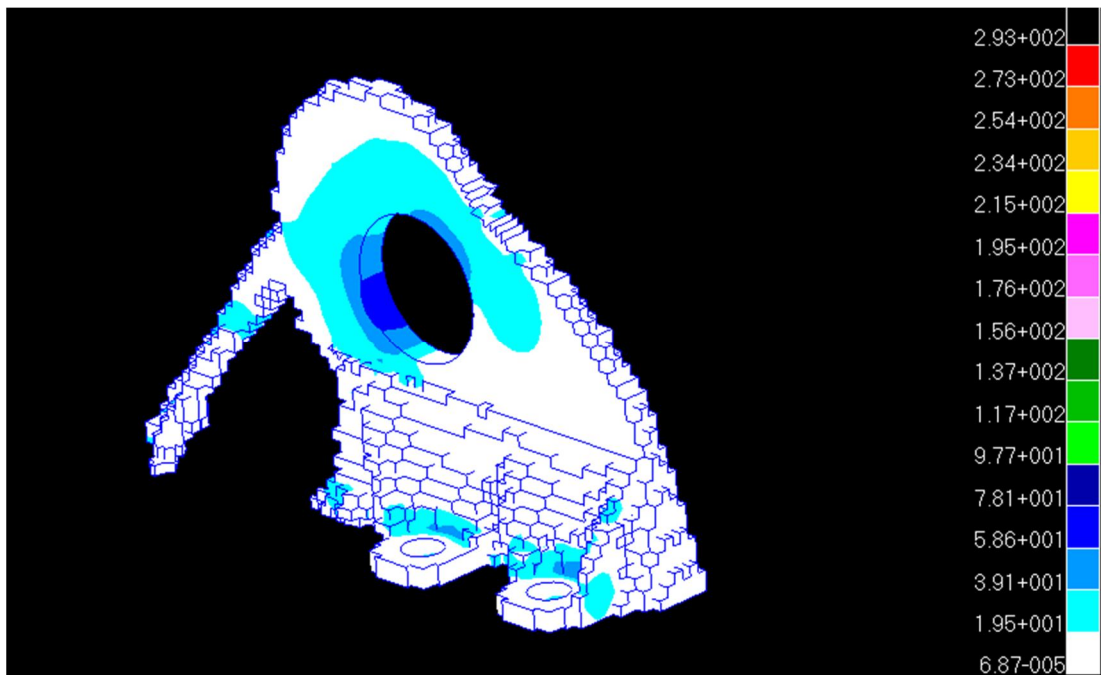


Figure B.6 The von Mises stress distribution of lug at RR=15% for load case 1.

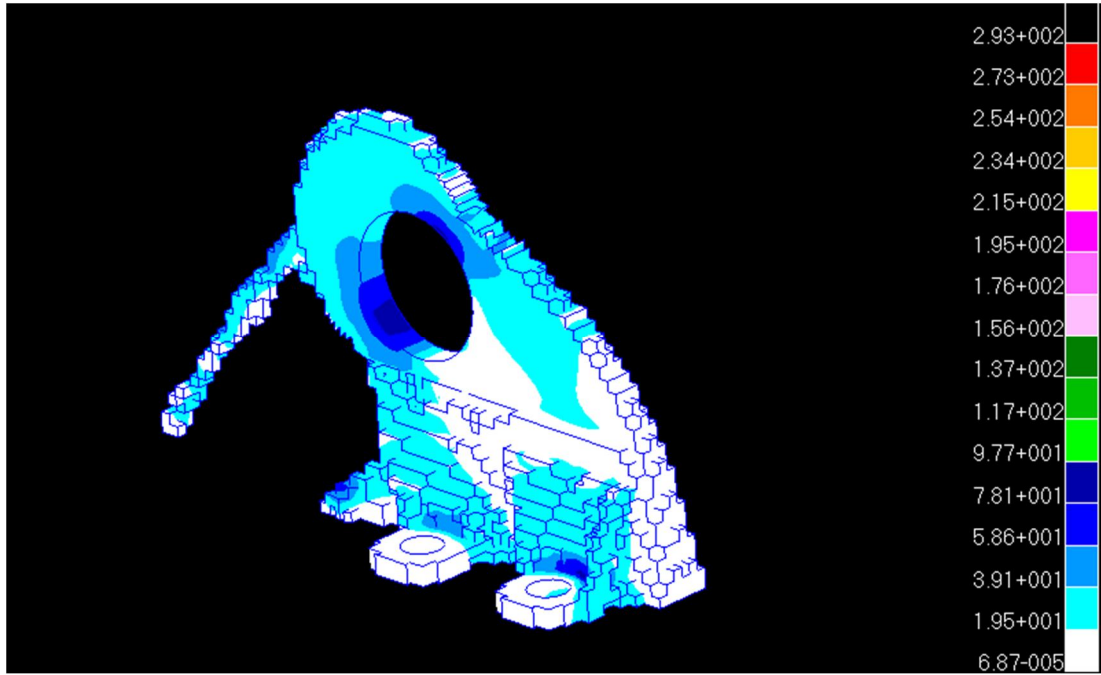


Figure B.7 The von Mises stress distribution of lug at RR=17.5% for load case 1.

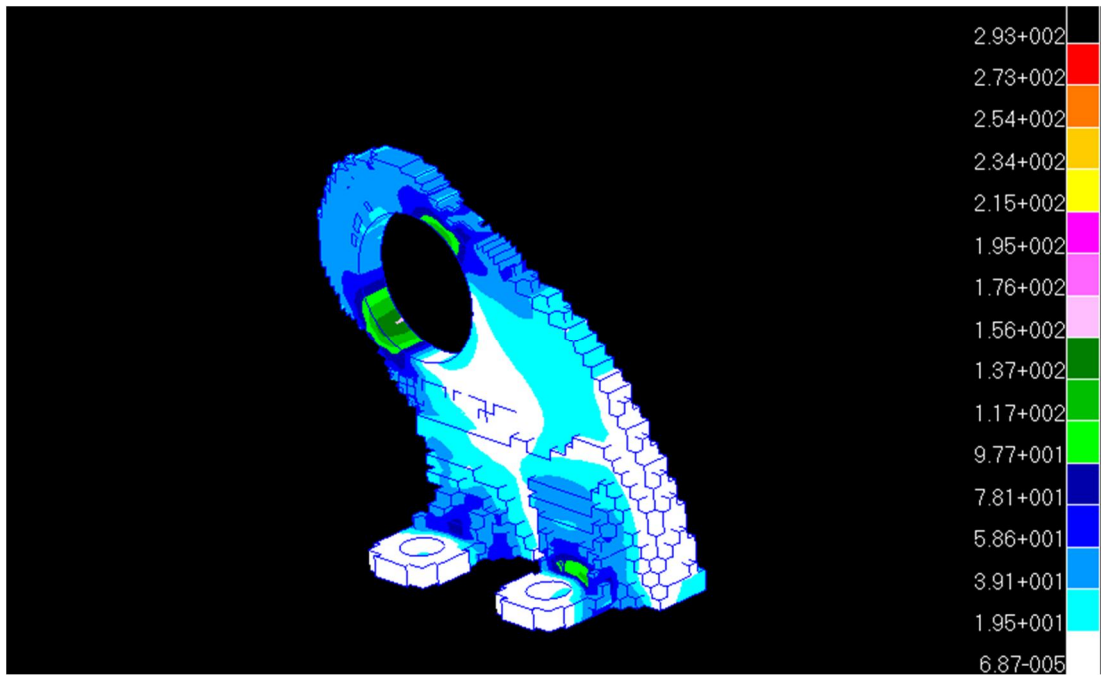


Figure B.8 The von Mises stress distribution of lug at RR=20% for load case 1.

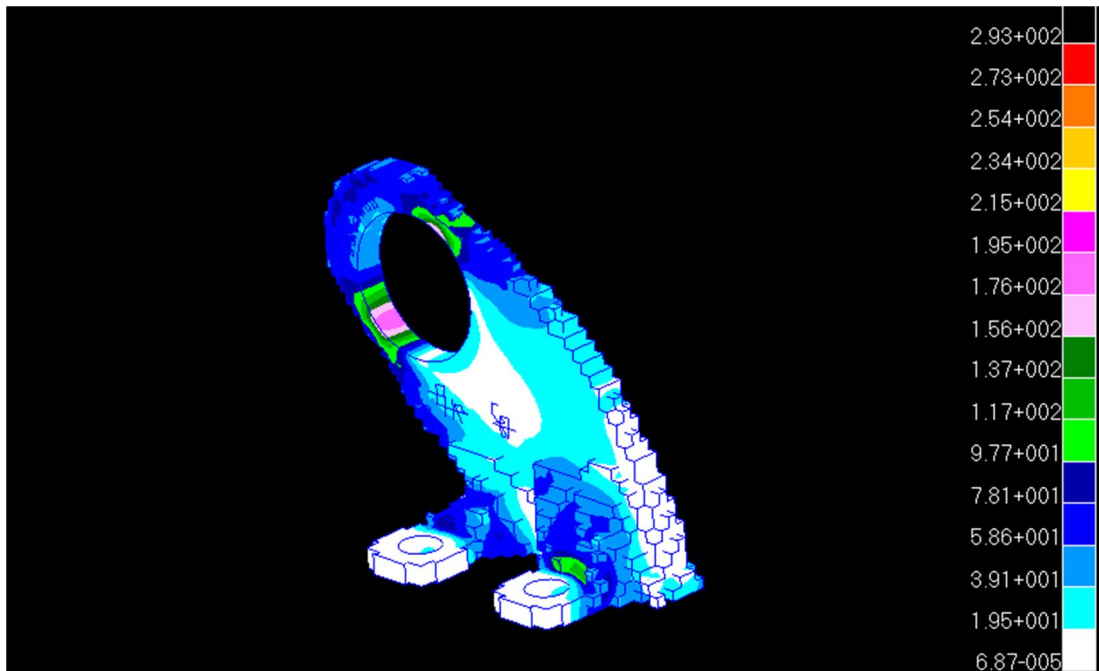


Figure B.9 The von Mises stress distribution of lug at RR=22.5% for load case 1.

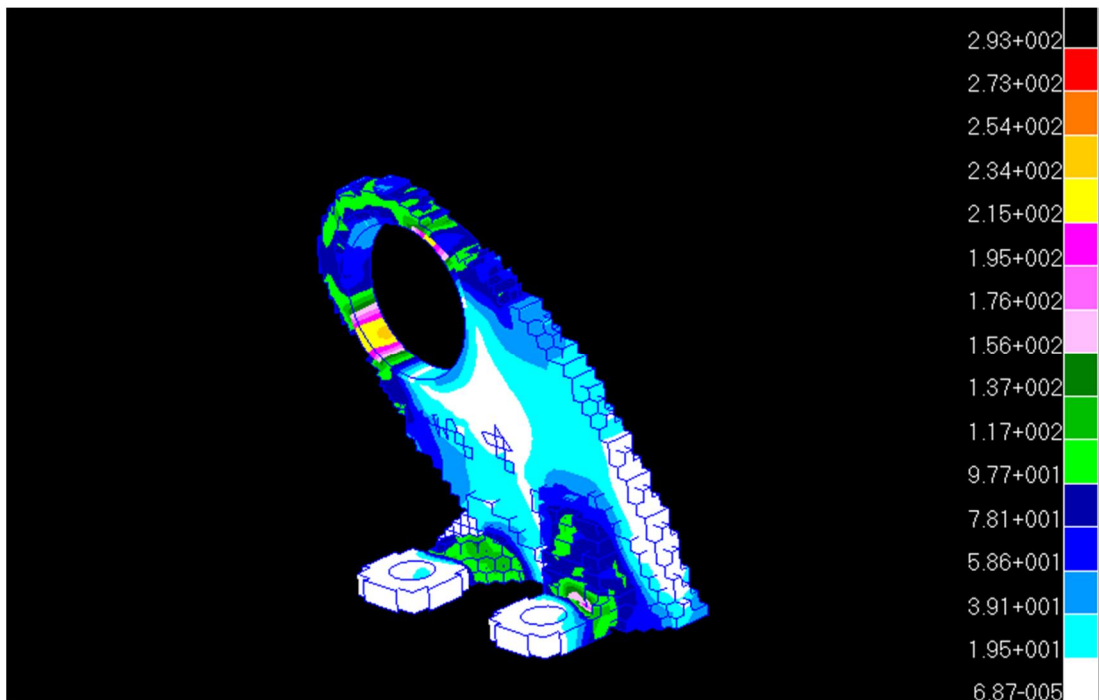


Figure B.10 The von Mises stress distribution of lug at RR=25% for load case 1.

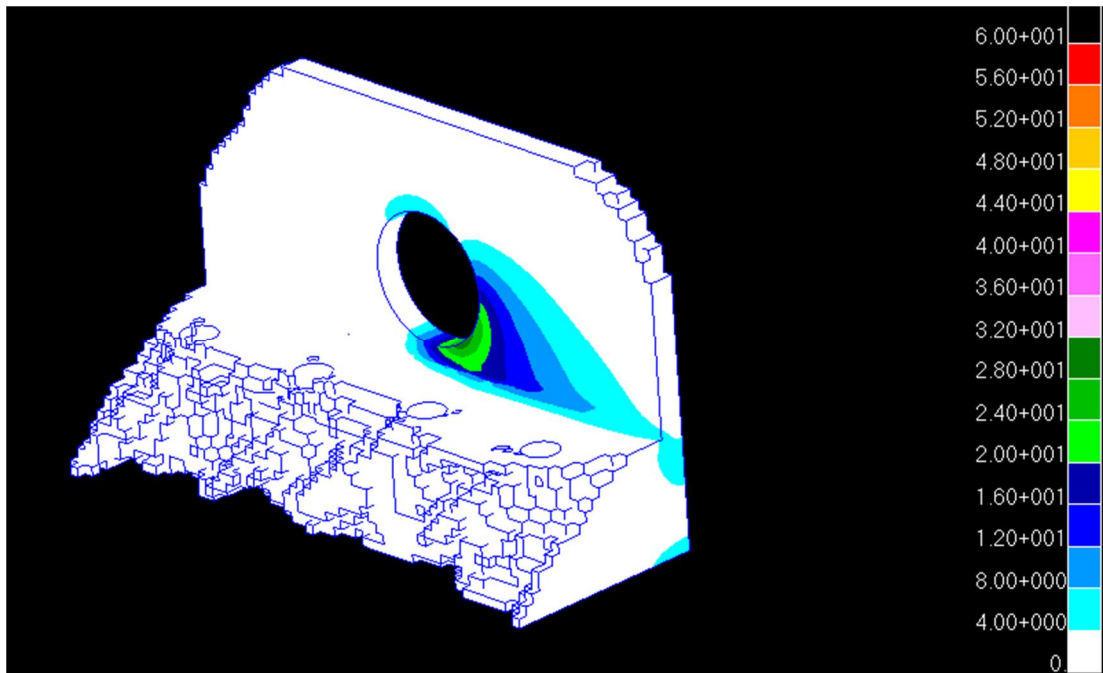


Figure B.11 The von Mises stress distribution of lug at RR=2.5% for load case 2.

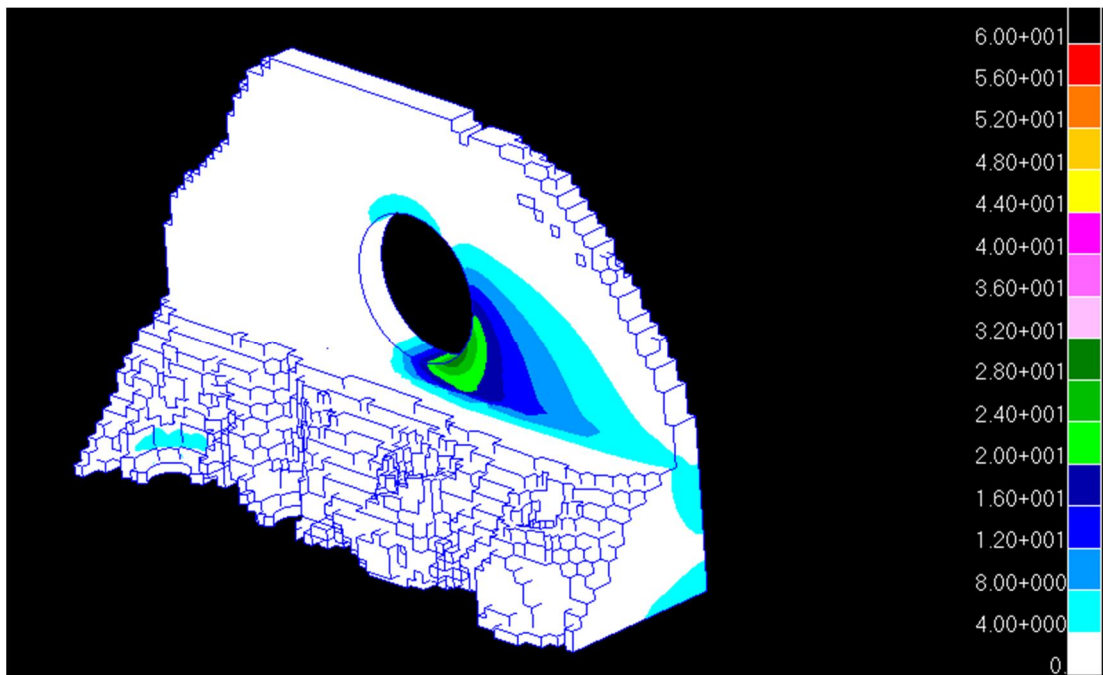


Figure B.12 The von Mises stress distribution of lug at RR=5% for load case 2.

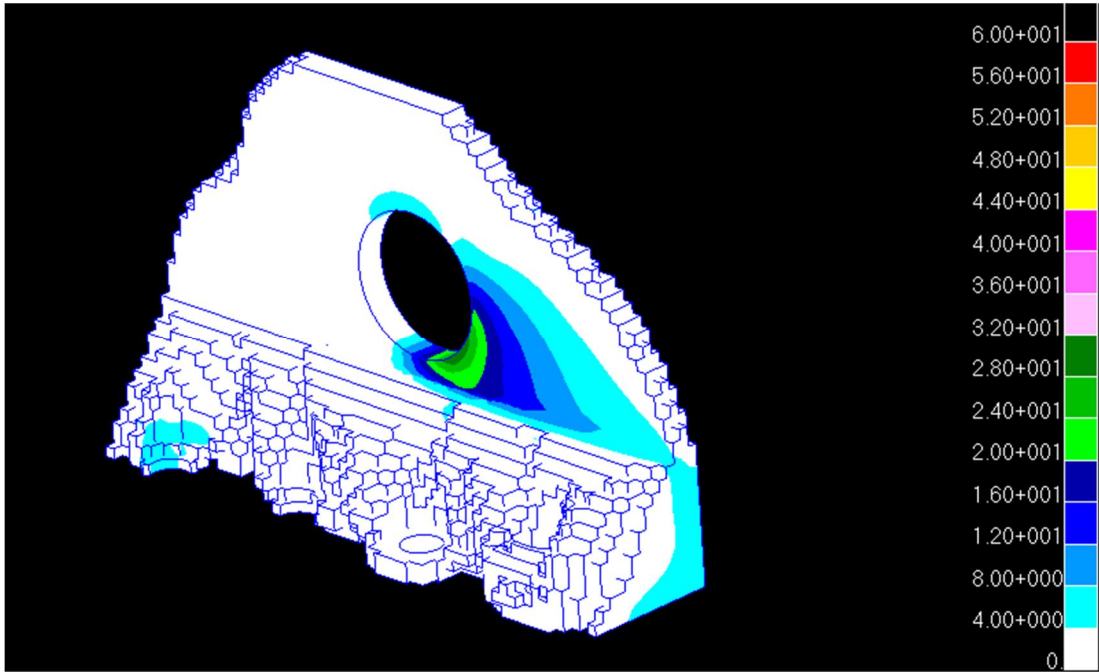


Figure B.13 The von Mises stress distribution of lug at RR=7.5% for load case 2.

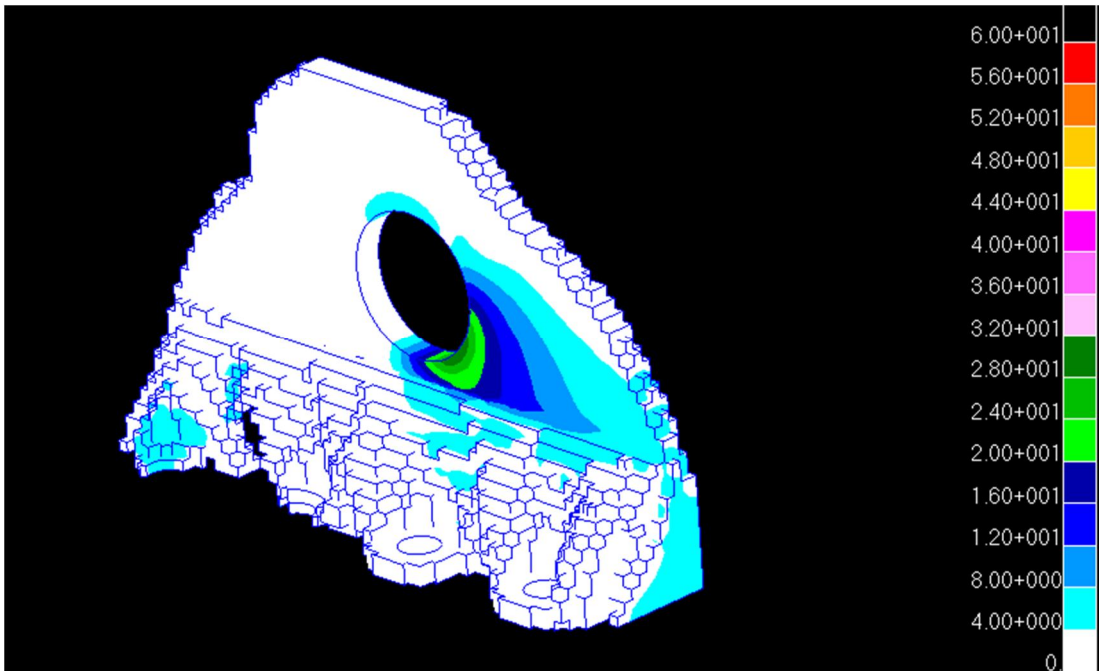


Figure B.14 The von Mises stress distribution of lug at RR=10% for load case 2.

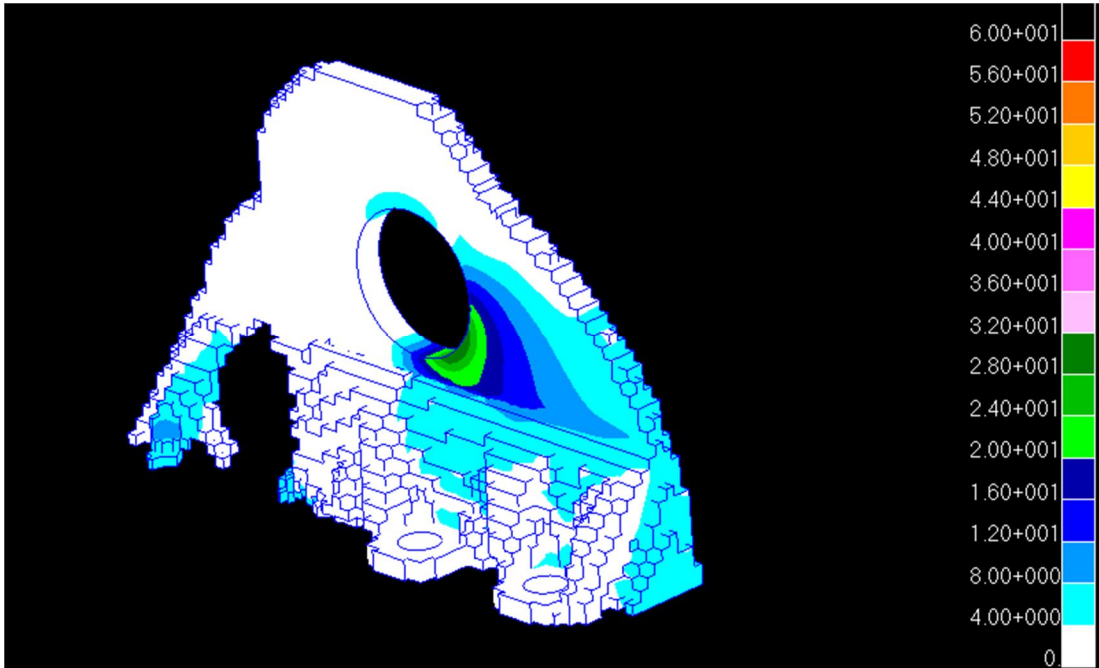


Figure B.15 The von Mises stress distribution of lug at RR=12.5% for load case 2.

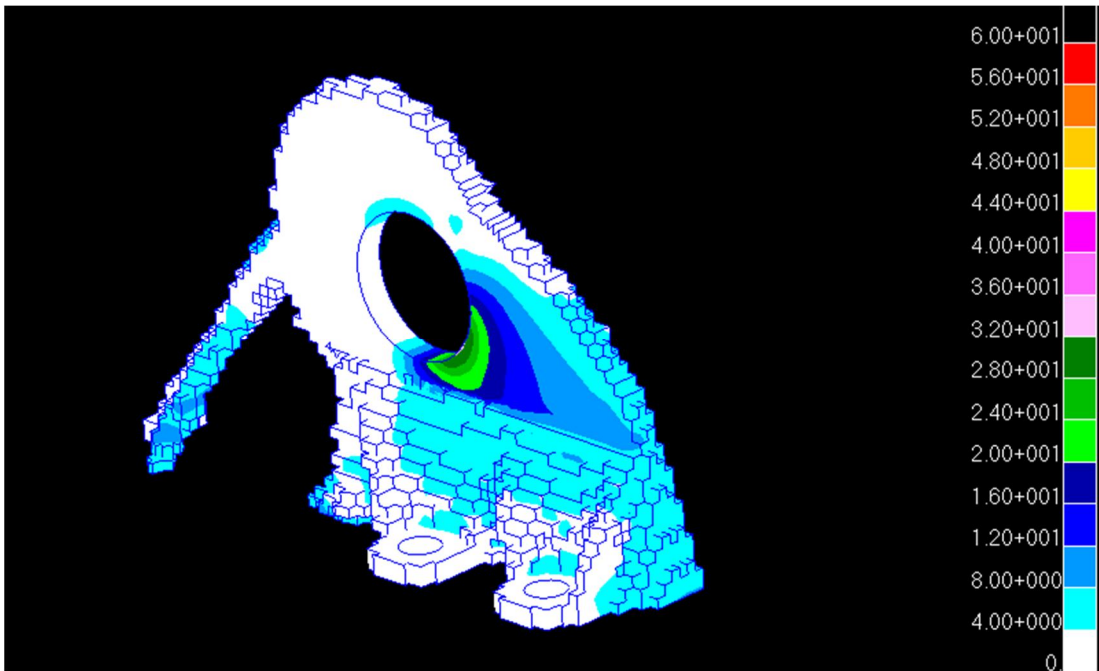


Figure B.16 The von Mises stress distribution of lug at RR=15% for load case 2.

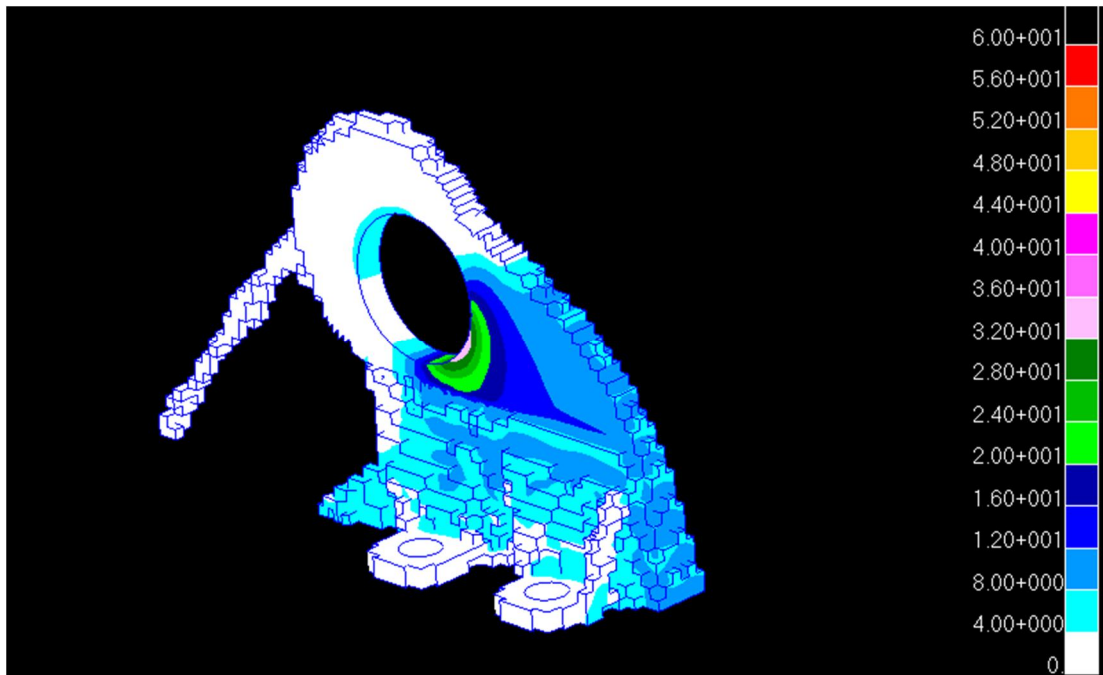


Figure B.17 The von Mises stress distribution of lug at RR=17.5% for load case 2.

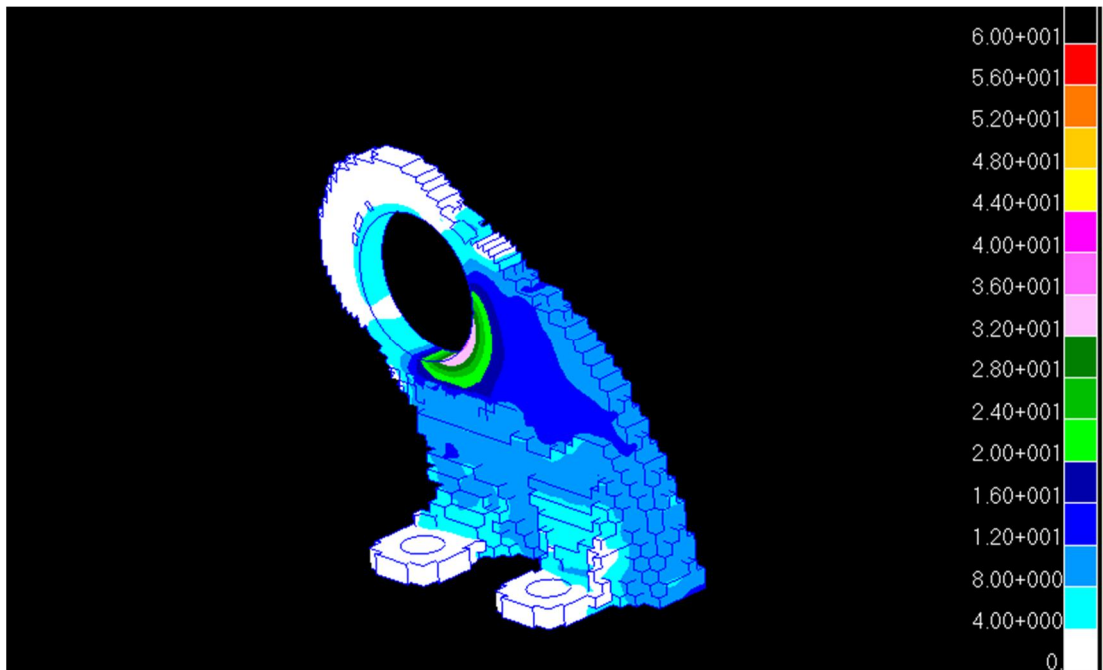


Figure B.18 The von Mises stress distribution of lug at RR=20% for load case 2.

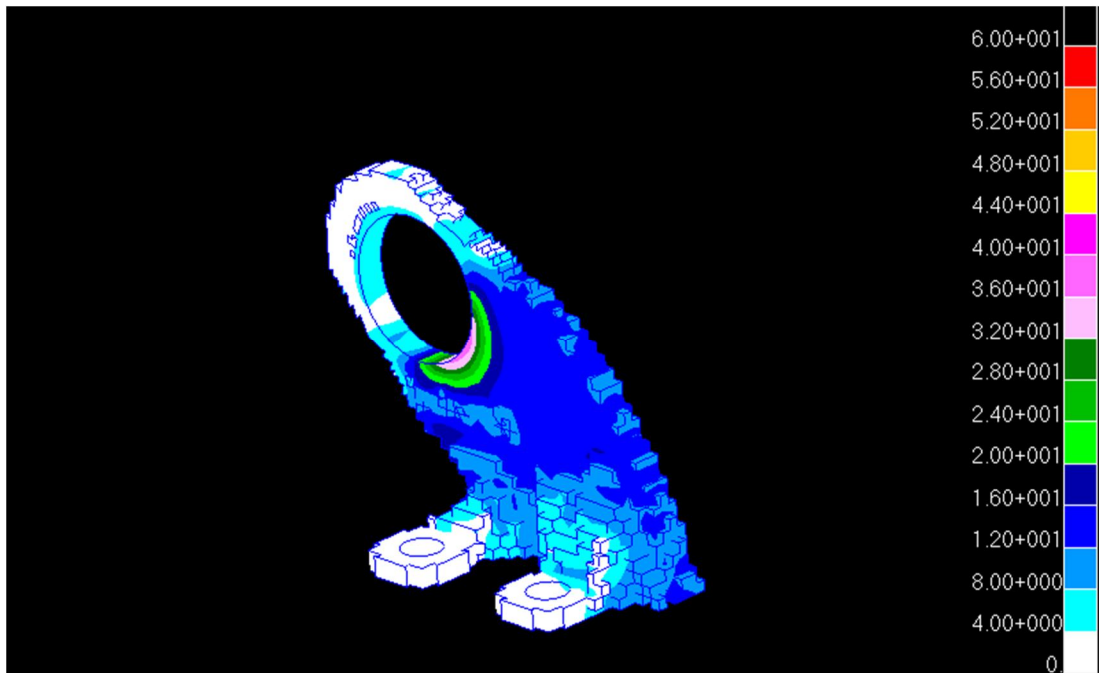


Figure B.19 The von Mises stress distribution of lug at RR=22.5% for load case 2.

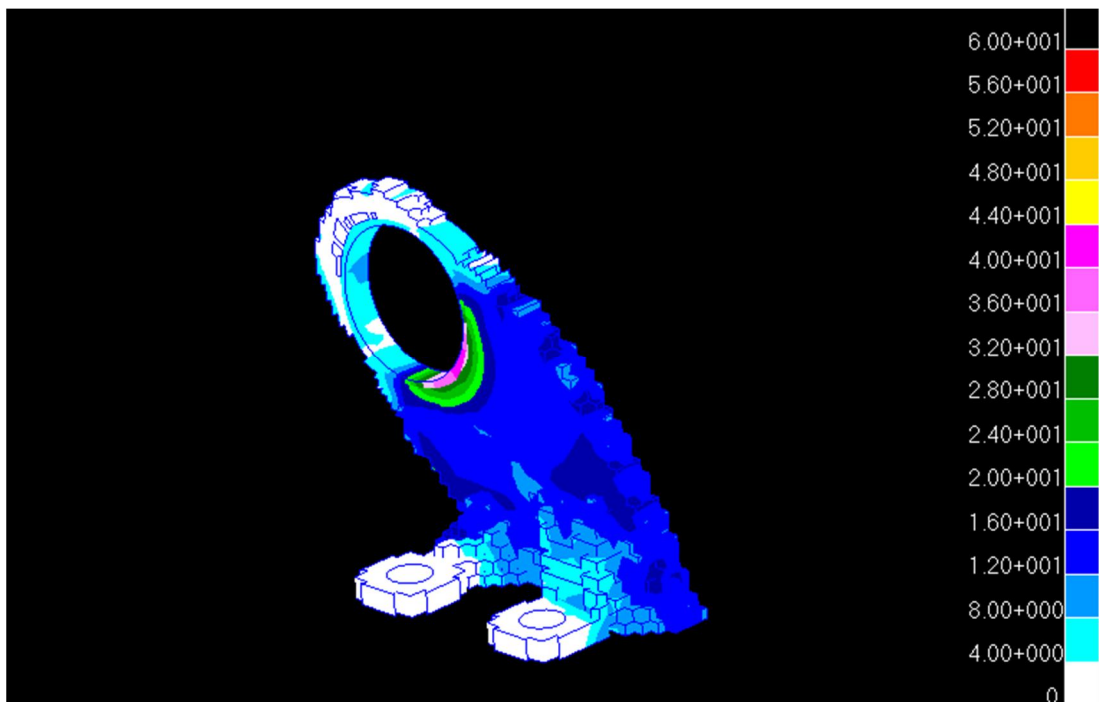


Figure B.20 The von Mises stress distribution of lug at RR=25% for load case 2.

B.2. THE EVALUATION OF CLEVIS

The optimization steps of clevis are presented from Figure B.21 to B.40. As mentioned in Chapter 4, the RR_o and ER are 0.25% and figures are inserted for each 12th iteration at each load case respectively. (i.e., $RR = 3\%$, 6%, 9%, 12%, 15%, 18%, 21%, 24%, 27%, 30%) Figure B.21 to B.30 present load case 1 and B.31 to B.40 present load case 2. Same von Mises spectrum is utilized with the Figure 4.33 and 4.35 for clarity.

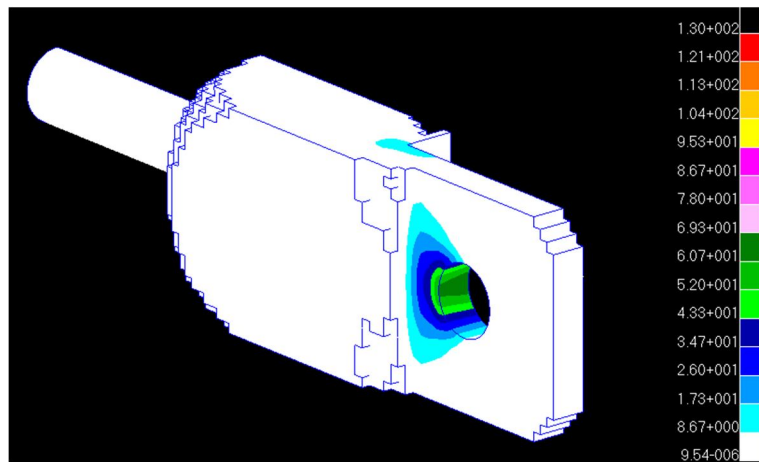


Figure B.21 The von Mises stress distribution of clevis at $RR=3\%$ for load case 1.

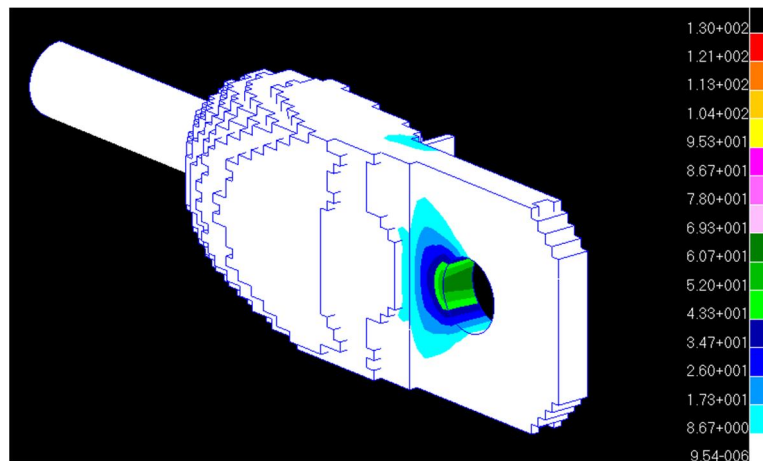


Figure B.22 The von Mises stress distribution of clevis at $RR=6\%$ for load case 1.

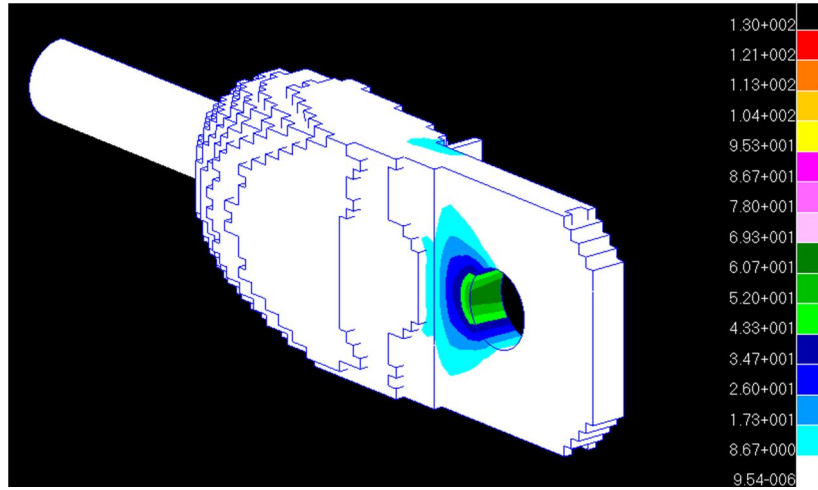


Figure B.23 The von Mises stress distribution of clevis at RR=9% for load case 1.

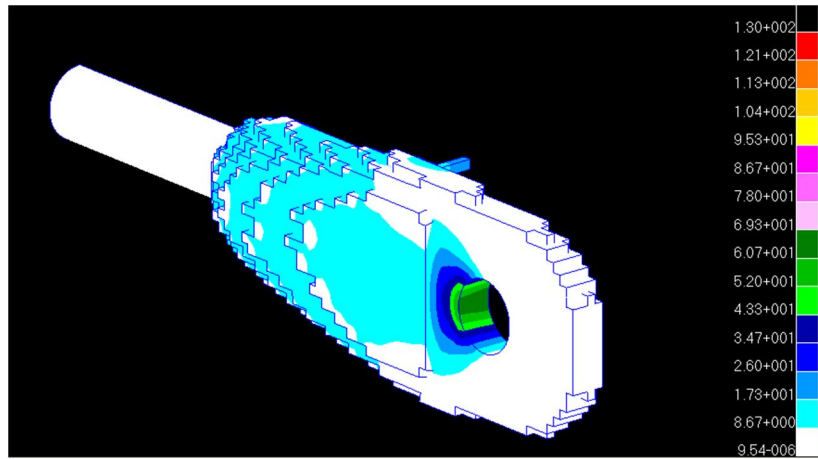


Figure B.24 The von Mises stress distribution of clevis at RR=12% for load case 1.

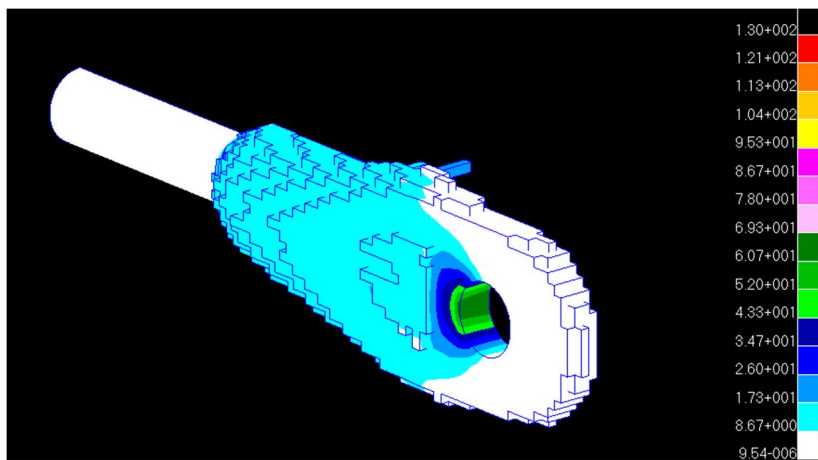


Figure B.25 The von Mises stress distribution of clevis at RR=15% for load case 1.

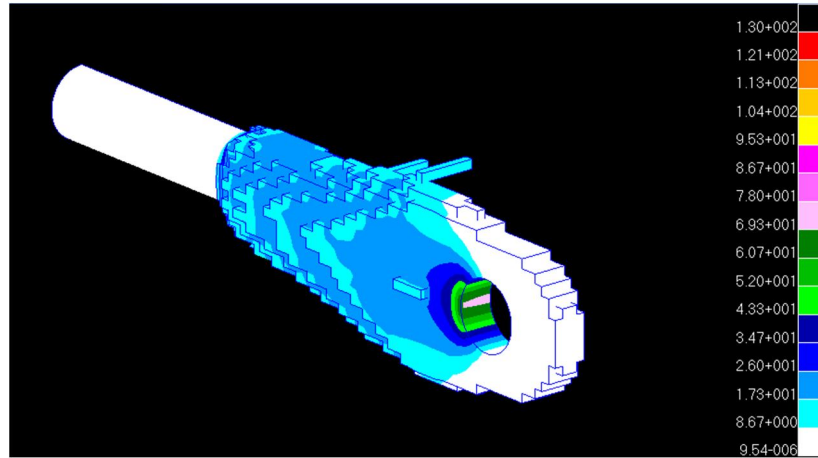


Figure B.26 The von Mises stress distribution of clevis at RR=18% for load case 1.

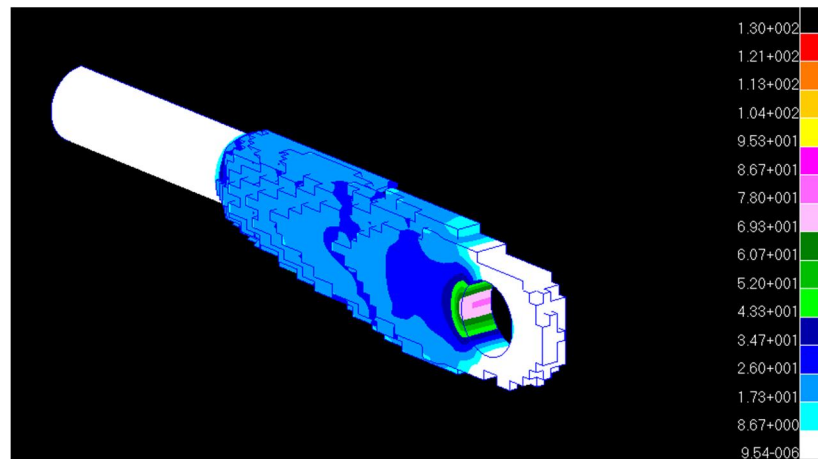


Figure B.27 The von Mises stress distribution of clevis at RR=21% for load case 1.

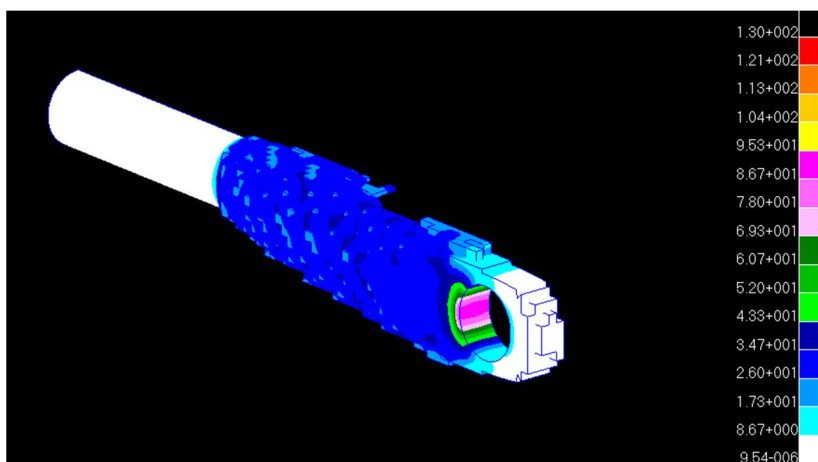


Figure B.28 The von Mises stress distribution of clevis at RR=24% for load case 1.

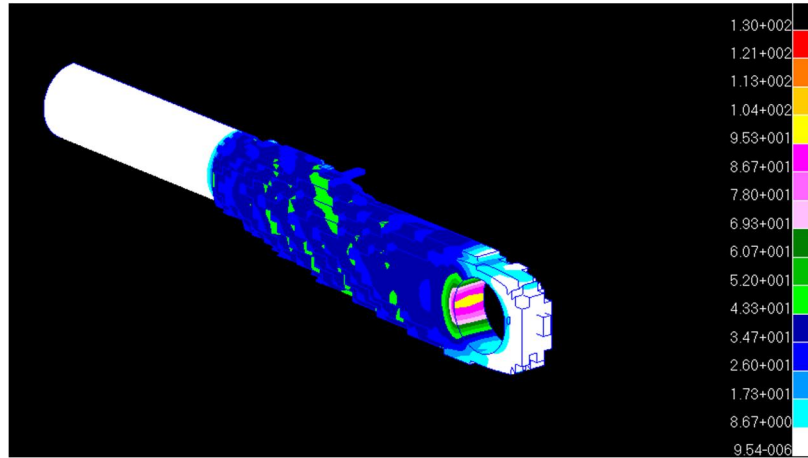


Figure B.29 The von Mises stress distribution of clevis at RR=27% for load case 1.



Figure B.30 The von Mises stress distribution of clevis at RR=30% for load case 1.

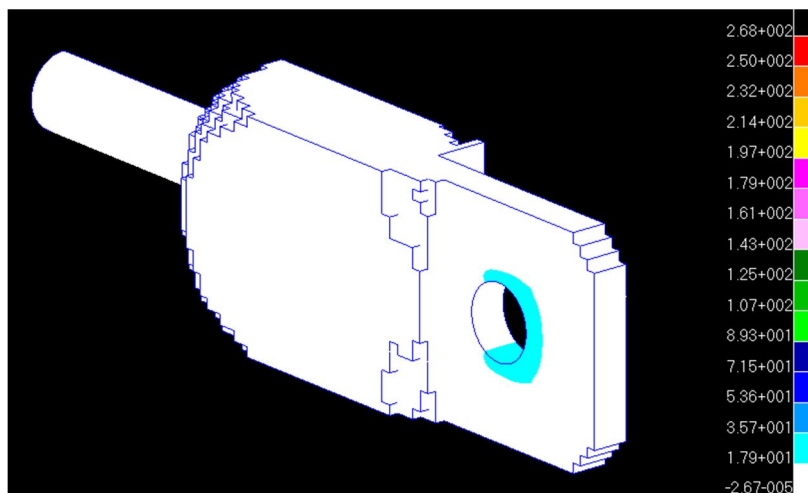


Figure B.31 The von Mises stress distribution of clevis at RR=3% for load case 2.

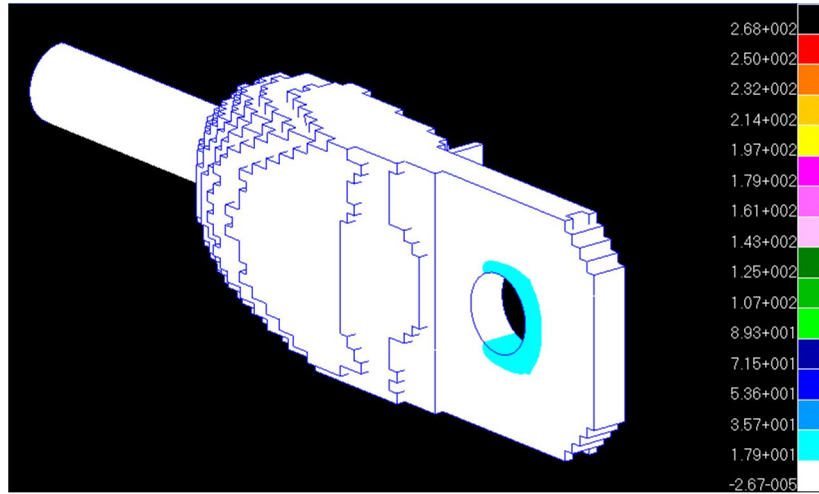


Figure B.32 The von Mises stress distribution of clevis at RR=6% for load case 2.

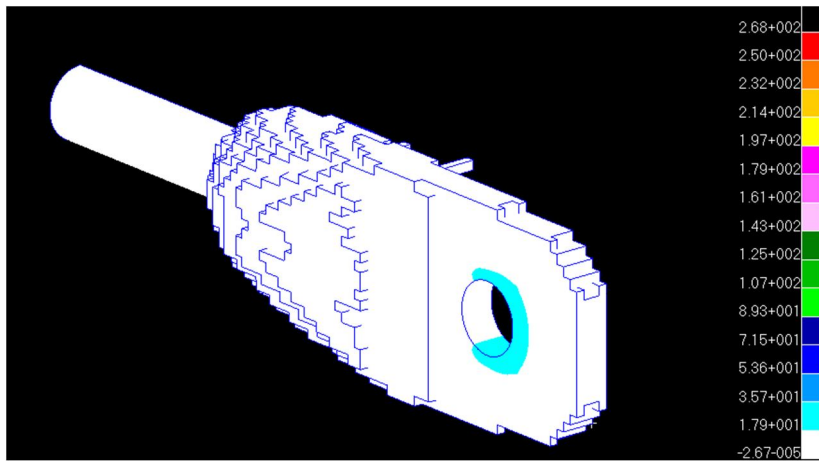


Figure B.33 The von Mises stress distribution of clevis at RR=9% for load case 2.

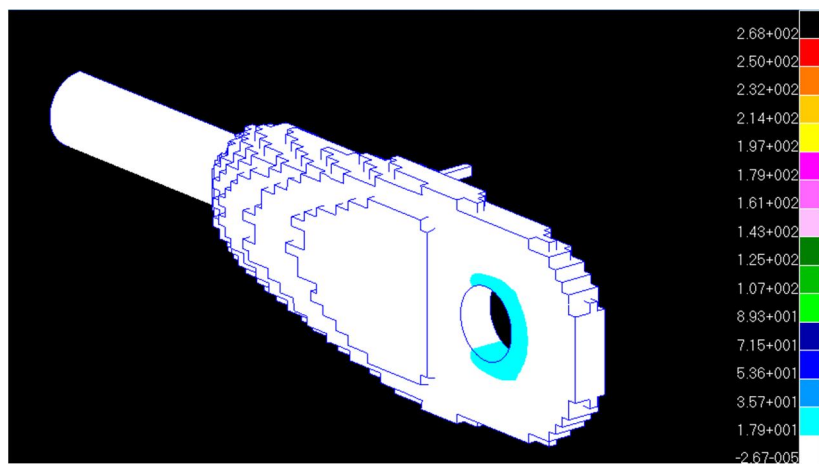


Figure B.34 The von Mises stress distribution of clevis at RR=12% for load case 2.

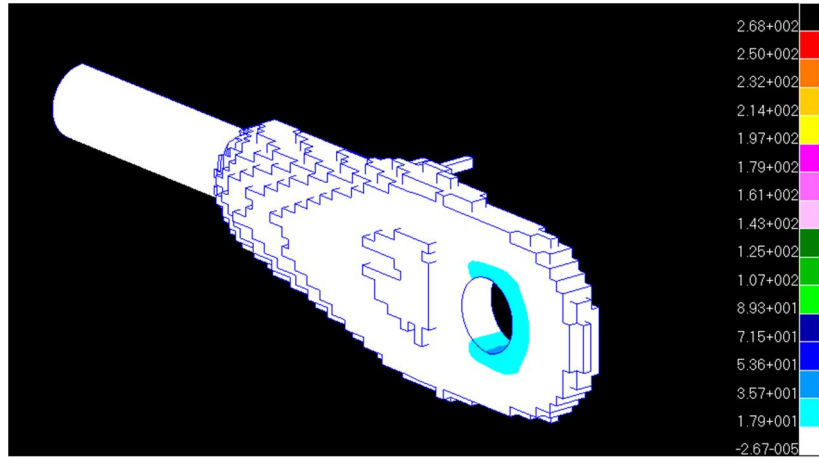


Figure B.35 The von Mises stress distribution of clevis at RR=15% for load case 2.

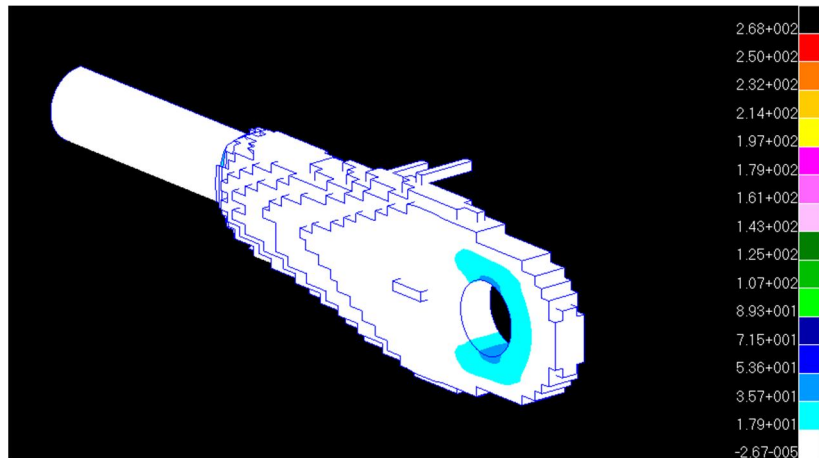


Figure B.36 The von Mises stress distribution of clevis at RR=18% for load case 2.

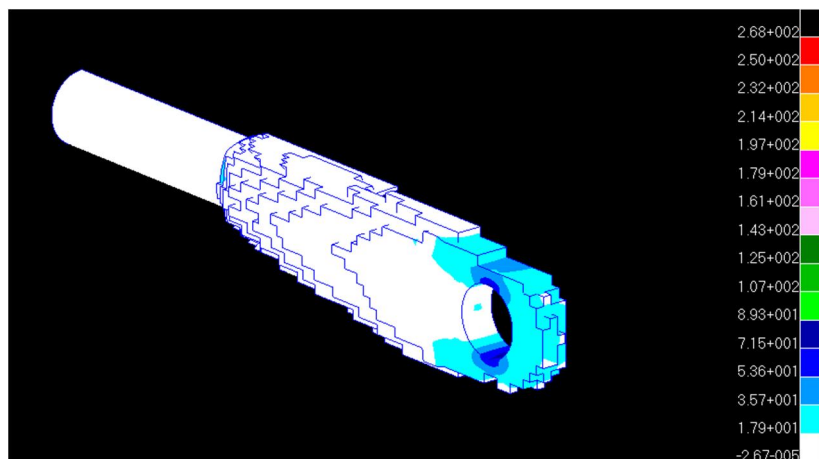


Figure B.37 The von Mises stress distribution of clevis at RR=21% for load case 2.

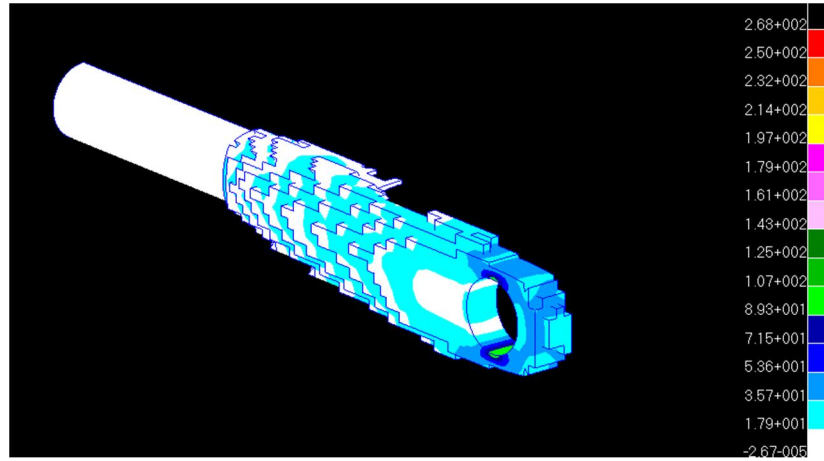


Figure B.38 The von Mises stress distribution of clevis at RR=24% for load case 2.

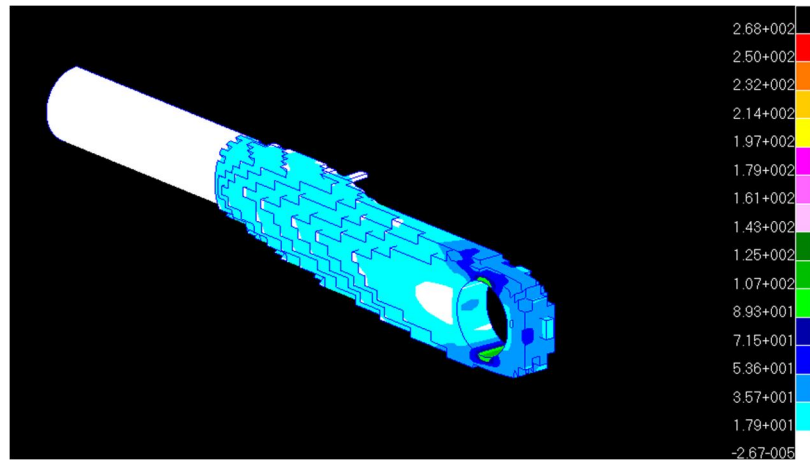


Figure B.39 The von Mises stress distribution of clevis at RR=27% for load case 2.

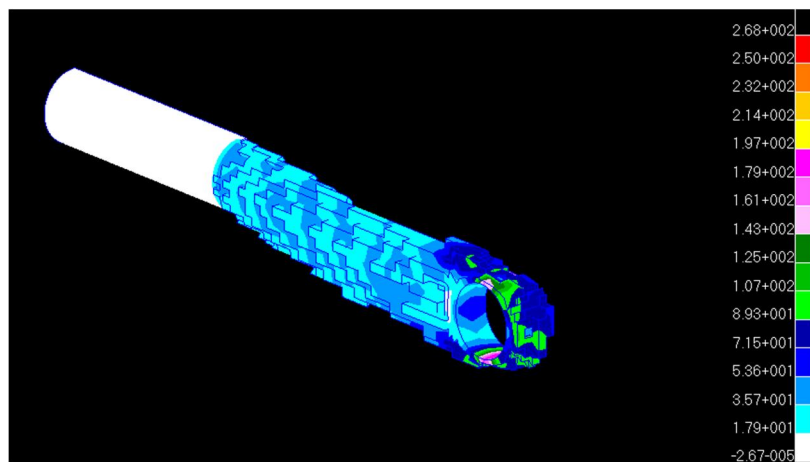


Figure B.40 The von Mises stress distribution of clevis at RR=30% for load case 2.

B.3. THE EVALUATION OF MAIN LANDING FITTING

The optimization steps of clevis are presented from Figure B.41 to B.46. As mentioned in Chapter 4, the RR_o and ER are 0.25% and figures are inserted for each 8th iteration at each load case respectively. (i.e., $RR = 2\%$, 4%, 6%, 8%, 10%, 12%) Same von Mises spectrum is utilized for clarity.

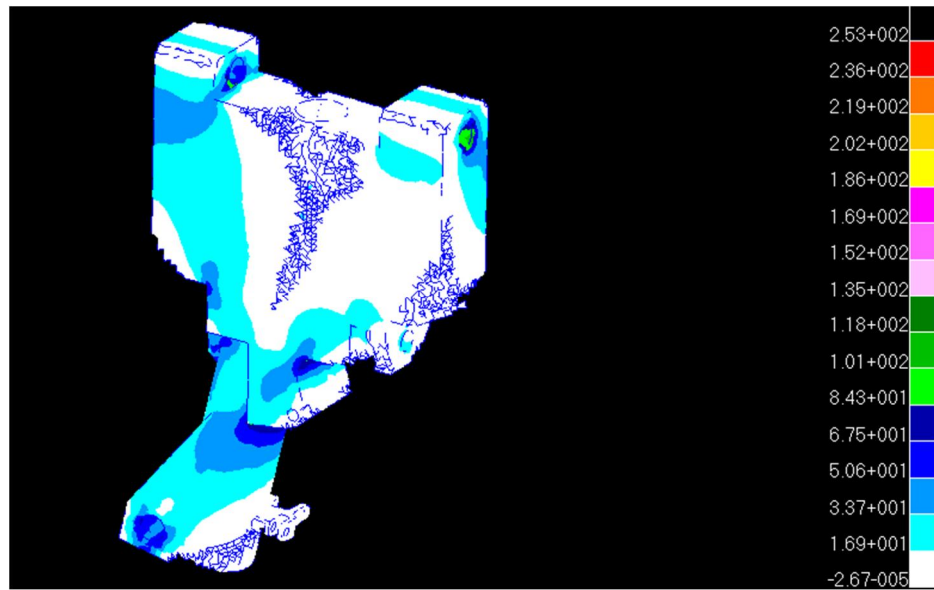


Figure B.41 The von Mises stress distribution of main landing fitting at $RR=2\%$.

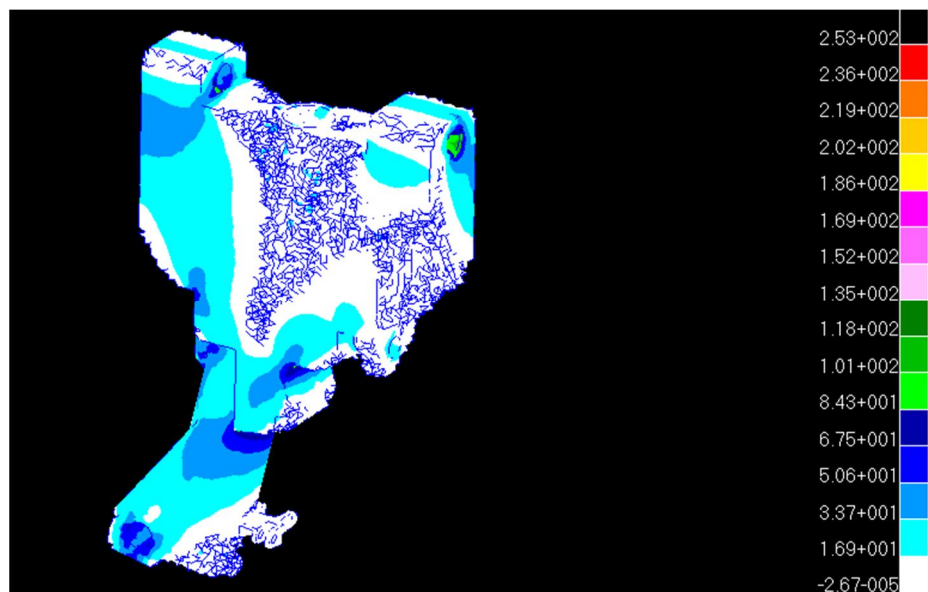


Figure B.42 The von Mises stress distribution of main landing fitting at $RR=4\%$.

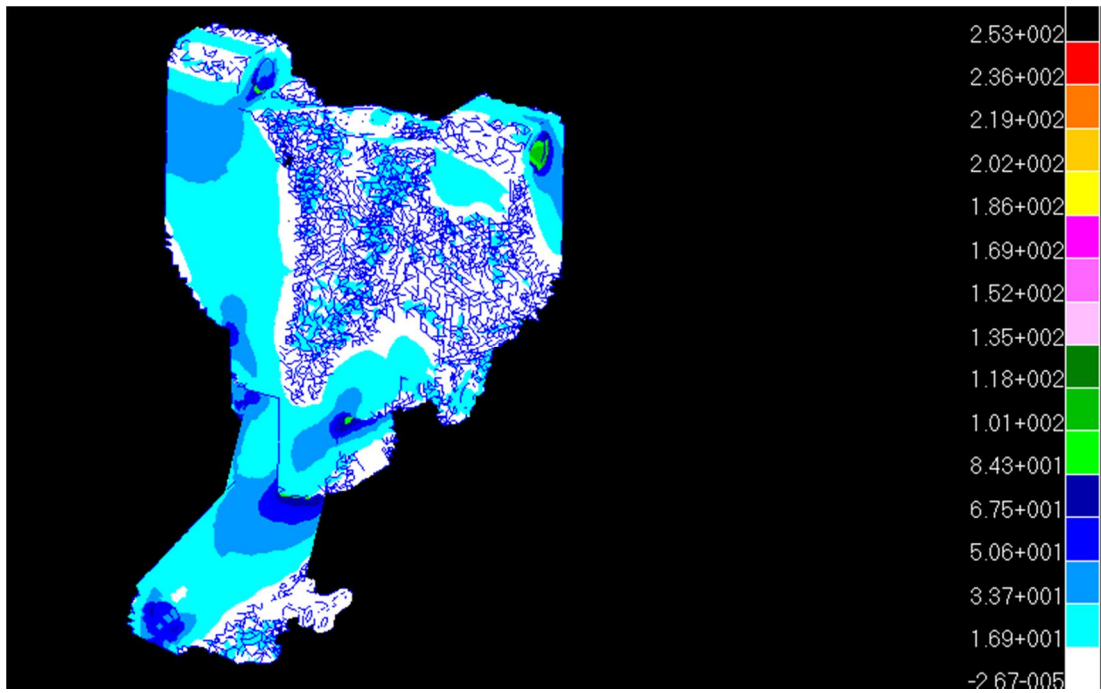


Figure B.43 The von Mises stress distribution of main landing fitting at RR=6%.

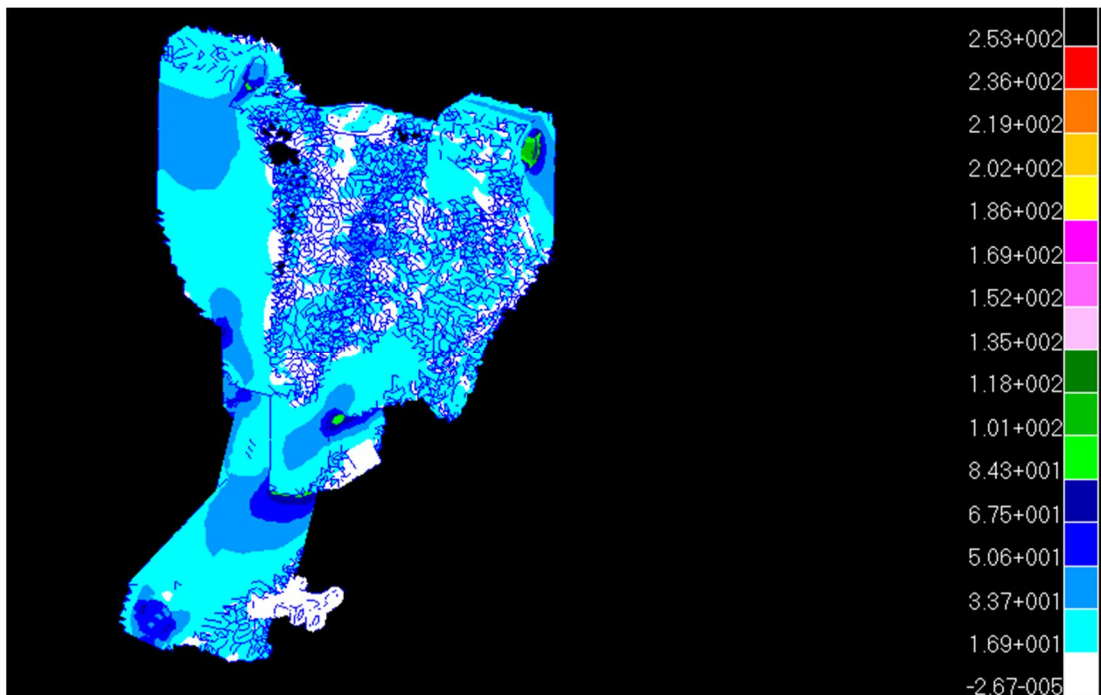


Figure B.44 The von Mises stress distribution of main landing fitting at RR=8%.

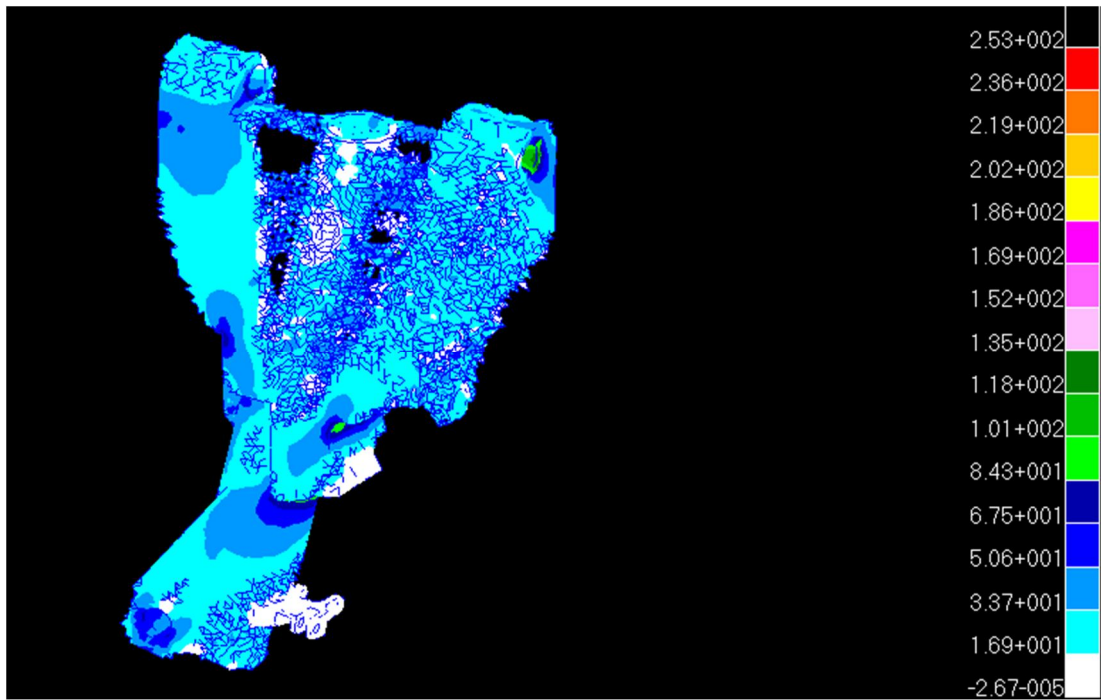


Figure B.45 The von Mises stress distribution of main landing fitting at RR=10%.

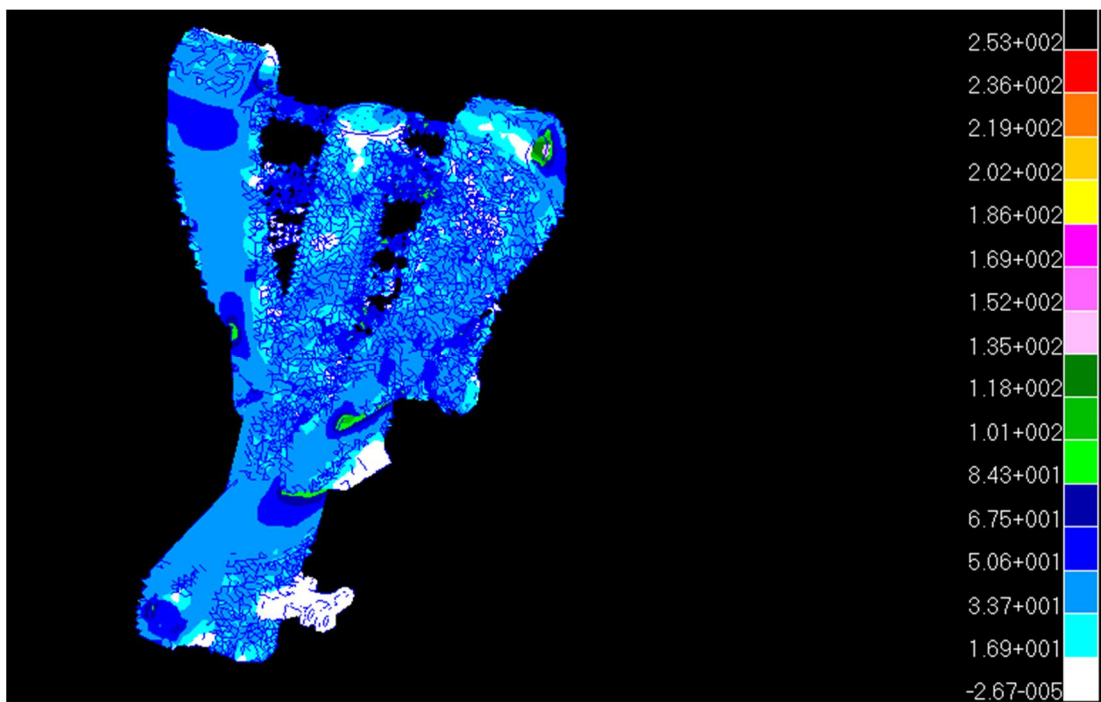


Figure B.46 The von Mises stress distribution of main landing fitting at RR=12%.

B.4. THE EVALUATION OF SUPPORT FITTING

The optimization steps of clevis are presented from Figure B.47 to B.58. As mentioned in Chapter 4, the RR_0 and ER are 1 % and figures are inserted for each 4th iteration at each load case respectively. (i.e., $RR = 4\%, 8\%, 12\%, 16\%, 20\%, 24\%$) Figure B.47 to B.52 present load case 1 and B.53 to B.58 present load case 2. Same von Mises spectrum is utilized for clarity.

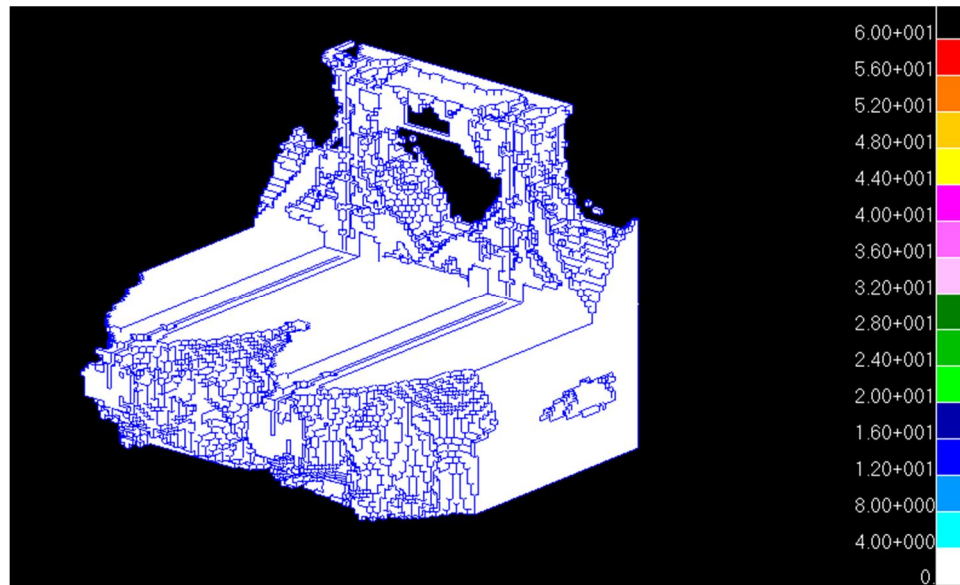


Figure B.47 The von Mises stress distribution of support fitting at $RR=4\%$ for load case 1.

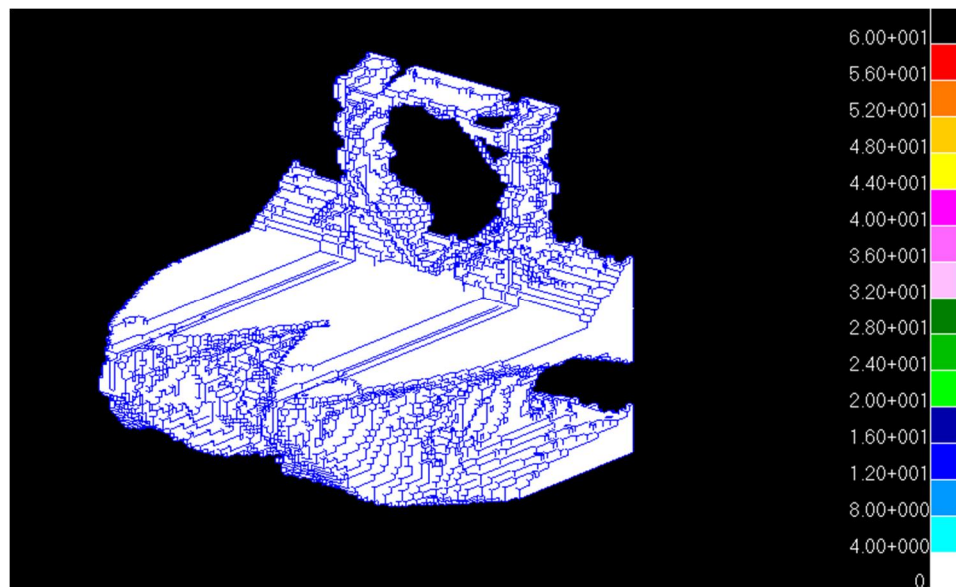


Figure B.48 The von Mises stress distribution of support fitting at $RR=8\%$ for load case 1.

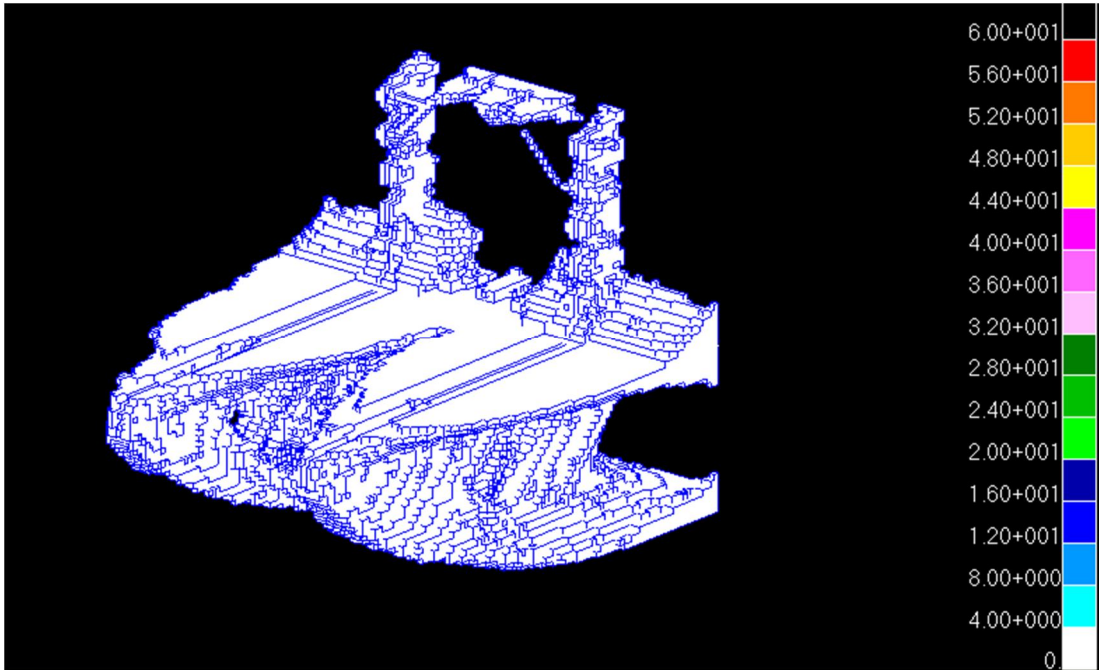


Figure B.49 The von Mises stress distribution of support fitting at RR=12% for load case 1.

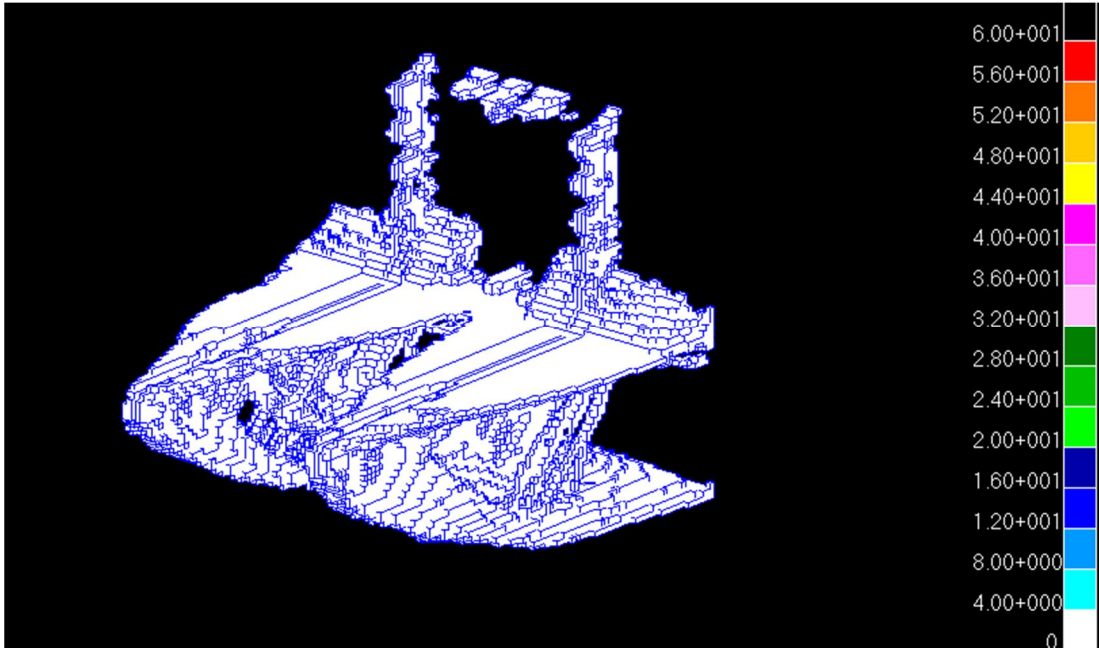


Figure B.50 The von Mises stress distribution of support fitting at RR=16% for load case 1.

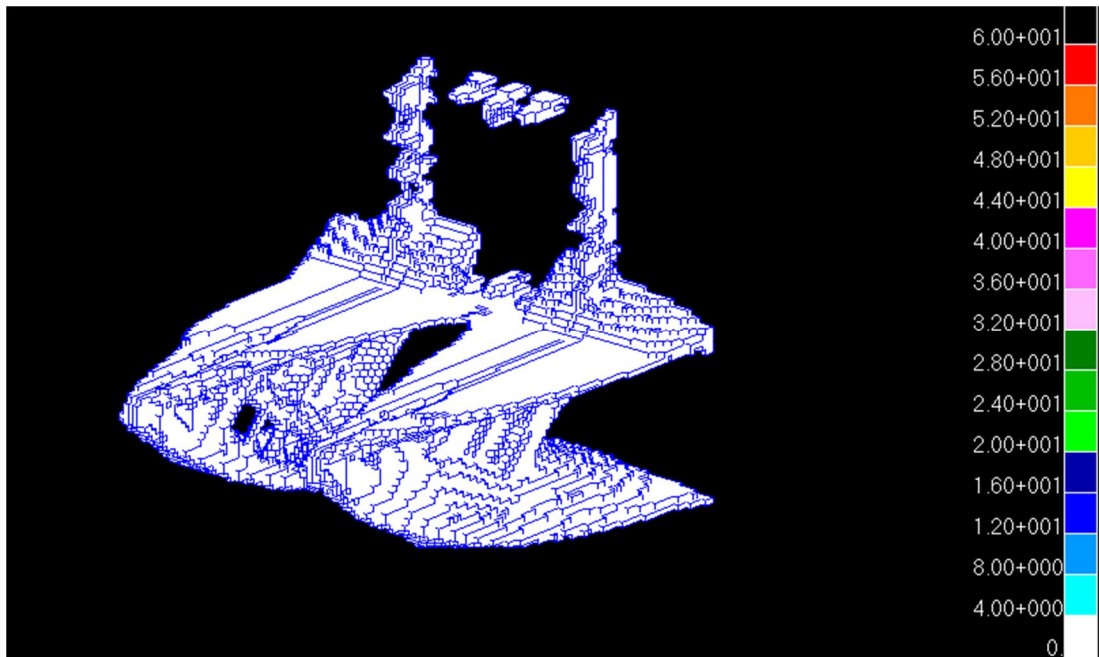


Figure B.51 The von Mises stress distribution of support fitting at RR=20% for load case 1.

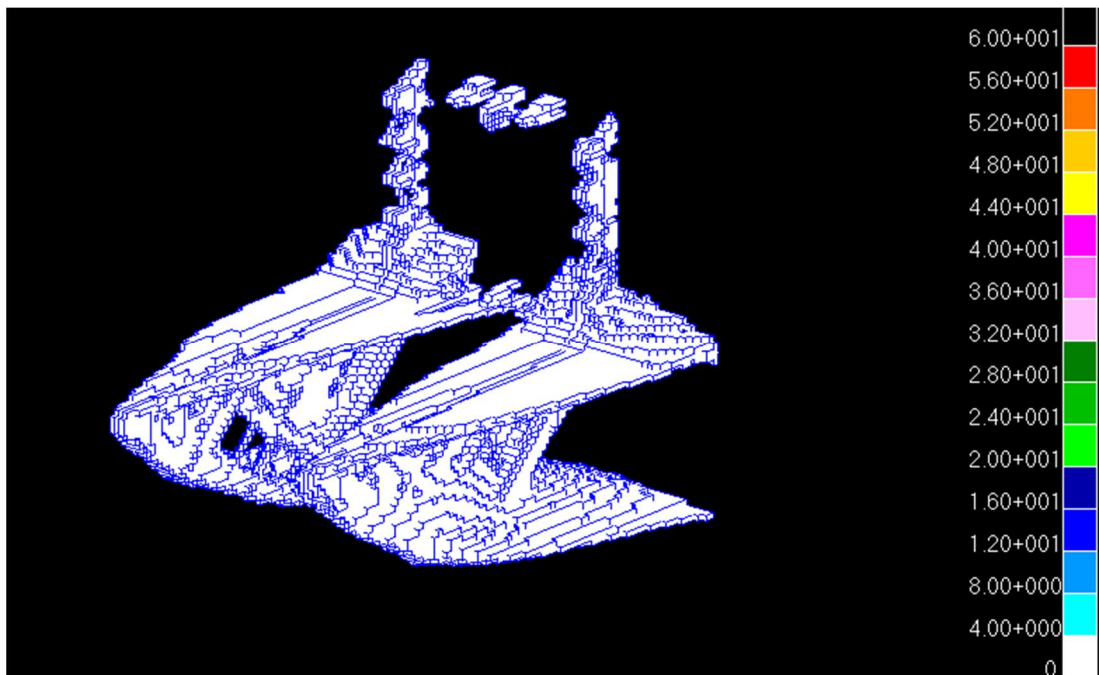


Figure B.52 The von Mises stress distribution of support fitting at RR=24% for load case 1.

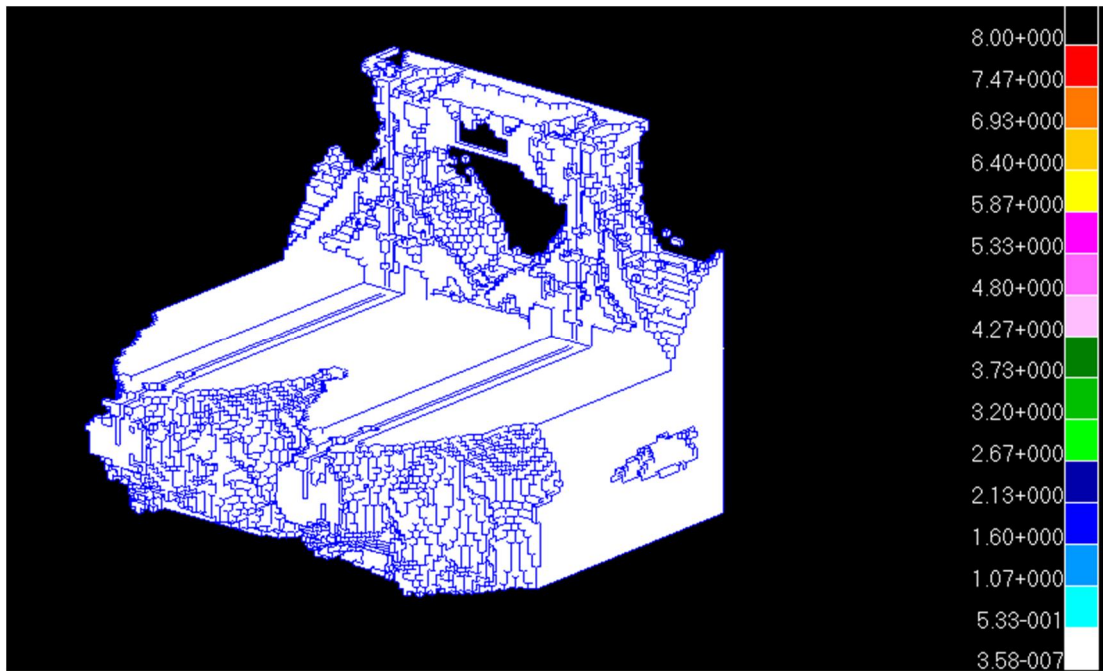


Figure B.53 The von Mises stress distribution of support fitting at RR=4% for load case 2.

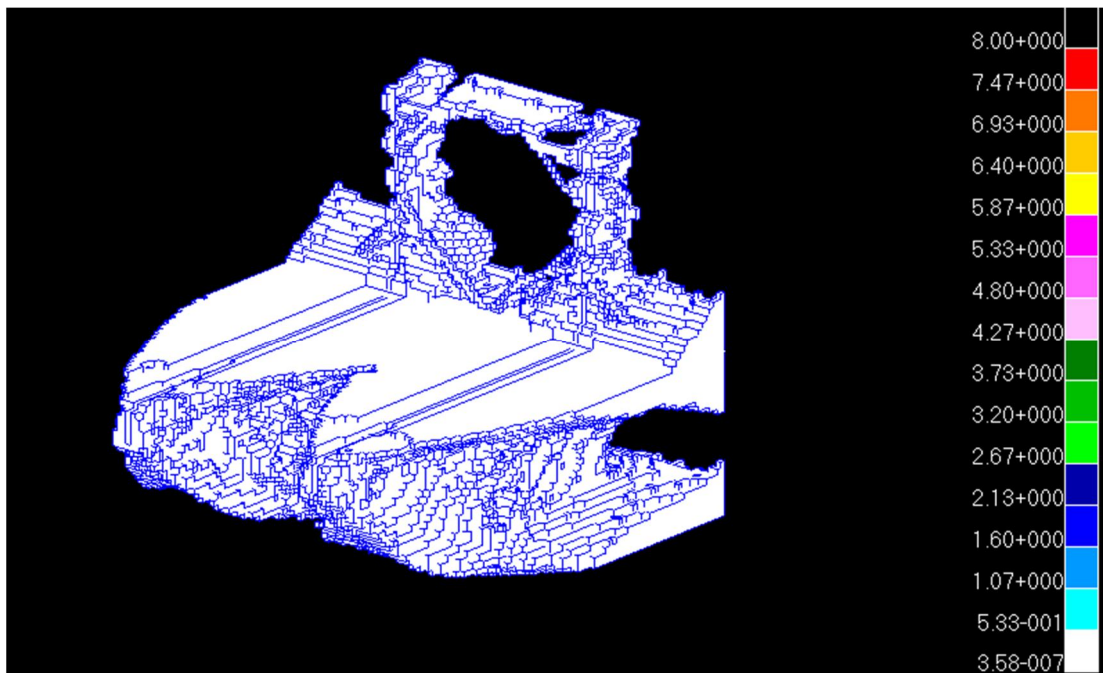


Figure B.54 The von Mises stress distribution of support fitting at RR=8% for load case 2.

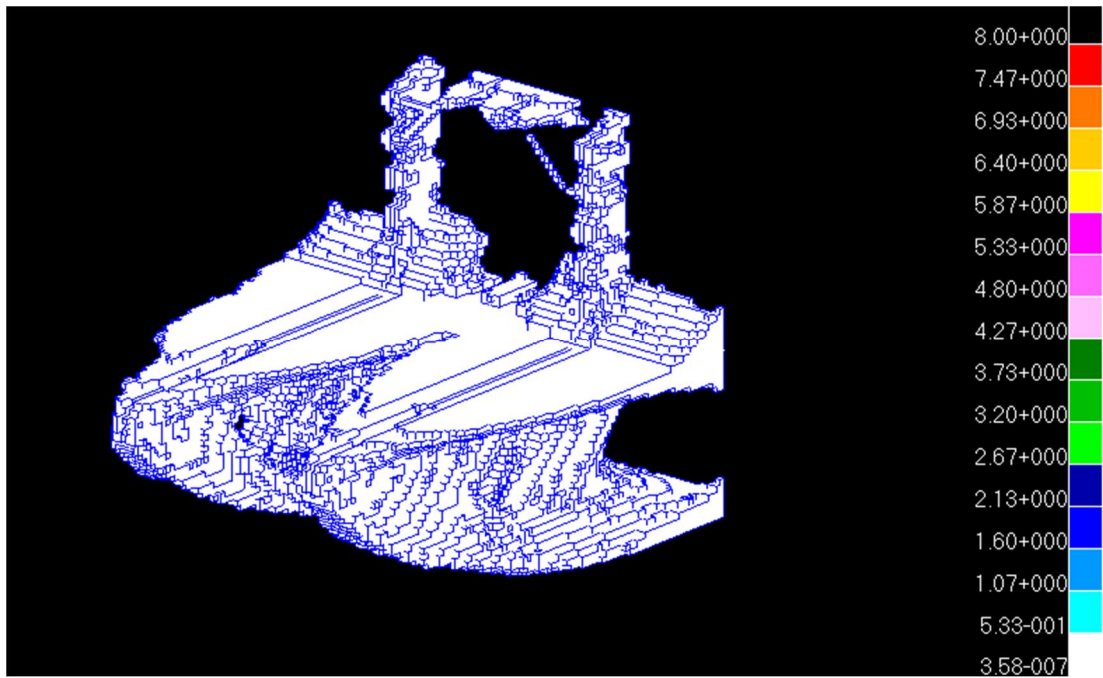


Figure B.55 The von Mises stress distribution of support fitting at RR=12% for load case 2.

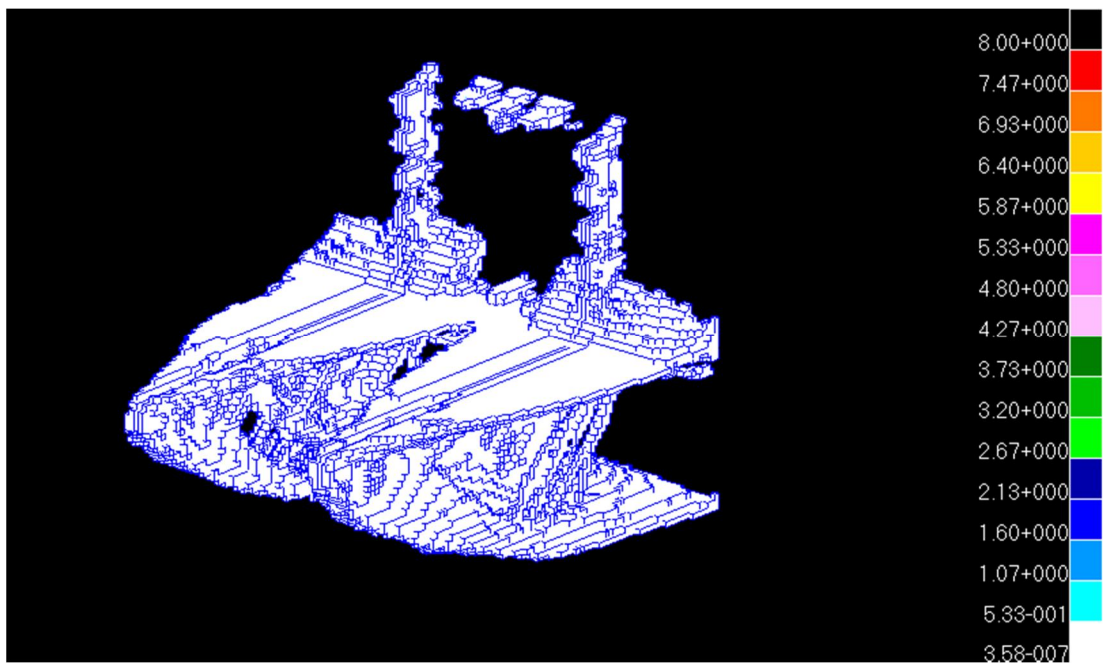


Figure B.56 The von Mises stress distribution of support fitting at RR=16% for load case 2.

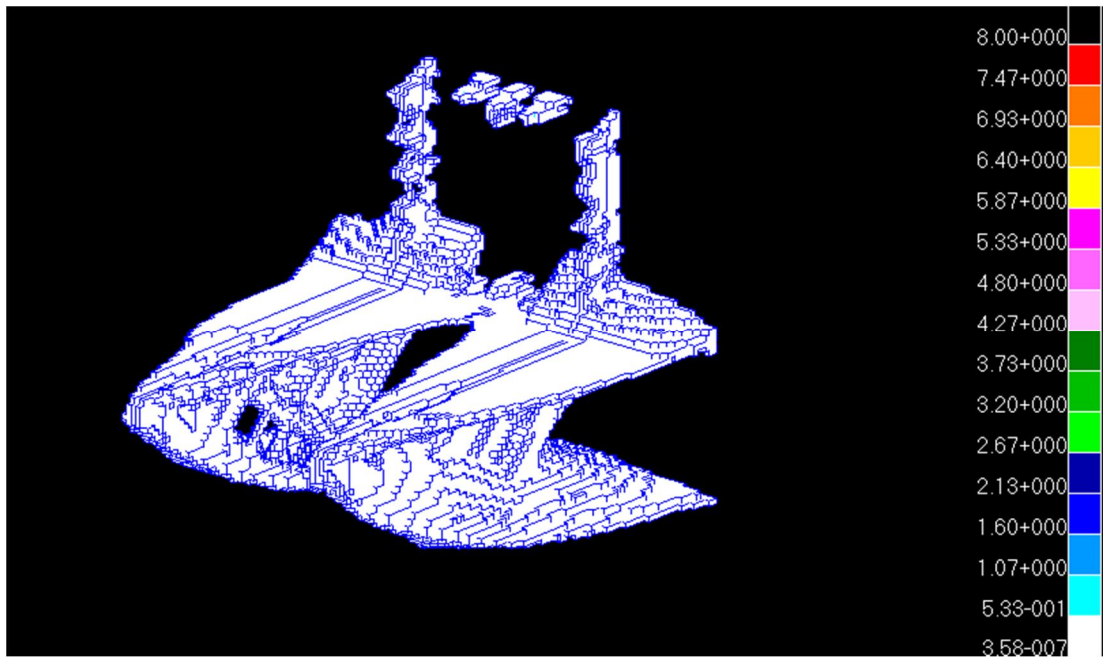


Figure B.57 The von Mises stress distribution of support fitting at RR=20% for load case 2.

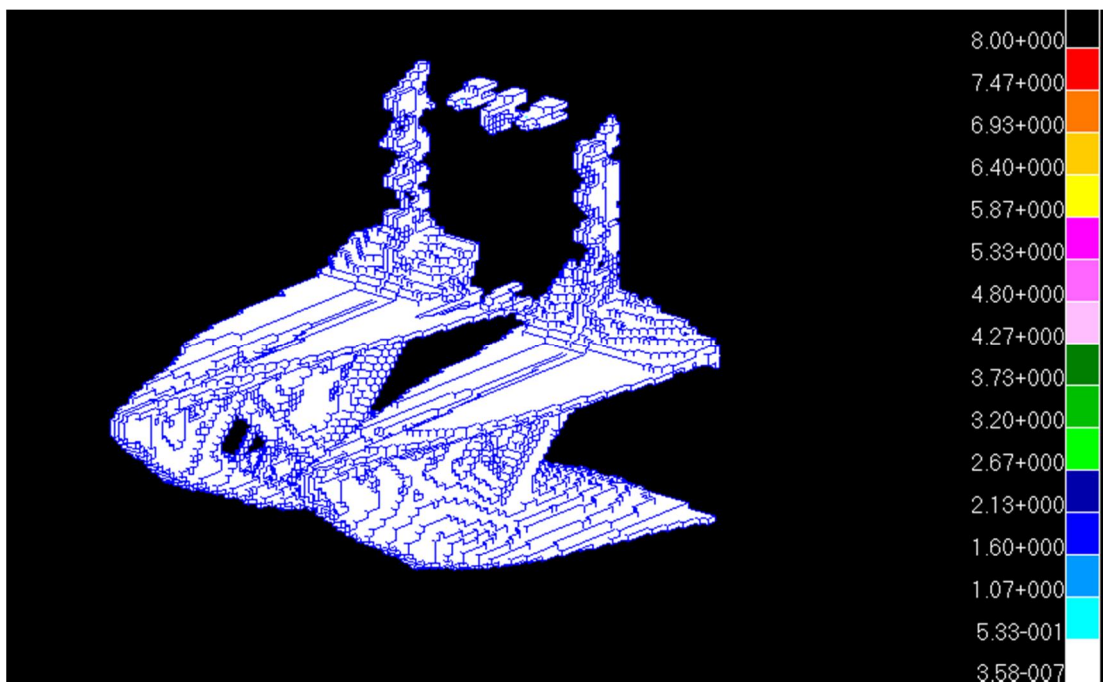


Figure B.58 The von Mises stress distribution of support fitting at RR=24% for load case 2.